Univerzita Karlova v Praze

Přírodovědecká fakulta

Vývojová a buněčná biologie

Mgr. Soňa Pecháčková

Potenciální využití WIP1 fosfatasy v terapii nádorového onemocnění prsu

WIP1 phosphatase as a potential pharmacological target in breast cancer

Disertační práce

Školitel: MUDr. Libor Macůrek, PhD.

Konzultant: Pavlína Řezáčová, PhD.

Praha 2017

Prohlášení:

Prohlašuji, že jsem závěrečnou práci zpracovala samostatně a že jsem uvedla všechny použité informační zdroje a literaturu. Tato práce ani její podstatná část nebyla předložena k získání jiného nebo stejného akademického titulu.

V Praze,

Podpis

In the first place, I have to thank my supervisor Libor Macůrek who gave me the opportunity to join the project and sacrificially help me to solve the scientific issues and finish Ph.D. thesis. I am indebted to Kamila Burdová for the professional teaching of advanced methods and for valuable consultations.

Many thanks goes to the Laboratory of structure biology, namely to a head of the department Pavlína Řezáčová for great knowhow about protein crystallization, further to Jana Škerlová and Petr Pachl who selflessly helped me with crystallization techniques and to Milan Fábry for cloning of protein constructs with the funny comments. My thank goes to Václav Urban who perfectly introduce me HPLC purification system.

My heartfelt thanks go to Monika Burocziová and Jan Benada for objective support but mostly for emotional support and their friendship. All my lab colleagues thank you for providing me help whenever I needed and for being such a great bunch of people to be around.

I would also like to extend my deepest gratitude to my parents and my sister for their continuous support during my studies and this thesis in particular. Most importantly, my biggest thanks belong to my beloved Pavel, thank you for being here for me.

Thank you all once again, and I wish you all the best!

ABBEREVIATION

53BP1	tumor suppressor p53-binding protein 1; enhances p53-mediated activation, plays a role in the response to DNA damage
aa	amino acid
APC	tumor suppressor; anaphase-promoting complex
APC/Cdc20	anaphase promoting complex (APC)/C in complex with activating cell-division cycle protein 20
APC/Cdh1	anaphase-promoting complex (APC)/C in complex with activating adaptor protein Cdh1
ATM	ataxia telangiectasia mutated; serine/threonine protein kinase
ATR	ataxia telangiectasia and Rad3-related protein; serine/threonine protein kinase
Aurora-A	serine/threonine-protein kinase 6
Bax	apoptosis regulator; accelerates programmed cell death
BER	base excision repair
B-loop	Basic amino acids region
BRCA1	breast cancer type 1 susceptibility protein; E3 ubiquitin-protein ligase
CCT007093	a potent PPM1D inhibitor with IC50 of 8.4 μM
Cdc25A	M-phase inducer phosphatase 1
Cdc25B	M-phase inducer phosphatase 2
Cdc25C	M-phase inducer phosphatase 3
CDK(s)	mammalian cyclin-dependent kinases; cyclin-dependent kinases (CDKs)
CDK1	cyclin-dependent kinase 1
CDK2	cyclin-dependent kinase 2
Chk1	serine/threonine-protein kinase; checkpoint kinase 1
Chk2	serine/threonine-protein kinase; checkpoint kinase 2
C-terminal	end of the protein (peptide) terminated by a free carboxyl group
cyclin-B	a member of the cyclin family; mitotic cyclin
cyclin-E	a member of the cyclin family; transition from G1 to S phase
D	Asp; an amino acid aspartic acid
DAXX	death domain-associated protein 6
DDR	DNA Damage Response Pathways
DSB(s)	DNA double strand breaks
E3	ubiquitin-protein ligase
EDTA	ethylene-diamine-tetraacetic acid; 2,2’,2”,2”’-(Ethane-1,2 diyldinitrilo)tetraacetic acid; a chelating agent

ERBB2	a proto-oncogene that encodes a member of the epidermal growth factor (EGF) receptor family of receptor tyrosine kinases
G1	cell cycle growth phase 1
G1/S	transition from G1 to S phase
G2	cell cycle growth phase 2
G2/M	transition from G2 to M phase
GSK2830371	specific inhibitor of Wip1 phosphatase with IC50 of 6 nM
H2AX	histone that replaces conventional H2A in a subset of nucleosomes
HCT116	human colorectal carcinoma cell line
HEPES	4-(2-hydroxyethyl)-1-piperazineethanesulfonic acid; a zwitterionic organic chemical buffering agent;
HER2	human epidermal growth factor receptor 2
HIPK2	homeodomain interacting protein kinase 2
HRAS1	HRas proto-oncogene; harvey rat sarcoma viral oncogene homolog
HTP	high throughput method
IC50	the half maximal inhibitory concentration
IEC	ion exchange chromatography
IR	ionizing irradiation
JNK	c-Jun N-terminal kinases
KAP1	Krüppel-Associated Box Domain-Associated Protein 1
Ki	the inhibitory constant
LB	Lysogeny broth; Luria broth; a nutritionally rich medium, used for the growth of bacteria
LSD1	lysine (K)-specific demethylase 1A
M	mitosis
MAP(K)	mitogenactivated protein kinases
MCF7	human breast adenocarcinoma cell line
MDC1	mediator of DNA damage checkpoint protein 1
MDM2	E3 ubiquitin-protein ligase; mediates ubiquitination of p53/TP53
MDMX	murine double minute, an important negative regulator of the p53 tumor suppressor, homolog Mdm2
MEFs	murine embryonic fibroblasts
Mg^{2+}/Mn^{2+}	magnesium/manganese cation
MMTV	mouse mammary tumor virus
Myc	family of retrovirus-associated DNA sequences (myc) originally isolated from an avian myelocytomatosis virus
Myt1	myelin transcription factor 1
NF-κB	nuclear factor of κ light polypeptide gene enhancer in B-cells 1

NLS	nuclear localization signal
NMR	Nuclear magnetic resonance
N-terminal	end of the protein (peptide) terminated by a free amino group
nutlin-3	MDM2 antagonist
P	phosphate group
P	Pro; an amino acid proline
p21	cyclin-dependent kinase inhibitor 1; CDK-interacting protein 1;
p38 MAPK	mitogen-activated protein kinase 14; mitogen-activated protein kinase p38 alpha
p53	cellular tumor antigen; acts as a tumor suppressor in many tumor types
p53-pS15	phosphorylated p53 at serine 15
p65	human transcription factor 65; nuclear factor NF-_B p65 subunit
Plk1	polo-like kinase 1; serine/threonine-protein kinase
PP1	serine/threonine protein phosphatase 1
PP2A	serine/threonine protein phosphatase 2A
PP2B	serine/threonine protein phosphatase 2B
PP2C	serine/threonine-protein phosphatase 2C
PP2Cδ	serine/threonine-protein phosphatase 2C delta = PPM1D = Wip1
PP4	serine/threonine-protein phosphatase 4
PP5	serine/threonine-protein phosphatase 5
PP6	serine/threonine-protein phosphatase 6
PP7	serine/threonine-protein phosphatase 7
PPM	serine/threonine Protein phosphatase metal-dependent
PPM1A	serine/threonine Protein phosphatase metal-dependent 1A
PPM1B	serine/threonine Protein phosphatase metal-dependent 1B
PPM1D	serine/threonine Protein phosphatase metal-dependent 1D (Wip1)
PPP	serine/threonine Phosphoprotein phosphatase
pRb	retinoblastoma protein
Pro-loop	Proline rich region of catalytic domain of Wip1
pSQ/pTQ	ATM/ATR phosphorylable serine or threonine residues with glutamine (Q) at the +1 position; the so-called SQ/TQ motif
pTXpY	phosphorylation motif phospho-threonine followed by phospho-tyrosine at the +2 position
Q	Gln; an amino acid glutamine
Ras	rat sarcoma, oncogene, encodes a single-subunit small GTPase
RBM38	RNA Binding Motif Protein 38

RG7388	an oral, selective, small molecule MDM2 antagonist
S	cell cycle synthetic phase
S	Ser; an amino acid serine
SCF	ubiquitin ligase; SCF(β-TrCP) ubiquitin ligase, SKP1 Cullin Ubiquitin Ligase, Cullin-F-box protein
SDS-PAGE	sodium Dodecyl Sulfate Polyacrylamide Gel Electrophoresis
siRNA /RNAi	small interfering ribonucleotide acid / RNA interference
SQ/TQ	ATM/ATR substrate motif; serine or threonine residues with glutamine (Q) at the +1 position
ssDNA	single stranded DNA
T	Thr; an amino acid threonine
T4L	T4 phage lysozyme
TP53	gene encoded p53
Tris	tris(hydroxymethyl)aminomethane; 2-Amino-2-hydroxymethyl-propane-1,3-diol; a component of buffer solutions
U2OS	human osteosarcoma cell line
UNG2	uracil-DNA glycosylase 2; removes uracil near replication forks and in nonreplicating DNA
UV	ultraviolet, electromagnetic radiation
Wee1	Wee1-like protein kinase
Wip1	wild-type p53-induced phosphatase 1
Wip1–7A	non-phosphorylated mutant of WIP1 at sites T34/S40/S44/S46/S54/ S85/ S97A
Wip-7D	phospho-mimicking mutant of WIP1 at sites T34/S40/S44/S46/S54/ S85/ S97D
WT	wild type
XPA	xeroderma pigmentosum, complementation group A, DNA damage recognition and repair factor
XPC	xeroderma pigmentosum, complementation group C, XPC complex subunit, DNA damage recognition and repair factor
Y	Tyr; an amino acid tyrosine
γ-H2AX	phosphorylated H2AX at serine 139

TABLE OF CONTENS

Abstract

Cells in our body respond to genotoxic stress by activation of a conserved DNA damage response pathway (DDR). Depending on the level DNA damage, DDR signaling promotes temporary cell cycle arrest (checkpoint), permanent growth arrest (senescence) or programmed cell death (apoptosis). Checkpoints prevent progression through the cell cycle and facilitate repair of damaged DNA. DDR represents an intrinsic barrier preventing genome instability to protect cells against cancer development. WIP1 (encoded by *PPM1D*) phosphatase is a major negative regulator of DDR pathway and is essential for checkpoint recovery. This thesis contributed to the understanding of molecular mechanisms of WIP1 function and revealed how WIP1 can be involved in tumorigenesis. Firstly, we described that WIP1 protein levels decline during mitosis by APC-Cdc20 dependent proteasomal degradation. WIP1 is phosphorylated at multiple residues which inhibit its enzymatic activity. We propose that inhibition of WIP1 in mitosis allows sensing of low levels of DNA damage that appear during unperturbed mitosis. Further, we identified novel gain-of-function mutations of *PPM1D* which result in expression of C-terminally truncated WIP1. These truncated WIP1 variants are enzymatically active and exhibit increased protein stability. As result, cells have more of catalytically active WIP1 that impairs the p53-dependent G1 checkpoint. These mutations were identified in cancer cell lines U2OS and HCT116 and also in the peripheral blood of breast and colorectal cancer patients. We suggest that these gain-of-mutations of *PPM1D* could predispose to cancer development. Finally, we validated commercially available inhibitors of WIP1 using cells with a CRISPR/Cas9-mediated knock-out of *PPM1D*. We confirmed the specificity of a small-molecule allosteric modulator GSK2830371 towards WIP1. Specific inhibition of WIP1 significantly reduced the cell proliferation in cancer cell lines which carry amplification of *PPM1D*. WIP1 inhibition did not affect the proliferation of non-transformed cells with low levels of WIP1. Importantly, we showed that inhibition of WIP1 by GSK2830371 sensitizes breast cancer cells with amplified *PPM1D* and wild-type p53 to DNA damage-induced chemotherapy (doxorubicin) and to MDM2 antagonist (Nutlin-3) treatment. In an effort to contribute the knowledge of WIP1 phosphatase we also aimed to determine its crystal structure. However, we have not optimized any crystallization condition for crystal growth. This part is included as unpublished results. In conclusion, the results obtained during the work on this thesis contribute to our knowledge of how the WIP1 negatively regulates DDR. Our results also support WIP1 phosphatase as a potential pharmacological target inhibition of which can sensitize cancer cells to chemotherapy.

Abstract (Czech)

Buňky našeho těla reagují na genotoxický stres aktivací signální dráhy, která se nazývá buněčná odpověď na poškození DNA (DNA damage response; DDR). V závislosti na typu poškození DNA, DDR dráha vede k dočasnému zastavení buněčného cyklu v kontrolních bodech (tzv. checkpointech), trvalému zastavení růstu (senescence) nebo k programované buněčné smrti (apoptóza). Aktivace kontrolních bodů buněčného cyklu brání progresi buněk a usnadňuje opravu poškozené DNA. DDR představuje bariéru před nárůstem genomové nestability a chrání buňky před vznikem rakoviny. WIP1 (kódovaná genem *PPM1D*) fosfatasa je hlavním negativním regulátorem DDR dráhy a je nezbytná pro ukončení kontrolních bodů buněčného cyklu. Tato práce přispěla k pochopení molekulárních mechanismů funkce WIP1 fosfatasy a popisuje, jak může být WIP1 fosfatasa zapojena při vzniku nádorů. Nejprve jsme popsali, že hladina WIP1 klesá během mitózy pomocí APC-Cdc20 komplexu, který způsobuje proteasomální degradaci proteinu. WIP1 je v průběhu mitózy fosforylovaná na několika aminokyselinách, což vede k inhibici její enzymatické aktivity. Navrhujeme, že inhibice WIP1 v mitóze umožňuje reagovat na nízkou hladinu DNA poškození, ke které dochází v průběhu nenarušené mitózy. Dále jsme identifikovali nové aktivační (gain-of-function) mutace genu *PPM1D*, které vedou k expresi zkráceného proteinu WIP1 z C-konce. Zkrácené varianty WIP1 jsou enzymaticky aktivní a vykazují se zvýšenou stabilitou proteinu v buňkách. V důsledku, že buňky mají více katalyticky aktivní WIP1, dochází k účinné inhibici p53 a k narušení kontrolního bodu v G1. Tyto mutace byly identifikovány v nádorových buněčných linií U2OS a HCT116 a také v periferní krvi pacientů s nádorem prsu a kolorektálním karcinomem. Navrhujeme, že tyto mutace genu *PPM1D* mohou predisponovat nositele k rozvoji rakoviny. V poslední části jsme *in vitro* validovali komerčně dostupné inhibitory WIP1 na buňkách s inaktivovaným genem *PPM1D* pomocí CRISPR-Cas9 technologie. Potvrdili jsme, že alosterický modulátor GSK2830371 specificky inhibuje WIP1 fosfatasu. Inhibice WIP1 významně snižuje proliferaci nádorových buněčných linií, které nesou amplifikaci *PPM1D*. Inhibice WIP1 neovlivnila proliferaci netransformovaných buněk, které mají nízkou hladinu WIP1 proteinu. Ukázali jsme, že inhibice WIP1 pomocí GSK2830371 zvyšuje citlivost buněk rakoviny prsu s amplifikací *PPM1D* a wild-type alelou p53 k účinkům drog způsobující DNA poškození a k antagonistům MDM2 (Nutlin-3). Ve snaze přispět k dalšímu poznání WIP1 fosfatasy jsme si také dali za cíl určit její krystalovou strukturu. Avšak do této doby se nám nepodařilo optimalizovat žádné krystalizační podmínky. Tato část je zahrnuta jako nepublikované výsledky. Ve shrnutí, získané výsledky během této doktorské práce přispívají k porozumění, jak WIP1 negativně reguluje DDR. WIP1 fosfatasa se podle našich výsledku jeví, jako vhodný farmakologický cíl, jehož inhibice může zvýšit odpověď nádorových buněk na chemoterapii.

1 INTRODUCTION

1.1 DNA damage response pathway

Cells in our body are continuously exposed to genotoxic stress caused either by exogenous agents (UV, IR, viral infection, and chemicals) or by endogenous action in cells (cellular metabolism and replication stress). In presence of DNA lesions, proliferating cells activate a conserved DNA damage response pathway (DDR) that temporary abrogates cell cycle to facilitate DNA repair. Depending on the level of DNA damage, DDR signalization promotes temporary cell cycle arrest (checkpoint), permanent growth arrest (senescence) or programmed cell death (apoptosis). DDR pathway represents an intrinsic barrier protecting genome stability and preventing tumor development. [1, 2]. DDR is regulated by posttranslational modifications (PTMs) of proteins involved in DDR pathways such as phosphorylation and ubiquitylation [3]. A central role in DNA damage-induced signal transduction has group of serine/threonine (S/T) kinases that are often mutated during cancer development [4]. DNA damage is recognized by various sensors proteins that activate phosphatidyl-inositol 3-kinase-related kinase protein kinases ATM/ATR, which spread the signal through the phosphorylation [5]. Subsequently, ATM/ATR phosphorylate histone H2AX which mediates recruitment of DNA damage mediators (BRCA1, 53BP1), activates downstream checkpoint kinases Chk1/Chk2 and other key effectors to promote appropriate outcomes of damage (Figure 1) [6].

A key downstream player is the tumor suppressor p53 that upregulates the transcription of genes involved in cell cycle arrest, DNA repair, apoptosis, senescence, and metabolism. [7, 8] The proper function of DDR signalization leads to inactivation of the cyclin-dependent kinases (CDKs) that regulate cell cycle progression. After genotoxic stress p53 is stabilized by multiple posttranslational modifications to increase the transcription of CDKN1A/p21, the inhibitor of CDKs. According to the damage type, DNA double-strand breaks (DSBs) trigger ATM/Chk2 activity to contribute p53/p21 pathway and promote apoptosis or checkpoint [9]. Single-stranded DNA damage (ssDNA) activates ATR/Chk1 kinases that regulate Cdc25A/B/C phosphatase and Wee1 kinase, to control inhibitory phosphorylation of CDKs and cause cell cycle arrest [9]. Transcriptional activity of p53

is stimulated by ATM kinase through the phosphorylation at serine 15 (S15) on the N-terminus of p53 [10].

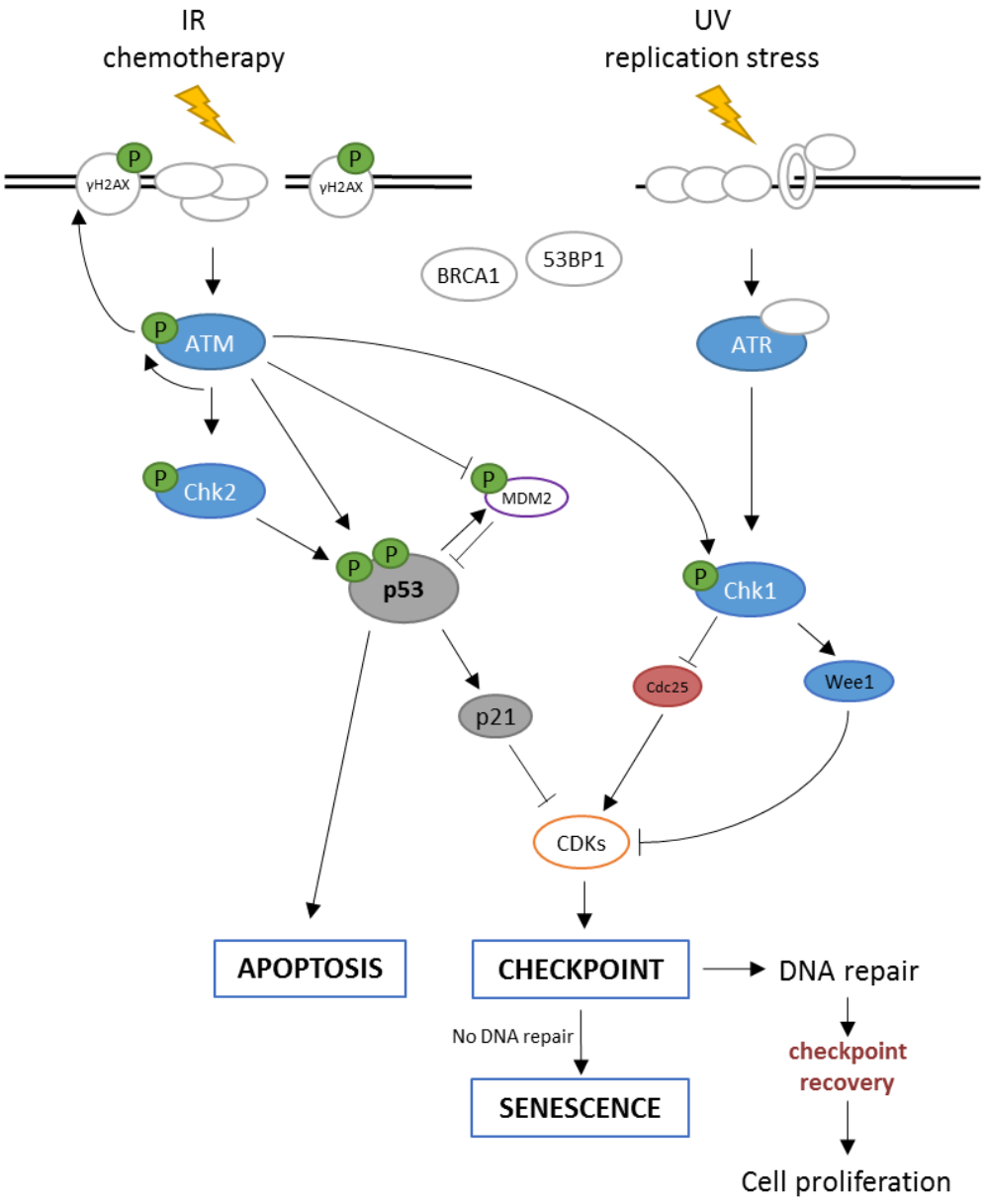

Figure 1. The key players of signal transmission in DNA damage response. The signalization in DNA damage response is primarily extended by apical kinases of the phosphatidyl-inositol 3-kinase-related (PIKK)3 kinase family - ATM and ATR that phosphorylates downstream kinases Chk2 and Chk1. ATM/Chk2 signaling is triggered by DNA double-strand breaks. ATR/Chk1 signaling is activated by exposed ssDNA which appears either during replication stress or during DNA repair processes involving resection of DNA ends. DDR pathway targets to deactivate Cdc25 phosphatases which regulate CDKs and to stabilize tumor suppressor p53, which is required for transcription of CDK inhibitor p21. These DDR effectors turn on cycle checkpoints to facilitate DNA repair. Senescence and program cell death by apoptosis protects the organism against uncontrolled cells transformation and potential tumorigenesis.

The phosphorylated p53 at S15 recruits lysine acetyltransferases to modify DNA binding and carboxy-terminal domains of p53 and allows stabilization of p53 by blocking its ubiquitylation. Moreover, ATM/ATR kinases phosphorylate histone variant H2AX at serine 139 (S139) upon DNA damage [11]. This phosphorylated form of histone H2AX is also known as γ-H2AX that is required for the efficient recruitment of DNA repair mediators BRCA1 and 53BP1 to damage sites [12].

The proliferation of cells is organized into cell cycle consisting of series of phases, G1 (growth phase 1), S (synthetic phase for DNA replication), G2 (growth phase 2) and M-phase (mitosis = nuclear division) and cell division (cytokinesis). The cell cycle is controlled by stable CDK kinases in complex with various cyclins which oscillate during cells progression [13]. Mainly, the CDK2/cyclin-E complex is required for G1/S transition and CDK1/cyclin-B controlled G2/M transition (Figure 2). CDKs are inactivated by phosphorylation of T14 and Y15 by Wee1 and Myt1 kinases [14, 15]. Conversely, CDKs are activated by dephosphorylation of the same residues by Cdc25 family phosphatases (isoforms Cdc25A, B, and C).

The DNA damage signalling activates cell cycle checkpoints in G1, intra-S, and G2/M, depending on the phase in which the damage occur. To promptly activate cell cycle checkpoints, the DDR targets Cdc25 phosphatases and Wee1 kinase. After DNA damage, Cdc25A, B and C phosphatases are rapidly deactivated through the phosphorylation by Chk1 and Chk2 kinases which decreases activation of CDK2 or CDK1 and causes a G1 or G2 checkpoint arrest, respectively [9, 16-19]. Additionally, Chk1 kinase also targets Wee1 kinase which phosphorylation enhances negative regulation toward CDKs [20]. In late response after DNA damage, DDR triggers p53-dependent transcription of p21, which functions as an inhibitor of CDKs and controls the G1 checkpoint [21]. The role of p53 is important for the G2/M checkpoint maintenance [22]. The key activator of p53 is the Chk2 in DSBs response. DNA damage can also induce activity of the p38 mitogen-activated protein kinase (p38 MAPK) pathway that activates p53 and inhibits Cdc25A/B/C to control G2/M checkpoint [23]. Altogether, ATR-Chk1, ATM-Chk2 and p38 MAPK pathways have been described to contribute to the checkpoint activation and maintenance after genotoxic stress (reviewed in [24]).

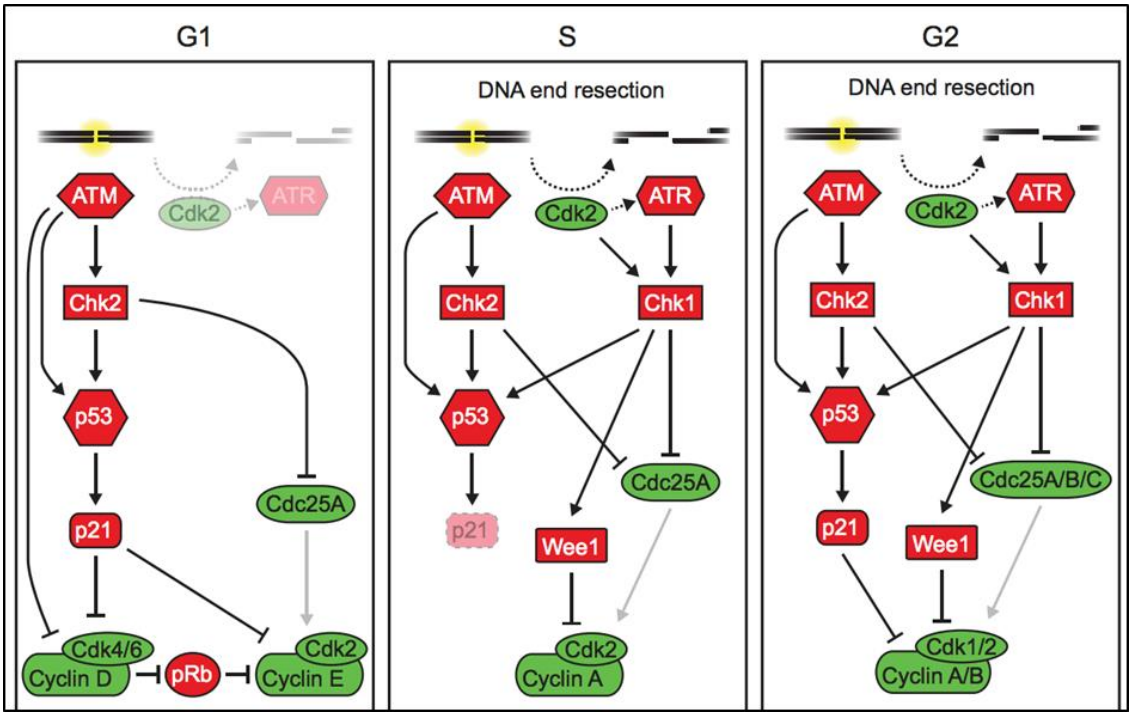

Figure 2. Cell cycle checkpoint signaling in different phases of cell cycle. The cell cycle is controlled by cyclin-dependent kinases CDKs and their cofactors, cyclins. Major regulatory cyclins and CDKs are CDK2/cyclin-E complexes is required for G1/S transition and CDK1/cyclin-B which control G2/M transition. G1 checkpoint depends on the ATM-Chk2-p53-p21 pathway. Intra-S phase checkpoint is governed by ATR-Chk1-Wee1 signaling in p21-independent response. In G2, DNA damage response contributes by ATM-Chk2-P53-p21 to the checkpoint, but major role plays ATR-Chk1-Wee1 signaling. (adapted with modifications from [25])

1.2 Checkpoint recovery

When the DNA lesions are successful repaired, cells re-enter to the proliferation by checkpoint recovery pathway that attenuates DNA damage response signals and terminates cell cycle arrest. During checkpoint recovery, phosphorylation sites previously modified by DDR kinases are dephosphorylated by phosphatases. In the same manner, checkpoint recovery pathway is dependent mostly on the action of protein S/T phosphatases and Plk1 and Aurora-A kinases to stop DDR signalization (reviewed in [24]). The PLK1 kinase is regulated by Aurora-A kinase to promote mitotic entry after a checkpoint-dependent arrest and downregulates checkpoint mediators Chk1, Wee1 and Cdc25C [26-28]. Moreover, PLK1 indirectly targets p53 to promote G2 checkpoint recovery [29]. However, the activity of PLK1kinase is not essential for mitotic entry but is required for checkpoint recovery. Several

protein S/T phosphatases have opposed actions of DDR kinases and negatively regulate phosphorylation levels during DDR.

1.2.1 Serine/threonine protein phosphatases silencing the checkpoints

Termination of DDR-induced checkpoints is regulated by two major families of protein serine/threonine (S/T) phosphatases which inactivate the key DDR kinases and other components triggered by apical kinases and checkpoint kinases to promote checkpoint recovery after sufficient DNA repair (Figure 3).

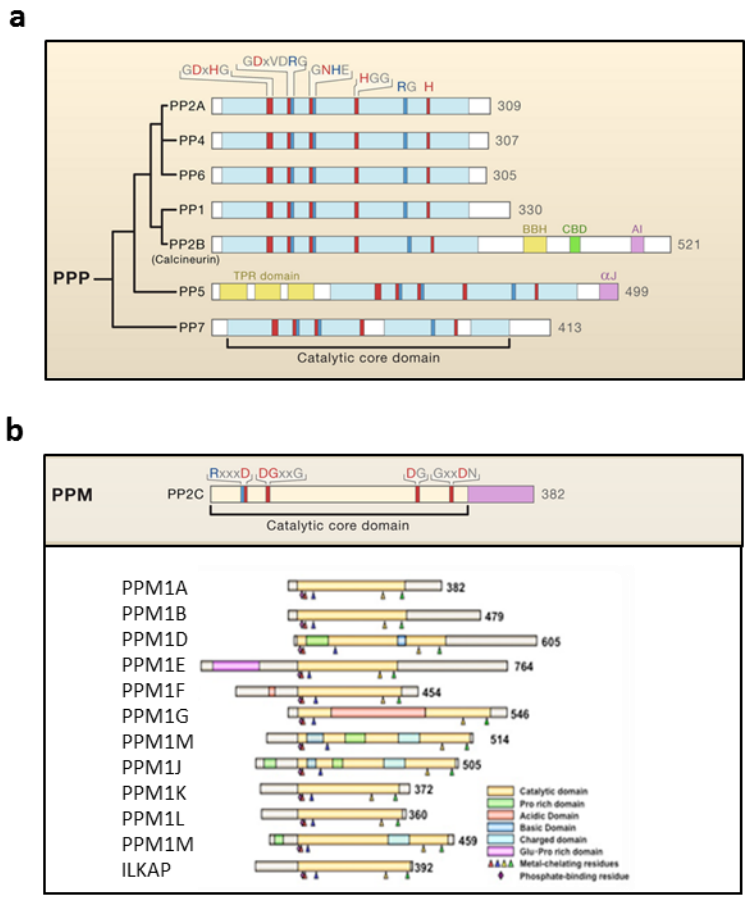

Figure 3. Protein serine/threonine phosphatases family involved in regulation of DNA damage response. Two protein S/T phosphatases family are presented here. **a)** Protein phosphatases (PPPs). **b)** Protein metal-dependent phosphatases (PPMs). The catalytic core domains of each protein are indicated below the diagram or colored in blue (a) and yellow (b). Conserved sequence motifs are labeled above the diagram. Residues that contribute to metal coordination and phosphate binding are colored in red and blue, respectively. (adapted with modifications from [30])

The phosphoprotein phosphatases (PPPs) family includes PP1, PP2A, PP2B (also known as calcineurin), PP4, PP5, PP6, and PP7 (Figure 3a). The PPPs are important for basal and non-specific dephosphorylation and their function catalytic subdomain C is directed by interaction with the regulatory subunits B and/or A [30]. PP1, PP2A and PP4 are implicated in DDR regulation and are specifically required for cell cycle restart after DNA damage-induced cell cycle arrest [31] (Figure 4).

PP1 and PP2A targets DDR kinases ATM, Chk1, and Chk2 to promote checkpoint recovery [32-34]. DNA damage marker histone γ-H2AX has been reported to be dephosphorylated by PP1, PP2A, PP4 and PP6 in complex with their specific catalytic subunit [35-38]. Nevertheless, the function of PP1 and PP2A in DDR and checkpoint recovery seems to be rather homeostatic [35]. Since their inhibition by okadaic acid was not sufficient to activate cell cycle arrest indicating that PP1 and PP2A are not essential for checkpoint recovery [39]. PP1 and PP2A can regulate also p53 at S15, and S46 and T55, respectively [40]. Interestingly, PP2A in complex with regulatory subunit B56γ stabilized DNA damage-induced p53 function by dephosphorylation of T55 which mediates p53 proteasomal degradation [41]. This underlying that PP2A can function as positive as well as negative regulator of checkpoint recovery. PP2A in complex with specific subunits A and/or B are the most characterized S/T phosphatases active in eukaryotic cells and is regarded as a tumor suppressor because it plays an important role in multiple cellular processes, including development, cell proliferation and death, the control of the cell cycle and cell mobility (reviewed in [35, 42]). Recently, PP2A was suggested as a therapeutic target, because its inhibition promotes cell death via mitotic catastrophe or sensitizes cancer cells to chemotherapy [43, 44].

One of the most important phosphatases in checkpoint recovery seems to be PP4 that has been proposed to play a dominant role in recovery from G1 phase [31]. In G1 checkpoint recovery, the catalytic subunit of PP4 with regulatory subunit 2 (PP4R2) dephosphorylates Krüppel-associated box domain-associated protein 1 (KAP1) at S473 which results in repression p21 transcription [31]. Overexpression of PP4 occurs frequently in multiple cancers and is associated with poor prognosis [45]. In conclusion, it seems that PP phosphatases help to reverse phosphorylation level established by DDR pathway and silence the checkpoint.

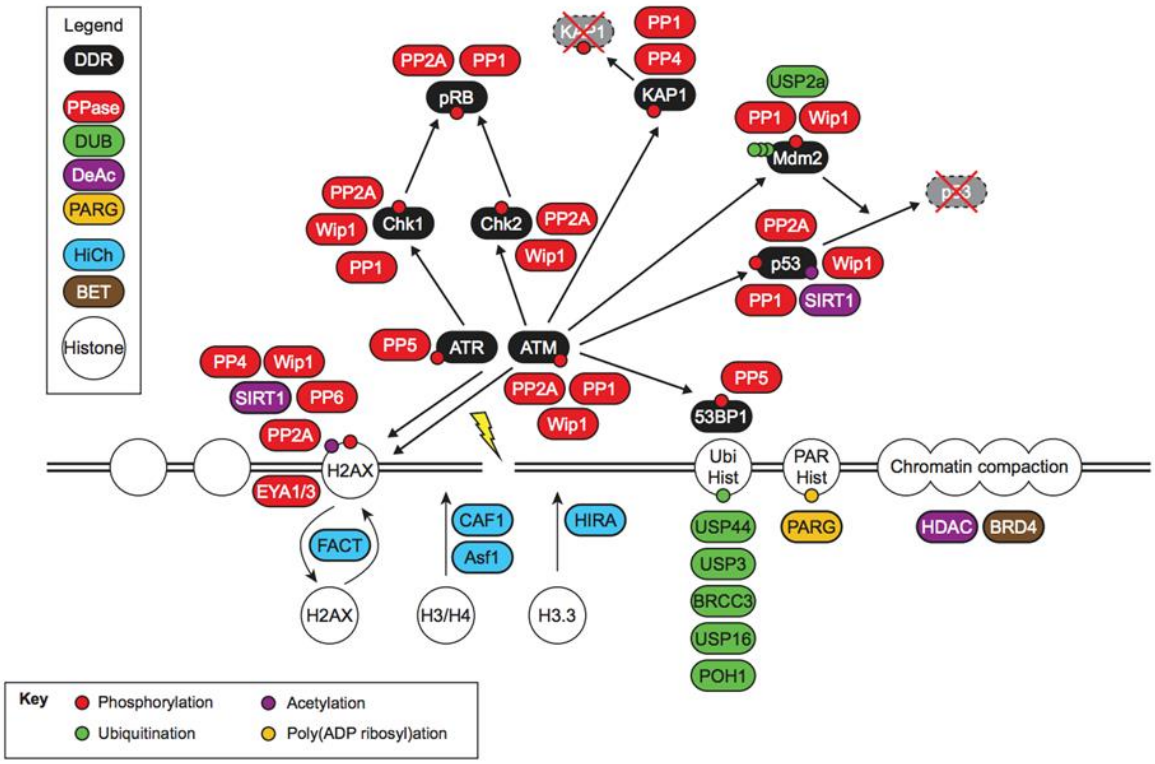

Figure 4. Scheme of DNA damage response silencing by protein serine/threonine phosphatases for checkpoint recovery. Prime role plays the dephosphorylation of ATM/ATR substrates. Protein phosphatases, including WIP1, PP2A, PP1, PP4, PP5 and PP6 (in red), has been reported to reverse the phosphorylation of checkpoint components. Besides phosphatases, the termination of DNA damage-induced checkpoints is contributed by corresponding enzymes to remove other PTMs – ubiquitination, acetylation, and PARylation. For further details see [25].

Second, the most active phosphatase in checkpoint recovery is WIP1 (Wild-type induced p53 phosphatase 1) phosphatase that belongs to metal-dependent S/T protein phosphatase (PPMs) family (Figure 4). PPM family includes PP2C phosphatases which are located within 16 distinct genes in the human genome that express at least 22 different isoforms [46] (Figure 3b). All PP2Cs function as monomer enzymes with conserved N-terminal phosphatase domain and non-catalytic carboxy-terminal (C-teminal) part. Enzymatic activity of these phosphatases is dependent on metal ions Mg^{2+} or Mn^{2+} and in contrast with other S/T phosphatases, PP2Cs are not sensitive to the common S/T phosphatase inhibitor okadaic acid. PP2Cs play an essential role in multiple processes including stress response signaling, cell differentiation, growth, apoptosis, and others [30, 47]. Isoforms PP2Cα (also PPM1A), PP2Cβ (also PPM1B), and PH domain leucine-rich repeat protein phosphatase (PHLPP) are involved in normal cell

cycle regulation and are suggested as tumor suppressor proteins [30, 46]. Isoform PP2Cδ is the WIP1 phosphatase (also known as *PPM1D*) which was showed as an essential regulator of G2/M checkpoint recovery in consequence to DNA damage response [31, 48]. Since WIP1 represents a major focus of this thesis, it will be discussed in larger details in the following chapters.

1.3 WIP1 phosphatase and its role in checkpoint recovery

WIP1 is important to regulate of cell cycle progression after DNA damage that was properly repaired. In the following section will discuss how WIP1 participate in checkpoint recovery pathway.

1.3.1 WIP1 phosphatase recognize ATM/ATR phosphorylated SQ/TQ

Main function of WIP1 in termination of the checkpoint is based on its substrates specificity. WIP1 preferentially dephosphorylates phospho-SQ/TQ (pSQ/pTQ) sites modified by ATM/ATR kinases and thus can modify DDR pathway on different levels (Figure 5). WIP1 modulates also autophosphorylated S1981 of ATM, a regulatory site for activation of ATM [49]. Further, WIP1 recognizes pSQ/pTQ sites and inhibits checkpoint kinases Chk1 and Chk2 which are activated by ATM/ATR after DNA damage [50, 51]. The ATM-targeted Chk2 and ATR-activated Chk1 kinases are dephosphorylated by WIP1 at T68 and S345, respectively [50, 52]. Importantly, ATM kinase phosphorylates tumor suppressor p53 at S15 and this site is recognized by WIP1 during checkpoint recovery. The regulation of p53 by WIP1 is the essential to terminate checkpoints and in more details will be discussed in the following chapter 1.3.3.

Beyond the main substrates of DDR pathway, WIP1 has been reported to target other ATM/ATR substrates including the histone chaperone DAXX (S564), nucleotide excision repair proteins XPA (S196) and XPC (S892) that both play role in DDR [53, 54]. Lately, WIP1 was observed to dephosphorylate LSD1 and RBM38 which are revered by different types of stress response S/T kinases, casein kinase 2 (CK2) and glycogen synthase kinase 3 (GSK3), respectively [55, 56]. The WIP1 function has been also defined in context of NF-kappaB signaling pathway that may promote tumorigenesis through the inflammation. The p65 subunit of NF-kappaB can bind to the *PPM1D* promoter and positively regulates expression

of WIP1 [57]. Conversely, WIP1 targets p65 at S536 that is known to be essential for the transactivation [58]. All described WIP1 substrates and their cellular functions are summarized in the following table (Table 1).

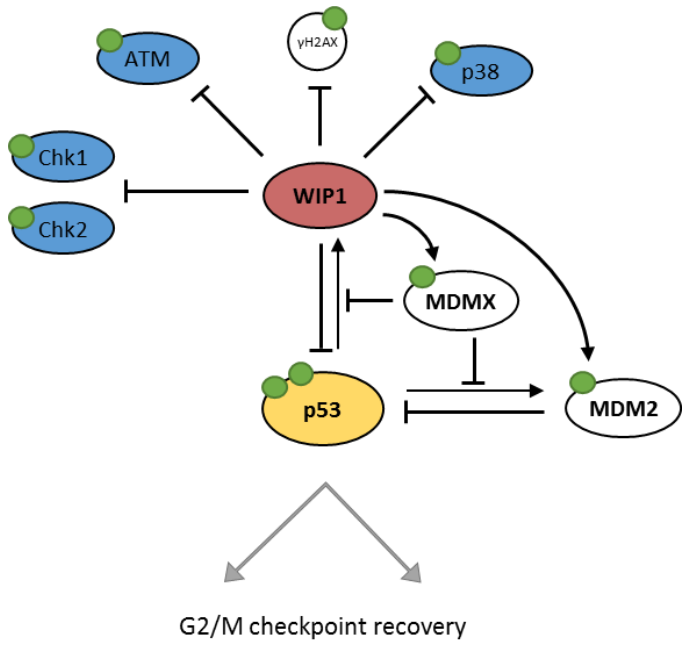

Figure 5. The function of WIP1 in checkpoint recovery. WIP1 dephosphorylates and inactivates keys DDR components - ATM, γH2AX, Chk2, Chk1, and p38. The major function of WIP1 is direct inhibitory dephosphorylation of p53. Moreover, WIP1 also remove inhibitory phosphorylations from MDM2 and MDMX, leading to p53 downregulation. WIP1 is as essential phosphatase in DNA damage-induced G2 checkpoint recovery.

1.3.2 WIP1 phosphatase dephosphorylates γ-H2AX at chromatin

WIP1 phosphatase functions in the nucleus where is tightly bound to the chromatin [59]. In the chromatin region flanking the DSB, histone H2AX is phosphorylated at S139 by ATM/ART kinases. Formation of γ-H2AX at the damage site provides a platform for recruitment and retention of components that stimulates DNA repair. It was described that WIP1 directly dephosphorylates γ-H2AX after induction of DNA damage and cells with depleted WIP1 delayed dephosphorylation of γ-H2AX during checkpoint recovery [59-61]. WIP1 has an essential role in negative regulation of γ -H2AX to silence the checkpoint and to restore chromatin structure after DNA repair.

Table 1 - Substrates of WIP1

Target Protein	Site(s)	Function	Ref.
pSQ/pTQ motif			
ATM	S1981; S365	DNA damage response	[49]
Chk1	S345		[50]
Chk2	S19; S33/35; T68; T432		[52]
DAXX	S564		[53]
H2AX	S139		[59]
p53	S15		[50]
MDM2	S395	regulator of p53	[62]
MDMX	S403		[63]
XPA	S196	nucleotide excision repair	[54]
XPC	S892		
pTXpY motif			
p38 MAPK	T180	stress response	[64]
UNG2	T6	base excision repair	[65]
Unclassified			
LSD1	S131; S137	DNA damage response	[55]
p65	S536	NF-KB signaling	[58]
RBM38	S195	RNA-binding protein; regulate translation of both *PPM1D* and p53	[56]

1.3.3 WIP1 phosphatase negatively regulates tumor suppressor p53

Originally, WIP1 phosphatase has been identified as a gene expressed after induction of DNA damage by UV or γ-irradiation in a p53-dependent manner [66]. Later, it was described that WIP1 directly regulates p53 by removal of ATM-dependent S15 phosphorylation in DNA damage response [50]. Under normal conditions, a half-life of the p53 is very short and mainly regulated by MDM2 E3 ubiquitin ligase and its enzymatically inactive homologue MDMX [67-69]. MDM2 suppress p53 transcriptional activity and trigger p53 to proteasomal degradation [69-72]. MDMX was showed to potentiate activation of MDM2 and negatively regulate p53 transcription activity [73]. Moreover, MDM2 is a transcriptional target of p53 resulting in a negative feedback loop [74].

WIP1 phosphatase has an additional function in p53 regulation because it dephosphorylates MDM2 at S395 and MDMX at S403, sites that are phosphorylated by ATM [62, 63, 75]. Simultaneously, WIP1 phosphatase directly inhibits the p53 pathway and

stimulates MDM2 and MDMX to destabilize p53 [76]. Moreover, as MDM2 and WIP1 are transcriptionally controlled by p53 resulting in a negative feedback loop to terminate p53-dependent cell cycle arrest (Figure 5) [66, 69].

Tumor suppressor p53 is a crucial factor which protects genome stability and decides about cells outcomes after genotoxic stress, to establish cell cycle arrest, facilitate DNA repair, senescence or apoptosis. As WIP1 is a negative regulator of p53, its abnormal activity can predispose to premature checkpoint recovery before completion of DNA repair and to allow division of cells with harmed genome. Enhanced WIP1 activity has been reported to suppress senescence of damaged cells thus overcoming a p53-dependent barrier against cell transformation [77, 78]. Moreover, the inaccurate function of WIP1 can impair apoptosis no only through the p53, but also directly by inhibition of pro-apoptotic BAX translocation to the mitochondria and BAX-related apoptosis [79].

1.3.4 WIP1 phosphatase has specificity towards pTXpY motif

There are several physiological substrates of WIP1 with sequence motif pTXpY - p38MAPK kinase and a nuclear uracil DNA glycosylase UNG2 [64, 65]. The p38 MAPK is activated in various stress responses and also by DNA damage. WIP1 directly dephosphorylates p38 MAPK kinase at pT180 resulting in attenuation of p38 MAPK-dependent p53 phosphorylation after exposure to UVC [64]. UGN2 initiates base excision repair (BER) and its dephosphorylation by WIP1 may inhibit its activity in BER and impair completion of DNA repair [65].

1.3.5 WIP1 phosphatase and its post-translational regulation

For the time being, regulation of WIP1 by specific post-translational modifications is still unclear. It has been reported that WIP1 is phosphorylated at S54 and S85 by homeodomain-interacting protein kinase 2 (HIPK2) in unstressed cells [80]. HIPK2 functions as a homeostatic regulator to enzymatically inactivate WIP1 and target it to proteasomal degradation. Upon stress condition caused by γ-irradiation, HIPK2 kinase is phosphorylated in the ATM-dependent manner by protein kinase AMP-activated catalytic subunit alpha 2 (AMPKa2) which mediates the dissociation of HIPK2 and WIP1 and subsequent stabilization of WIP1.

1.4 WIP1 phosphatase and predicted structure

WIP1 belongs to PP2C subfamily of S/T protein phosphatases which represent a family of highly conserved protein phosphatases. As the other PP2C phosphatases, WIP1 functions as a monomer and recognizes two different substrate motifs, pSQ/pTQ or pTXpY (Table 1) [81]. Two alternative spliced variants of WIP1 transcript have been identified in cells [82]. Full-length protein of WIP1 has 605 amino acids with highly conserved N-terminal phosphatase domain from amino acids 1-375 and non-catalytic C-terminal part from amino acids 376-605 (Figure 6). The second spliced variant of WIP1 resulting in shortening of the C-terminal part to 430 amino acids. The shorter variant of WIP1 is exclusively expressed in the testis and leukocytes whereas the full-length WIP1 is ubiquitous, indicating that the second splice variant may have specific functions in immune response and/or spermatogenesis [82]. The C-terminal part of WIP1 is less conserved across species than the catalytic domain but is noticeably high conserved among mammals in comparison with non-mammalian WIP1 and other phosphatases [47]. C-terminal domain is unique for WIP1 but its function is unclear.

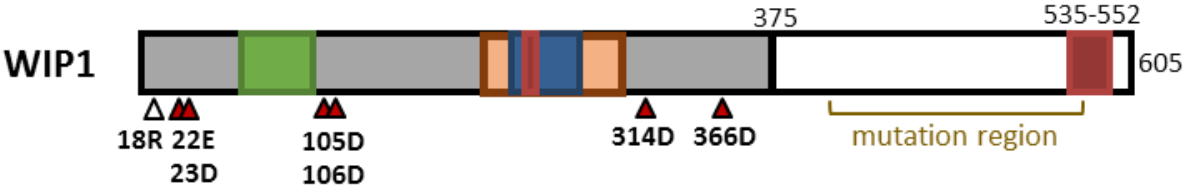

Figure 6. Schematic structure of WIP1 phosphatase. WIP1 consist from catalytic core domain (gray) and C-terminal part (white). In the catalytic domain is located proline-rich sequence, termed Pro-loop (green). Additionally, WIP1 contains "flap" subdomain from P219 to P295 (orange) which includes a basic amino acids rich region (V235-F268), called B-loop (blue) conserved across the species. Nuclear localization sequences (red) are located in the B-loop and on the C-terminus. Red arrow show amino acids binding of Mg^{2+} ions required for enzymatic activity. White arrow marked arginine 18 that binds of phosphate groups on the substrates.

Within the otherwise conserved PP2C catalytic domain of WIP1, proline-rich region (termed Pro-loop) is localized and whereas it does not affect the enzymatic activity it may be important for protein-protein interactions. More important is the unique basic amino acid-rich part of WIP1, termed B-loop (V235 to F268) that utilizes affinity for negatively charged phosphate group on the specific substrates [83]. Amino acid R18 is required for binding of a phosphate group into the catalytic site of WIP1. Negatively charged amino acids E22, E23, D105, D106, D314, and D366 binds Mg^{2+}/Mn^{2+} cations that stabilize interaction with the phosphorylated substrate. These amino acids and B-loop sequence are highly conserved through the PP2C subfamily in vertebrates. Since WIP1 is enzymatically active only in the nucleus, two nuclear localization sequences (NLS) provide WIP1 translocation to the nucleus. One NLS has been found directly in the B-loop (247-KRPR-250) and second lies in the C-terminus (from amino acids 535-552) [82, 84]. Recently, new subdomain termed 'flap' was established (aa 219-295) and it has been described to bind allosteric, small-molecule inhibitors of WIP1 (Figure 7) [85]. So far, the native structure of WIP1 has not been determined and currently described inhibitors do not affect specifically the catalytic site of WIP1 phosphatase.

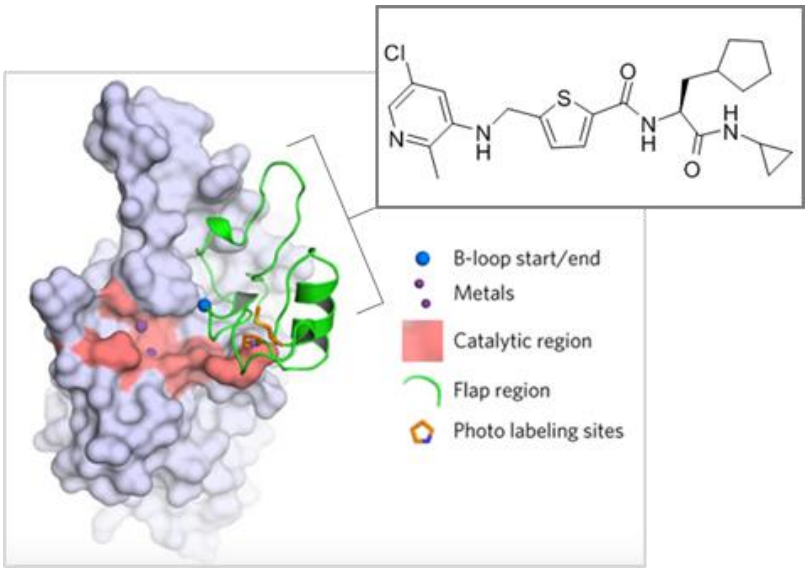

Figure 7. *In silico* predicted structure of WIP1 phosphatase. Designed model of WIP1 was based on PPM1A crystal structure [85]. In green, "flap" region, which includes B-loop (blue); purple - Mg^{2+}; pink - residues of the catalytic site (R18, E22, D23, D105, G106, D192, K218, D314, and D366). The crystal structure of WIP1 has not been determined.

1.5 Role of WIP1 phosphatase in tumorigenesis

Almost half of human tumors exhibit a defect in DDR pathway caused by inactivating somatic mutations in the *TP53* gene. These mutations lead to deficient response to genotoxic stress and are commonly associated with poor prognosis in cancer patients. [86, 87] On the other hand, tumors carrying wild-type *TP53* frequently accumulate other mutations in genes which can provide cell growth advantages, for example, a mutation in DDR pathway. As we described above, WIP1 phosphatase is a negative regulator of DDR pathway that predisposes to genomic instability and could be implicated in cancer development. WIP1 phosphatase is encoded on chromosome 17q23 that is often amplified in breast cancer [88, 89]. The amplification of chromosomal locus carrying the *PPM1D* gene for WIP1 phosphatase has been observed in human cancers including breast, ovarian, colorectal and gastric cancer, neuroblastoma, medulloblastoma and lung adenocarcinoma [88, 90-97]. Therefore, WIP1 phosphatase was suggested as an oncoprotein and promising pharmacological target. Approximately 11% of primary breast tumors with overexpressed *PPM1D* gene retain wild-type TP53 [94]. In about one-third of breast tumors *PPM1D* overexpression was reported to promote breast cancer development in cooperation with different oncogenes such as amplification of the ERBB2/HER2 [98]. First findings revealed that *PPM1D* amplification contributes to the development of human cancers through the inactivation of p38 MAPK and suppression of p53 [91]. WIP1 null mice showed different postnatal defects like a reduced spermatogenesis, immunity, and rate in cell cycle progression [99, 100]. Bulavin et.al. reported that deletion of *PPM1D* impaired breast tumorigenesis in mice bearing MMTV-driven oncogenes ERBB2 or HRAS1 through the inactivation of p38 MAPK and p53 [101]. Another in vivo study demonstrated that WIP1-null mice dramatically delayed development of Eμ-myc-induced lymphomas in an ATM and p53 dependent manner [102]. Since high expression of WIP1 has been observed in intestinal stem cells, abnormal function of WIP1 is implicated also in colorectal cancer. Indeed, the ablation of WIP1 suppressed APC(Min)-driven polyposis formation in mouse colon [103]. The role of *PPM1D* overexpression has been suggested in the generation of point mutations by regulation of heterochromatin silencing through the deactivation of ATM/BRCA1-dependent methylation [104]. The relationship between *PPM1D* and tumor development is still under the investigation but current

knowledge supports the hypothesis that high levels of WIP1 act as rather a weak oncogene to contribute tumorigenesis

1.6 Inhibition of WIP1 phosphatase

Discovery of highly potent drugs and specific small molecules ligand is dependent on 3D structural data of target protein or enzyme [105]. Current X-ray crystallography, NMR or cryo-electron microscopy are major technologies to determine the native structure of proteins. Structure-driven drug design allows development of molecules that affect active site of the target enzyme or target the protein-protein interaction in cells. Novel therapeutic compounds are usually discovered by high-throughput screening of libraries containing thousands of small molecules. Until now the structure of WIP1 has not been determined but several models of WIP1 (Figure 7) was structured based on protein homology with PP2C phosphatases that already had been crystallized (PPM1A and PPM1B) [83, 85]. Therefore, existing published inhibitors of WIP1 have been found by HTP screening of libraries.

Compound M321237 was discovered as first potential WIP1 inhibitor but the selectivity for *PPM1D* amplified cancer cells has not been confirmed [106]. Initially, promising compound was discovered by HTP screening and *in vitro* validation of the hit compound, CCT007093 showed IC50 = 8.4 µM [107]. Cell viability in presence of CCT007093 was suppressed in human *PPM1D* amplified/wild-type p53 cancer cell lines. On the other hand specificity of CCT007093 to WIP1 has not been proved in comparison with other PP2C phosphatases. Moreover, specificity of CCT007093 to inhibit WIP1 in cells seems to be limited due to its interaction with cellular thiols and amines. This chemical feature of CCT007093 strengthens the secondary effects on cellular viability. However, CCT007093 had the low efficiency to inhibit of endogenous WIP1 in skin keratinocytes, suggesting off-target effects of the inhibitor [108]. Other potential inhibitors of WIP1 phosphatase SPI-001 and its analogue SL-176 were determined as a non-competitive inhibitor with low IC50 value at 110 and 86.9 nM, respectively [109, 110]. SPI-001 was determined to be approximately 50-fold more specific against WIP1 then to another PP2C phosphatase, PPM1A [109]. Both, SPI-001 and SL-176 suppressed the cell proliferation in human breast cancer MCF7 cells with overexpressed *PPM1D* in a dose-dependent manner [110]. In conclusion, SL-176 could be potentially used in combination therapy to sensitize *PPM1D* mutated cancer cells, but further analysis

of specificity and efficiency of SL-176 need to be proved. The more structure-based design of WIP1 inhibitors led to development of cyclic-thioether peptides that mimic substrates of WIP1 and were designed according to pTXpY substrate motifs recognized by WIP1 [81, 111, 112]. Cyclic peptide inhibitors can block WIP1 enzymatic activity *in vitro* with Ki = 2.9 µM [111]. However, due to the chemical properties of cyclic peptides, they have low bioavailability and have not been tested in cells to address their anti-proliferative effect in tumor cells [113]. The cyclic peptide could be used in different drug delivery system, such as nanoparticles in future.

Recently, novel promising compounds GSK2830371 with potent bioavailability and high selectivity to inhibit of WIP1 phosphatase was discovered [85]. Two independent HTP screens of a library of small molecules were determined compounds with overlapping structures containing an amino acid-like core region flanked by organic molecules improving pharmacological parameters. These compounds have been classified as capped amino acid (CAA) and from this series compound 8, marked as GSK2830371 has been developed and it showed advanced cell permeability and pharmacokinetics. According to WIP1 homology model with PPM1A structure, it was found that GSK2830371 binds as an allosteric modulator to the "flap" region of WIP1 and disrupts access to the catalytic site of WIP1 (Figure 7). GSK2830371 selectively inhibits WIP1 *in vitro* with IC50 = 13 nM compared to other 21 phosphatases. Importantly, GSK2830371 efficiently suppresses proliferation of hematological tumor cells exhibiting *PPM1D* amplification and wild-type *TP53* [85]. In vivo analysis of WIP1 inhibitor GSK2830371 in a xenografted tumor mice models of B-cell lymphoma and neuroblastoma significantly inhibited tumor growth through activation of the p53 pathway [85, 114].

1.7 Targeting WIP1 phosphatase in cancer therapy

Independent studies showed that inhibition of WIP1 by RNA interference sensitized cancer cells to DNA damage-induced chemotherapy (doxorubicin) and caused apoptosis [115-117]. The amplification *PPM1D* correlates with p53 proficient type of cancer mainly in breast cancer. This supports the possibility that the WIP1 may function in tumor development principally through inhibition of p53. WIP1 inhibition can serve as novel view in personalized chemotherapy medicine to recover p53 response and promote cell cycle arrest or apoptosis

of tumor cells (Figure 8). The pharmacological reactivation of p53 function is also supported in mouse models for tumor regression [118].

Reactivation of the p53 pathway by inhibition of MDM2/MDMX has been suggested as a strong therapeutic strategy of cancers with TP53 wild-type locus [119-122]. MDM2 antagonists nutlin-3 (cis-imidazoline) and its orally bioavailable analogue RG7388 disrupted the interaction between p53 and MDM2/MDMX to maintain the function of p53 [123, 124]. Treatment with nutlin-3 prevents degradation of p53 by MDM2 and induces cell cycle arrest or apoptosis in dose-dependent manner [123]. RG7388 efficiently induced apoptosis in p53-proficient neuroblastoma cell lines and blocked tumor growth *in vivo* in xenograft models [124-126]. Currently, the biologically active derivate of nutlin-3, RG7388 is in clinical trials to test the efficiency of the drug in cancer therapy.

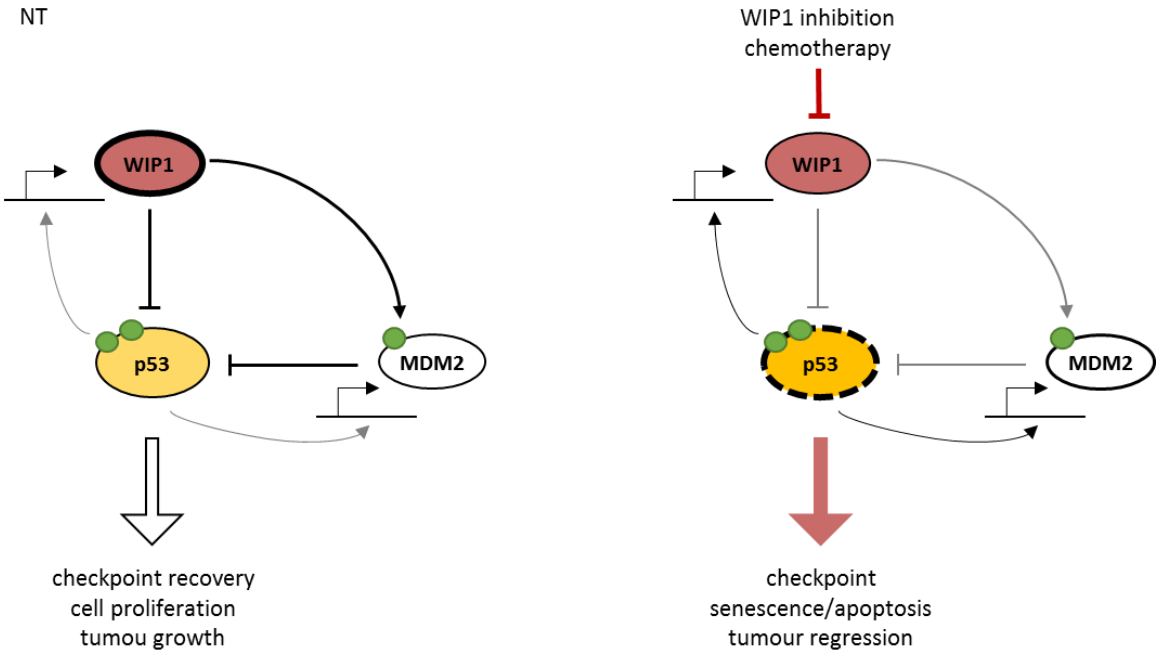

Figure 8. Scheme of the WIP1-p53 pathway in cancer cells. Cancer cells carrying amplification *PPM1D* and intact *TP53* cannot establish cell cycle arrest by WIP1-mediated inhibition of p53 and activation of MDM2/MDMX that destabilized p53. It has been proposed that inhibition of WIP1 upregulates p53 activity and can enhance the sensitivity of cancer cells to chemotherapy, for example, agents which cause genotoxic stress (doxorubicin).

2 AIMS

This thesis aims to contribute understanding of how WIP1 phosphatase functions at the molecular level in cells. It was shown that WIP1 is required for G2 checkpoint recovery, but its regulation during cell cycle phases is unclear. Since that WIP1 is a negative regulator of DDR pathway its abnormal function has been observed in tumor cells which exhibit *PPM1D* amplification. Therefore, WIP1 has been suggested as an oncoprotein and potential pharmacological target in cancer therapy. The crystal structure of WIP1 is unknown and structure-based design of specific small molecule inhibitors is impossible yet. Presently available inhibitors of WIP1 are poorly validated in cancer cells and their specificity needs to be analysed.

The aims of this thesis can be summarized as follows:

- How is WIP1 regulated during the cell cycle?
- How newly identified truncated variants of WIP1 function in cancer cells?
- Validation of commercially available inhibitors of WIP1.
- What is the effect of WIP1 inhibition in cancer cell lines?
- Determination of crystal structure of WIP1 phosphatase.

3 RESEARCH PAPERS

Downregulation of WIP1 phosphatase modulates the cellular threshold of DNA damage signaling in mitosis.

Macurek L, Benada J, Müllers E, Halim VA, Krejčíková K, Burdová K, Pecháčková S, Hodný Z, Lindqvist A, Medema RH, Bartek J.

Cell Cycle. 2013; 12:251-62. doi: 10.4161/cc.23057

Impact Factor (2013): 5.006

Gain-of-function mutations of *PPM1D*/WIP1 impair the p53-dependent G1 checkpoint.

Kleiblova P, Shaltiel IA, Benada J, Ševčík J, Pecháčková S, Pohlreich P, Voest EE, Dundr P, Bartek J, Kleibl Z, Medema RH, Macurek L.

Journal Cell of Biology. 2013; 201:511-21. doi: 10.1083/jcb.201210031

Impact Factor (2013): 9.688

Inhibition of WIP1 phosphatase sensitizes breast cancer cells to genotoxic stress and to MDM2 antagonist nutlin-3.

Pechackova S, Burdova K, Benada J, Kleiblova P, Jenikova G, Macurek L.

Oncotarget. 2016 ; 7:14458-75. doi: 10.18632/oncotarget.7363.

Impact Factor (2015/2016): 5.008

WIP1 phosphatase as pharmacological target in cancer therapy

manuscript - Review

Pecháčková S, Burdová K, Macůrek L.

Journal of Molecular Medicine (under consideration)

3.1 Downregulation of WIP1 phosphatase modulates the cellular threshold of DNA damage signaling in mitosis

Macurek L, Benada J, Müllers E, Halim VA, Krejčíková K, Burdová K, Pecháčková S, Hodný Z, Lindqvist A, Medema RH, Bartek J.

Cell Cycle. 2013 Jan 15; 12(2):251-62. doi: 10.4161/cc.23057. Epub 2012 Jan 15.

Here we have examined how WIP1 is regulated during the cell cycle, mainly in mitosis. We have identified that WIP1 activity is downregulated by phosphorylation at multiple residues that lead to inhibition of its enzymatic activity during mitosis. Further, we showed that protein abundance of WIP1 peaks in G2 and declines in mitosis. Moreover, we found a responsible ubiquitin ligase which leads to degradation of WIP1 in the proteasome.

P. S. contributed to creating plasmids and performed the in vitro kinase assay.

Cell Cycle 12:2, 1–12; January 15, 2013; © 2013 Landes Bioscience

Downregulation of Wip1 phosphatase modulates the cellular threshold of DNA damage signaling in mitosis

Libor Macurek,[1,*] Jan Benada,[1] Erik Müllers,[2] Vincentius A. Halim,[3] Kateřina Krejčíková,[1] Kamila Burdová,[1] Soňa Pecháčková,[1] Zdeněk Hodný,[1] Arne Lindqvist,[2] René H. Medema[3] and Jiri Bartek[1,4,*]

[1]Department of Genome Integrity; Institute of Molecular Genetics; Academy of Sciences of the Czech Republic; Prague, Czech Republic; [2]Department of Cell and Molecular Biology; Karolinska Institutet; Stockholm, Sweden; [3]Division of Cell Biology; The Netherlands Cancer Institute; Amsterdam, Netherlands; [4]Danish Cancer Society Research Center; Copenhagen, Denmark

Key words: cell cycle, Wip1 phosphatase, DNA damage response, mitotic progression, γH2AX

Abbreviations: 53BP1, p53-binding protein 1; APC/C, anaphase-promoting complex/cyclosome; ATM, ataxia telangiectasia-mutated kinase; ATR, Ataxia telangiectasia and Rad3-related kinase; BRCA1, breast cancer type 1 susceptibility protein; Cdk, cyclin-dependent kinase; DDR, DNA damage response; FUCCI, fluorescent, ubiquitination-based cell cycle indicator; γH2AX, histone variant H2AX, phosphorylated on serine 139; IR, ionizing radiation; MDC1, mediator of DNA damage checkpoint protein 1; NZ, nocodazole; PPM1D, Protein phosphatase Mg2+/Mn2+ dependent 1D; SCF, Skp, Cullin, F-box containing complex; WCL, whole-cell lysate; Wip1, wild-type p53 induced phosphatase 1

Cells are constantly challenged by DNA damage and protect their genome integrity by activation of an evolutionary conserved DNA damage response pathway (DDR). A central core of DDR is composed of a spatiotemporally ordered net of post-translational modifications, among which protein phosphorylation plays a major role. Activation of checkpoint kinases ATM/ATR and Chk1/2 leads to a temporal arrest in cell cycle progression (checkpoint) and allows time for DNA repair. Following DNA repair, cells re-enter the cell cycle by checkpoint recovery. Wip1 phosphatase (also called PPM1D) dephosphorylates multiple proteins involved in DDR and is essential for timely termination of the DDR. Here we have investigated how Wip1 is regulated in the context of the cell cycle. We found that Wip1 activity is downregulated by several mechanisms during mitosis. Wip1 protein abundance increases from G_1 phase to G_2 and declines in mitosis. Decreased abundance of Wip1 during mitosis is caused by proteasomal degradation. In addition, Wip1 is phosphorylated at multiple residues during mitosis, and this leads to inhibition of its enzymatic activity. Importantly, ectopic expression of Wip1 reduced γH2AX staining in mitotic cells and decreased the number of 53BP1 nuclear bodies in G_1 cells. We propose that the combined decrease and inhibition of Wip1 in mitosis decreases the threshold necessary for DDR activation and enables cells to react adequately even to modest levels of DNA damage encountered during unperturbed mitotic progression.

Introduction

Following DNA damage, eukaryotic cells protect their genome integrity by activation of a conserved DNA damage response pathway (DDR) that temporally arrests progression through the cell cycle (checkpoint) and promotes DNA repair. Depending on the mode of DNA damage, DDR is triggered by activation of the phosphatidylinositol 3-kinase-related kinases, namely ATM and DNA-PK in case of double-stranded DNA breaks or ATR in case of diverse types of lesions, mainly associated with DNA replication.[1] Recent studies and phosphoproteomic screens identified several hundred ATM/ATR substrates, including also checkpoint kinases Chk1/2 and tumor-suppressor protein p53. Activation of checkpoint kinases Chk1/2 promotes a fast establishment of the checkpoint by a direct inactivation or degradation of cdc25-family phosphatases. Phosphorylation of p53 by ATM/ATR and Chk1/2 leads to its stabilization and promotes its binding to promoters resulting in extensive changes in gene expression. Checkpoint is further strengthened by a p53-dependent expression of the cdk inhibitor p21 and by transcriptional repression of mitotic inducers cyclin B and cdc25B. In parallel to the checkpoint arrest, chromatin flanking the DNA lesion is extensively post-translationally modified to allow recruitment of various proteins involved in DNA repair (recently reviewed in ref. 2). Rapidly after DNA damage, ATM/ATR kinases phosphorylate the histone variant H2AX at Ser139 (referred to as γH2AX), and this modification generates a docking site for a large adaptor protein MDC1.[3]

*Correspondence to: Libor Macurek and Jiri Bartek; Email: libor.macurek@img.cas.cz or jb@cancer.dk
Submitted: 11/15/12; Accepted: 11/28/12
http://dx.doi.org/10.4161/cc.23057

In turn, various ubiquitin E3 ligase complexes are recruited to the site of damage and mediate ubiquitination of the chromatin. Recent studies identified multiple protein complexes that control DNA-damage induced histone ubiquitination, and these include E3 ligases RNF8,[4,5] RNF168[6] and HERC2;[7] E2-conjugating enzyme Ubc13 and E1 ubiquitin-activating enzyme UBA1.[8] Both histone phosphorylation and ubiquitination are necessary for recruitment of 53BP1 and BRCA1 proteins, essential regulators of non-homologous end joining and homologous recombination DNA repair pathways, respectively.[2,9] Besides the well-established role in DNA repair of lesions caused by ionizing radiation (IR) or by genetic rearrangements during maturation of the immune system, for example, 53BP1 is also involved in protecting endogenous underreplicated DNA regions (such as fragile sites) during interphase.[10,11] According to this model, progression through unperturbed mitosis may generate DNA damage in these underreplicated regions. Since ubiquitination does not occur on mitotic chromatin, 53BP1 cannot localize to sites of DNA damage during mitosis, while γH2AX remains and provides a marker of mitotic DNA damage.[12,13] In the subsequent G_1 phase, 53BP1 is recruited to the damaged regions and prevents undesired DNA end processing until lesion is repaired during the next S phase. However, the precise molecular mechanisms regulating formation of these endogenous 53BP1 nuclear bodies remain to be elucidated.

Various phosphatases have been implicated in timely inactivation of the DDR following DNA repair.[14] Among these, the PP2C family serine/threonine phosphatase Wip1 seems to play an essential role, since it can dephosphorylate multiple proteins involved in DDR signaling including, ATM, Chk1, Chk2, p53, mdm2 and γH2AX[15-21] and, thus, is considered as a major regulator of the cellular DDR.[22] Since Wip1 is a direct transcriptional target of p53, its expression increases following genotoxic stress.[23] Early after DNA damage, translation of Wip1 mRNA is blocked by miR-16 preventing premature termination of the DDR.[24] Later during the DDR, when the bulk of the lesions had been repaired, increased abundance of Wip1 allows termination of the DDR and by a negative feedback loop inactivates p53. However, a basal Wip1 activity needs to be present throughout the G_2 checkpoint to limit the p53-dependent transcriptional repression of cyclin B and to maintain the recovery competence.[25] Importantly, loss of Wip1 strongly protects knockout mice from cancer development, suggesting that deregulated Wip1 may act as an oncogene.[26-28] In addition, amplification of the *PPM1D* gene (encoding Wip1) was identified in various human tumors, pointing toward a role of Wip1 in cancer development.[27,29-34] Whereas the role of Wip1 in termination of DDR is relatively well-known, molecular mechanisms that control its function are still poorly understood. Here, we investigated how Wip1 is regulated during the cell cycle and found that the level of Wip1 is low in G_1, increases toward G_2 and declines during mitosis. Besides regulation at the protein level, Wip1 is extensively post-translationally modified, which contributes to its inactivation during mitosis. Our findings offer an explanation for the observed activation of the DDR pathway during unperturbed mitosis without exposure to exogenous DNA damaging insults.[10]

Results

Protein abundance of Wip1 peaks in G_2 and declines during mitosis. To gain insight into the regulation of Wip1 protein levels during the cell cycle, we synchronized HeLa cells at G_1/S transition by a double thymidine block and then released them to fresh media containing nocodazole to allow progression to and arrest in mitosis. We noticed that whereas Wip1 was detectable throughout the S and G_2 phases, its expression dramatically declined at 10–12 h post-thymidine release when cells entered mitosis (**Fig. 1A**). Interestingly, cells released into media without nocodazole progressed through mitosis to G_1 phase after 12 h and expressed Wip1, suggesting that the observed decrease of Wip1 may reflect a regulatory mechanism specific to mitosis. The same staining pattern was observed using two antibodies recognizing distinct epitopes in Wip1, thus indicating that the low signal is unlikely to reflect masking of the epitopes in mitosis. In addition, similar behavior of Wip1 was observed in U2OS cells, suggesting that the low abundance of Wip1 in mitosis is not restricted to a particular cell type (data not shown). Since synchronization of cells with thymidine may cause undesired stress response and potentially impair protein expression, we aimed to develop a system that would allow investigation of asynchronously growing cells.[35] We made use of the published fluorescent, ubiquitination-based cell cycle indicator (FUCCI) and established a stable cell line expressing markers of G_1 and S/G_2 phases.[36] After fluorescence-activated sorting of asynchronously growing cells, we obtained fractions highly enriched in G_1 and G_2 cells (**Fig. 1B**; **Fig. S1**). Notably, we observed that G_2 cells expressed approximately 2-fold more Wip1 compared with G_1 cells (**Fig. 1C**). Since transcription of Wip1 is controlled by p38/MAPK-p53 and JNK/c-Jun stress-responsive pathways, we hypothesized that the moderate difference in expression of Wip1 in G_1 and G_2 phases may be masked in cells synchronized with thymidine.[23,37]

To substantiate our findings obtained by biochemical analysis of mixed cell populations, we set up an automated microscopic analysis of multiple individual cells. Total intensity of the DAPI signal was proportional to the DNA content and, as expected, was 2-fold higher in G_2 cells compared with G_1 cells. In addition, mitotic cells with condensed chromatin showed slightly higher DAPI signal compared with G_2 cells. Remarkably, higher Wip1 staining intensity was found in interphase cells with higher DAPI signal compared with those with lower DAPI signal, thus supporting our conclusion that expression of Wip1 is higher in G_2 cells compared with G_1 cells (**Fig. 1D**). Importantly, the observed immunofluorescence signal of Wip1 in interphase cells was specific, since it increased after treatment of cells with etoposide and was greatly reduced after depletion of Wip1 by RNAi (**Fig. 1D**). Despite the commonly observed higher fluorescence staining background in mitosis, mitotic cells showed a lower intensity of the Wip1 staining compared with G_2 cells, which is consistent with our analysis of the whole-cell lysates using immunoblotting (**Fig. 1D**).

Recently, we reported that overexpressed EGFP-Wip1 is bound to chromatin throughout the cell cycle.[19] In good agreement with

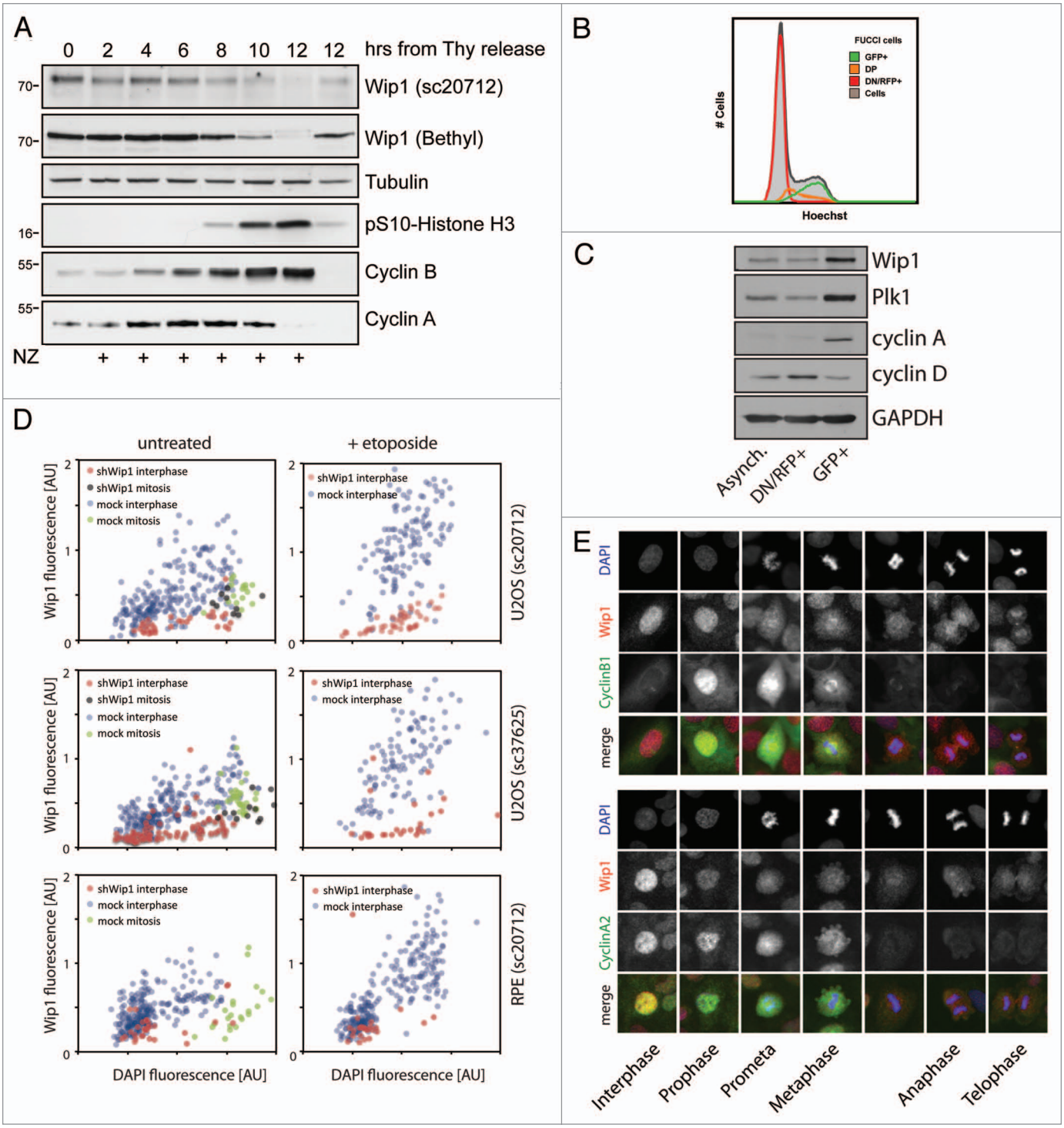

Figure 1. For figure legend, see page 4.

our previous findings, we observed that endogenous Wip1 was enriched in the nucleus during interphase (**Fig. 1E**). In a striking contrast, we did not observe any specific signal of the endogenous Wip1 at the metaphase plate, suggesting that endogenous Wip1 might be absent from chromatin during mitosis (**Fig. 1E**). To exclude the possibility that the antibody does not recognize the chromatin-bound Wip1 during mitosis, we examined cells expressing Wip1-mCherry and observed an identical staining pattern (**Fig. S2**).

Wip1 is degraded in mitosis by proteasome in APC/C^{cdc20}-dependent manner. Since our biochemical and microscopic analyses revealed decreased abundance of Wip1 in mitotic cells, we hypothesized that protein stability of Wip1 might be regulated during mitosis. To assess this possibility, we released cells from

Figure 1. Wip1 protein abundance during the cell cycle. (**A**) HeLa cells were synchronized by a double thymidine block, released into fresh media supplemented or not with nocodazole, and samples were collected at 2-h intervals and probed with indicated antibodies. pSer10-H3 was used as a marker of mitotic entry; degradation of cyclin A as a marker of prometaphase and degradation of cyclin B as a marker of mitotic exit. (**B**) Asynchronously growing FUCCI indicator expressing U2OS cells were pretreated with Hoechst DNA dye and the following populations of cells were sorted: double-negative (DN) and single RFP-positive cells (RNF+); single GFP-positive cells (GFP+); double-positive (DP) cells and samples were analyzed by flow cytometry. Note that the DN/RFP+ population corresponds to cells with a low DNA content (G_1 phase), whereas GFP+ population corresponds to 4 n cells (G_2 phase) and DP show intermediate DNA content (S phase). (**C**) Populations of cells from (**B**) analyzed by immunoblotting. Cyclin D was used as a marker of G_1, cyclin A and Plk1 as markers of G_2. (**D**) U2OS and RPE cells were cotransfected by Wip1 shRNA plasmid (shWip1) together with a mCherry marker and probed with polyclonal Wip1 (sc20712) or monoclonal Wip1 (sc37625) antibodies and with DAPI. Neighboring untransfected cells were used as a control (mock). Shown is quantification of immunofluorescence staining in interphase and mitotic cells. Note higher Wip1 signal intensity in cells with higher DAPI corresponding to G_2 cells and decreased Wip1 signal in mitotic cells. As additional control of signal specificity, cells were treated with Etoposide (2.5 μM for 16 h), which caused accumulation of G_2 cells with high intensity of Wip1. (**E**) Asynchronously growing U2OS cells were fixed and probed with indicated antibodies and DAPI. Note decreased Wip1 signal in mitosis and absence of the signal on mitotic chromatin.

the thymidine block to a media supplemented with nocodazole and added a proteasomal inhibitor MG132 for the last 4 h. Interestingly, treatment with MG132 completely prevented the mitosis-associated decrease of Wip1, suggesting that Wip1 is normally degraded by the proteasome upon entry into mitosis (**Fig. 2A**). Similarly, microscopic analysis of mitotic cells revealed that the intensity of the Wip1 staining increased after a short treatment with MG132 (**Fig. 2B**). Finally, we wished to exclude the possibility that the low abundance of Wip1 in mitosis is caused by the absence of Wip1 mRNA. We synchronized cells in late G_2 phase by treatment with a selective Cdk1-inhibitor Ro-3306 and released them into media with or without nocodazole for 3 h to obtain mitotic and G_1 cells, respectively.[38] Similarly to the above experiments with the thymidine block/release synchronization, we noticed that protein levels of Wip1 declined in mitosis (**Fig. 2C**). Importantly, both samples analyzed in parallel showed similar levels of Wip1 mRNA, suggesting that Wip1 abundance during mitosis is not regulated at the level of mRNA (**Fig. 2C**).

Next, we aimed to identify the mechanism of Wip1 degradation in mitosis. Given similar kinetics of cyclin A and Wip1 loss during prometaphase (**Fig. 1A and E**), we argued that Wip1 might be degraded upon ubiquitylation by either SCF or APC/C^{cdc20} E3 ubiquitin ligase complexes, both of which are active in early mitosis.[39] First, we depleted cells of an essential SCF complex component Cul1 and F-box proteins βTrCP1/2 or Fbw7 using siRNA and assayed the protein level of Wip1 in cells synchronized at G_1/S transition or in mitosis (**Fig. 2D**; **Fig. S3**). As expected, depletion of Cul1 or Fbw7 caused stabilization of the SCF^{Fbw7} substrate cyclin E.[40] Similarly, depletion of Cul1 or βTrCP1/2 led to stabilization of hBora protein during mitosis.[41] Although we were able to efficiently deplete all indicated proteins, we did not observe any significant changes in levels of Wip1, either in interphase or in mitosis, suggesting that stability of Wip1 is not regulated by the SCF complex. Next, we depleted the APC/C activator cdc20 by RNAi and assayed the protein level of Wip1 in mitotic cells (**Fig. 2E**; **Fig. S3**). As expected, efficient depletion of cdc20 enriched the population of mitotic cells and led to stabilization of cyclin $A^{42\text{-}44}$ (**Fig. 2E**). Importantly, depletion of cdc20 resulted in stabilization of Wip1 protein to levels comparable to those observed in interphase cells (**Fig. 2E**). From these results we conclude that proteasomal degradation of Wip1 in mitosis is controlled by the APC/C^{cdc20} complex.

Catalytic domain of Wip1 is phosphorylated at multiple sites in mitosis. Apart from the decreased protein level of endogenous Wip1, we noticed that an additional slower migrating band recognized by antibodies to Wip1 appeared in mitotic cell extracts, indicative of a possible post-translational modification. Indeed, Wip1-FLAG purified from mitotic cells showed a similar mobility shift that disappeared after treatment with lambda phosphatase, suggesting that Wip1 is phosphorylated during mitosis (**Fig. 3A**). To better characterize the timing of the Wip1 phosphorylation during the cell cycle, we synchronized cells expressing a phosphatase-dead Wip1-D314A-FLAG fusion protein in G_2 by adriamycine treatment and followed the occurrence of the slower migrating band corresponding to phosphorylated Wip1 during the progression to mitosis. Interestingly, behavior of Wip1 closely mimicked that of an established mitotic marker cdc27 (**Fig. 3B**). Consistently, neither Wip1 nor cdc27 showed a mobility shift when mitotic entry was prevented by exposure of cells to the CDK inhibitor roscovitine, suggesting that phosphorylation of Wip1 occurs in mitosis (**Fig. 3B**). In addition, the mobility shift of Wip1-D314A-FLAG rapidly disappeared when cells were released from nocodazole arrest and exited mitosis, further supporting the notion that such phosphorylation of Wip1 is restricted to mitosis (**Fig. 3C**). To get insight into protein kinases responsible for modification of Wip1 during mitosis, we treated nocodazole-arrested cells expressing Wip1-FLAG with roscovitine or an MAPK inhibitor SB202190 and assayed the mobility of Wip1 separated on a PhosTag gel.[45] Whereas mitotic Wip1 migrates as three separate bands under these conditions, the band showing the slowest mobility disappeared upon treatment of cells with roscovitine (but not with the MAPK inhibitor), suggesting that Wip1 might be phosphorylated by Cdk1 during mitosis (**Fig. 3D**). Consistent with this possibility, we observed no mobility shift in cells arrested in late G_2 by exposure to the Cdk1 selective inhibitor Ro-3306 (data not shown). Moreover, bacterially expressed His-Wip1 was a good substrate for the Cdk1/cyclin B kinase in vitro (**Fig. 3E**).

To identify the mitotically phosphorylated residues of Wip1, we purified a phosphatase-dead Wip1-D314A-FLAG from nocodazole-arrested cells and analyzed post-translational modifications by mass spectrometry. This analysis revealed seven phosphorylation sites within the catalytic domain of Wip1 and an additional six modified residues in the C-terminal domain (**Fig. 3F**). Bioinformatic analysis of short linear motifs in the primary sequence of Wip1 revealed Ser40 as the only putative phosphorylation site by Cdk1.[46] Indeed, mutagenesis of Ser40 to alanine almost completely blocked the phosphorylation of Wip1

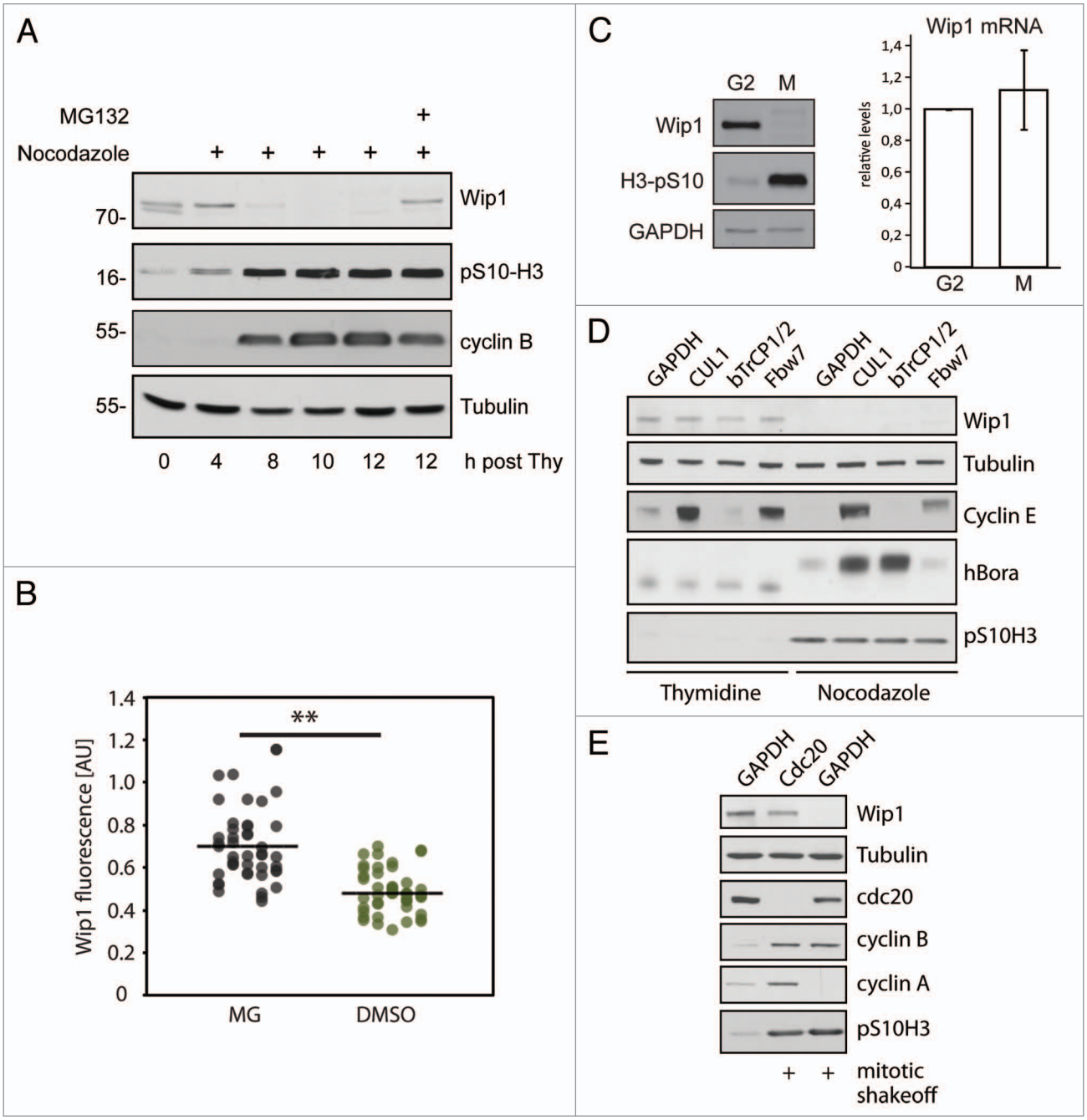

Figure 2. Degradation of Wip1 during mitosis. (**A**) U2OS cells were synchronized by a double thymidine block, released into media with NZ and after 8 h, treated or not with 5 μM MG132. (**B**) Asynchronously growing cells were treated for 60 min with 5 μM RO-3306 to release cells from mitosis and prevent new cells from entering. Subsequently, cells were treated for 60 min with MG132 (5 μM) or DMSO, fixed, stained for Wip1 and the signal was quantified. Each dot corresponds to one cell. The dashed lines indicate the respective mean values. The difference between the means was analyzed by Student's t-test (** $p < 0.01$). (**C**) Cells were synchronized in late G_2 by Ro-3306 and released into fresh media with NZ for 2 h. Mitotic cells were collected by shake-off and analyzed by immunoblotting (left) or qPCR (right). (**D**) Cells were transfected with siRNAs targeting indicated proteins. One-third of the cells were synchronized for last 24 h with thymidine, and adherent cells were collected. One-third of the cells were treated with NZ for the last 12 h and collected by mitotic shake-off. Cell extracts were collected at 48 h after transfection and probed with indicated antibodies. RNA was extracted from the last part of cells and analyzed by qPCR (**Fig. S3**). (**E**) Cells were transfected with siRNAs targeting cdc20 or GAPDH (negative control). Mitotic cells were collected by shake-off 24 h after transfection and probed with indicated antibodies.

by Cdk1 in vitro, suggesting that Ser40 is the major phosphorylation site of Cdk1 (**Fig. 3G**). In addition, Wip1-S40A mutant protein ectopically expressed in mitotic cells showed increased gel mobility compared with wild-type Wip1, confirming that Ser40 is phosphorylated also in vivo (**Fig. 3H**). However, the observed partial impact of mutating Ser40 on the overall mobility shift in

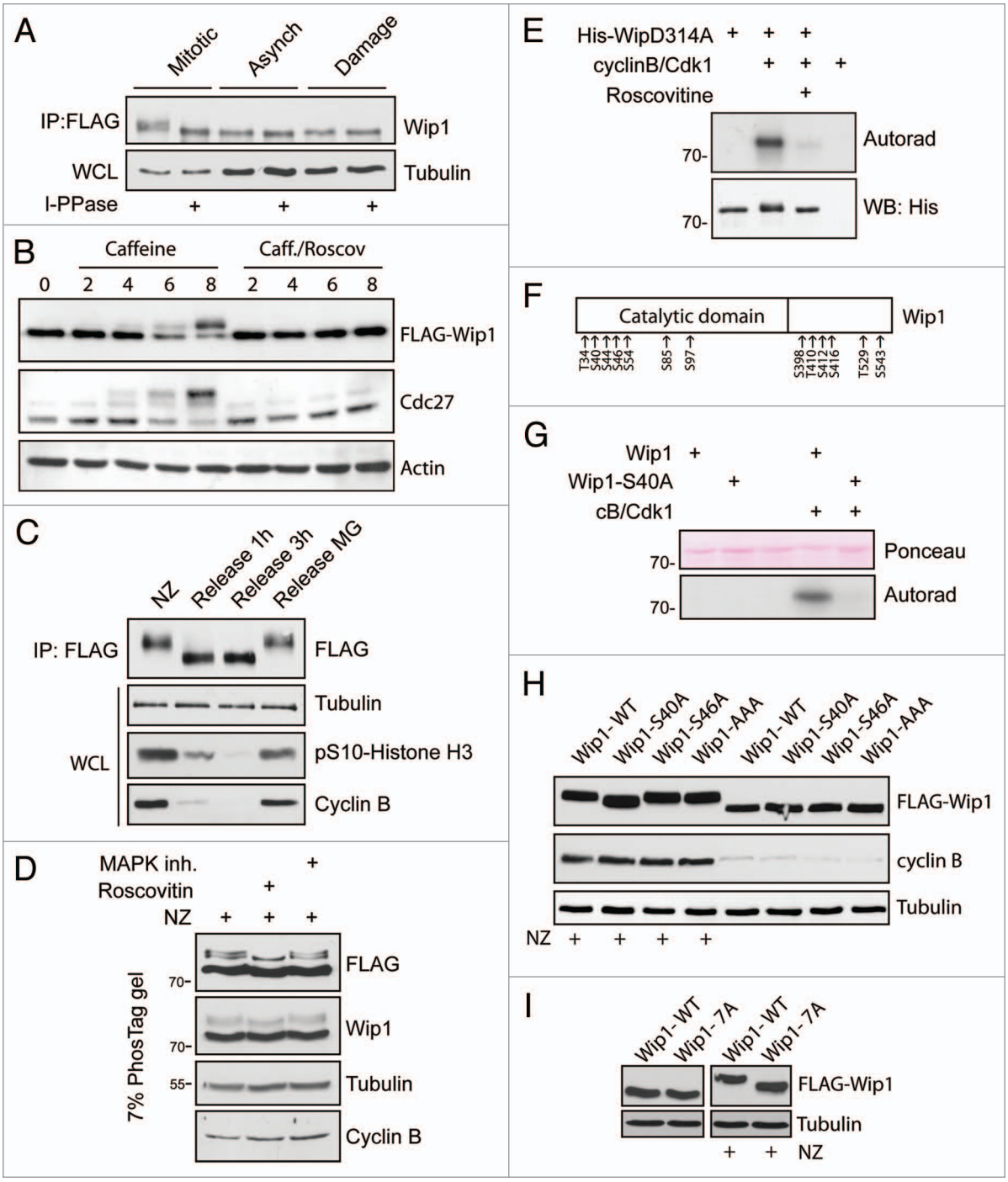

Figure 3. Wip1 is extensively phosphorylated in mitosis. (**A**) Expression of Wip1-FLAG was induced by tetracycline and Wip1-FLAG was immunoprecipitated from asynchronously growing cells (Asynch.), from mitotic cells arrested in NZ and collected by shake-off (Mitotic) or from cells treated with 0.5 μM adriamycine (Damage). Half of the immunopurified material was subjected to treatment with lambda phosphatase. (**B**) Cells expressing Wip1-D314A-FLAG were arrested in G_2 by treatment with adriamycine and forced to enter mitosis by treatment with caffeine. Alternatively, roscovitine was added to prevent mitotic entry. (**C**) Cells expressing Wip1-D314A-FLAG were arrested in mitosis by treatment with NZ and released into fresh media for indicated time. Alternatively, mitotic exit was blocked by addition of MG132. (**D**) Cells expressing Wip1-FLAG were arrested in mitosis by NZ and treated with DMSO, roscovitine (12 μM) or p38i (3 μM, SB202190) for 90 min. Cell lysates were separated on Phostag SDS-PAGE and probed with indicated antibodies. (**E**) Phosphatase dead His-Wip1-D314A was subjected to in vitro kinase assay with Cdk1/cyclin B, separated on SDS-PAGE and phosphorylation was detected by autoradiography. (**F**) Wip1-D314A-FLAG was purified from mitotic cells and analyzed by MS. Scheme of identified phosphorylated residues is shown. (**G**) His-Wip1 or His-Wip1-S40A was subjected to in vitro kinase assay with Cdk1/cyclin B, separated on SDS-PAGE and phosphorylation was detected by autoradiography. (**H**) Cells expressing Wip1-FLAG, Wip1-S40A, Wip1-S46A or Wip1-AAA were synchronized in mitosis by NZ or grown asynchronously. Note a partial loss of mobility shift in the S40A mutant purified from mitotic cells. (**I**) Cells expressing Wip1-WT or Wip1–7A were grown asynchronously or arrested in mitosis by addition of nocodazole for 12 h and probed with indicated antibodies. Note decreased mobility shift of Wip1–7A in mitotic cells.

Wip1-S40A indicates that other phosphosites also exist on mitotic Wip1 (**Fig. 3H**). Interestingly, mutagenesis of residues Thr410, Ser412 and Thr416 (identified as phosphosites by MS) to alanine did not affect the mobility of such Wip1-AAA protein in mitosis, suggesting that the extent of modification of these sites might be low, or such phosphorylations do not significantly affect Wip1 gel mobility (**Fig. 3H**). In contrast, Wip1–7A mutant, in which all seven identified phosphorylated residues within the catalytic domain were mutated to alanine, showed a strongly reduced mobility shift in mitosis, suggesting that these residues are phosphorylated in mitosis (**Fig. 3I**). Since Cdk1 phosphorylated only one of these seven phosphosites that we identified within the catalytic domain of Wip1, additional mitotic kinases likely also modify Wip1 during mitosis.

Loss of Wip1 activity coincides with the positivity of γH2AX during mitosis. Since we observed a decreased protein level of Wip1 in mitotic cells, we argued that also total enzymatic activity of Wip1 should be reduced during mitosis. To test this prediction, we established an assay for measuring the activity of endogenous Wip1 and indeed we found that the global Wip1 activity was decreased in mitotic cells (**Fig. 4A**; **Fig. S4**). DDR kinases have recently been reported to support genome integrity by responding to and phosphorylating proteins at underreplicated DNA regions during unperturbed mitosis.[10,11] According to this model, DNA lesions may accumulate in underreplicated DNA regions (such as chromosomal fragile sites) due to the mechanical forces acting during chromosome condensation or sister chromatid segregation.[10] These regions are marked by γH2AX during mitosis, followed by 53BP1 binding early in the G_1 and protected throughout G_1 until repair occurs in the following S phase.[10,11] We and others have previously demonstrated that Wip1 dephosphorylates γH2AX during checkpoint recovery in interphase cells, thereby contributing to silencing of the DDR after successful DNA repair.[19-21,47] We hypothesized that removal of Wip1 during mitosis may contribute to the activation and impact of ATM and to the formation of γH2AX foci in mitotic cells. In good agreement with published data, we observed that mitotic cells are positive for γH2AX foci (**Fig. 4B**).[10,48,49] Reduction of the number of mitotic γH2AX foci in the presence of selective ATM[50] and DNA-PK[51] (but not ATR[52]) inhibitors suggests that both ATM and DNA-PK contribute to sensing of DNA damage in mitosis (**Fig. S5**). Importantly, overexpression of ectopic Wip1-WT impaired formation of γH2AX foci in mitotic cells (**Fig. 4B**). Similarly, automated microscopic analysis revealed that expression of Wip1 (but not of a phosphatase dead Wip1-D314A) interfered with formation of 53BP1 nuclear bodies in G_1 cells (**Fig. 4C**).

Furthermore, since we observed extensive mitotic phosphorylation of Wip1, we asked whether such modification might also contribute to the regulation of Wip1 enzymatic activity. Analysis of the activity of the modified Wip1-WT proved to be technically challenging, since immunopurified Wip1-WT showed a largely decreased mobility shift compared with Wip1-D314A, indicating that there is a considerable level of auto-dephosphorylation of overexpressed Wip1-WT during mitosis. Nevertheless, we observed a slightly decreased enzymatic activity of Wip1-WT purified from mitotic cells compared with that isolated from asynchronously growing cells (**Fig. S6A**). Next we investigated the enzymatic activity of Wip1 mutants. Whereas, there were no significant differences in the activities of Wip1-WT, Wip1-S40D and Wip1–7A, the activity of the phospho-mimicking mutant Wip1–7D was severely impaired (**Fig. 4D**; **Fig. S6B**). In agreement with the differential enzymatic activity determined in vitro, induced expression of Wip1-WT or Wip1–7A (but not Wip1–7D) reduced the number of 53BP1 nuclear bodies in G_1 cells (**Fig. 4E**). In addition, Wip1-WT and Wip1–7A (but not Wip1–7D) impaired phosphorylation of the p53 tumor suppressor on Ser15 and γH2AX, both targets of the apical DDR kinases ATM and ATR, after exposure of cells to adriamycine (**Fig. 4F**). From these experiments, we conclude that modification of a single Ser40 residue by Cdk1 during mitosis is not sufficient for inhibition of Wip1 activity but extensive modification of multiple residues within the catalytic domain impairs the activity of Wip1.

Overall, our data indicate that the observed decreased activity of Wip1 phosphatase during mitosis is ensured by coordinated complex phosphorylations of the Wip1 catalytic domain and decreased abundance of Wip1 protein due to enhanced proteolytic turnover.

Discussion

Whereas the roles of Wip1 in termination of signaling and in control of the recovery competence in response to genotoxic insults are well-established,[22,25,53,54] molecular mechanisms that regulate Wip1 have remained largely unexplored. In this study, we investigated how human Wip1 phosphatase is regulated during the cell cycle. Here, we report that protein abundance of Wip1 increases from G_1 to G_2 and then rapidly declines in mitosis. The observation of differential expression of Wip1 during interphase was facilitated by development of models and techniques that allow analysis of live asynchronously growing cells, thus avoiding the need for cellular synchronization involving the treatment of cells with stress-inducing drugs (such as thymidine). These novel approaches include sorting of cells engineered to express fluorescent markers of the cell cycle progression and microscopic analysis of cells using intensity of the DAPI signal as the readout of the DNA content. Identification of higher levels of Wip1 in G_2 compared with G_1, reported here, is consistent with the fact that a complete loss of Wip1 in knockout mice resulted in an increase in the population of G_2 cells.[55,56] Wip1-knockout animals are viable, indicating that Wip1 is not essential for cell division.[56] Similarly, RNAi-mediated depletion of Wip1 in tissue culture cells caused a transient delay in G_2/M transition, but eventually all cells enter mitosis.[25] Thus, Wip1 is not absolutely required for mitotic entry but might be involved in a tight control of the timing of the G_2/M transition. Since expression of Wip1 is induced by various forms of genotoxic stress, it is plausible that higher levels of Wip1 observed in G_2 may reflect the endogenous stress emanating from the unresolved replication intermediates of genomic DNA.[57] In turn, increased expression of Wip1 in G_2 may timely counteract the ATR/Chk1 and ATM/Chk2 signaling modules that respond to replication stress and DNA breakage. In this way, the

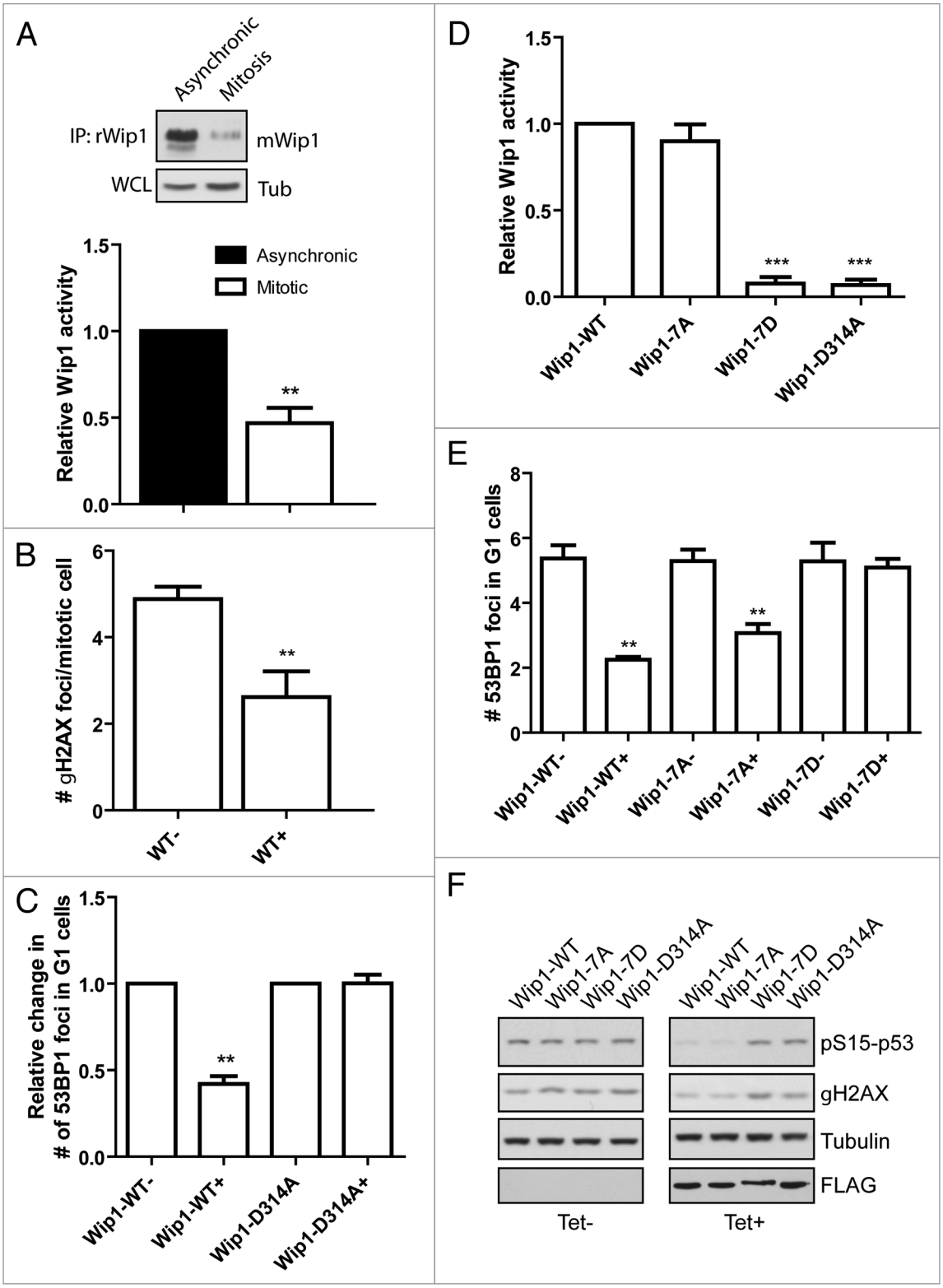

Figure 4. For figure legend, see page 9.

G_2-associted elevation of Wip1 may facilitate cell cycle progression from G_2 phase into mitosis.

In contrast to high levels in G_2, abundance of Wip1 is dramatically decreased in early phases of mitosis. We have observed similar results using two antibodies recognizing distinct regions on Wip1 and ectopically expressed fluorescence-labeled Wip1, thereby excluding the possibility of epitope masking during mitosis. Given that the proteasomal inhibitor MG132 stabilized

Figure 4. Activity of Wip1 is decreased in mitosis. (**A**) Endogenous Wip1 was immunoprecipitated using rabbit anti-Wip1 (H300) from asynchronously growing or NZ-arrested cells and phosphatase activity was measured in vitro. (**B**) Expression of Wip1-WT was induced or not by tetracycline in asynchronously growing cells. Number of γH2AX positive foci was determined by a manual evaluation of immunofluorescence staining in 70 mitotic cells (n = 3, error bars indicate, ** $p < 0.01$). (**C**) Expression of Wip1 or Wip1-D314A was induced (+) or not (-) by tetracycline and cells were probed for 53BP1. Number of 53BP1 positive nuclear bodies in G_1 cells was determined by automated microscopy in 1000 cells (n = 3, error bars indicate SD, ** $p < 0.01$). (**D**) Expression of Wip1-WT, Wip1–7A, Wip1–7D and Wip1-D314A was induced by tetracycline, FLAG-tagged proteins were immunoprecipitated and the phosphatase activity was determined in vitro (n = 3, error bars indicate SD, ** $p < 0.01$). (**E**) Expression of Wip1-WT, Wip1–7A, Wip1–7D and Wip1-D314A was induced (+) or not (-) by tetracycline and number of 53BP1 nuclear bodies was determined by automated microscopy. Intensity of DAPI signal was used for gating of G_1 cells (n = 3, error bars indicate SD, ** $p < 0.01$). (**F**) Expression of Wip1-WT, Wip1–7A, Wip1–7D and Wip1-D314A was induced (+) or not (-) by tetracycline; cells were treated with 0.5 μM adriamycine for 4 h, and whole-cell lysates were probed for pSer15p53 and γH2AX.

the mitotic Wip1 protein, and that no changes of Wip1 mRNA levels were detected throughout the cell cycle, we suggest that Wip1 is proteolytically degraded in mitosis. Whereas the degradation of Wip1 was apparently independent of SCF, depletion of the cdc20 caused stabilization of Wip1 in mitotic cells, indicating that Wip1 protein levels are controlled by the APC/C^{cdc20} E3 ligase complex.

Induction of Wip1 expression using a tetracycline inducible system allowed us to investigate the phenotype of mitotic cells containing high levels of active Wip1 phosphatase. Since Wip1 can counteract the activity of ATM in response to DNA damage, and since ATM has recently been implicated in control of mitotic progression,[58] we tested the effect of Wip1 expression during mitosis. Although induction of Wip1-WT expression resulted in increased Wip1 activity in mitotic cells, we did not observe any major differences in the timing of mitotic progression, architecture of the mitotic spindle and cytokinesis (data not shown). In contrast, we observed that forced expression of Wip1-WT led to a dramatic decrease in the number of γH2AX foci in mitotic cells and also to a reduction of 53BP1 nuclear bodies in G_1 cells. Since DNA lesions cannot be repaired during mitosis, it is essential to mark these regions by γH2AX to allow repair in the following cell cycle. Moreover, due to the lacking ubiquitination of mitotic chromatin, 53BP1 cannot bind to DNA lesions until cells exit from mitosis and enter the next G_1.[12,13] Thus, γH2AX appears to be an essential marker of endogenous DNA lesions present in unperturbed mitosis. Previously, we have shown that Wip1 associates with the chromatin and dephosphorylates γH2AX. Thus, it is likely that Wip1 activity needs to be eliminated from mitotic cells to allow formation of γH2AX foci at mitotic chromatin. Removing the phosphatase that has the ability to counteract the activity of ATM may allow cells to adequately respond to low levels of DNA damage present in unperturbed mitosis. Apart from the degradation of Wip1 during mitosis, we have also observed extensive phosphorylation of the catalytic domain of Wip1. Importantly, whereas the nonphosphorylatable Wip1–7A mutant protein showed normal enzymatic activity, the phosphomimicking Wip-7D mutant was enzymatically inactive. Therefore, we propose that cells efficiently reduce the net activity of Wip1 during mitosis through a combination of proteasomal degradation and phosphorylation-mediated inhibition of its enzymatic activity. After 53BP1 nuclear bodies form around and protect the DNA lesions in the following G_1, Wip1 expression can increase again. In summary, we have shown here that protein abundance of Wip1 is not constant during the cell cycle but increases from G_1 to G_2, and then declines during mitosis. Degradation of Wip1 and inhibition of Wip1 enzymatic activity by extensive post-translational modifications at multiple residues within the catalytic domain of Wip1 in mitosis, allow more sensitive DNA damage signaling during mitosis, including appearance of γH2AX foci at mitotic chromatin. Such cell cycle-regulated modulation of the DDR signaling threshold through changes in Wip1 abundance and activity seem to facilitate formation of the 53BP1 nuclear (OPT) bodies[10,11] in the subsequent G_1 phase, thereby contributing to the ability of mammalian cells to adequately deal with consequences of replication stress and, indeed, to the global maintenance of genome integrity.

Materials and Methods

Antibodies and reagents. The following antibodies were used in this study: rabbit Wip1 (H300; sc20712), mouse Wip1 (clone F-10; sc37625), p53 (sc-6243), cyclin A (sc-53230), cdc20 (sc-8358) and 53BP1 (sc-22760; Santa Cruz Biotechnology); Wip1/PPM1D (A300–664A, Bethyl Laboratories), pSer15p53 (#9284S), β-TrCP (#4394), cyclin B1 (V152; #4135), γH2AX (#2577; Cell Signaling Technology); α-tubulin (T5168) and FLAG (F1804; Sigma Aldrich); Cyclin B (ab7957; Abcam); pSer10-H3 (06–570; Millipore-Upstate); GAPDH (GTX30666; GeneTex); cdc27 (#610454, BD Transduction Laboratories), Alexa Fluor fluorescently labeled secondary antibodies were from Life Technologies. Lambda phosphatase was from New England Biolabs. PhosTag acrylamide was from Wako Pure Chemical Industries (AAL-107).

Plasmids. pRS-Wip1 construct targeting GGA TGA CTT TGT CAG AGC T of the human Wip1, FLAG tagged pcdna4/TO-Wip1-WT, pcdna4/TO-Wip1-D314A and pWip1-mCherry were described previously.[19,25] Mutagenesis was performed using QuickChange II site-directed mutagenesis kit (Agilent Technologies), and fragments encoding Wip1-S40A, S40D, T410A-S412A-S416A (Wip1-AAA), S97A, S97D were inserted into pcdna4/TO (Life Technologies) or pQE81L (Qiagen). Mutants Wip1–7A (containing T34/S40/S44/S46/S54/S85/S97A) and Wip1–7D (containing T34/S40/S44/S46/S54/S85/S97D) were generated by GenArt Synthesis (Life Technologies), and fragments were inserted into pcdna4/TO. pFucci-S/G_2/M-Green and pFucci-G_1 orange plasmids expressing hGeminin (1–110) and hCdt1 (30–120) fragments fused with fluorescent reporters are based on published fluorescent ubiquitination-based cell cycle indicator (FUCCI) and were from MBL International.[36]

Cell lines. Human HeLa, MCF7 and U2OS cell lines were cultured in Dulbecco's modified Eagle's medium (DMEM)

under standard conditions as described.[59] Human hTERT-immortalized retinal pigment epithelial cells (RPE) were grown in DMEM supplemented with nutrient mixture F-12 (DMEM/F12). Cells expressing Wip1, or its point mutants, under control of tetracycline-inducible promoter were generated as described[25] and routinely grown in media containing Tet system-approved serum.[25] Enhanced expression was induced by addition of tetracycline (1 μg/ml) for 12 h. Monoclonal cell line stably expressing FUCCI indicator was generated by transfection of U2OS cells followed by hygromycine/neomycine selection and two steps of clonal selection using limited dilution on a 96-well plate. Live cells positive for GFP (corresponding to G_2 cells) or double-negative cells (DN) and RFP-positive cells (corresponding to G_1 cells) were sorted using Influx cell sorter (BD Biosciences) and lysed for biochemical analysis. In parallel, cells pre-incubated with a cell permeable dye Hoechst 33342 as a DNA marker were analyzed by flow cytometry.

Cell synchronization. Cells were synchronized at G_1/S transition using a double thymidine (2.5 mM) block (12 h-Thy/8 h-release/12 h-Thy), washed in PBS and released into fresh media supplemented with nocodazole to arrest cells in mitosis (most cells entered M after 10–12 h). Cells were collected in 2-h intervals. Mitotic cells were collected by shake-off. Alternatively, cells were synchronized at late G_2 using Ro-3306 (9 μM for 20 h; Tocris Bioscience) and released into fresh media (most cells entered M after 1–2 h). Where indicated, MG132 (5 μM, Sigma) was added to media to block proteasomal degradation.

Immunofluorescence and live-cell imaging. Cells were grown in 96-well imaging plates (BD Biosciences) and immunofluorescence was performed as described.[60] For each image, the background signal of an area without cells was subtracted. Nuclei were identified based on DAPI staining before measurement of nuclear Wip1 staining. Images were acquired on a DeltaVision Spectris imaging system equipped with a 20× objective, NA 0.7 (Applied Precision). For automated microscopic analysis of 53BP1 or γH2AX-positive foci, cells were cultured on glass coverslips, fixed using 4% formaldehyde (10 min at RT), permeabilized by ice-cold methanol, blocked with 3% BSA in PBS supplemented with 0.1% Tween-20 (PBST) and incubated with the primary 53BP1 or γH2AX antibodies for 1 h at RT. After washing with PBST, coverslips were incubated with AlexaFluor-conjugated secondary antibodies for 1 h at RT. DNA was stained with DAPI (Sigma) for 2 min and coverslips were mounted using Vectashield reagent (Vector Laboratories). Automated image acquisition was done using Scan^R high-content screening station equipped with a motorized stage and 40× objective (Olympus). Nuclei were identified based on the DAPI signal and the median number of 53BP1 or γH2AX foci was determined using a spot detection module. Mitotic cells were gated based on higher DAPI intensity of condensed chromatin with manual correction for false-positive events. At least 1,000 nuclei for interphase cells and at least 100 mitotic cells were counted per condition in three independent experiments. For live-cell imaging cells expressing FUCCI, indicator were grown in LabTek II chamber slides in CO_2-independent L15 media (Gibco) and imaged at 30 min intervals using Leica DMI6000 inverted microscope.

Transfection. U2OS cells were transfected with plasmid DNA using a standard calcium phosphate method. Silencer Select siRNAs targeting Cul1 (GGC UUG UGG UCG CUU CAU), βTrCP1 (GAA CUA UAA AGG UAU GGA A), βTrCP2 (GGU UGU UAG UGG AUC AUC A), Fbx7 (GGG UUG UUA GUG GAG CAU A) and cdc20 (CGA AAU GAC UAU UAC CUG A) were obtained from Ambion (Life Technologies) and were transfected at 5 nM concentration using RNAiMAX (Life Technologies) and collected at indicated times post-transfection.

In vitro phosphatase assay. Cells were induced by tetracycline to express FLAG-tagged Wip1-Wt or its point mutants, extracted by EBC buffer (50 mM Tris pH 7.5, 150 mM NaCl, 0.5% NP-40, 1 mM EGTA) and subsequent sonication (3 × 10 sec, amplitude 7, 100W) and extracts were spinned down (16.000 g, 10 min, 4°C) and normalized for protein concentration. FLAG-tagged proteins were immunopurified from tetracycline-induced cells with anti-FLAG agarose (Sigma). Alternatively, endogenous Wip1 was immunoprecipitated using a polyclonal anti-Wip1 antibody (H300, 2 μg/reaction) and 30 μl protein A/G Ultra link resin (Thermo Scientific). Phosphatase assay was performed using synthetic phosphopeptide, corresponding to pSer15p53 (100 μM, GeneScript) and Biomol Green reagent (Enzo Life Sciences) as described.[19] Statistical analysis was performed using Student's t-test in GraphPad Prism software.

In vitro kinase assay. *E. coli*-(BL21) transformed with pQE81L-Wip1-D314A or its point mutants were induced with 0.5 mM IPTG for 4 h at 37°C and His-tagged Wip1 was purified using Ni-NTA agarose (Qiagen). His-Wip1 (2 mg) was mixed with 50 ng of active protein kinases Cdk1/cyclin B (Sigma) in kinase buffer (25 mM MOPS pH 7.2, 12.5 mM glycerol 2-phosphate, 25 mM $MgCl_2$, 5 mM EGTA, 2 mM EDTA and 0.25 mM DTT) supplemented with 100 μM ATP and 5 μCi ^{32}P-γ-ATP and a sample was incubated for 20 min at 30°C. Proteins were separated using SDS-PAGE as described,[61] and phosphorylation was detected by autoradiography.

Quantitative real-time PCR (qPCR). Total RNA samples were isolated using the TRI Reagent (Sigma) according to the manufacturer's protocol. First-strand cDNA was synthesized from 200 ng of total RNA with random hexamer primers using TaqMan Reverse Transcription Reagents (Applied Biosystems). qRT-PCR was performed in ABI Prism 7300 (Applied Biosystems) using SYBR Green I Master Mix with the following set of primers: Wip1 (GGG AGT GAT GGA CTT TGG AA and CAA GAT TGT CCA TGC TCA CC), tubulin (GAG TGC ATC TCC ATC CAC GTT and TAG AGC TCC CAG CAG GCA TT). The relative quantity of cDNA was estimated by ΔΔCt, and data were normalized to tubulin. Samples were measured in triplicate in three independent experiments.

Mass spectrometry. Phosphatase dead FLAG-Wip1-D314A was immunoprecipitated from mitotic cells obtained by mitotic shake-off of nocodazole-arrested cells. The sample was separated on SDS-PAGE, stained by CBB and a slice of the gel corresponding to the Wip1 was digested by trypsin or V8 protease and peptides were subjected to MS. Peptide mass was analyzed using Mascot software (Matrix Science). Combined sequence coverage was 82%.

Disclosure of Potential Conflicts of Interest

No potential conflicts of interest were disclosed.

Acknowledgments

We are thankful to Dr. Stanek (IMG) for making the Scan^R imaging station available and all members of our laboratories for helpful discussions. This work was supported by the Grant Agency of the Czech Republic (projects P305/10/P420 and P301/10/1525), the Netherlands Genomic Initiative of NWO (CGC), the Danish Cancer Society and the European Commission (project DDResponse). A.L. was supported by Swedish cancer foundation and Swedish childhood cancer foundation.

Supplemental Materials

Supplemental materials may be found here:
www.landesbioscience.com/journals/cc/article/23057/

References

1. Shiloh Y. ATM and related protein kinases: safeguarding genome integrity. Nat Rev Cancer 2003; 3:155-68; PMID:12612651; http://dx.doi.org/10.1038/nrc1011.
2. Lukas J, Lukas C, Bartek J. More than just a focus: The chromatin response to DNA damage and its role in genome integrity maintenance. Nat Cell Biol 2011; 13:1161-9; PMID:21968989; http://dx.doi.org/10.1038/ncb2344.
3. Stucki M, Clapperton JA, Mohammad D, Yaffe MB, Smerdon SJ, Jackson SP. MDC1 directly binds phosphorylated histone H2AX to regulate cellular responses to DNA double-strand breaks. Cell 2005; 123:1213-26; PMID:16377563; http://dx.doi.org/10.1016/j.cell.2005.09.038.
4. Huen MSY, Grant R, Manke I, Minn K, Yu X, Yaffe MB, et al. RNF8 transduces the DNA-damage signal via histone ubiquitylation and checkpoint protein assembly. Cell 2007; 131:901-14; PMID:18001825; http://dx.doi.org/10.1016/j.cell.2007.09.041.
5. Mailand N, Bekker-Jensen S, Faustrup H, Melander F, Bartek J, Lukas C, et al. RNF8 ubiquitylates histones at DNA double-strand breaks and promotes assembly of repair proteins. Cell 2007; 131:887-900; PMID:18001824; http://dx.doi.org/10.1016/j.cell.2007.09.040.
6. Doil C, Mailand N, Bekker-Jensen S, Menard P, Larsen DH, Pepperkok R, et al. RNF168 binds and amplifies ubiquitin conjugates on damaged chromosomes to allow accumulation of repair proteins. Cell 2009; 136:435-46; PMID:19203579; http://dx.doi.org/10.1016/j.cell.2008.12.041.
7. Bekker-Jensen S, Rendtlew Danielsen J, Fugger K, Gromova I, Nerstedt A, Lukas C, et al. HERC2 coordinates ubiquitin-dependent assembly of DNA repair factors on damaged chromosomes. Nat Cell Biol 2010; 12:80-6, 1-12; PMID:20023648; http://dx.doi.org/10.1038/ncb2008.
8. Moudry P, Lukas C, Macurek L, Hanzlikova H, Hodny Z, Lukas J, et al. Ubiquitin-activating enzyme UBA1 is required for cellular response to DNA damage. Cell Cycle 2012; 11:1573-82; PMID:22456334; http://dx.doi.org/10.4161/cc.19978.
9. Chapman JR, Taylor MR, Boulton SJ. Playing the end game: DNA double-strand break repair pathway choice. Mol Cell 2012; 47:497-510; PMID:22920291; http://dx.doi.org/10.1016/j.molcel.2012.07.029.
10. Lukas C, Savic V, Bekker-Jensen S, Doil C, Neumann B, Pedersen RS, et al. 53BP1 nuclear bodies form around DNA lesions generated by mitotic transmission of chromosomes under replication stress. Nat Cell Biol 2011; 13:243-53; PMID:21317883; http://dx.doi.org/10.1038/ncb2201.
11. Harrigan JA, Belotserkovskaya R, Coates J, Dimitrova DS, Polo SE, Bradshaw CR, et al. Replication stress induces 53BP1-containing OPT domains in G1 cells. J Cell Biol 2011; 193:97-108; PMID:21444690; http://dx.doi.org/10.1083/jcb.201011083.
12. Giunta S, Belotserkovskaya R, Jackson SP. DNA damage signaling in response to double-strand breaks during mitosis. J Cell Biol 2010; 190:197-207; PMID:20660628; http://dx.doi.org/10.1083/jcb.200911156.
13. Giunta S, Jackson SP. Give me a break, but not in mitosis: the mitotic DNA damage response marks DNA double-strand breaks with early signaling events. Cell Cycle 2011; 10:1215-21; PMID:21412056; http://dx.doi.org/10.4161/cc.10.8.15334.
14. Harris DR, Bunz F. Protein phosphatases and the dynamics of the DNA damage response. Cell Cycle 2010; 9:861-9; PMID:20348842; http://dx.doi.org/10.4161/cc.9.5.10862.
15. Shreeram S, Demidov ON, Hee WK, Yamaguchi H, Onishi N, Kek C, et al. Wip1 phosphatase modulates ATM-dependent signaling pathways. Mol Cell 2006; 23:757-64; PMID:16949371; http://dx.doi.org/10.1016/j.molcel.2006.07.010.
16. Fujimoto H, Onishi N, Kato N, Takekawa M, Xu XZ, Kosugi A, et al. Regulation of the antioncogenic Chk2 kinase by the oncogenic Wip1 phosphatase. Cell Death Differ 2006; 13:1170-80; PMID:16311512; http://dx.doi.org/10.1038/sj.cdd.4401801.
17. Lu X, Ma O, Nguyen T-A, Jones SN, Oren M, Donehower LA. The Wip1 Phosphatase acts as a gatekeeper in the p53-Mdm2 autoregulatory loop. Cancer Cell 2007; 12:342-54; PMID:17936559; http://dx.doi.org/10.1016/j.ccr.2007.08.033.
18. Lu X, Nannenga B, Donehower LA. PPM1D dephosphorylates Chk1 and p53 and abrogates cell cycle checkpoints. Genes Dev 2005; 19:1162-74; PMID:15870257; http://dx.doi.org/10.1101/gad.1291305.
19. Macurek L, Lindqvist A, Voets O, Kool J, Vos HR, Medema RH. Wip1 phosphatase is associated with chromatin and dephosphorylates gammaH2AX to promote checkpoint inhibition. Oncogene 2010; 29:2281-91; PMID:20101220; http://dx.doi.org/10.1038/onc.2009.501.
20. Moon S, Lin L, Zhang X, Nguyen T, Darlington Y, Waldman A. Wildtype p53-induced phosphatase 1 dephosphorylates histone variant {gamma}-H2AX and suppresses DNA double strand break repair. J Biol Chem 2010; 23:12935-47; http://dx.doi.org/10.1074/jbc.M109.071696.
21. Cha H, Lowe JM, Li H, Lee J-S, Belova GI, Bulavin DV, et al. Wip1 directly dephosphorylates γ-H2AX and attenuates the DNA damage response. Cancer Res 2010; 70:4112-22; PMID:20460517; http://dx.doi.org/10.1158/0008-5472.CAN-09-4244.
22. Lu X, Nguyen TA, Moon SH, Darlington Y, Sommer M, Donehower LA. The type 2C phosphatase Wip1: an oncogenic regulator of tumor suppressor and DNA damage response pathways. Cancer Metastasis Rev 2008; 27:123-35; PMID:18265945; http://dx.doi.org/10.1007/s10555-008-9127-x.
23. Fiscella M, Zhang H, Fan S, Sakaguchi K, Shen S, Mercer WE, et al. Wip1, a novel human protein phosphatase that is induced in response to ionizing radiation in a p53-dependent manner. Proc Natl Acad Sci USA 1997; 94:6048-53; PMID:9177166; http://dx.doi.org/10.1073/pnas.94.12.6048.
24. Zhang X, Wan G, Mlotshwa S, Vance V, Berger FG, Chen H, et al. Oncogenic Wip1 phosphatase is inhibited by miR-16 in the DNA damage signaling pathway. Cancer Res 2010; 70:7176-86; PMID:20668064; http://dx.doi.org/10.1158/0008-5472.CAN-10-0697.
25. Lindqvist A, de Bruijn M, Macurek L, Brás A, Mensinga A, Bruinsma W, et al. Wip1 confers G2 checkpoint recovery competence by counteracting p53-dependent transcriptional repression. EMBO J 2009; 28:3196-206; PMID:19713933; http://dx.doi.org/10.1038/emboj.2009.246.
26. Nannenga B, Lu X, Dumble M, Van Maanen M, Nguyen T-A, Sutton R, et al. Augmented cancer resistance and DNA damage response phenotypes in PPM1D null mice. Mol Carcinog 2006; 45:594-604; PMID:16652371; http://dx.doi.org/10.1002/mc.20195.
27. Bulavin DV, Phillips C, Nannenga B, Timofeev O, Donehower LA, Anderson CW, et al. Inactivation of the Wip1 phosphatase inhibits mammary tumorigenesis through p38 MAPK-mediated activation of the p16(Ink4a)-p19(Arf) pathway. Nat Genet 2004; 36:343-50; PMID:14991053; http://dx.doi.org/10.1038/ng1317.
28. Shreeram S, Hee WK, Demidov ON, Kek C, Yamaguchi H, Fornace AJ Jr., et al. Regulation of ATM/p53-dependent suppression of myc-induced lymphomas by Wip1 phosphatase. J Exp Med 2006; 203:2793-9; PMID:17158963; http://dx.doi.org/10.1084/jem.20061563.
29. Rauta J, Alarmo E-L, Kauraniemi P, Karhu R, Kuukasjärvi T, Kallioniemi A. The serine-threonine protein phosphatase PPM1D is frequently activated through amplification in aggressive primary breast tumours. Breast Cancer Res Treat 2006; 95:257-63; PMID:16254685; http://dx.doi.org/10.1007/s10549-005-9017-7.
30. Bulavin DV, Demidov ON, Saito S, Kauraniemi P, Phillips C, Amundson SA, et al. Amplification of PPM1D in human tumors abrogates p53 tumor-suppressor activity. Nat Genet 2002; 31:210-5; PMID:12021785; http://dx.doi.org/10.1038/ng894.
31. Li J, Yang Y, Peng Y, Austin RJ, van Eyndhoven WG, Nguyen KCQ, et al. Oncogenic properties of PPM1D located within a breast cancer amplification epicenter at 17q23. Nat Genet 2002; 31:133-4; PMID:12021784; http://dx.doi.org/10.1038/ng888.
32. Castellino RC, De Bortoli M, Lu X, Moon S-H, Nguyen T-A, Shepard MA, et al. Medulloblastomas overexpress the p53-inactivating oncogene WIP1/PPM1D. J Neurooncol 2008; 86:245-56; PMID:17932621; http://dx.doi.org/10.1007/s11060-007-9470-8.
33. Saito-Ohara F, Imoto I, Inoue J, Hosoi H, Nakagawara A, Sugimoto T, et al. PPM1D is a potential target for 17q gain in neuroblastoma. Cancer Res 2003; 63:1876-83; PMID:12702577.
34. Tan DSP, Lambros MBK, Rayter S, Natrajan R, Vatcheva R, Gao Q, et al. PPM1D is a potential therapeutic target in ovarian clear cell carcinomas. Clin Cancer Res 2009; 15:2269-80; PMID:19293255; http://dx.doi.org/10.1158/1078-0432.CCR-08-2403.
35. Bolderson E, Scorah J, Helleday T, Smythe C, Meuth M. ATM is required for the cellular response to thymidine induced replication fork stress. Hum Mol Genet 2004; 13:2937-45; PMID:15459181; http://dx.doi.org/10.1093/hmg/ddh316.
36. Sakaue-Sawano A, Kurokawa H, Morimura T, Hanyu A, Hama H, Osawa H, et al. Visualizing spatiotemporal dynamics of multicellular cell-cycle progression. Cell 2008; 132:487-98; PMID:18267078; http://dx.doi.org/10.1016/j.cell.2007.12.033.

37. Song JY, Han H-S, Sabapathy K, Lee B-M, Yu E, Choi J. Expression of a homeostatic regulator, Wip1 (wild-type p53-induced phosphatase), is temporally induced by c-Jun and p53 in response to UV irradiation. J Biol Chem 2010; 285:9067-76; PMID:20093361; http://dx.doi.org/10.1074/jbc.M109.070003.
38. Vassilev LT, Tovar C, Chen S, Knezevic D, Zhao X, Sun H, et al. Selective small-molecule inhibitor reveals critical mitotic functions of human CDK1. Proc Natl Acad Sci USA 2006; 103:10660-5; PMID:16818887; http://dx.doi.org/10.1073/pnas.0600447103.
39. Skaar JR, Pagano M. Control of cell growth by the SCF and APC/C ubiquitin ligases. Curr Opin Cell Biol 2009; 21:816-24; PMID:19775879; http://dx.doi.org/10.1016/j.ceb.2009.08.004.
40. Koepp DM, Schaefer LK, Ye X, Keyomarsi K, Chu C, Harper JW, et al. Phosphorylation-dependent ubiquitination of cyclin E by the SCFFbw7 ubiquitin ligase. Science 2001; 294:173-7; PMID:11533444; http://dx.doi.org/10.1126/science.1065203.
41. Chan EH, Santamaria A, Silljé HH, Nigg EA. Plk1 regulates mitotic Aurora A function through betaTrCP-dependent degradation of hBora. Chromosoma 2008; 117:457-69; PMID:18521620; http://dx.doi.org/10.1007/s00412-008-0165-5.
42. Wolthuis R, Clay-Farrace L, van Zon W, Yekezare M, Koop L, Ogink J, et al. Cdc20 and Cks direct the spindle checkpoint-independent destruction of cyclin A. Mol Cell 2008; 30:290-302; PMID:18471975; http://dx.doi.org/10.1016/j.molcel.2008.02.027.
43. den Elzen N, Pines J. Cyclin A is destroyed in prometaphase and can delay chromosome alignment and anaphase. J Cell Biol 2001; 153:121-36; PMID:11285279; http://dx.doi.org/10.1083/jcb.153.1.121.
44. Geley S, Kramer E, Gieffers C, Gannon J, Peters J-M, Hunt T. Anaphase-promoting complex/cyclosome-dependent proteolysis of human cyclin A starts at the beginning of mitosis and is not subject to the spindle assembly checkpoint. J Cell Biol 2001; 153:137-48; PMID:11285280; http://dx.doi.org/10.1083/jcb.153.1.137.
45. Yamada S, Nakamura H, Kinoshita E, Kinoshita-Kikuta E, Koike T, Shiro Y. Separation of a phosphorylated histidine protein using phosphate affinity polyacrylamide gel electrophoresis. Anal Biochem 2007; 360:160-2; PMID:17092477; http://dx.doi.org/10.1016/j.ab.2006.10.005.
46. Dinkel H, Michael S, Weatheritt RJ, Davey NE, Van Roey K, Altenberg B, et al. ELM--the database of eukaryotic linear motifs. Nucleic Acids Res 2012; 40(Database issue):D242-51; PMID:22110040; http://dx.doi.org/10.1093/nar/gkr1064.
47. Moon S-H, Nguyen T-A, Darlington Y, Lu X, Donehower LA. Dephosphorylation of γ-H2AX by WIP1: an important homeostatic regulatory event in DNA repair and cell cycle control. Cell Cycle 2010; 9:2092-6; PMID:20495376; http://dx.doi.org/10.4161/cc.9.11.11810.
48. Ichijima Y, Sakasai R, Okita N, Asahina K, Mizutani S, Teraoka H. Phosphorylation of histone H2AX at M phase in human cells without DNA damage response. Biochem Biophys Res Commun 2005; 336:807-12; PMID:16153602; http://dx.doi.org/10.1016/j.bbrc.2005.08.164.
49. McManus KJ, Hendzel MJ. ATM-dependent DNA damage-independent mitotic phosphorylation of H2AX in normally growing mammalian cells. Mol Biol Cell 2005; 16:5013-25; PMID:16030261; http://dx.doi.org/10.1091/mbc.E05-01-0065.
50. Hickson I, Zhao Y, Richardson CJ, Green SJ, Martin NMB, Orr AI, et al. Identification and characterization of a novel and specific inhibitor of the ataxia-telangiectasia mutated kinase ATM. Cancer Res 2004; 64:9152-9; PMID:15604286; http://dx.doi.org/10.1158/0008-5472.CAN-04-2727.
51. Leahy JJJ, Golding BT, Griffin RJ, Hardcastle IR, Richardson C, Rigoreau L, et al. Identification of a highly potent and selective DNA-dependent protein kinase (DNA-PK) inhibitor (NU7441) by screening of chromenone libraries. Bioorg Med Chem Lett 2004; 14:6083-7; PMID:15546735; http://dx.doi.org/10.1016/j.bmcl.2004.09.060.
52. Reaper PM, Griffiths MR, Long JM, Charrier J-D, Maccormick S, Charlton PA, et al. Selective killing of ATM- or p53-deficient cancer cells through inhibition of ATR. Nat Chem Biol 2011; 7:428-30; PMID:21490603; http://dx.doi.org/10.1038/nchembio.573.
53. Le Guezennec X, Bulavin DV. WIP1 phosphatase at the crossroads of cancer and aging. Trends Biochem Sci 2010; 35:109-14; PMID:19879149; http://dx.doi.org/10.1016/j.tibs.2009.09.005.
54. Lu X, Nguyen T-A, Donehower LA. Reversal of the ATM/ATR-mediated DNA damage response by the oncogenic phosphatase PPM1D. Cell Cycle 2005; 4:1060-4; PMID:15970689; http://dx.doi.org/10.4161/cc.4.8.1876.
55. Zhu Y-H, Zhang C-W, Lu L, Demidov ON, Sun L, Yang L, et al. Wip1 regulates the generation of new neural cells in the adult olfactory bulb through p53-dependent cell cycle control. Stem Cells 2009; 27:1433-42; PMID:19489034; http://dx.doi.org/10.1002/stem.65.
56. Choi J, Nannenga B, Demidov ON, Bulavin DV, Cooney A, Brayton C, et al. Mice deficient for the wild-type p53-induced phosphatase gene (Wip1) exhibit defects in reproductive organs, immune function, and cell cycle control. Mol Cell Biol 2002; 22:1094-105; PMID:11809801; http://dx.doi.org/10.1128/MCB.22.4.1094-1105.2002.
57. Petermann E, Caldecott KW. Evidence that the ATR/Chk1 pathway maintains normal replication fork progression during unperturbed S phase. Cell Cycle 2006; 5:2203-9; PMID:16969104; http://dx.doi.org/10.4161/cc.5.19.3256.
58. Yang C, Tang X, Guo X, Niikura Y, Kitagawa K, Cui K, et al. Aurora-B mediated ATM serine 1403 phosphorylation is required for mitotic ATM activation and the spindle checkpoint. Mol Cell 2011; 44:597-608; PMID:22099307; http://dx.doi.org/10.1016/j.molcel.2011.09.016.
59. Hubackova S, Novakova Z, Krejcikova K, Kosar M, Dobrovolna J, Duskova P, et al. Regulation of the PML tumor suppressor in drug-induced senescence of human normal and cancer cells by JAK/STAT-mediated signaling. Cell Cycle 2010; 9:3085-99; PMID:20699642; http://dx.doi.org/10.4161/cc.9.15.12521.
60. Lindqvist A, van Zon W, Karlsson Rosenthal C, Wolthuis RMF. Cyclin B1-Cdk1 activation continues after centrosome separation to control mitotic progression. PLoS Biol 2007; 5:e123; PMID:17472438; http://dx.doi.org/10.1371/journal.pbio.0050123.
61. Kosar M, Bartkova J, Hubackova S, Hodny Z, Lukas J, Bartek J. Senescence-associated heterochromatin foci are dispensable for cellular senescence, occur in a cell type- and insult-dependent manner and follow expression of p16(ink4a). Cell Cycle 2011; 10:457-68; PMID:21248468; http://dx.doi.org/10.4161/cc.10.3.14707.

3.2 Gain-of-function mutations of *PPM1D*/WIP1 impair the p53-dependent G1 checkpoint

Kleiblova P, Shaltiel IA, Benada J, Ševčík J, Pecháčková S, Pohlreich P, Voest EE, Dundr P, Bartek J, Kleibl Z, Medema RH, Macurek L.

Journal Cell of Biology. 2013 May 13; 201(4):511-21. doi: 10.1083/jcb.201210031. Epub 2013 May 6.

In this publication, we describe novel gain-of-function mutations of *PPM1D* (WIP1) cancer cell lines. These variants of WIP1 are created by nonsense mutations in exon 6 of *PPM1D* that result in expression of the C-terminally truncated protein with higher stability in the cells. Further, we identified that the mutations of *PPM1D* are present in the tumors and in the peripheral blood of breast and colorectal cancer patients, indicating that they may predispose to cancer development. We show that mutations in *PPM1D* affect the DNA damage response pathway and propose that they could predispose to cancer.

P. S. performed in vitro phosphatase assay and epitope mapping of anti-WIP1 antibodies.

Published May 6, 2013

Gain-of-function mutations of PPM1D/Wip1 impair the p53-dependent G1 checkpoint

Petra Kleiblova,[1,4] Indra A. Shaltiel,[2,3] Jan Benada,[4,5] Jan Ševčík,[1] Soňa Pecháčková,[4,5] Petr Pohlreich,[1] Emile E. Voest,[3] Pavel Dundr,[6] Jiri Bartek,[5,7,8] Zdenek Kleibl,[1] René H. Medema,[2,3] and Libor Macurek[4,5]

[1]Institute of Biochemistry and Experimental Oncology, First Faculty of Medicine, Charles University in Prague, CZ-12853 Prague, Czech Republic
[2]Division of Cell Biology, The Netherlands Cancer Institute, 1066CX Amsterdam, Netherlands
[3]Department of Medical Oncology, University Medical Center Utrecht, 3584CG Utrecht, Netherlands
[4]Department of Cancer Cell Biology and [5]Department of Genome Integrity, Institute of Molecular Genetics v.v.i., Academy of Sciences of the Czech Republic, CZ-14220 Prague, Czech Republic
[6]Institute of Pathology, First Faculty of Medicine, Charles University in Prague and General University Hospital in Prague, CZ-12000 Prague, Czech Republic
[7]Institute of Molecular and Translational Medicine, Palacky University, CZ-77515 Olomouc, Czech Republic
[8]Danish Cancer Society Research Center, DK-2100 Copenhagen, Denmark

The DNA damage response (DDR) pathway and its core component tumor suppressor p53 block cell cycle progression after genotoxic stress and represent an intrinsic barrier preventing cancer development. The serine/threonine phosphatase PPM1D/Wip1 inactivates p53 and promotes termination of the DDR pathway. Wip1 has been suggested to act as an oncogene in a subset of tumors that retain wild-type p53. In this paper, we have identified novel gain-of-function mutations in exon 6 of *PPM1D* that result in expression of C-terminally truncated Wip1. Remarkably, mutations in *PPM1D* are present not only in the tumors but also in other tissues of breast and colorectal cancer patients, indicating that they arise early in development or affect the germline. We show that mutations in *PPM1D* affect the DDR pathway and propose that they could predispose to cancer.

Introduction

Proliferating cells respond to genotoxic stress by activating a conserved DNA damage response (DDR) pathway that blocks cell cycle progression (checkpoint) and facilitates DNA repair. Activation of ATM (ataxia telangiectasia mutated)/Chk2, ATR (ataxia telangiectasia and Rad3 related)/Chk1, and p38/MK2 kinases converges on the tumor suppressor p53, which plays a central role in regulating cell fate decisions in response to genotoxic stress (Jackson and Bartek, 2009; Medema and Macůrek, 2012). In general, genotoxic stress induces stabilization, oligomerization, and binding of p53 to promoters, causing a widespread modulation of gene expression (Vogelstein et al., 2000). Although high doses of DNA damage (such as therapeutic irradiation or radiomimetic drugs) lead to p53-induced programmed cell death or permanent withdrawal from the cell cycle (senescence), more moderate DNA damage (originating from erroneous DNA metabolism or from environmental factors) triggers expression of DNA repair genes and a cyclin-dependent kinase inhibitor p21(WAF1/CIP1) that controls the G1 checkpoint (el-Deiry et al., 1993). After completion of DNA repair, cells recover from the temporal checkpoint arrest and return to the proliferation program. Wip1 (also known as PPM1D) is a monomeric serine/threonine phosphatase of the PP2C family, and its expression is increased after DNA damage (Fiscella et al., 1997). Wip1 has been implicated in dephosphorylation of multiple DDR components, including ATM, Chk1/2, γ-H2AX, and p53, all contributing to timely inactivation of DDR after DNA repair (Le Guezennec and Bulavin, 2010). In addition, Wip1-dependent inactivation of p53 is thought to play a major role in control of checkpoint recovery (Lindqvist et al., 2009).

Recent work has identified oncogene-induced replication stress and DNA breakage that trigger the DDR as an intrinsic barrier against progression of early preinvasive stages of solid tumors to malignant lesions (Bartkova et al., 2005, 2006; Gorgoulis et al., 2005; Di Micco et al., 2006; Halazonetis et al., 2008). According to this model, cells that accumulate mutations circumventing the checkpoint barrier have a selective advantage

P. Kleiblova and I.A. Shaltiel contributed equally to this paper.

Correspondence to Libor Macurek: libor.macurek@img.cas.cz; or René H. Medema: r.medema@nki.nl

Abbreviations used in this paper: DDR, DNA damage response; FL, full length; FUCCI, fluorescent, ubiquitination-based cell cycle indicator; IR, ionizing radiation; IRIF, IR-induced foci; MS, mass spectrometry; STLC, S-trityl-L-cysteine.

Supplemental Material can be found at:
/content/suppl/2013/05/01/jcb.201210031.DC1.html

The Rockefeller University Press $30.00
J. Cell Biol. Vol. 201 No. 4 511–521
www.jcb.org/cgi/doi/10.1083/jcb.201210031

Published May 6, 2013

and can thus promote further development of cancer. The most common example of such DDR defect is an inactivating somatic mutation in the *TP53* gene that disables proper response to genotoxic stress, leads to genomic instability, and is found in about half of human tumors (Hollstein et al., 1991). On the other hand, tumors that retain wild-type p53 are likely to accumulate other genetic defects that would allow them to overcome the DDR barrier, providing a growth advantage in the presence of replicative stress. Importantly, amplification of the 17q23 locus carrying the *PPM1D* gene has been reported in various p53 wild-type tumors, pointing toward a role of Wip1 in cancer development, and Wip1 overexpression is associated with poor prognosis (Bulavin et al., 2002, 2004; Li et al., 2002; Saito-Ohara et al., 2003; Rauta et al., 2006; Castellino et al., 2008; Liang et al., 2012). The oncogenic behavior of Wip1 is further supported by mouse genetics showing that loss of Wip1 protects from cancer development (Bulavin et al., 2004; Nannenga et al., 2006). However, point mutations that affect Wip1 function have not been reported. Here, we have identified novel truncating mutations of Wip1 that show a gain-of-function effect and impair p53-dependent responses to genotoxic stress. Strikingly, mutations in the *PPM1D* gene were found also in breast and colorectal cancer patients, suggesting that such truncating mutations of Wip1 may predispose to a wider range of cancer types.

Results and discussion

Because amplification of the *PPM1D* gene occurs mainly in tumors that retain the wild-type p53, we have screened a panel of p53-proficient tumor cell lines to determine the expression level of Wip1 in tumors derived from various tissues (Bulavin et al., 2002; Rauta et al., 2006). Predictably, we could confirm high expression of Wip1 in MCF7 cells that are known to carry an extensive amplification of the *PPM1D* locus (Fig. 1 A; Pärssinen et al., 2008). All other tested cell lines expressed substantially lower amounts of full-length (FL) Wip1. Surprisingly, we noticed an abundant, faster migrating band, recognized by two distinct Wip1 antibodies in HCT116 and U2OS cells derived from colorectal adenocarcinoma and osteosarcoma, respectively (Fig. 1, A and B). Notably, antibodies recognizing an epitope corresponding to the amino acid residues 380–410 of Wip1 stained both bands, whereas an antibody directed against an epitope corresponding to the amino acid residues 500–550 of Wip1 recognized only the slower migrating band (Figs. 1 A and S1 A). In addition, both bands were depleted by three independent Wip1 siRNAs, indicating that the two protein bands correspond to various forms of Wip1 (Fig. S1 B). Consistent with this, sequencing of genomic DNA revealed heterozygous mutations (c.1349delT and c.1372C>T) within exon 6 of the *PPM1D* gene that caused truncation of the Wip1 protein (p.L450X in HCT116 and p.R458X in U2OS cells; Fig. 1 C). Expression of both the FL and truncated versions of Wip1 in U2OS and HCT116 cells was further confirmed by immunopurification of Wip1 and subsequent mass spectrometry (MS) analysis (Fig. S1, C and D). Importantly, epitope-tagged versions of truncated Wip1 proteins expressed from plasmid DNA showed electrophoretic mobility that closely resembled that of the aberrant endogenous Wip1 proteins (Fig. S1 E).

To understand whether truncation of Wip1 affects its function in the DDR, we asked whether the respective truncation mutants were capable of suppressing formation of ionizing radiation (IR)–induced foci (IRIF) as has been described for FL Wip1 (Macůrek et al., 2010). Both, Wip1-L450X and Wip1-R458X localized properly in the nucleus and were bound to the chromatin, suggesting that overall subcellular distribution of Wip1 is not affected by the exon 6 truncations (Fig. 2 A). As expected, overexpression of FL-Wip1 resulted in a reduction in IRIF formation, as determined by the number of 53BP1 foci induced after irradiation (Fig. 2 B). Similarly, overexpression of Wip1-L450X and Wip1-R458X (but not phosphatase-dead Wip1-D314A) also caused a dramatic reduction in IRIF formation, suggesting that the mutants retain normal phosphatase activity that opposes IRIF assembly (Fig. 2 B). In addition, expression of FL-Wip1, Wip1-L450X, and Wip1-R458X significantly decreased levels of radiation-induced phosphorylation of histone H2AX (γ-H2AX) and pSer15-p53 (both established markers of DDR and substrates of Wip1; Lu et al., 2005; Macůrek et al., 2010), suggesting that all tested Wip1 proteins are capable of silencing the DDR (Fig. 2 C). Wip1 is a monomeric phosphatase, and because all identified truncating mutations reside in the C-terminal region of Wip1 leaving the N-terminal catalytic domain intact, we hypothesized that the truncation mutants retain phosphatase activity. Indeed, immunopurified FL-Wip1, Wip1-L450X, and Wip1-R458X showed comparable phosphatase activity in vitro, and therefore, it is unlikely that mutation of *PPM1D* leads to production of a hyperactive Wip1 (Fig. 2 D).

Because mutations in oncogenes are expected to cause a gain-of-function effect, we wondered whether the C-terminal region coded by exon 6 reduces the stability of Wip1. Consistent with this notion, we found that both U2OS and HCT116 cells expressed ∼10–20-fold more of the truncated Wip1 compared with the FL-Wip1 (Fig. 2 E). In contrast, no substantial differences between wild-type and mutated Wip1 expression were found at the mRNA level, indicating that these are not differentially regulated at the transcriptional level and that the high levels of the mutant Wip1 proteins reflect enhanced protein stability (Fig. S1 F). Indeed, the FL-Wip1 disappeared rapidly after treatment of cells with cycloheximide (half-life of 1–2 h), whereas both truncated mutants exhibited enhanced stability (half-life of >6 h; Fig. 3, A and B). In addition, treatment with the proteasomal inhibitor MG-132 reversed the effect of the cycloheximide on destabilization of the FL-Wip1 (Fig. 3 C). This suggests that the C-terminal domain of Wip1 somehow renders the FL protein unstable and that its turnover is regulated by the proteasome. To further corroborate this notion, we fused the C-terminal noncatalytic part of Wip1 (aa 380–605) to GFP and analyzed its effect on protein stability. Similar to what we observed for FL-Wip1, we found that the GFP fusion containing the C-terminal tail of Wip1 was less stable than GFP itself (Fig. 3 D). From this, we conclude that nonsense mutations in exon 6 of the *PPM1D* gene lead to increased protein levels of enzymatically active truncated Wip1 and thus result in increased total Wip1 activity in cells.

Published May 6, 2013

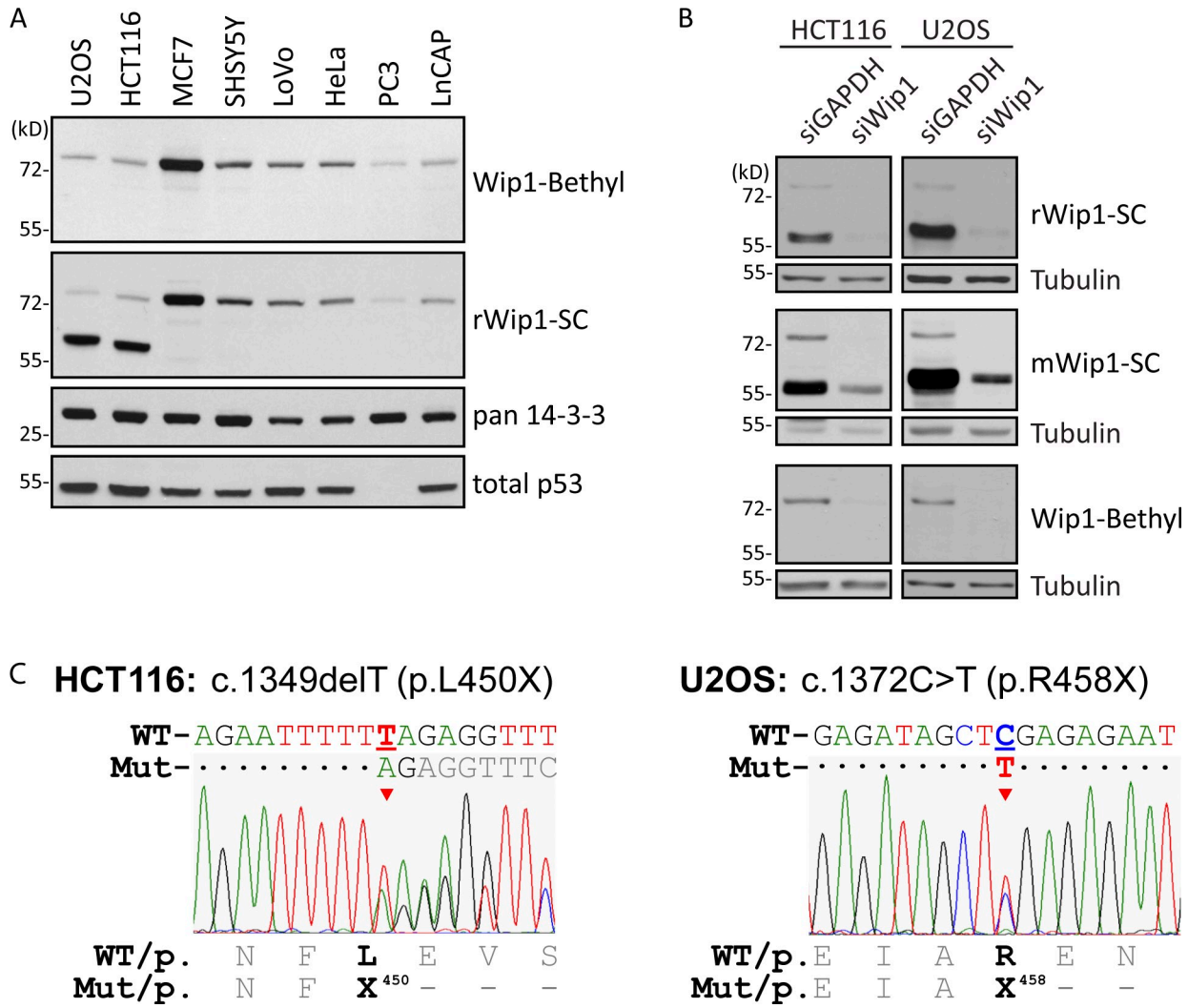

Figure 1. **The *PPM1D* gene is mutated in selected cancer cell lines.** (A) Whole-cell lysates from indicated cell lines were probed with anti-Wip1 (Bethyl Laboratories, Inc.), anti-Wip1 (Santa Cruz Biotechnology, Inc. [SC]), and anti–14-3-3 (loading control) antibodies. Note the additional Wip1-reactive band around 60 kD in U2OS and HCT116 cells. PC3 cells are p53 negative and served as a control. (B) Wip1 was depleted in U2OS and HCT116 cells by siRNA, and lysates were probed with the indicated antibodies. (C) Sequencing chromatograms of *PPM1D* from genomic DNA isolated from U2OS and HCT116 cells. Numbering is based on NCBI GenBank reference sequence NT_010783.15. Mutations are indicated by arrowheads and underlined. WT, wild-type *PPM1D*; Mut, mutated *PPM1D*; c., nucleotide sequence; p., Wip1 peptide sequence.

Despite the fact that U2OS and HCT116 contain wild-type p53, they fail to arrest in G1 in response to IR and preferentially arrest in the G2 checkpoint that remains intact (Fig. S2, A and B). This is reminiscent of the behavior of cells lacking p53 or expressing mutant p53 and suggests that the p53 pathway is somehow compromised in U2OS and HCT116 cells. To test whether this may be caused by enhanced Wip1 levels and/or activity, we depleted Wip1 by RNAi and measured the ability of cells exposed to IR to arrest in G1. Indeed, we observed that U2OS cells did arrest in G1 after depletion of Wip1 and exposure to IR (Figs. 4 A and S2 C). Moreover, this arrest was fully dependent on p53 because codepletion of Wip1 and p53 or depletion of Wip1 in p53-negative cell lines SW480, DLD1, and HT29 did not restore any G1 checkpoint function (Fig. 4 A and not depicted). In addition, depletion of the truncated Wip1 (but not of the FL-Wip1) by isoform-specific RNAi was sufficient to rescue the G1 arrest in irradiated U2OS cells, thus further supporting the conclusion that expression of the truncated variant of Wip1 abrogates the G1 checkpoint (Fig. 4 B). As an alternative approach, we followed the progression from G1 to S phase by time-lapse analysis of living HCT116 cells expressing fluorescent markers to monitor cell cycle progression (Fig. 4 C). HCT116 cells treated with control siRNA were delayed in G1 after irradiation (Fig. 4 C), consistent with previous observations that degradation of Cdc25A and Cyclin D1 can delay S-phase entry in a p53-independent manner (Agami and Bernards, 2000; Mailand et al., 2000). However, the majority of control cells eventually entered S phase (Fig. 4 C). In contrast, HCT116 cells depleted of Wip1 mounted a lasting G1 checkpoint arrest (Fig. 4 C). In accordance with restoration of p53 function upon depletion of Wip1, we observed increased levels of p21 after exposure to IR in U2OS and HCT116 cells treated with Wip1 RNAi (Fig. 4, D and E).

We conclude that cells with mutations that enhance Wip1 protein stability are unable to engage p53 function, fail to arrest

Published May 6, 2013

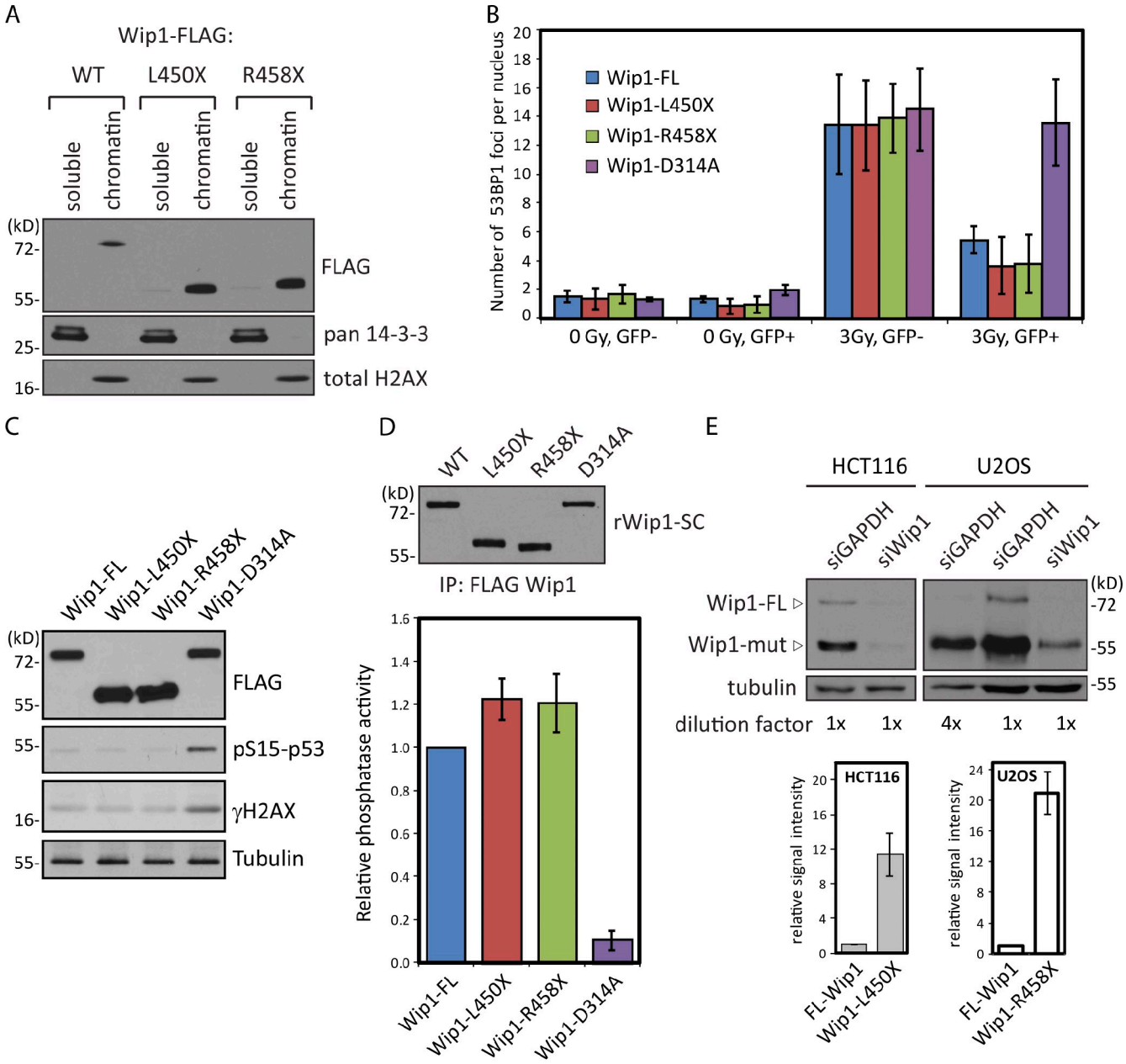

Figure 2. **Truncated Wip1 mutants are enzymatically active.** (A) Soluble and chromatin fractions from cells expressing FL or truncated FLAG-Wip1 were probed with the indicated antibodies. (B) Cells expressing EGFP-Wip1-FL (FL), EGFP-Wip1-D314A (phosphatase dead), or truncated EGFP-Wip1 were fixed 3 h after irradiation (3 Gy). 53BP1 nuclear foci were counted by automated image analysis (1,000 cells per condition). Average number of 53BP1 foci per nucleus in transfected (GFP+) and neighboring control cells (GFP−) is shown. (C) Expression of Wip1-FL, Wip1-D314A, or truncated FLAG-Wip1 was induced by tetracycline 12 h before irradiation (3 Gy). Whole-cell lysates were probed with the indicated antibodies. (D) Phosphatase activity of immunopurified FLAG-Wip1-FL, -L450X, -R458X, or -D314A (phosphatase dead) was measured in vitro using a synthetic phosphopeptide corresponding to pSer15-p53 (bottom), and the precipitated material was probed with anti-Wip1 antibody as a control of equal loading (top). $n = 4$. (E) Quantification of the signal intensity corresponding to the endogenous levels of FL and truncated Wip1 in HCT116 and U2OS cells. siRNA of Wip1 was used as a control of the signal specificity. Error bars indicate standard deviations. mut, mutated; WT, wild type.

in G1 after DNA damage, and progress to S phase. Thus, the genome integrity of cells expressing truncated Wip1 versions may be compromised by replication of the genome that contains unrepaired DNA lesions, including the highly pro-oncogenic DNA double-strand breaks. Increased expression of truncated Wip1 impairs the cellular responses to genotoxic stress also via a reduction in H2AX phosphorylation, which is an established substrate of Wip1. In addition, it is likely that high levels of truncated Wip1 may also directly cause accumulation of mutations through the described negative role of Wip1 in regulation of nucleotide excision repair (Nguyen et al., 2010). All these mechanisms may contribute to the elimination of the intrinsic DDR-mediated barrier against tumor development in cells carrying gain-of-function mutations of Wip1.

Finally, we wished to address the clinical relevance of the identified Wip1 mutations. We therefore performed mutational

Published May 6, 2013

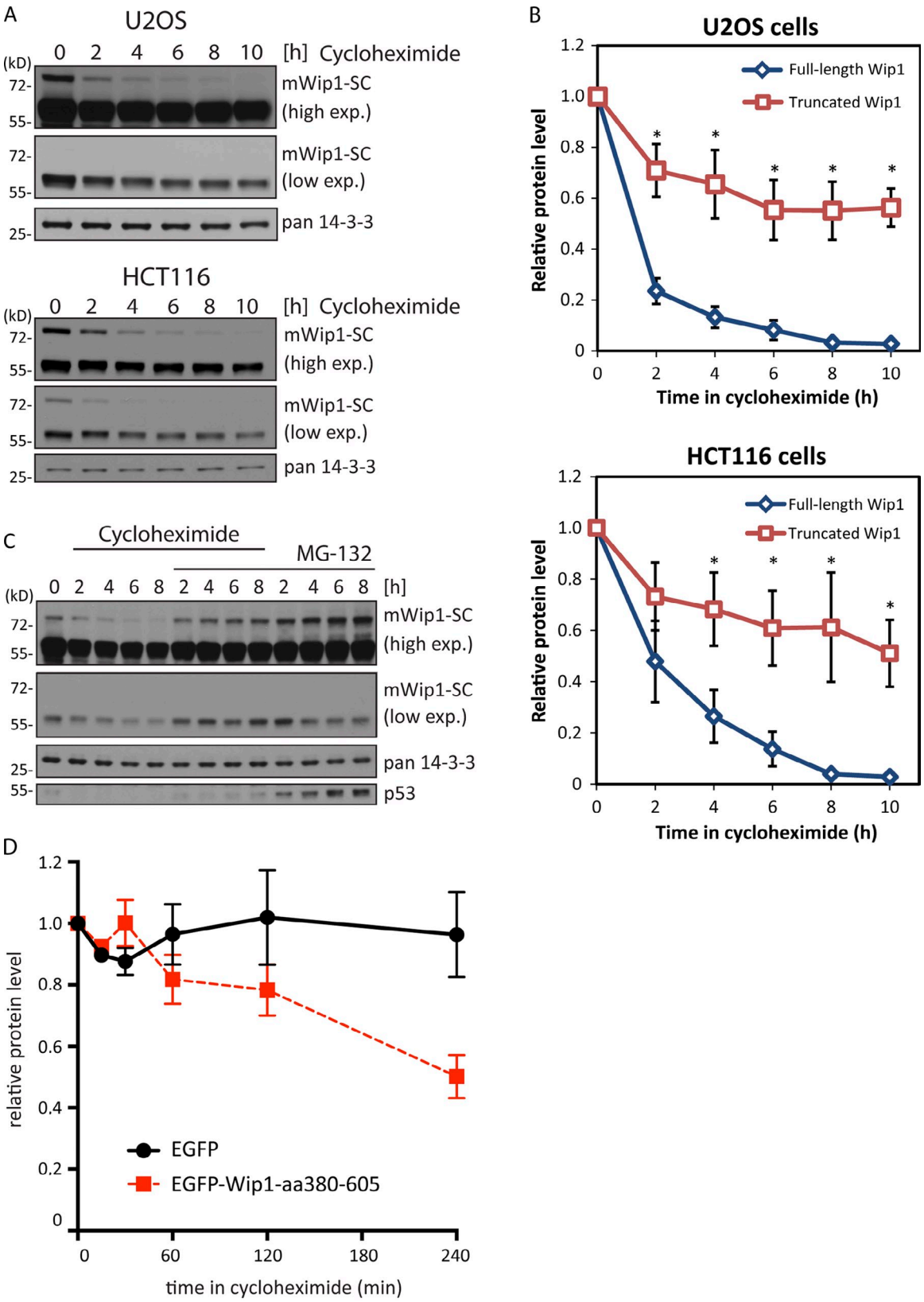

Figure 3. **Truncated Wip1 mutants show increased protein stability.** (A) HCT116 and U2OS cells were treated for the indicated times with cycloheximide. Normalized cell lysates were probed using the monoclonal anti-Wip1 antibody (Santa Cruz Biotechnology, Inc. [SC]). (B) Signal intensity corresponding to the FL-Wip1 and truncated Wip1 from A was quantified using ImageJ software. The relative change in signal intensity is shown. Statistical significance was determined by unpaired two-tailed *t* test ($n = 3$; *, $P < 0.05$). (C) U2OS cells were treated with cycloheximide, proteasomal inhibitor MG132 or a combination of both for the indicated times and analyzed as in A. (D) U2OS cells were transfected with plasmid DNA coding for EGFP or EGFP fused to the C-terminal region of Wip1 (aa 380–605). Cells were treated for the indicated times with cycloheximide. Normalized cell lysates were probed with an anti-GFP antibody, and the signal intensity was quantified using ImageJ software. $n = 3$. Error bars indicate standard deviations. exp., exposure.

Published May 6, 2013

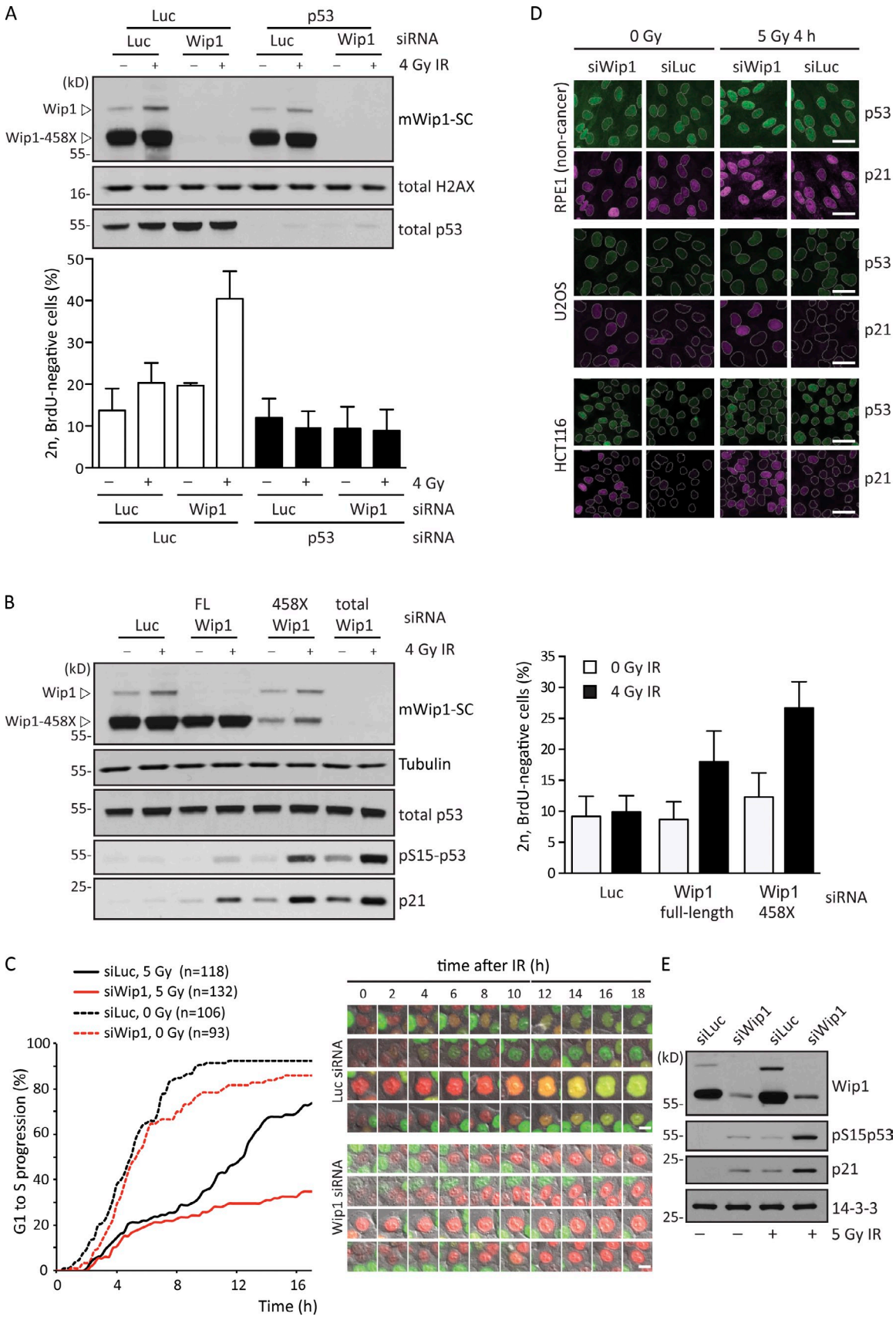

Figure 4. **Mutated Wip1 impairs the p53-dependent G1 checkpoint.** (A) U2OS cells were transfected by siRNA targeting luciferase, Wip1 and/or p53 and grown for 48 h. Cells were treated with BrdU and STLC, irradiated or not irradiated with 4 Gy, and grown for a further 16 h. Cells were analyzed by immunoblotting (top) or by flow cytometry (bottom) to determine the fraction of G1 cells (2n; BrdU negative). (B) U2OS cells were transfected by

Published May 6, 2013

analysis of the *PPM1D* gene in a panel of unselected colorectal cancer patients (n = 304) and a panel of high-risk patients with *BRCA1/2*-negative breast and ovarian cancer (n = 728) and identified four deleterious mutations in exon 6 (c.1372C>T and c.1602insT in patients with colorectal cancer and c.1601del15 and c.1451T>G in patients with breast cancer) compared with no such mutations present in noncancer control samples (n = 450; Fig. 5 A and Table S1). All identified Wip1-truncating mutations (p.R458X, p.L484X, p.K535X, and p.F534X) and showed a striking similarity to mutations identified in the tumor cell lines. Functional analysis of all Wip1 mutants present in cancer patients confirmed that these truncations retain the enzymatic activity as well as the ability to bind to chromatin (Fig. 5, B and C; and not depicted). In addition, we analyzed protein levels of Wip1 in leukocytes in one of the mutant carriers and found that the truncated Wip1 is expressed at a much higher level than the FL-Wip1, thus phenocopying the situation in tumor cell lines (Fig. 5 D). Finally, we analyzed a noncancer mammary tissue and tumor tissue from one mutation carrier and identified a heterozygous mutation in the tumor tissue (Fig. 5 E).

Remarkably, all truncating mutations identified in the *PPM1D* gene in patients and cancer cell lines were heterozygous gain-of-function mutations, which is consistent with the role of Wip1 as an oncogene. Of note, alterations in cancer patients were identified in peripheral blood samples, excluding the possibility that these mutations arise in the developing tumor simply as a consequence of genetic instability. The targeting to a discrete hot-spot region in the exon 6 of the *PPM1D* oncogene—their gain-of-function character proven by in vitro experiments—the variable onset of cancer in affected individuals, and the versatile spectrum of cancer types appearing in mutation carriers and cancer cell lines all indicate that mutations in *PPM1D* may represent an unusual and novel genetic risk factor of general cancer predisposition not associated with a single specific cancer type.

Although the majority of hereditary cancers is caused by mutations in tumor suppressor genes, germline mutations in oncogenes are not unprecedented (Knudson, 2002). For example, germline mutations of oncogenic tyrosine kinases *RET*, *MET*, and *KIT* are linked with medullary thyroid carcinoma, hereditary papillary renal carcinoma, and hereditary gastrointestinal stromal tumor syndrome, respectively (Mulligan et al., 1993; Schmidt et al., 1997; Nishida et al., 1998). Whereas tumor development is substantially boosted by inactivation of the second allele of the tumor suppressor genes, monoallelic gain-of-function mutations are usually sufficient to activate oncogenes (Vogelstein and Kinzler, 2004). In agreement with this, identified mutations of *PPM1D* in the tumor cell lines were heterozygous, and both wild-type and truncated *PPM1D* alleles were expressed. We propose that the high expression level of truncated Wip1 impairs the p53-dependent genome surveillance system in mutation carriers, making their genomic DNA hypersensitive to various genotoxic insults. By this mechanism, mutations in other tumor-promoting genes may accumulate throughout the entire life span of the *PPM1D* mutation carriers and promote cancer development. The clinical significance of truncating *PPM1D* mutations in predisposition to breast and ovarian cancer was recently documented by an extensive case control study (Ruark et al., 2013). Further studies are needed to address the possibility that mutations in *PPM1D* may represent a hereditary cancer predisposition and that truncated Wip1 might be a suitable candidate for pharmacological intervention in cancer patients carrying *PPM1D* mutations.

Materials and methods

Antibodies

Antibodies used were rabbit anti-Wip1 (H300), mouse anti-Wip1 (F-10), anti-p53 (DO1), anti-p21 (C19), and anti-53BP1 (Santa Cruz Biotechnology, Inc.); anti-PPM1D (A300-664A; Bethyl Laboratories, Inc.); anti-pSer15p53, anti-p53, and anti-pSer139-H2AX (Cell Signaling Technology); anti–α-tubulin and anti-FLAG (Sigma-Aldrich); anti-BrdU (clone BU1/75; Abcam); and Alexa Fluor–conjugated secondary antibodies (Life Technologies).

Plasmids

DNA fragments coding for FLAG-tagged human FL or truncated (R458X, L450X, and F534X) Wip1 were generated by PCR and subcloned into BamHI–XbaI sites of the pcDNA4/TO plasmid. Alternatively, coding sequence for EGFP was inserted in HindIII site of pcDNA4/TO and FL, or truncated Wip1 was cloned in frame into BamHI–XbaI sites.

Cell culture

Human U2OS, HCT116, LoVo, MCF7, HeLa, SH-SY5Y, and PC3 or nontumor diploid retinal pigment epithelium cells were grown in DMEM (Gibco) supplemented with 10% FCS, 2 mM L-glutamine, 100 U/ml penicillin, and 100 µg/ml streptomycin. Tetracycline repressor–expressing U2OS-TR cells were grown in media containing tetracycline system–approved FCS, and protein expression was induced by tetracycline. A stable cell line expressing the fluorescent, ubiquitination-based cell cycle indicator (FUCCI) was generated by transduction of HCT116 cells with pCSII-EF-MCS-mKO2-hCdt1(30–120) and pCSII-EF-MCS-mAG-hGeminin(1–110) plasmids (Sakaue-Sawano et al., 2008) followed by FACS sorting of double-positive cells from which a single clone was expanded. Transfections of plasmid DNA were performed using a standard calcium phosphate technique. ON-TARGET*plus* siRNAs targeting Wip1 (5′-GGCCAAGGGUGAAUUCUAA-3′, 5′-CGAAAUGGCUUAAGUCGAA-3′, and 5′-AGUAACGUCCUCCAUGUAC-3′) and control siRNAs (Thermo Fisher Scientific) were transfected (5–10 nM) using RNAiMAX (Invitrogen). Alternatively, isoform-specific siRNAs targeting the FL-Wip1 (5′-AUAGCUCGAGAGAAUGUCC-3′) or the 458X-Wip1 (5′-AUAGCUUGAGAGAAUGUCC-3′) were used.

Immunofluorescence and microscopic analysis

Cells cultured on glass coverslips were left untreated or exposed to IR (dose 3–5 Gy as indicated) and fixed at the indicated times by 4% formaldehyde for 10 min at RT, permeabilized by ice-cold methanol, blocked with 3% BSA in PBS supplemented with 0.1% Tween 20, and incubated with the primary antibodies 60 min at RT. After washing, coverslips were

siRNA targeting various isoforms of Wip1, irradiated, and probed with the indicated antibodies (left) or analyzed by cytometry (right). The fraction of BrdU-negative 2n cells corresponds to cells arrested in G1. (C, left) FUCCI-expressing HCT116 cells were transfected with Wip1 or luciferase siRNA (siLuc), irradiated (4 Gy), and followed by live-cell imaging. Cumulative progression into S phase was determined based on the loss of FUCCI-G1 marker (red) and appearance of the FUCCI-S/G2 marker (green) Numbers of analyzed cells are indicated in parentheses. (right) Representative images of four individual cells transfected with Wip1 or Luciferase siRNA are shown. Bars, 10 µm. (D) Retinal pigment epithelium (RPE1), U2OS, and HCT116 cells were transfected with Wip1 or luciferase siRNA and grown for 48 h before irradiation (5 Gy). Cells were fixed 4 h after IR and probed for total p53 and p21. Bars, 50 µm. (E) U2OS cells were treated as in D, collected 6 h after IR, and probed with the indicated antibodies. SC, Santa Cruz Biotechnology, Inc.

Published May 6, 2013

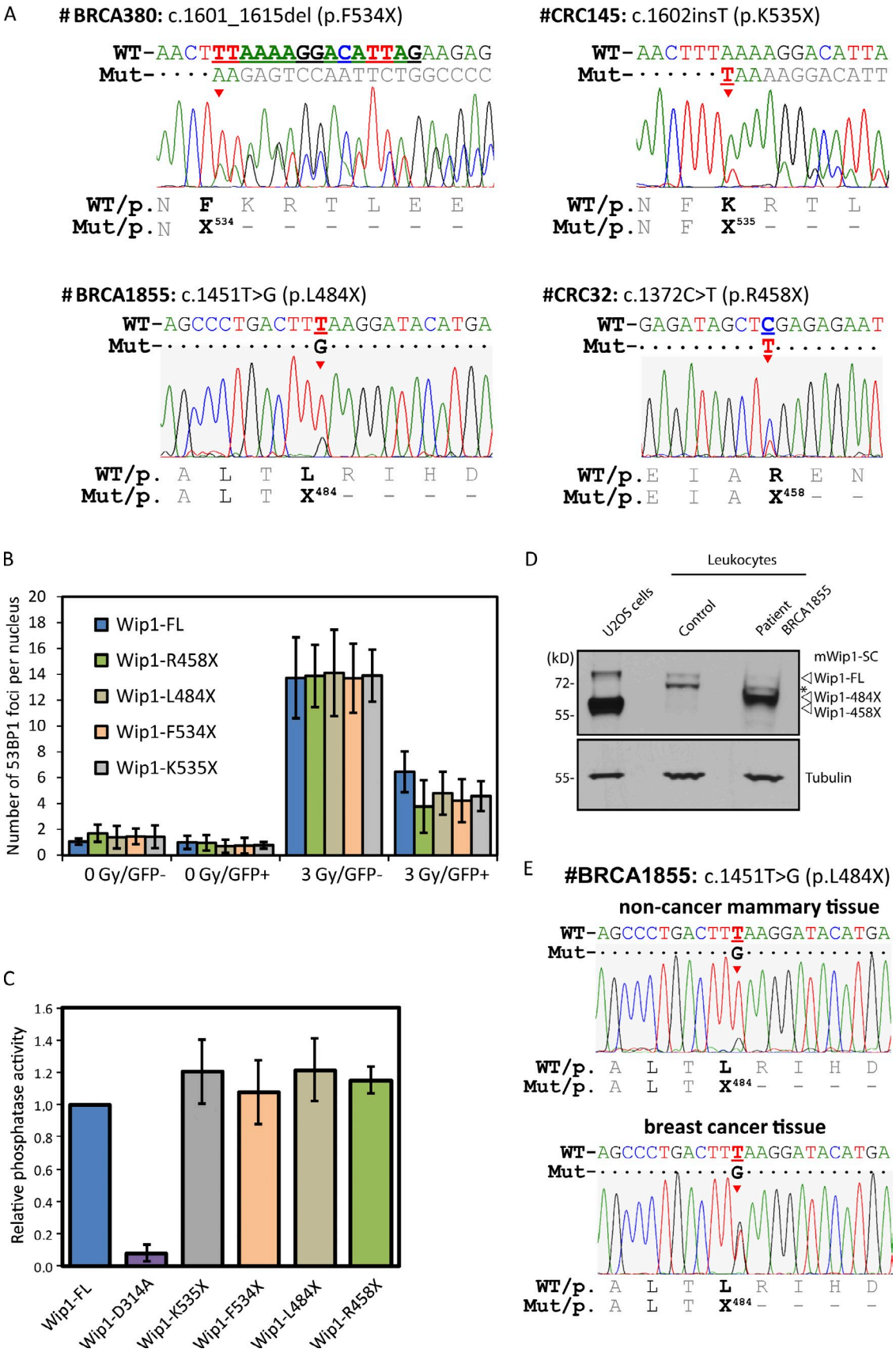

Figure 5. **Truncation mutations of Wip1 are present in cancer patients.** (A) Chromatograms of four truncating mutations identified by screening of the *PPM1D* gene in cancer patients. Mutations are indicated by arrowheads and underlined. WT, wild-type *PPM1D*; Mut, mutated *PPM1D*; c., nucleotide sequence; p., Wip1 peptide sequence. (B) Cells expressing EGFP–Wip1-FL, -R458X, -L484X, -F534X, or -K535X mutants were irradiated, and the number

Published May 6, 2013

incubated with Alexa Fluor–conjugated secondary antibodies and mounted using Vectashield reagent (Vector Laboratories) supplemented with 1 µg/ml DAPI. Imaging was performed on DeltaVision Imaging System using NA 1.4 objectives (Applied Precision). Automated image acquisition was performed using a high-content screening station (Scan^R; Olympus; using charge-coupled device camera [IX81 and ORCA-285; Olympus]) equipped with a 40×/1.3 NA objective (RMS40X-PFO; Olympus). Nuclei were identified based on the DAPI signal, and the average number of 53BP1 foci was determined using a spot detection module. At least 1,000 nuclei were counted per condition in three independent experiments. Cells transiently transfected with FL- or mutant EGFP-Wip1 were gated according to the EGFP signal, and neighboring EGFP-negative cells were used as controls. Alternatively, HCT116-FUCCI cells were grown at 37°C in Lab-Tek II chamber slides in L15 media (Gibco) containing all supplements. Cells were irradiated or not irradiated, and videos were acquired using DeltaVision system equipped with a 10×/0.40 NA U-Plan S-Apochromat objective (Olympus), a camera (CoolSNAP HQ2; Photometrics), Quad-mCherry polychroic filter, and mCherry/GFP emission filter sets. Nuclei negative for Geminin-mAG1 (corresponding to G1) directly after irradiation were followed until the appearance of Geminin-mAG1 signal (corresponding to S) detectable over background in two consecutive frames (15 min).

Immunoprecipitation and in vitro phosphatase assay

U2OS cells were extracted by EBC buffer (50 mM Tris, pH 7.5, 150 mM NaCl, 0.5% NP-40, and 1 mM EGTA) followed by sonication (3 × 10 s) and spinning down (20,000 *g* for 10 min). Polyclonal anti-Wip1 (H300; 2 µg/reaction) antibody was incubated with 30 µl protein A/G resin (UltraLink; Thermo Fisher Scientific) and with cell extracts for 4 h at 4°C. As specificity controls, cell extract was incubated with empty beads, and alternatively immobilized antibody was not incubated with cell extract. After extensive washing, beads were mixed with SDS sample buffer and boiled. Immunoprecipitates were probed with polyclonal anti-Wip1 (Bethyl Laboratories, Inc.) and monoclonal anti-Wip1 (Santa Cruz Biotechnology, Inc.). Alternatively, the gel was stained by Coomassie brilliant blue, and immunoprecipitated bands were subjected to MS analysis. Normalized cell extracts from cells expressing FL or truncated FLAG-Wip1 were incubated with M2 agarose (Sigma-Aldrich). In vitro phosphatase assay was performed in a phosphatase buffer (40 mM Hepes, pH 7.4, 100 mM NaCl, 50 mM KCl, 1 mM EGTA, and 50 mM $MgCl_2$) supplemented with 100 µM VEPPLpSQETFS synthetic phosphopeptide (GenScript). Release of phosphate was measured after incubation at 30°C for 20 min using BIOMOL Green reagent (Enzo Life Sciences) and was described previously (Macůrek et al., 2010). Finally, beads containing all immunoprecipitated material were separated by SDS-PAGE and probed for Wip1.

Subcellular fractionation

Soluble and chromatin fractions were prepared as previously described (Macůrek et al., 2010). In brief, soluble cytosolic proteins were extracted from U2OS cells by incubating cells in buffer A (10 mM Hepes, pH 7.9, 10 mM KCl, 1.5 mM $MgCl_2$, 0.34 M sucrose, 10% glycerol, 1 mM DTT, 0.1% Triton X-100, and protease inhibitor cocktail) at 4°C for 10 min and spinning down at 1,500 *g* for 2 min. Soluble nuclear fraction was obtained by extraction of cell nuclei with an equal amount of buffer B (10 mM Hepes, pH 7.9, 3 mM EDTA, 0.2 mM EGTA, and 1 mM DTT) and spinning down at 2,000 *g* for 2 min. Both soluble fractions were mixed (1:1). Insoluble chromatin was washed with buffer B and finally resuspended in SDS sample buffer.

Flow cytometry analysis

Asynchronous cells were transfected with indicated siRNAs (20 nM) and cultured for 48 h before γ-irradiation. To allow determination of cell cycle progression, cells were grown further for 16 h in the presence of 10 µM BrdU and 10 µM S-trityl-L-cysteine (STLC). Cells were collected by trypsinization and either lysed in SDS sample buffer for Western Blot or fixed in ice-cold ethanol for flow cytometry. After incubation in 2M hydrochloric acid and 0.1% Triton X-100, cells were stained with anti-BrdU (replication marker) and anti-mpm2 (mitotic marker) followed by incubation with Alexa Fluor–coupled secondary antibodies. DNA was stained with propidium iodide. Flow cytometry was performed on a cytometer (FACSCalibur; BD), and single cells were analyzed with CellQuest software (BD). As STLC inhibits mitotic kinesin Eg5, cells that progress into mitosis remain arrested in mitosis. This allows identification of cells that were in G1 at the time of IR and remained arrested in the G1 checkpoint (2n DNA content, $BrdU^-mpm2^-$), cells that were in G1/S and progressed to G2 (4n DNA content, $BrdU^+mpm2^-$), cells that were in G1/S and progressed to mitosis (4n DNA content, $BrdU^+mpm2^+$), cells that were in G2 and remained arrested in the G2 checkpoint (4n DNA content, $BrdU^-mpm2^-$), and cells that were in G2 and progressed to mitosis or were in mitosis at the start of the experiment (4n DNA content, $BrdU^-mpm2^+$). The 4n BrdU-negative populations were used to exclude differences in cell cycle distribution at the moment of irradiation. 2n $BrdU^-$ populations were used for quantification of cells remaining in G1. Alternatively, cells were pulsed with 10 µM BrdU (15 min) before irradiation, and BrdU-positive cells were assayed for progression through the G2 phase by FACS analysis of the DNA content (Chen et al., 2001).

Protein stability assay

Cells treated for the indicated times with 50 µg/ml cycloheximide were lysed, and equal amounts of protein were separated on 4–12% Bis-Tris precast gels (NuPAGE; Life Technologies) and probed with the indicated antibodies. Where indicated, cells were treated with 5 µg/ml DMSO or MG-132. Unsaturated films were scanned at 600 dpi as 16-bit grayscale TIFF-formatted images. The densitometry analysis was performed using ImageJ software (National Institutes of Health). No image adjustments were made before the analysis. Signal intensities were normalized to the loading control from the same gel.

MS

Wip1 was immunoprecipitated from U2OS or HeLa cells using a monoclonal anti-Wip1 antibody (Santa Cruz Biotechnology, Inc.; 2 µg/reaction) immobilized on protein A/G UltraLink resin. Samples were separated by SDS-PAGE and stained by protein stain (GelCode; Thermo Fisher Scientific). Proteins corresponding to both forms of Wip1 were digested in gel by trypsin (Promega) and analyzed by peptide mass fingerprinting (9.4T Apex-Qe; Bruker Daltonics). Mass spectra were analyzed and interpreted using DataAnalysis 4.0 and BioTools 3.2 software (Bruker Daltonics).

Mutational analysis

Genomic DNA was isolated from peripheral blood of high-risk, *BRCA1/2*-negative, familial and/or early onset breast (*n* = 280)/ovarian (*n* = 50) cancer patients, unselected colorectal cancer patients (*n* = 304), and noncancer controls (*n* = 450) as described previously (Pohlreich et al., 2005; Kleibl et al., 2009; Ticha et al., 2010). All patients and controls were Caucasians of the Czech descent that gave written informed consent with the genetic testing approved by local ethics committees. PCR amplicons covering all *PPM1D* exons with flanking intronic sequences were obtained using PCR master mix (High Resolution Melting; Roche) and a real-time PCR system (LightCycler 480; Roche). PCR amplification was performed using the following sets of primers: 5′-GCGAGCGCCTAGTGTGTCTCC-3′ and 5′-GCGCCAAACAAGCCAGGGAAC-3′ (exon 1); 5′-GTTGCCATTTGTATCCTGACAGTG-3′ and 5′-CTTCAGTAAAAGGGACAGTAGTAGGTC-3′ (exon 2); 5′-CAGGAATTTTGGCTTATGCATCTTTG-3′ and 5′-AGTAAGGGTTTAGTTCTGTCTCCTC-3′ (exon 3); 5′-CTGTTGCTGTTGTACTATTAGCTTCC-3′ and 5′-TGCAAAAATCTACCCAAGGTCAATG-3′ (exon 4); 5′-GATACAGATGTAGTGGCAGCTAAATC-3′; and 5′-CGCTAACCAAAGAACTGGTGTC-3′ (exon 5); 5′-TGCCATCCTACTAGCTTCATAAGAAG-3′ and 5′-TTGGTCCATGACAGTGTTTGTTG-3′ (exon 6a); and 5′-TTCCAATTGGCCTTGTGCCTA-3′ and 5′-AAAAAAGTTCAACATCGGCACCA-3′ (exon 6b). Altered DNA sequences were identified by subjecting PCR amplicons corresponding to the exons 2–6 to a high-resolution melting analysis (Roche), and samples with aberrant melting profile were bidirectionally sequenced using a genetic analyzer (ABI 3130; Life Technologies). Direct sequencing analysis was performed for the analysis of exon 1. All identified *PPM1D* alterations were reconfirmed by sequencing

of 53BP1 foci was analyzed as in Fig. 2 B. (C) FLAG–Wip1-FL, -R458X, -L484X, -F534X, or -K535X mutants were immunoprecipitated, and phosphatase activity was determined as in Fig. 2 D. (D) Wip1 expression in leukocytes from a healthy control or the #BRCA1855 patient was analyzed by immunoblotting. The asterisk indicates a cross-reacting band in the blood sample. Note the increased expression level of the truncated Wip1 in leukocytes from cancer patient. (E) Mutation of *PPM1D* was analyzed in microdissected mammary noncancer tissue and in cancer tissue from the #BRCA1855 patient. Error bars indicate standard deviations.

Published May 6, 2013

from an independent PCR amplification. The same method was used for the analysis of DNAs isolated from human tumor cell lines. Mutation analysis of amplicon covering exon 6 only was performed in the validation set of another 398 high-risk, *BRCA1/2*-negative breast cancer patients. Mutation analysis in the formalin-fixed, paraffin-embedded breast cancer specimen from a number BRCA1855 patient was performed by sequencing after PCR amplification of exon 6 from DNA isolated from microdissected cancer and noncancer tissue by DNeasy Blood & Tissue kit (QIAGEN).

Online supplemental material

Fig. S1 shows validation of anti-Wip1 antibodies used in this study and data from MS analysis of truncated and FL forms of Wip1 purified from U2OS cells. Fig. S2 demonstrates that the G1 but not G2 checkpoint is affected in cells with truncated Wip1. Table S1 contains data from mutational analysis of the *PPM1D* gene and anamnestic data of *PPM1D* mutation carriers. Online supplemental material is available at http://www.jcb.org/cgi/content/full/jcb.201210031/DC1.

We are thankful to Dr. Staňek for making the Scan^R microscope available, Dr. Novák (Institute of Molecular Genetics, Prague) for MS analysis, and Dr. Zimovjanová and Dr. Novotný (Department of Oncology, General University Hospital in Prague) for help with clinical samples.

This work was supported by the Grant Agency of the Czech Republic (P301/10/1525, P305/12/2485 and 13-18392S), an institutional grant from the Academy of Sciences of the Czech Republic (RVO68378050), the European Commission (Trireme and Biomedreg), Netherlands Genomic Initiative of Nederlandse organisatie voor Wetenschappelijk Onderzoek (Cancer Genomics Center), Dutch Cancer Society (UU2009-4478), Grant Agency of the Ministry of Health of the Czech Republic (NT13343-4), and Charles University in Prague (PRVOUK-P27/LF1/1).

Submitted: 5 October 2012
Accepted: 11 April 2013

References

Agami, R., and R. Bernards. 2000. Distinct initiation and maintenance mechanisms cooperate to induce G1 cell cycle arrest in response to DNA damage. *Cell*. 102:55–66. http://dx.doi.org/10.1016/S0092-8674(00)00010-6

Bartkova, J., Z. Horejsí, K. Koed, A. Krämer, F. Tort, K. Zieger, P. Guldberg, M. Sehested, J.M. Nesland, C. Lukas, et al. 2005. DNA damage response as a candidate anti-cancer barrier in early human tumorigenesis. *Nature*. 434:864–870. http://dx.doi.org/10.1038/nature03482

Bartkova, J., N. Rezaei, M. Liontos, P. Karakaidos, D. Kletsas, N. Issaeva, L.-V.F. Vassiliou, E. Kolettas, K. Niforou, V.C. Zoumpourlis, et al. 2006. Oncogene-induced senescence is part of the tumorigenesis barrier imposed by DNA damage checkpoints. *Nature*. 444:633–637. http://dx.doi.org/10.1038/nature05268

Bulavin, D.V., O.N. Demidov, S.i. Saito, P. Kauraniemi, C. Phillips, S.A. Amundson, C. Ambrosino, G. Sauter, A.R. Nebreda, C.W. Anderson, et al. 2002. Amplification of PPM1D in human tumors abrogates p53 tumor-suppressor activity. *Nat. Genet.* 31:210–215. http://dx.doi.org/10.1038/ng894

Bulavin, D.V., C. Phillips, B. Nannenga, O. Timofeev, L.A. Donehower, C.W. Anderson, E. Appella, and A.J. Fornace Jr. 2004. Inactivation of the Wip1 phosphatase inhibits mammary tumorigenesis through p38 MAPK-mediated activation of the p16(Ink4a)-p19(Arf) pathway. *Nat. Genet.* 36:343–350. http://dx.doi.org/10.1038/ng1317

Castellino, R.C., M. De Bortoli, X. Lu, S.-H. Moon, T.-A. Nguyen, M.A. Shepard, P.H. Rao, L.A. Donehower, and J.Y. Kim. 2008. Medulloblastomas overexpress the p53-inactivating oncogene WIP1/PPM1D. *J. Neurooncol.* 86:245–256. http://dx.doi.org/10.1007/s11060-007-9470-8

Chen, M.-S., J. Hurov, L.S. White, T. Woodford-Thomas, and H. Piwnica-Worms. 2001. Absence of apparent phenotype in mice lacking Cdc25C protein phosphatase. *Mol. Cell. Biol.* 21:3853–3861. http://dx.doi.org/10.1128/MCB.21.12.3853-3861.2001

Di Micco, R., M. Fumagalli, A. Cicalese, S. Piccinin, P. Gasparini, C. Luise, C. Schurra, M. Garre', P.G. Nuciforo, A. Bensimon, et al. 2006. Oncogene-induced senescence is a DNA damage response triggered by DNA hyper-replication. *Nature*. 444:638–642. http://dx.doi.org/10.1038/nature05327

el-Deiry, W.S., T. Tokino, V.E. Velculescu, D.B. Levy, R. Parsons, J.M. Trent, D. Lin, W.E. Mercer, K.W. Kinzler, and B. Vogelstein. 1993. WAF1, a potential mediator of p53 tumor suppression. *Cell*. 75:817–825. http://dx.doi.org/10.1016/0092-8674(93)90500-P

Fiscella, M., H. Zhang, S. Fan, K. Sakaguchi, S. Shen, W.E. Mercer, G.F. Vande Woude, P.M. O'Connor, and E. Appella. 1997. Wip1, a novel human protein phosphatase that is induced in response to ionizing radiation in a p53-dependent manner. *Proc. Natl. Acad. Sci. USA*. 94:6048–6053. http://dx.doi.org/10.1073/pnas.94.12.6048

Gorgoulis, V.G., L.-V.F. Vassiliou, P. Karakaidos, P. Zacharatos, A. Kotsinas, T. Liloglou, M. Venere, R.A. Ditullio Jr., N.G. Kastrinakis, B. Levy, et al. 2005. Activation of the DNA damage checkpoint and genomic instability in human precancerous lesions. *Nature*. 434:907–913. http://dx.doi.org/10.1038/nature03485

Halazonetis, T.D., V.G. Gorgoulis, and J. Bartek. 2008. An oncogene-induced DNA damage model for cancer development. *Science*. 319:1352–1355. http://dx.doi.org/10.1126/science.1140735

Hollstein, M., D. Sidransky, B. Vogelstein, and C.C. Harris. 1991. p53 mutations in human cancers. *Science*. 253:49–53. http://dx.doi.org/10.1126/science.1905840

Jackson, S.P., and J. Bartek. 2009. The DNA-damage response in human biology and disease. *Nature*. 461:1071–1078. http://dx.doi.org/10.1038/nature08467

Kleibl, Z., O. Havranek, I. Hlavata, J. Novotny, J. Sevcik, P. Pohlreich, and P. Soucek. 2009. The CHEK2 gene I157T mutation and other alterations in its proximity increase the risk of sporadic colorectal cancer in the Czech population. *Eur. J. Cancer*. 45:618–624. http://dx.doi.org/10.1016/j.ejca.2008.09.022

Knudson, A.G. 2002. Cancer genetics. *Am. J. Med. Genet.* 111:96–102. http://dx.doi.org/10.1002/ajmg.10320

Le Guezennec, X., and D.V. Bulavin. 2010. WIP1 phosphatase at the crossroads of cancer and aging. *Trends Biochem. Sci.* 35:109–114. http://dx.doi.org/10.1016/j.tibs.2009.09.005

Li, J., Y. Yang, Y. Peng, R.J. Austin, W.G. van Eyndhoven, K.C.Q. Nguyen, T. Gabriele, M.E. McCurrach, J.R. Marks, T. Hoey, et al. 2002. Oncogenic properties of PPM1D located within a breast cancer amplification epicenter at 17q23. *Nat. Genet.* 31:133–134. http://dx.doi.org/10.1038/ng888

Liang, C., E. Guo, S. Lu, S. Wang, C. Kang, L. Chang, L. Liu, G. Zhang, Z. Wu, Z. Zhao, et al. 2012. Over-expression of wild-type p53-induced phosphatase 1 confers poor prognosis of patients with gliomas. *Brain Res.* 1444:65–75. http://dx.doi.org/10.1016/j.brainres.2011.12.052

Lindqvist, A., M. de Bruijn, L. Macurek, A. Brás, A. Mensinga, W. Bruinsma, O. Voets, O. Kranenburg, and R.H. Medema. 2009. Wip1 confers G2 checkpoint recovery competence by counteracting p53-dependent transcriptional repression. *EMBO J.* 28:3196–3206. http://dx.doi.org/10.1038/emboj.2009.246

Lu, X., B. Nannenga, and L.A. Donehower. 2005. PPM1D dephosphorylates Chk1 and p53 and abrogates cell cycle checkpoints. *Genes Dev.* 19:1162–1174. http://dx.doi.org/10.1101/gad.1291305

Macůrek, L., A. Lindqvist, O. Voets, J. Kool, H.R. Vos, and R.H. Medema. 2010. Wip1 phosphatase is associated with chromatin and dephosphorylates gammaH2AX to promote checkpoint inhibition. *Oncogene*. 29:2281–2291. http://dx.doi.org/10.1038/onc.2009.501

Mailand, N., J. Falck, C. Lukas, R.G. Syljuâsen, M. Welcker, J. Bartek, and J. Lukas. 2000. Rapid destruction of human Cdc25A in response to DNA damage. *Science*. 288:1425–1429. http://dx.doi.org/10.1126/science.288.5470.1425

Medema, R.H., and L. Macůrek. 2012. Checkpoint control and cancer. *Oncogene*. 31:2601–2613. http://dx.doi.org/10.1038/onc.2011.451

Mulligan, L.M., J.B.J. Kwok, C.S. Healey, M.J. Elsdon, C. Eng, E. Gardner, D.R. Love, S.E. Mole, J.K. Moore, L. Papi, et al. 1993. Germ-line mutations of the RET proto-oncogene in multiple endocrine neoplasia type 2A. *Nature*. 363:458–460. http://dx.doi.org/10.1038/363458a0

Nannenga, B., X. Lu, M. Dumble, M. Van Maanen, T.-A. Nguyen, R. Sutton, T.R. Kumar, and L.A. Donehower. 2006. Augmented cancer resistance and DNA damage response phenotypes in PPM1D null mice. *Mol. Carcinog.* 45:594–604. http://dx.doi.org/10.1002/mc.20195

Nguyen, T.-A., S.D. Slattery, S.-H. Moon, Y.F. Darlington, X. Lu, and L.A. Donehower. 2010. The oncogenic phosphatase WIP1 negatively regulates nucleotide excision repair. *DNA Repair (Amst.)*. 9:813–823. http://dx.doi.org/10.1016/j.dnarep.2010.04.005

Nishida, T., S. Hirota, M. Taniguchi, K. Hashimoto, K. Isozaki, H. Nakamura, Y. Kanakura, T. Tanaka, A. Takabayashi, H. Matsuda, and Y. Kitamura. 1998. Familial gastrointestinal stromal tumours with germline mutation of the KIT gene. *Nat. Genet.* 19:323–324. http://dx.doi.org/10.1038/1209

Pärssinen, J., E.-L. Alarmo, R. Karhu, and A. Kallioniemi. 2008. PPM1D silencing by RNA interference inhibits proliferation and induces apoptosis in breast cancer cell lines with wild-type p53. *Cancer Genet. Cytogenet.* 182:33–39. http://dx.doi.org/10.1016/j.cancergencyto.2007.12.013

Pohlreich, P., M. Zikan, J. Stribrna, Z. Kleibl, M. Janatova, J. Kotlas, J. Zidovska, J. Novotny, L. Petruzelka, C. Szabo, and B. Matous. 2005. High proportion of recurrent germline mutations in the BRCA1 gene in breast and ovarian cancer patients from the Prague area. *Breast Cancer Res.* 7:R728–R736. http://dx.doi.org/10.1186/bcr1282

Rauta, J., E.-L. Alarmo, P. Kauraniemi, R. Karhu, T. Kuukasjärvi, and A. Kallioniemi. 2006. The serine-threonine protein phosphatase PPM1D is frequently activated through amplification in aggressive primary breast tumours. *Breast Cancer Res. Treat.* 95:257–263. http://dx.doi.org/10.1007/s10549-005-9017-7

Ruark, E., K. Snape, P. Humburg, C. Loveday, I. Bajrami, R. Brough, D.N. Rodrigues, A. Renwick, S. Seal, E. Ramsay, et al; Breast and Ovarian Cancer Susceptibility Collaboration; Wellcome Trust Case Control Consortium. 2013. Mosaic PPM1D mutations are associated with predisposition to breast and ovarian cancer. *Nature*. 493:406–410. http://dx.doi.org/10.1038/nature11725

Saito-Ohara, F., I. Imoto, J. Inoue, H. Hosoi, A. Nakagawara, T. Sugimoto, and J. Inazawa. 2003. PPM1D is a potential target for 17q gain in neuroblastoma. *Cancer Res.* 63:1876–1883.

Sakaue-Sawano, A., H. Kurokawa, T. Morimura, A. Hanyu, H. Hama, H. Osawa, S. Kashiwagi, K. Fukami, T. Miyata, H. Miyoshi, et al. 2008. Visualizing spatiotemporal dynamics of multicellular cell-cycle progression. *Cell*. 132:487–498. http://dx.doi.org/10.1016/j.cell.2007.12.033

Schmidt, L., F.-M. Duh, F. Chen, T. Kishida, G. Glenn, P. Choyke, S.W. Scherer, Z. Zhuang, I. Lubensky, M. Dean, et al. 1997. Germline and somatic mutations in the tyrosine kinase domain of the MET proto-oncogene in papillary renal carcinomas. *Nat. Genet.* 16:68–73. http://dx.doi.org/10.1038/ng0597-68

Ticha, I., Z. Kleibl, J. Stribrna, J. Kotlas, M. Zimovjanova, M. Mateju, M. Zikan, and P. Pohlreich. 2010. Screening for genomic rearrangements in BRCA1 and BRCA2 genes in Czech high-risk breast/ovarian cancer patients: high proportion of population specific alterations in BRCA1 gene. *Breast Cancer Res. Treat.* 124:337–347. http://dx.doi.org/10.1007/s10549-010-0745-y

Vogelstein, B., and K.W. Kinzler. 2004. Cancer genes and the pathways they control. *Nat. Med.* 10:789–799. http://dx.doi.org/10.1038/nm1087

Vogelstein, B., D. Lane, and A.J. Levine. 2000. Surfing the p53 network. *Nature*. 408:307–310. http://dx.doi.org/10.1038/35042675

3.3 Inhibition of WIP1 phosphatase sensitizes breast cancer cells to genotoxic stress and to MDM2 antagonist nutlin-3

Pechackova S, Burdova K, Benada J, Kleiblova P, Jenikova G, Macurek L.

Oncotarget. 2016 Mar 22; 7(12):14458-75. doi: 10.18632/oncotarget.7363.

Here we have validated the specificity of currently available inhibitors of WIP1 on the cellular model with the CRISPR-Cas9-mediated knock-out of the *PPM1D* in U2OS cells. We demonstrated that while the novel allosteric modulator GSK2830371 specifically inhibits the growth of cancer cells, the compound CCT007093 slightly suppressed cell growth, independently on the presence of WIP1. Significantly, we observed that inhibition of WIP1 by GSK2830371 suppressed the growth of the breast cancer cell lines with amplified *PPM1D* and upregulated their response to DNA damage.

In this type of the cancer cells, allosteric WIP1 inhibition was not sufficient to affect cell viability but we found the combined treatment with GSK2830371, doxorubicin and MDM2 antagonist (nutlin-3) promotes induction of senescence and/or apoptosis in a p53 and dose-dependent manner. Our results support that WIP1 inhibition is a promising candidate for the therapy of breast cancers with amplified *PPM1D* and wild-type *TP53*. Moreover, sensitization of cancer cells by WIP1 inhibition can be beneficial to decrease adverse effects of the genotoxic or cytotoxic effect of chemotherapy.

P. S. designed and performed the experiments, wrote materials and methods, and coordinated the manuscript.

Inhibition of WIP1 phosphatase sensitizes breast cancer cells to genotoxic stress and to MDM2 antagonist nutlin-3

Sona Pechackova[1,*], Kamila Burdova[1,*], Jan Benada[1], Petra Kleiblova[1,2], Gabriela Jenikova[1], Libor Macurek[1]

[1]Department of Cancer Cell Biology, Institute of Molecular Genetics of the ASCR, CZ-14220 Prague, Czech Republic

[2]Institute of Biochemistry and Experimental Oncology, Charles University in Prague, CZ-12853 Prague, Czech Republic

[*]These authors have contributed equally to this work

Correspondence to: *Libor Macurek,* ***e-mail:*** *libor.macurek@img.cas.cz*

Keywords: *WIP1 inhibitor, p53, checkpoint, nutlin-3, breast cancer*

Received: *October 31, 2015* ***Accepted:*** *January 29, 2016* ***Published:*** *February 13, 2016*

ABSTRACT

PP2C family serine/threonine phosphatase WIP1 acts as a negative regulator of the tumor suppressor p53 and is implicated in silencing of cellular responses to genotoxic stress. Chromosomal locus 17q23 carrying the *PPM1D* (coding for WIP1) is commonly amplified in breast carcinomas and WIP1 was proposed as potential pharmacological target. Here we employed a cellular model with knocked out *PPM1D* to validate the specificity and efficiency of GSK2830371, novel small molecule inhibitor of WIP1. We have found that GSK2830371 increased activation of the DNA damage response pathway to a comparable level as the loss of *PPM1D*. In addition, GSK2830371 did not affect proliferation of cells lacking *PPM1D* but significantly supressed proliferation of breast cancer cells with amplified *PPM1D*. Over time cells treated with GSK2830371 accumulated in G1 and G2 phases of the cell cycle in a p21-dependent manner and were prone to induction of senescence by a low dose of MDM2 antagonist nutlin-3. In addition, combined treatment with GSK2830371 and doxorubicin or nutlin-3 potentiated cell death through a strong induction of p53 pathway and activation of caspase 9. We conclude that efficient inhibition of WIP1 by GSK2830371 sensitizes breast cancer cells with amplified *PPM1D* and wild type p53 to chemotherapy.

INTRODUCTION

Cells exposed to genotoxic stress protect their genome integrity by activation of a conserved DNA damage response pathway that orchestrates DNA repair and represents an intrinsic barrier preventing genome instability and tumorigenesis [1, 2]. A core component of this pathway is the tumor suppressor p53 that controls cell fate decisions. Depending on the amplitude and duration of its activation, p53 promotes temporary cell cycle arrest (checkpoint), permanent withdrawal from the cell cycle (senescence) or programmed cell death (apoptosis) [3–5]. Under basal conditions, function of the p53 is suppressed by an E3 ubiquitin ligase MDM2 and its enzymatically inactive homologue MDMX that control p53 stability and transcriptional activity, respectively [6, 7]. Genotoxic stress triggers activation of ATM/ATR, Chk1/Chk2 and other kinases that extensively phosphorylate the N-terminal domain of p53, MDM2 and MDMX allowing stabilization of the p53 and promoting expression of its target genes [8–11]. One of the p53 target genes is *PPM1D* that codes for a Protein phosphatase 2C isoform delta (hereafter referred to as WIP1) [12]. Expression of WIP1 is induced by genotoxic stress and forming a negative feedback loop, WIP1 efficiently inhibits the p53 pathway by a direct dephosphorylation of p53 at Ser15 and also by dephosphorylation of its negative regulators MDM2 and MDMX [13–16]. By inactivating the p53 pathway, WIP1 promotes recovery from the G2 checkpoint [17, 18]. Moreover, WIP1 dephosphorylates other proteins including ATM, Chk1, Chk2, p38 and γH2AX which contributes to the termination of the DNA damage response [19–24]. In addition, WIP1 was reported to prevent premature senescence in various cell types and tissue compartments [21, 25, 26].

Chromosomal locus 17q23 carrying the *PPM1D* gene is commonly amplified in various human tumors including breast, ovarian and gastric cancer, neuroblastoma and lung adenocarcinoma [27–34]. In particular, amplification of the *PPM1D* occurs in approximately 10 % of breast tumors, typically those that retain wild type p53 [31, 35, 36]. In addition, about one third of breast tumors with amplified *PPM1D* locus also contain amplification of the *ERBB2/HER2* oncogene suggesting that both genes may jointly promote tumor development [36]. Indeed, MMTV-driven overexpression of *Ppm1d* potentiated *Erbb2*-induced breast tumor development in mice [37]. Comparably less common than *PPM1D* amplifications are rare nonsense mutations in the exon 6 of *PPM1D* that result in expression of abnormally stable WIP1 and promote development of breast and ovary cancer [38–40].

Reactivation of the p53 function by various MDM2 or MDMX antagonists and other small molecule p53 activators has been proposed as promising strategy for treatment of cancers with the wild-type p53 [41–45]. Nutlin-3 is a potent and selective antagonist of the interaction between MDM2 and p53 (IC50 of 90 nM) [46]. Treatment with nutlin-3 activates the p53 pathway and depending on the dose induces cell cycle arrest or cell death [46]. RG7388, an orally available analogue of nutlin-3, efficiently suppressed tumor growth *in vivo* [47]. Clinical trials are currently ongoing to prove clinical efficacy of MDM2 antagonists in cancer therapy. Reactivation of p53 pathway can be also achieved by inhibition of WIP1 and indeed WIP1 was proposed a potential pharmacological target in cancer therapy [21, 48]. Loss of *Ppm1d* dramatically delayed the development of Erbb2-induced breast cancer, MYC-induced lymphoma and APC^{min}-induced intestinal tumors in mice [49–52]. In addition, depletion of WIP1 using RNA interference has been shown to efficiently suppress growth of various human cancer cells [30, 53–55]. However, translation of these observations into clinics is challenging due to the lack of suitable WIP1 inhibitors with sufficient specificity and favourable pharmacokinetic properties. Cyclic phosphopeptides that mimic substrates of WIP1 can block its phosphatase activity *in vitro*, but their efficiency in cells still remains to be addressed [56, 57]. A high-throughput screening identified a small molecule CCT007093 that inhibited WIP1 *in vitro* (IC50 = 8.4 μM) and eradicated WIP1 overexpressing tumor cells [58]. However, the specificity of CCT007093 towards WIP1 may be low in cells [59]. Small molecules SPI-001 and its analogue SL-176 inhibited WIP1 *in vitro* (IC50 = 86.9 nM and 110 nM and, respectively) and supressed growth of cells with the C-terminally truncated or overexpressed WIP1 but their efficiency at organismal level still needs to be tested [60–62]. Novel orally available inhibitor of WIP1 phosphatase GSK2830371 has recently been shown to selectively inhibit WIP1 *in vitro* (IC50 = 6 nM) and to efficiently suppress growth of a subset of hematopoietic tumor cell lines and neuroblastoma cells with overexpression of WIP1 [63, 64].

Here we aimed to validate the specificity and efficiency of the commercially available WIP1 inhibitors in blocking proliferation of the breast cancer cells. We have found that GSK2830371 suppressed growth of breast cancer cells with amplified *PPM1D* gene in a p53-dependent manner which is in good agreement with previous RNAi-based studies. In addition, we have found that inhibition of WIP1 is not sufficient to induce cell death in cancer cells but rather slows down proliferation by extending G1 and G2 phases of the cell cycle. However, breast cancer cells treated with WIP1 inhibitor are more sensitive to DNA damage-inducing chemotherapy and to MDM2 antagonist nutlin-3. Combined treatment with these drugs triggers senescence or programmed cell death and can efficiently eradicate p53 positive breast cancer cells. Our data validate GSK2830371 as potent and selective inhibitor of WIP1 that sensitizes breast cancer cells to chemotherapy.

RESULTS

WIP1 inhibition impairs proliferation of breast cancer cells with amplified PPM1D and wt-p53

To test the specificity of the novel WIP1 inhibitors in a cellular model, we generated U2OS-*PPM1D*-KO cells with the CRISPR-mediated knock-out of the *PPM1D* gene and determined the effect of CCT007093 or GSK2830371 compounds on cell growth (Figure 1A). Surprisingly, we have found that the effect of CCT007093 was not dependent on the presence of WIP1. In contrast, GSK2830371 showed a dose-dependent suppression of cell growth in parental U2OS but not in U2OS-*PPM1D*-KO cells. Next, we compared the ability of both compounds to potentiate a DNA damage-induced phosphorylation of two established substrates of WIP1 phosphatase, histone variant H2AX phosphorylated at Ser139 (referred to as γH2AX) and p53 phosphorylated at Ser15 (Figure 1B and 1C). We have not observed any significant differences in cells treated with DMSO and CCT007093 (10 μM) suggesting that CCT007093 does not block the activity of WIP1 in cells. In contrast, levels of γH2AX and pS15-p53 were increased in cells treated with GSK2830371 (0.5 μM) consistent with the expected inhibition of WIP1 activity. In accordance with a previous report we also observed a reduced level of WIP1 in the presence of an allosteric inhibitor GSK2830371 [63]. To further assess the efficiency of WIP1 inhibition, we compared responses to ionizing radiation in U2OS-*PPM1D*-KO cells and U2OS cells treated with GSK2830371 (Figure 1D). We found that treatment with GSK2830371 (0.5 μM) increased the phosphorylation of γH2AX and pS15-p53 and expression of p21 to comparable levels as the knock-out of *PPM1D* strongly indicating that GSK2830371 efficiently blocks WIP1 activity in cells.

Having established efficient concentration of GSK2830371 that specifically affects growth of U2OS cells, we continued with testing the sensitivity of breast cancer cells to GSK2830371. First, we tested the effect of WIP1 inhibition on cell proliferation in MCF7 cells that have massively amplified *PPM1D* locus at 17q22/q23 and harbouring wild-type p53 [31, 65]. Using cell proliferation and colony formation assays we observed

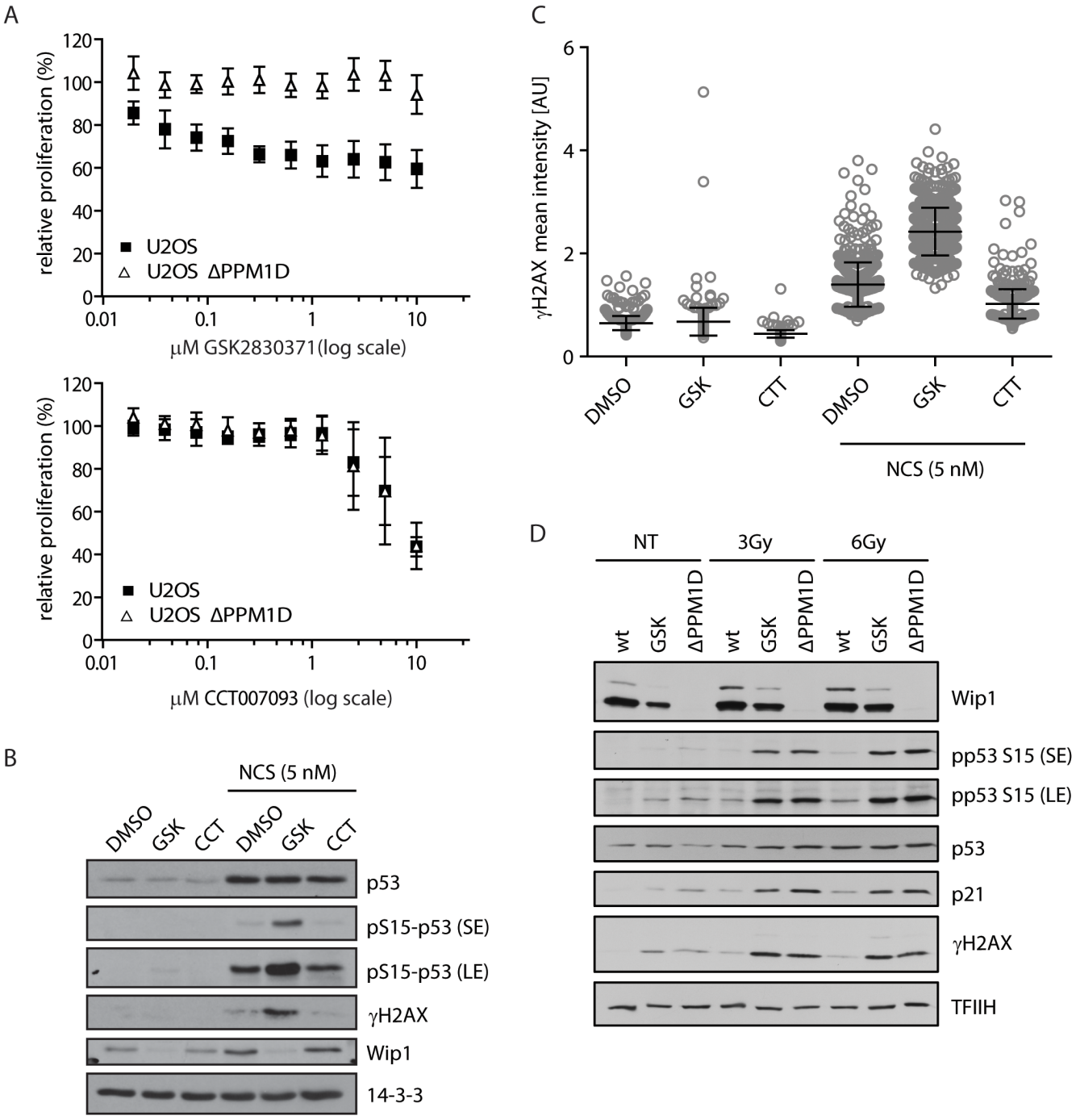

Figure 1: Validation of WIP1 inhibitors in U2OS-PPM1D-KO cells. A. U2OS or U2OS-*PPM1D*-KO cells were treated with DMSO, CCT007093 or GSK2830371 at indicated doses and relative cell proliferation was measured after 7 days. Error bars represent SD. **B, C.** U2OS cells were treated with DMSO, CCT007093 (10 μM, CCT) or GSK2830371 (0.5 μM, GSK) and DNA damage was induced by 5 nM neocarzinostatin (NCS) for 5 h. Cells were analyzed by immunoblotting (B) or fixed and nuclear γH2AX intensity was determined by immunofluorescent staining and microscopy analysis C. Dots represent individual cells. Error bars represent SD. **D.** U2OS or U2OS-*PPM1D*-KO (ΔPPM1D) cells were treated with DMSO or GSK2830371 (0.5 μM), exposed to ionizing radiation (3 and 6 Gy) and analysed by immunoblotting using indicated antibodies. Short exposure (SE) or long exposure (LE) is shown.

dramatic reduction of cell growth after inhibition of WIP1 (Figure 2A and 2B). Reduction of cell proliferation by GSK2830371 showed EC50=0.3 μM in MCF7 cells which is in good agreement with a previous report [63]. In contrast, we have found that MCF7 cells with knocked-out *TP53* were less sensitive to GSK2830371 (Figure 2A and 2C). Similarly, we observed only a minor effect of GSK2830371 in BT-474 cells that contain amplification of the *PPM1D* but have inactivating mutation in *TP53* [65] (Figure 2D). Thus the effect of WIP1 inhibition on breast cancer cell proliferation depends on the intact p53 pathway as previously reported for haematological cancer cells [63]. Next we tested the sensitivity of CAL-51 breast cancer cells that contain a normal number of *PPM1D* alleles and wild type p53 (Figure 2D). We have found that CAL-51 cells were resistant to the treatment with GSK2830371 suggesting that cells with amplified *PPM1D* might be addicted to the high WIP1 activity whereas cells with normal levels of WIP1 can tolerate inhibition of WIP1 and proliferate also in the presence of GSK2830371. Finally, we tested the impact of GSK2830371 on proliferation of nontransformed cells. A dose of GSK2830371 that efficiently supressed growth of U2OS and MCF7 cells did not affect proliferation of BJ fibroblasts, hTERT-immortalized human retinal pigment epithelial cells (RPE) or SV40-immortalized human colon epithelia cells (HCE) indicating that inhibition of WIP1 is well tolerated by nontransformed cells (Figure 2E)

WIP1 inhibition delays progression through G1 and G2 phases of the cell cycle

Since we observed a strong reduction of the proliferating breast cancer cells population following WIP1 inhibition, we asked what the fate of the cells treated with GSK2830371 was. We found that GSK2830371 did not significantly affect the viability of MCF7 cells, suggesting that inhibition of WIP1 is not sufficient to induce cell death (Figure 3A). Instead we found that inhibition of WIP1 slowed down proliferation of MCF7 cells monitored by a dilution of CFSE dye in daughter cells (Figure 3B). The effect of GSK2830371 on the proliferation rate was fully dependent on p53 and p21 since we observed no differences in dilution of CFSE dye in MCF7-P53-KO or MCF7-P21-KO cells treated with WIP1 inhibitor (Figure 3B). Next we determined the effect of GSK2830371 on the cell cycle progression in MCF7 and BT-474 cells (Figure 3C). We have noted an accumulation of MCF7 cells in G1 phase 24 h after treatment with GSK2830371 (0.5 μM), whereas fraction of G2 cells was enriched in the later time points (48-72 h). This suggests that progression through G1 is slowed down in MCF7 cells early after addition of GSK2830371. Eventually cells progress through S phase to the G2 where they also progress more slowly compared to control cells. We did not observe any enrichment in the fraction of mitotic cells in the presence of GSK2830371 indicating that progression through mitosis was not affected by inhibition of WIP1 which is in good agreement with described degradation of WIP1 during prometaphase [66]. In contrast, no effect on the cell cycle progression was observed in BT-474, suggesting that observed extension of G1 and G2 phases depends on the ability to activate the p53 pathway (Figure 3C). Immunoblot analysis of MCF7 cells revealed that addition of GSK2830371 resulted in a rapid phosphorylation of p53 at Ser15 (Figure 3D). Two days after addition of GSK2830371, MCF7 cells showed increased levels of p21 which indicated a strong activation of the p53 pathway (Figure 3D). Consistent with no effect on the cell cycle progression and with the impaired p53 pathway, BT-474 cells did not show any induction of p21 levels after GSK2830371 administration (Figure 3E). Finally, we have found no effect on the cell cycle distribution in MCF7-P53-KO and MCF7-P21-KO cells treated with GSK2830371 further confirming that the effect of WIP1 inhibition on the progression through the cell cycle fully depends on the p53/p21 pathway (Figure 3F).

WIP1 inhibition promotes DNA damage-induced checkpoint arrest

We have previously shown that WIP1 is required for recovery from the DNA damage-induced G2 checkpoint [17]. Therefore, we tested the effect of GSK2830371 inhibitor on the ability of MCF7 cells to establish the G2 checkpoint. Whereas about 70 % of the control cells progressed to mitosis at 20 h after exposure to ionizing radiation, cells treated with GSK2830371 remained arrested in the G2 (Figure 4A). It has been reported that normal diploid RPE cells do not require WIP1 activity for recovery from the G1 checkpoint [18]. In the same time, C-terminally truncated WIP1 present in U2OS and HCT116 cells impairs activation of the G1 checkpoint [39]. To determine the contribution of the overexpressed WIP1 in suppression of the G1 checkpoint in MCF7 cells we compared fractions of cells remaining in G1 after exposure to ionizing radiation. Following exposure to a low dose of ionizing radiation (3 Gy, IR), MCF7 cells treated with GSK2830371 showed stronger accumulation in the G1 checkpoint compared to untreated cells (Figure 4B). To test how long these effects of WIP1 inhibition can persist we followed MCF7 cells for 3 to 6 days after irradiation and treatment with GSK2830371. We have found that cells with inhibited WIP1 did not incorporate BrdU three days after irradiation and that a substantial fraction of cells was arrested in the G2 checkpoint (Figure 4C and 4D). At 6 days after irradiation, we noted a dramatically reduced growth of cells exposed to a low dose (3 Gy) of IR and GSK2830371 (Figure 4E and 4F). Comparably smaller differences were observed after high dose of IR (6 Gy) when similar fractions of cells remained arrested regardless of the activity of WIP1 (Figure 4E and 4F).

WIP1 inhibition sensitizes cells to genotoxic stress and to MDM2 inhibitor nutlin-3

Since we observed potentiation of the IR-induced checkpoint arrest after inhibition of WIP1 we decided to test the combination of GSK2830371 with various chemotherapeutics causing genotoxic stress. High dose of doxorubicin (0.5 μM) strongly suppressed proliferation of MCF7 cells, which is consistent with extensive DNA damage caused by inhibition of topoisomerase II (Figure 4A). In contrast, low dose of doxorubicin (0.05 μM) caused only mild activation of p53 pathway and was

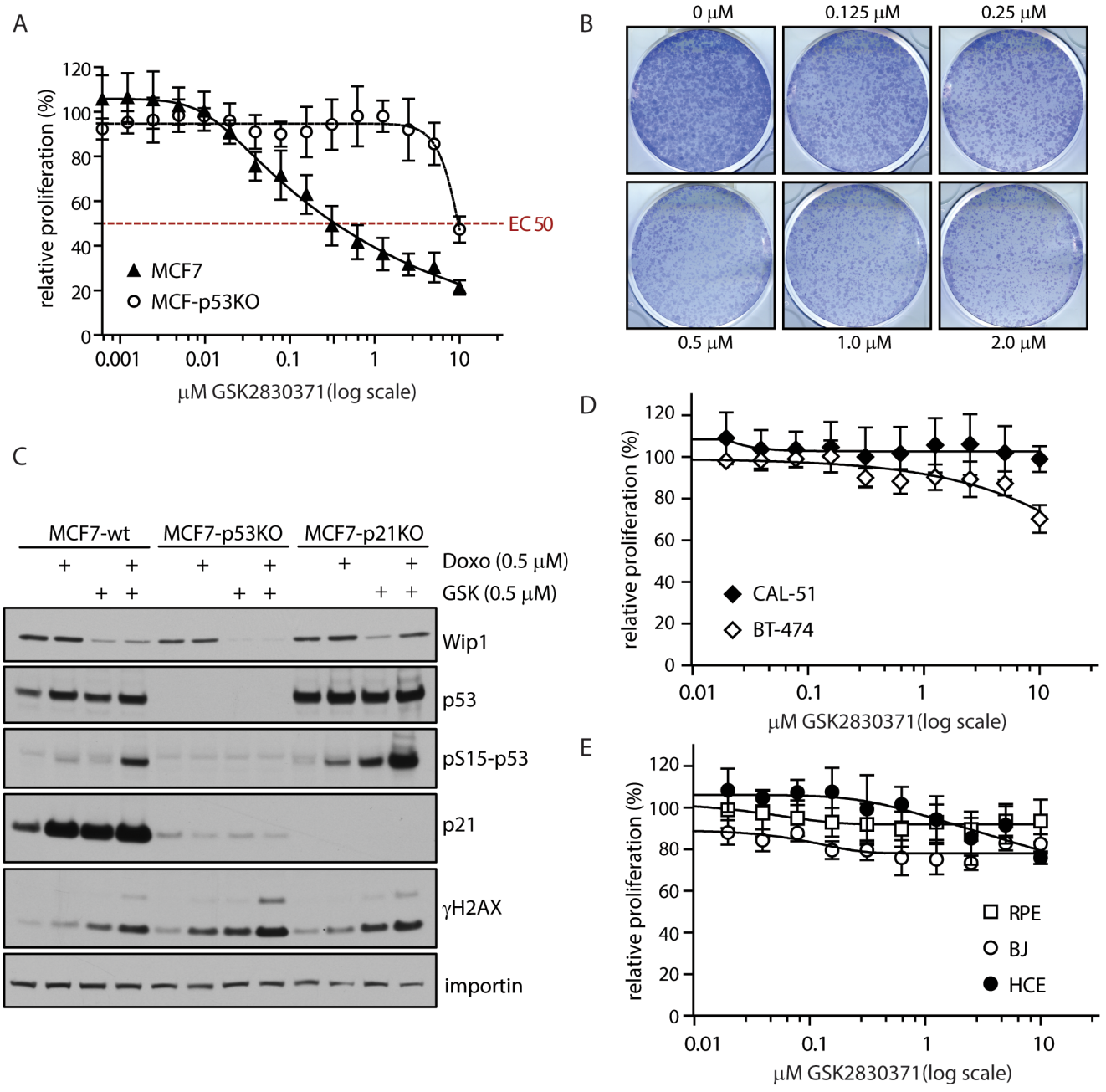

Figure 2: Inhibition of WIP1 impairs proliferation of cancer cells with amplified *PPM1D*. A. MCF7 or MCF7-P53-KO cells were treated with indicated doses of GSK2830371 and relative cell proliferation was measured after 7 days. Error bars represent SD. **B.** MCF7 cells were treated with indicated doses of GSK2830371 and cell proliferation was determined by colony formation assay after 7 days. Representative image from three independent experiments is shown. **C.** MCF7, MCF7-P53-KO or MCF7-P21-KO cells were treated with DMSO, GSK2830371 (0.5 μM), doxorubicin (0.5 μM) or combination of both and cells were analyzed by immunoblotting after 24 h. **D.** BT-474 or CAL-51 cells were treated with indicated doses of GSK2830371 and relative cell proliferation was measured after 7 days. Error bars represent SD. **E.** BJ fibroblasts, hTERT-RPE1 cells or human colon epithelia cells (HCE) were treated with indicated doses of GSK2830371 and relative cell proliferation was measured after 7 days. Error bars represent SD.

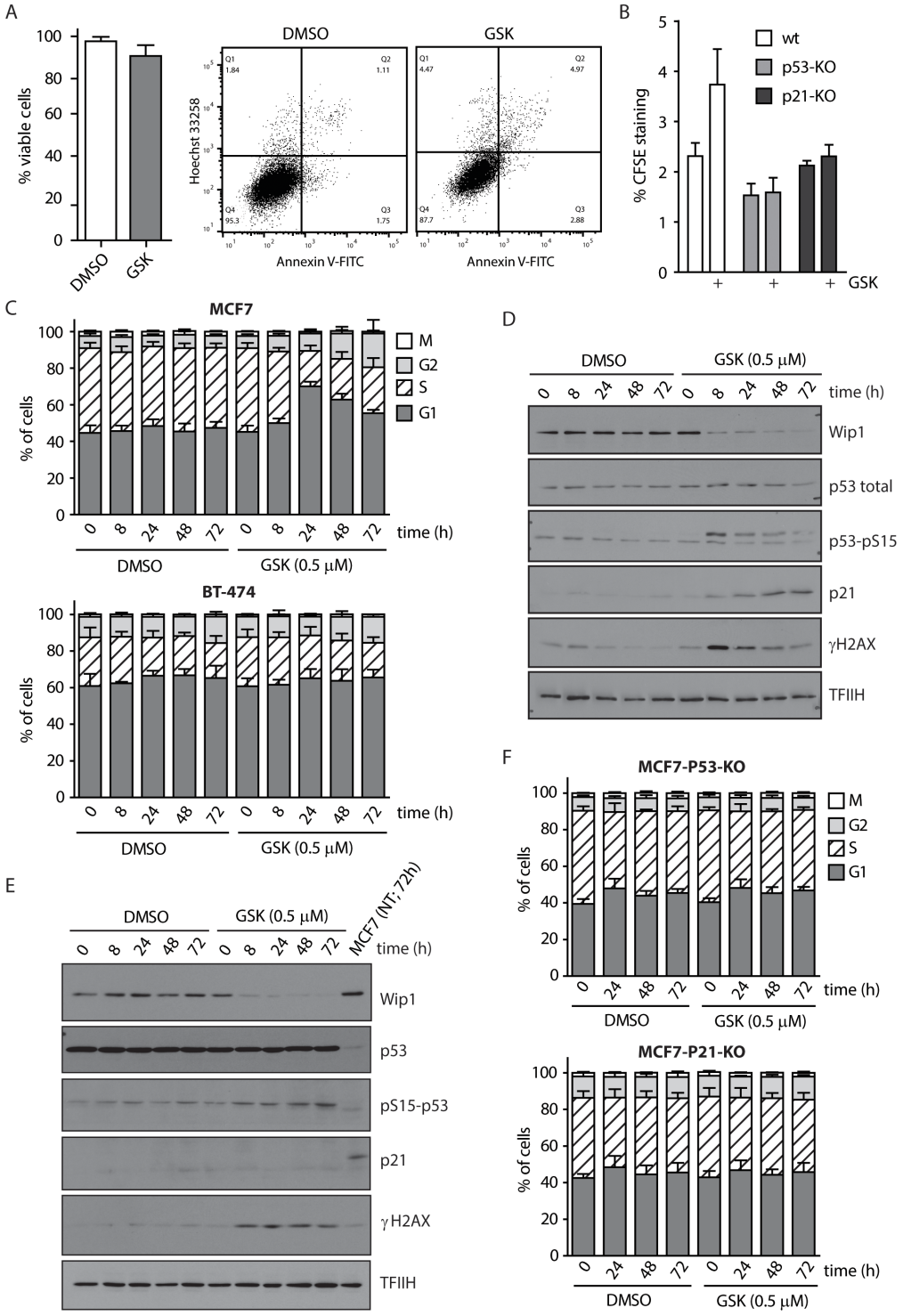

Figure 3: WIP1 inhibition leads to G1 and G2 phase accumulation in MCF7 cells. A. MCF7 cells were treated with DMSO or GSK2830371 (0.5 μM) for 5 days and percentage of living cells (Hoechst/Annexin V negative) was determined by flow cytometry. Error bars represent SD. **B.** MCF7, MCF7-P53-KO or MCF7-P21-KO cells were incubated with CFSE and subsequently treated with DMSO or GSK2830371 (0.5 μM) for 3 days. Fluorescent signal of CFSE was measured by flow cytometry. Plotted is the CFSE signal relative to the signal measured at day 0. Error bars represent SD. **C.** MCF7 or BT-474 cells were treated with DMSO or GSK2830371 (0.5 μM) for indicated times, pulsed with BrdU before fixation and distribution of cell cycle phases was determined by flow cytometry. BrdU incorporation was used as a marker of replication and pS10-H3 as a marker of mitotic cells. Error bars represent SD. **D.** MCF7 cells were treated as in C and analyzed by immunoblotting. **E.** BT-474 cells were treated as in C and analyzed by immunoblotting. **F.** MCF7-P53-KO or MCF7-P21-KO cells were treated with DMSO or GSK2830371 (0.5 μM) for indicated times, pulsed with BrdU before fixation and distribution of cell cycle phases was determined as in C. Error bars represent SD.

relatively well tolerated in MCF7 cells (Figure 5A and 5B). Combined treatment with doxorubicin (0.05 μM) and GSK2830371 increased activation of the p53 pathway and significantly reduced proliferation of MCF7 cells (Figure 5A and 5B). Similar potentiation was observed also in combination of GSK2830371 and low doses of etoposide and bleomycin (data not shown). Together with the observed response to ionizing radiation (Figure 4E and 4F) this suggests that loss of WIP1 activity can potentiate DNA damage response to the low level of genotoxic stress whereas extensive DNA damage can trigger activation of this signaling cascade leading to a sustained growth arrest despite high expression levels of WIP1 present in MCF7 cells.

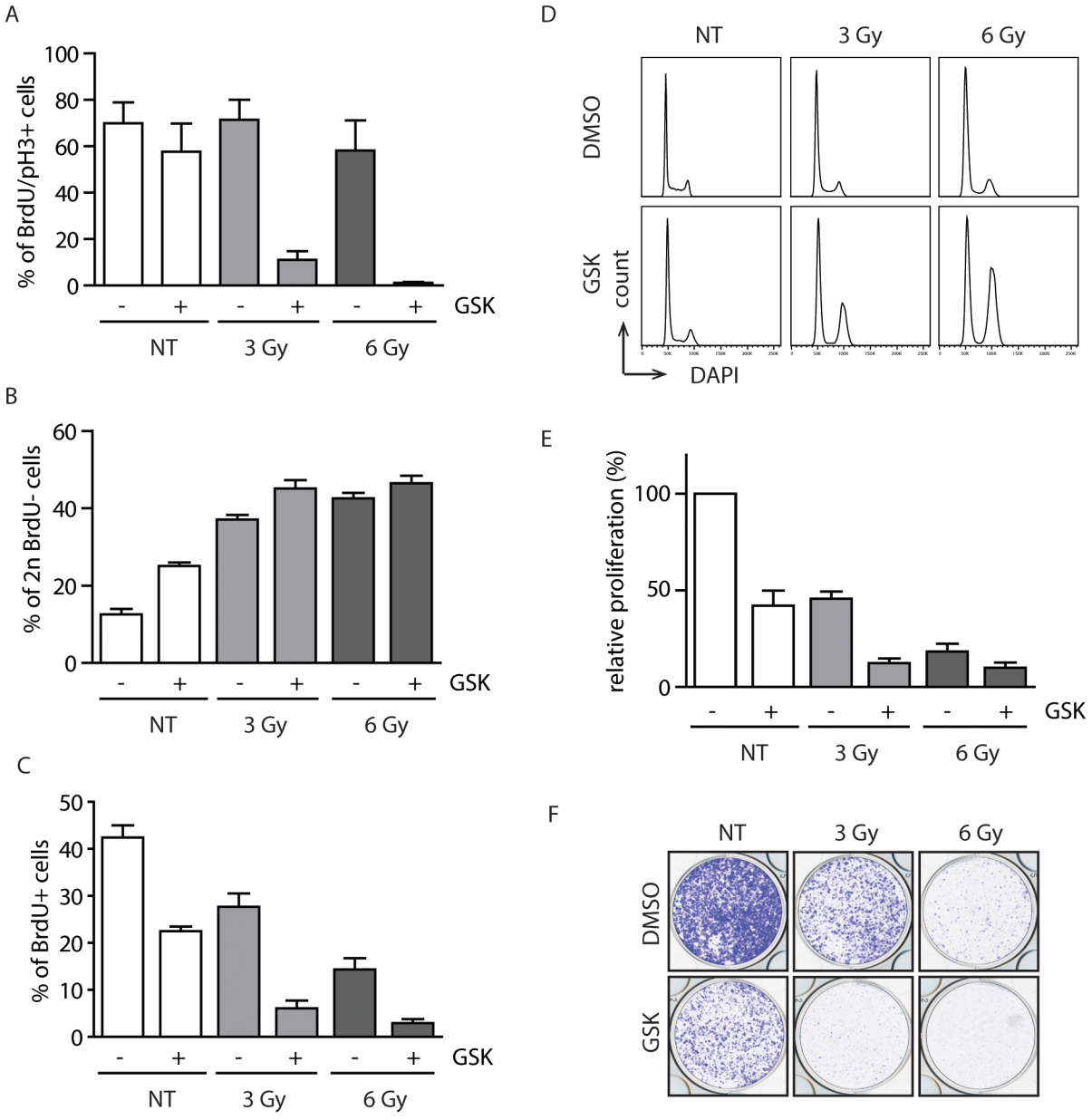

Figure 4: Inhibition of WIP1 potentiates the checkpoint through activation of the p53 pathway. A. MCF7 cells were pulsed with BrdU, treated with DMSO or GSK2830371 (0.5 μM) and exposed to IR. Cells were incubated in the presence of nocodazole and collected after 20 h. Fraction of BrdU positive cells that progressed to mitosis (pH3 marker) was determined by flow cytometry. Error bars represent SD. **B.** MCF7 cells were treated as in A. Fraction of BrdU negative cells with 2n DNA content (corresponding to G1) was determined by flow cytometry 20 h after treatment. Error bars represent SD. **C, D.** MCF7 cells were treated with DMSO or GSK2830371 (0.5 μM), exposed to IR and BrdU incorporation (C) or cell cycle profile (D) was determined after 3 days. Error bars represent SD. **E.** MCF7 cells were treated with DMSO or GSK2830371 (0.5 μM), exposed to IR and cell proliferation was analyzed after 6 days. Error bars represent SD. **F.** MCF7 cells were treated as in E and cell proliferation was determined by colony formation assay after 6 days. Representative image from three independent experiments is shown.

Transcriptional activity of the tumor suppressor p53 is regulated at multiple levels, including extensive phosphorylation in the transactivation and oligomerization domains and MDM2-dependent ubiquitination and degradation [67, 68]. Since inhibition of WIP1 increases phosphorylation of p53 at Ser15, we decided to test whether GSK2830371 could potentiate the effect of an MDM2 antagonist nutlin-3 that increases the total level of p53 [46]. As expected, treatment with high dose of nutlin-3 (10 μM) strongly suppressed cell proliferation of MCF7 cells (Figure 5C). Low dose of nutlin-3 (1 μM) showed an intermediate effect on cell proliferation of MCF7 cells that was further enhanced by simultaneous inhibition of WIP1 (Figure 5C). Consistent with an expected mode of action, we observed increased levels of total p53 after treatment with nutlin-3, increased phosphorylation of p53 at Ser15 after treatment with GSK2830371 and both effects after combined treatment with both inhibitors (Figure 5D). Efficient inhibition of WIP1 is documented by increased basal phosphorylation of γH2AX which is an established substrate of WIP1 and also by decreased levels of MDM2 which is destabilized in the absence of WIP1 activity (Figure 5B and 5D) [14, 20, 22]. Although inhibition of WIP1 slightly increased the basal phosphorylation of p38 at Thr180/Tyr182 (established substrate of WIP1), we did not observe any further increase of p38 activity in combination of GSK2830371 with doxorubicin or nutlin (Figure 5B and 5D). This suggests that p38 does not potentiate the cytotoxic effect of WIP1 and WIP1 impacts on p53 independently on the p38 pathway.

Finally, we tested the potentiation of the cytostatic effect by combining the GSK2830371 with low doses of nutlin-3 and doxorubicin. We found that this triple combination further decreased cell proliferation of MCF7 cells compared to treatments with individual drugs or with the double inhibitor combinations (Figure 5E). Triple combination of GSK2830371, nutlin-3 and doxorubicin also potentiated the cytostatic effect in ZR-75-1 cells that contain amplification of the *PPM1D* locus and harbour wild-type p53 (Figure 5F). In contrast no potentiation was observed in BT-474 and MCF7-P53-KO cells strongly indicating that status of p53 plays a key role in determining the cell sensitivity to WIP1 inhibition (Figure 5G and 5H).

Inhibition of WIP1 potentiates activation of p53 pathway

To quantify activation of the p53 pathway after treatment of MCF7 cells with combination of WIP1 inhibitor and chemotherapeutics we analyzed the expression profiles of selected established p53 target genes. As expected, expression of *CDKN1A* increased 3-5 fold after treatment with GSK2830371, nutlin-3 or doxorubicin administered individually (Figure 6A). Double combination of GSK2830371 with nutlin-3 or doxorubicin resulted in approximately 20 fold increase in *CDKN1* expression. The highest induction of *CDKN1A* expression (about 50 fold) was observed after triple combination of GSK2830371, nutlin-3 and doxorubicin. Similarly, expression of p53 up-regulated modulator of apoptosis (*PUMA*) or pro-apoptotic regulator *BAX* showed the strongest induction after triple combination of GSK2830371, nutlin-3 and doxorubicin. In contrast, we did not observe any significant change in expression of an apoptosis-promoting gene *NOXA*. Inversely, we observed a strongly reduced expression of *BIRC5* (coding for survivin), an anti-apoptotic gene that was reported to be suppressed in a p53-dependent manner [69, 70]. In addition, we have found strongly increased expression of *PPM1D* and *MDM2* after triple combination of GSK2830371, nutlin-3 and doxorubicin, which is consistent with the described transcriptional regulation of both genes by p53. Although expression of *PPM1D* mRNA was increased after triple combination of the drugs, protein levels of WIP1 were decreased (Figure 6B) due to the destabilization of WIP1 caused by binding of GSK2830371 to its catalytic domain [63]. After 3 days of GSK2830371 treatment we did not observe increased total levels of p53; however p53 was heavily phosphorylated at Ser15 known to stimulate its transcriptional activity [11].

Inhibition of WIP1 promotes induction of senescence and apoptosis

Since the expression profiling showed induction of the checkpoint and pro-apoptotic genes, we asked what the fate of cells treated with WIP1 inhibitor alone or in combination with other chemotherapeutics was. Although, cell proliferation was suppressed in MCF7 cells treated with GSK2830371, we observed only mild reduction in the fraction of viable cells compared to the control cells (Figure 3A). In contrast, GSK2830371 significantly decreased viability of MCF7 cells when administered concomitantly with a high dose of doxorubicin (0.5 μM) while having only mild effect when administered together with low dose of doxorubicin (0.05 μM) (Figure 7A, 7B). Similarly, GSK2830371 decreased viability of MCF7 cells treated with a high dose of nutlin-3 (10.0 μM) (Figure 7B). Consistent with a previous report, nutlin-3 increased sensitivity of cells to the low dose of doxorubicin (0.05 μM) [71]. Moreover, we have observed that GSK2830371 further increased the sensitivity of MCF7 cells to a combined treatment with nutlin-3 and doxorubicin (Figure 7B). This suggests that inhibition of WIP1 can potentiate cytotoxic effects of doxorubicin and the MDM2 antagonist nutlin-3. In addition, we observed induction of caspase 9 activity after combined treatment with GSK2830371, nutlin-3 and doxorubicin which is consistent with activation of an intrinsic apoptotic pathway (Figure 7C) [72].

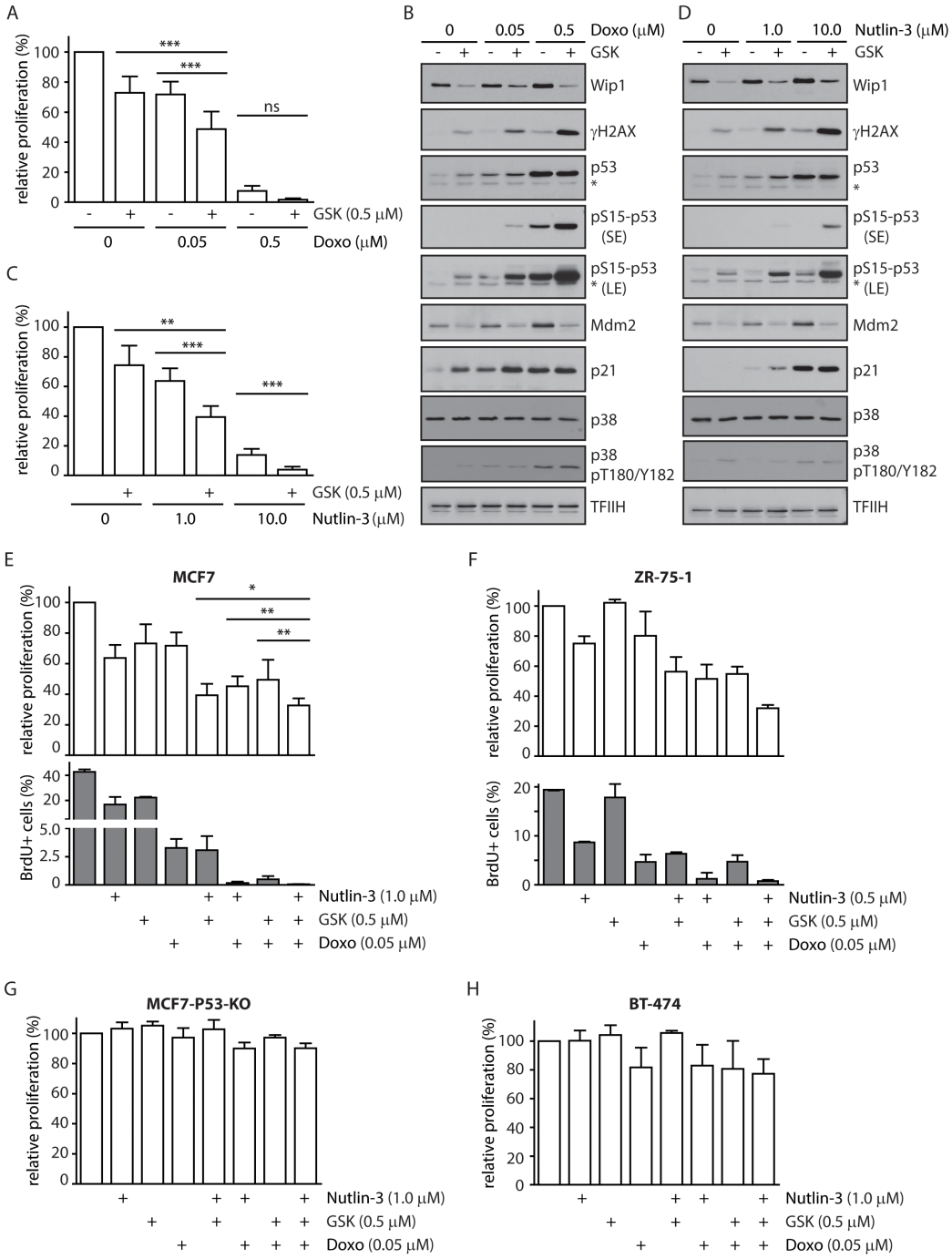

Figure 5: Inhibition of WIP1 increases sensitivity of cells to DNA damage and to nutlin-3. A. MCF7 cells were incubated with indicated doses of doxorubicin in combination with DMSO or GSK2830371 and relative fraction of proliferating cells was determined after 3 days. Error bars represent SD. **B.** MCF7 cells were incubated as in A and analysed by immunoblotting. Staining for TFIIH was used as loading control. Asterisk indicates an unspecific reactivity band. Short exposure (SE) or long exposure (LE) is shown. **C.** MCF7 cells were incubated with indicated doses of nutlin-3 in combination with DMSO or GSK2830371 and relative fraction of proliferating cells was determined after 3 days. Error bars represent SD. **D.** MCF7 cells were incubated with indicated doses of nutlin-3 and GSK2830371 for 1 day and analysed by immunoblotting. Staining for TFIIH was used as loading control. Asterisk indicates an unspecific reactivity band. Short exposure (SE) or long exposure (LE) is shown. **E.** MCF7 cells were incubated for 3 days with indicated doses of doxorubicin, nutlin-3 and GSK2830371 and fraction of proliferating cells was determined by cell survival assay (top) or by incorporation of BrdU (bottom). Error bars represent SD. **F.** ZR-75-1 cells were incubated for 6 days with indicated doses of doxorubicin, nutlin-3 and GSK2830371 and fraction of proliferating cells was determined by cell proliferation assay (top) or by incorporation of BrdU (bottom). Error bars represent SD. **G.** MCF7-P53-KO cells were incubated with indicated doses of doxorubicin, nutlin-3 and GSK2830371 and relative fraction of proliferating cells was determined after 3 days. Error bars represent SD. **H.** BT-474 cells were incubated with indicated doses of doxorubicin, nutlin-3 and GSK2830371 and relative fraction of proliferating cells was determined after 6 days. Error bars represent SD.

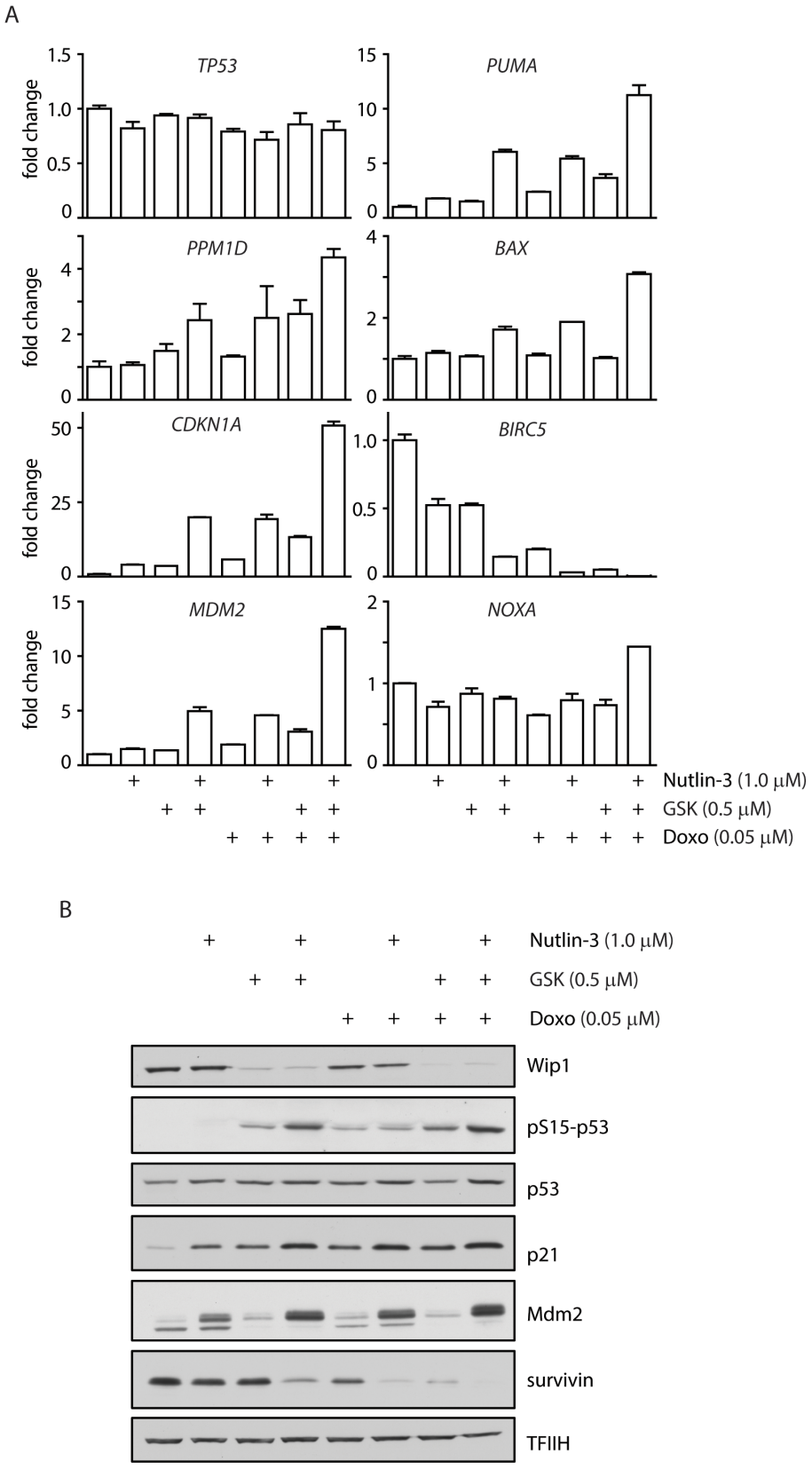

Figure 6: Inhibition of WIP1 increases transcription of p53 target genes. A. MCF7 cells were incubated for 3 days with indicated doses of doxorubicin, nutlin-3 and GSK2830371 and expression of indicated genes was determined by qRT-PCR. Levels are presented as the ratio of mRNA to GAPDH mRNA and are normalized to untreated cells. Error bars correspond to SEM. **B.** MCF7 cells were incubated as in A and expression of selected proteins was analysed by immunoblotting.

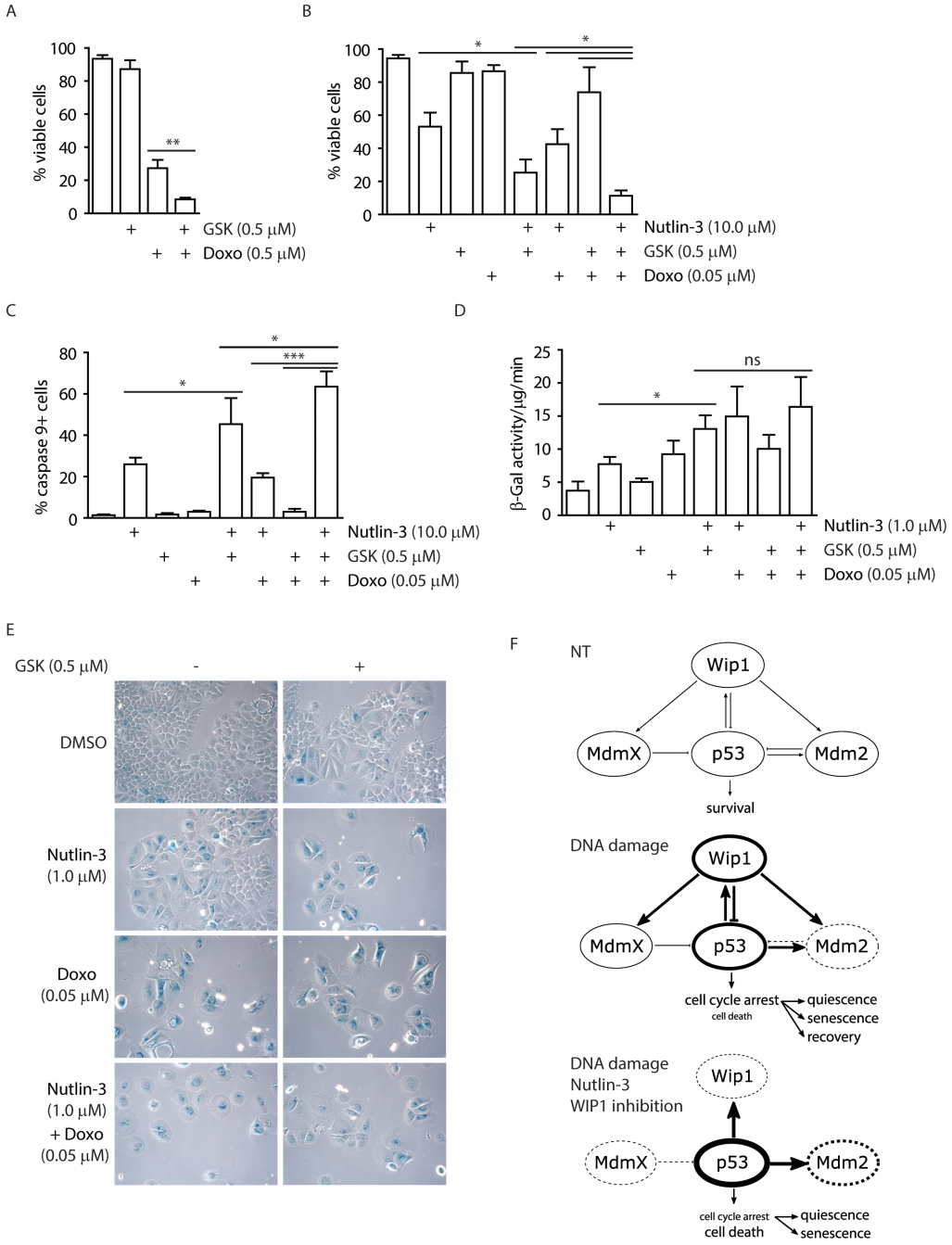

Figure 7: Inhibition of WIP1 potentiates induction of senescence or apoptosis. A. MCF7 cells were incubated with GSK2830371 (0.5 μM) and doxorubicin (0.5 μM) for 3 days and fraction of viable cells (Hoechst/Annexin V negative) was determined by flow cytometry. Error bars represent SD. **B.** MCF7 cells were incubated with indicated combinations of GSK2830371 (0.5 μM), nutlin-3 (10.0 μM) and doxorubicin (0.05 μM) for 3 days and fraction of viable cells (Hoechst/Annexin V negative) was determined by flow cytometry. Error bars represent SD. **C.** MCF7 cells were treated as in (B) and fraction of cells with active caspase 9 was determined by flow cytometry. Error bars represent SD. **D.** MCF7 cells were incubated with indicated combinations of GSK2830371, nutlin-3 (1.0 μM) and doxorubicin (0.05 μM) for 7 days. Activity of SA-β-galactosidase was measured in cell extracts using fluorimetric assay. Error bars represent SD. **E.** MCF7 cells were incubated as in D and SA-β-galactosidase activity was evaluated by light microscopy. **F.** Model for outcomes of treatment with p53/mdm2/Wip1 pathway modulators. Under non-treated conditions, p53 activity is tightly controlled by MDM2 and MDMX. Upon mild DNA damage, MDM2 is inhibited and destabilized leading to stabilization of p53 that in turn leads to increased transcription of its targets including WIP1 phosphatase. Subsequently WIP1 inactivates p53 pathway by direct dephosphorylation of p53 Ser15 and through activation of MDM2 and possibly also MDMX by their dephosphorylation. When MDM2-p53 interaction inhibitor nutlin-3 and WIP1 inhibitor are combined with DNA damage, MDM2 cannot ubiquitinate and thus degrade p53 and WIP1 cannot oppose activation of p53. This leads to further increase of p53 protein levels and its phosphorylation at Ser15 and results mainly in cell death. Thickness of the circle lines represents protein levels; dashed lines mean inhibition of the protein activity.

Whereas combination of the high dose of nutlin-3 and GSK2830371 efficiently induced cell death, most cells survived treatment with the low dose of nutlin-3. Since these cells did not incorporate BrdU (Figure 5E), we hypothesized that they corresponded to the population of cells permanently withdrawn from the cell cycle. Indeed, MCF7 cells treated with GSK2830371 and 1.0 μM nutlin-3 exhibited flattened and enlarged morphology; and showed induction of β-galactosidase activity, both established markers of cellular senescence (Figure 7D and 7E) [73].

In summary, we have validated GSK2830371 as potent and specific inhibitor of WIP1 phosphatase. Our data suggest that mild activation of p53 pathway caused by a partial stabilization (through low levels of nutlin-3) or phosphorylation of p53 (through inhibition of WIP1) is sufficient to slow down proliferation and eventually promotes cellular senescence. Conversely, full activation of p53 pathway achieved by combined effects of genotoxic stress with inhibition of two negative regulators of p53, MDM2 and WIP1 can potentiate cell death in breast cancer cells (Figure 7F).

DISCUSSION

Taking advantage of the U2OS cells with knocked-out *PPM1D*, we compared effects of the two commercially available inhibitors of WIP1 phosphatase in a cellular model. Data presented here and also by others strongly suggest that CCT007093 compound suppresses the cell growth independently of WIP1 inhibition [59]. It is possible that CCT007093 stimulates the p38 pathway as originally reported, however caution should be taken when interpreting these effects as a result of WIP1 inhibition. In contrast, our cellular model confirmed the specificity of the novel allosteric inhibitor GSK2830371 that interfered with dephosphorylation of γH2AX (an established substrate of WIP1) and suppressed cell growth in a WIP1-dependent manner. Notably, an impact of GSK2830371 on activation of the DNA damage response pathway was comparable to that of the *PPM1D* knock out indicating that GSK2830371 can efficiently inhibit WIP1 in cells.

We have found that GSK2830371 administered at doses that specifically block WIP1 activity does not affect proliferation of nontransformed cells but impairs proliferation of breast cancer cells with amplified *PPM1D*. MCF7 cells treated with GSK2830371 accumulate over time in the G2 phase of the cell cycle. This observation is in good agreement with the higher ratio of the G2 cells reported in the population of PPM1D-/- MEFs compared to the wild type MEFs and also with the increased expression level of WIP1 during the G2 in human cells [66, 74]. Analyzis of the MCF7-P53-KO and MCF7-P21-KO cells has shown that this effect of WIP1 on the cell cycle progression is mediated by the p53/p21 pathway. Level of p21 present during G2 was recently identified as an important factor that determines the fate of proliferating cells [75, 76]. Low level of p21 in G2 allows immediate building up of the CDK2 activity following mitotic exit and results in continuous proliferation. In contrast, cells with high level of p21 during G2 remain temporarily arrested in a quiescence after completing cell division and do not proliferate unless stimulated with excessive dose of growth factors [75]. It is plausible that these cells eventually become senescent after long period of sustained p21-dependent inhibition of cyclin dependent kinases. It appears that cells progressing through G2 phase are very sensitive to activation of the p53/p21 pathway. Indeed, short activation of p53 during G2 triggered nuclear retention and subsequent degradation of Cyclin B1 and was sufficient to induce a permanent withdrawal from the cell cycle [77, 78]. Here we have shown that inhibition of WIP1 potentiates an effect of a low dose of nutlin-3 resulting in increased induction of senescence in breast cancer cells.

Although GSK2830371 efficiently suppressed growth of breast cancer cells with amplified *PPM1D* and wild type *TP53*, it did not affect viability of MCF7 cells suggesting that inhibition of WIP1 alone may not be sufficient to eradicate tumor cells. On the other hand, we have found that inhibition of WIP1 by GSK2830371 potentiated doxorubicin-induced cell death in breast cancer cells. This data is consistent with previously reported high sensitivity of Wip1-depleted MCF7 cells to doxorubicin [79]. Similar potentiation of the cytotoxic effect of doxorubicin by WIP1 inhibition has recently been reported in neuroblastoma cells and in a colorectal carcinoma cells with a C-terminally truncated *PPM1D* [61, 64]. In addition, we have found that inhibition of WIP1 potentiated cell death induced by nutlin-3. Synergistic effect of nutlin-3 and doxorubicin has been reported in B-cell leukemia and in breast cancer cells [71, 80]. Here we show that combination of GSK2830371 with doxorubicin and nutlin-3 further increased activation of the p53 pathway and resulted in massive cell death. Clinical outcome of doxorubicin therapy can be impaired by induction of senescence in breast cancer cells with wild-type p53 [81, 82]. Strong induction of p53 function by concomitant inhibition of WIP1 and/or MDM2 could increase the fraction of cells eliminated by cell death and thus could improve the response to doxorubicin. In addition, therapeutic effect of doxorubicin is limited by a cumulative, dose-related cardiotoxicity [83]. Possible reduction of the doxorubicin dose administered in combination with WIP1 inhibitor could be beneficial for breast cancer patients by decreasing undesired side effects of chemotherapy.

WIP1 has been reported to directly target several proteins implicated in apoptosis (including BAX and RUNX2) in p53 negative cells [84–86]. However, suppression of cell growth and induction of cell death by WIP1 depletion or inhibition fully depends on the p53 pathway. In addition, inhibition of WIP1 efficiently affects growth of cells with amplified or truncated *PPM1D* whereas little effect is observed in cells with normal levels of WIP1. This suggests that determination of the status of *TP53* and *PPM1D* in the tumors will be important for predicting the therapeutical outcome of WIP1 inhibitors. Further research is needed to identify additional factors determining the sensitivity of cancer cells to WIP1 inhibitors. Response of cancer cells to nutlin-3 depends on the level of MDM2 and is commonly impaired by overexpression of MDMX [71, 87, 88]. Since GSK2830371 potentiates the cytotoxic effect of nutlin-3, we hypothesize that *MDMX* overexpressing tumors might be attractive candidates for testing the sensitivity to WIP1 inhibition.

MATERIALS AND METHODS

Cell lines

Human osteosarcoma U2OS and breast cancer MCF7 cells were generous gifts from Dr. Medema (NKI, Amsterdam), BT474 from Dr. Truksa (IBT, Prague), CAL-51 and BJ fibroblasts (population doubling 40-50) from Dr. Bartek (IMG, Prague). ZR-75-1 cells were obtained from European Collection of Cell Cultures, hTERT-RPE1 from ATCC and human SV40-immortalized colon epithelia HCE cells from Applied Biological Materials (ABM, #T0570). Cells were grown at 37°C and 5% CO2 in DMEM, RPMI (ZR-75-1 and BT-474) or Prigrow III media (HCE cells) supplemented with 6-10% FBS (Gibco), penicillin (100 U/ml), and streptomycin (0.1 mg/ml). All cell lines were regularly checked for absence of mycoplasma infection using MycoAlert Plus reagent (Lonza). To knock-out *TP53* or *CDKN1A* gene, MCF7 cells were transfected with a combination (1:1) of p53 CRISPR/Cas9 KO Plasmid (Santa Cruz, sc-416469) or p21 CRISPR/Cas9 KO Plasmid (sc-400013) and corresponding HDR Plasmids and stable clones were selected by puromycin (10 μg/ml). Integration of the HDR cassette to genomic loci was confirmed by sequencing and loss of protein expression by immunoblotting. To generate *PPM1D* knock-out cells, U2OS cells were transfected with a CAS9-2A-GFP plasmid expressing the gRNA corresponding to the tgagcgtcttctccgaccaggg sequence in exon 1 of the human *PPM1D* (Sigma). Individual GFP positive clones were expanded and loss of WIP1 expression was determined by immunoblotting. Transfection of plasmid DNA was performed using Lipofectamine LTX according to recommendations of manufacturer (Life Technologies). Where indicated, cells grown on culture plates were exposed to ionizing radiation generated by X-ray instrument T-200 (16.5 Gy/min, Wolf-Medizintechnik).

Antibodies and chemicals

The following antibodies were used: WIP1 (sc-130655), p53 (sc-6243), TFIIH (sc-293), importin (sc-137016), p21 (sc-397) from Santa Cruz; pSer15-p53 (#9284), γH2AX (#9718), p38 MAPK Thr180/Tyr182 (#9216S) and p38 MAPK (#9212) from Cell Signaling Technology); γH2AX (05-636, Millipore); MDM2 (Calbiochem); Alexa Fluor-labelled secondary antibodies (Life Technologies); anti-BrdU FITC-conjugated antibody (#347583, BD Biosciences) and anti-pSer10-H3 antibody (Upstate). Doxorubicin hydrochloride (Sigma), GSK2830371 and nutlin-3 (both MedChem Express) were diluted in DMSO and used at indicated doses. Resazurin, neocarzinostatin (NCS) and carboxyfluorescein diacetate succinimidyl ester (CFSE) were purchased from Sigma.

Cell proliferation assay

MCF7 or BT-474 cells were seeded into 96-well plates at $2x10^3$ or $0.5x10^3$ cells/well, treated with a compound dilution series and analyzed after 3 or 7 days, respectively. CAL-51, RPE, HCE, BJ or ZR-75-1 cells were seeded into 96 well plates at $0.02\text{-}2x10^4$ cells/well and grown for 7 days. Resazurin (30 μg/mL) was added to growth media and fluorescence signal (excitation wavelength 560 nm, emission wavelength 590 nm) was measured after 1 to 5 h using EnVision plate reader (PerkinElmer).

Alternatively, rate of cell proliferation was determined using CFSE Cell Proliferation assay as previously described [89]. Cells were stained with 50 μM CFSE in complete media for 15 min in 37°C, washed with complete media and seeded to 12-well plate at $2.5x10^4$ cells/well. Where indicated, GSK2830371 (0.5 μM) was added to the media. Cells were harvested and fixed by 4% paraformaldehyde 3 days after treatment. Percentage of the remaining CFSE staining compared to the cells harvested immediately after staining was determined by flow cytometry.

Clonogenic assay

Cells were seeded in 6-well plates at $2x10^4$ cells/well. Cells were treated with a compound dilution series on day 1. After 6-7 days, cells were washed with PBS, fixed by 70 % ethanol for 15 min and stained with crystal violet dye.

Cell cycle assay

Cells were grown for indicated times in the presence of DMSO or GSK2830371 (0.5 μM), pulsed with BrdU (10 μM for 30 min; Sigma), harvested by trypsinization and fixed in ice-cold 70 % ethanol. Following the protocol from manufacturer, cells were stained with anti-BrdU-FITC (replication marker, BD Biosciences), anti-pSer10H3 (mitotic marker) and DAPI and analyzed by flow cytometry using LSRII (BD Biosciences) and FlowJo software (FlowJo).

Checkpoint analysis

Evaluation of the cell cycle checkpoints was performed as described previously with minor modifications [39]. Cells were pulsed with BrdU (10 μM for 30 min) and treated with GSK2830371 (0.5 μM) or DMSO before irradiation with 3 or 6 Gy and were grown for further 20 h in the presence of nocodazole (250 ng/ml). Cells were processed as mentioned above and analyzed by flow cytometry. BrdU-positive cells were assayed for progression through the G2 phase to mitosis (4n DNA content, pH3+). BrdU-negative cells with 2n content were used for quantification of cells arrested in G1 checkpoint.

Cell viability assay

MCF7 cells were seeded into 12-well plates at $2x10^4$ cells/well, treated with Nutlin-3 (10 μM or 1 μM), GSK2830371 (0.5 μM) and doxorubicin (0.05 μM or 0.05 μM) and grown for 3 days. Cells were trypsinized, washed with PBS and incubated with FITC-conjugated Annexin V (BD Biosciences) and Hoechst-33258 for 15 minutes. Fraction of living cells was determined as Annexin V negative and Hoechst negative population analyzed by flow cytometry.

β-galactosidase assay

Senescence-associated β-galactosidase activity was quantified in cell extracts as previously described [90]. Briefly, MCF7 cells were seeded into 6 cm plates at $0.5x10^5$ cells/plate and grown in media supplemented with indicated combinations of nutlin-3 (1 μM), GSK2830371 (0.5 μM) and doxorubicin (0.05 μM) for 7 days. Cells were washed in PBS, collected to ice cold lysis buffer (5 mM CHAPS, 40 mM citric acid, 40 mM sodium phosphate, 0.5 μM benzamidine and 0.25 mM PMSF, pH 6.0), vortexed and centrifuged for 5 min at 12,000g. Cell extract was mixed 1:1 with 2x reaction buffer supplemented with 4-MUG (1.7 mM, Sigma) and MgCl2 (4 mM) and incubated at 37°C for 0.5 – 4 hours. Reaction was stopped by addition of sodium carbonate (400 mM) and fluorescence signal was measured at excitation wavelength 360 nm and emission wavelength 465 nm using EnVision plate reader. β-galactosidase activity was determined as the rate of 4-MUG conversion to the fluorescent 4-MU and normalized to the protein concentration measured by BCA assay. Alternatively, cells were grown on coverslips, fixed by 0.2 % glutaraldehyde 7 days after treatment with indicated combinations of nutlin-3 (1 μM), GSK2830371 (0.5 μM) and doxorubicin (0.05 μM) and β-galactosidase activity was determined by colorimetric staining as previously [73].

Caspase assay

Activity of caspase-9 was measured using SR-FLICA Caspase-9 assay according to manufacturer protocol (Immunochemistry Technologies). Briefly, cells were seeded to 12-well plates, treated as indicated, harvested by trypsinization after 48 h and re-suspended in complete media containing SR-FLICA caspase-9 and incubated 1 h at 37°C. After incubation, cells were washed with Apoptosis wash buffer for 10 min at 37°C. Percentage of cells positive for caspase-9 activity was determined by flow cytometry.

Immunofluorescence microscopy

U2OS cells grown on coverslips were treated with DMSO, CCT007093 or GSK2830371 for 1 h and DNA damage was induced by neocarzinostatin for 5 h. Cells were fixed by 4 % formaldehyde (10 min at RT), permeabilized by ice-cold methanol and stained with antibody against γH2AX and with DAPI. Average nuclear intensity of γH2AX signal was quantified using Scan^R high-content screening station as described previously [66].

Quantitative real-time PCR (qPCR)

Total RNA was isolated using RNeasy mini kit (Qiagen). cDNA was synthetized using 0.5 μg RNA, random hexamer, and RevertAid H Minus Reverse Transcriptase (Thermo Scientific). RT-qPCR was performed using LightCycler 480 SYBR Green I Master mix; Light Cycler LC480 (Roche) and following cycle conditions: initial denaturation 95°C for 7 min, followed by 45 cycles of denaturation 95°C for 15 s, annealing 60°C for 15s and extension 72°C for 15s. A melting curve analysis was used to confirm the specificity of amplification, and Ct values were determined using LigtCycler480 software. All data are presented as the ratio of the tested mRNA to *GAPDH* mRNA. Primers are listed in the table.

Gene	Forward sequence	Reverse sequence
PPM1D	CTGAACCTGACTGACAGCCC	CTTGGCCATGGATCCTCCTC
BIRC5	CTGCCTGGTCCCAGAGTG	GTGGCACCAGGGAATAAACC
MDM2	TCGACCTAAAAATGGTTGCAT	GGCAGGGCTTATTCCTTTTC
PUMA	TCTCGGTGCTCCTTCACTCT	ACGTTTGGCTCATTTGCTCT
BAX	GCTGGACATTGGACTTCCTC	GTCTTGGATCCAGCCCAAC
CDKN1A	GGCGGCAGACCAGCATGACA	CCTCGCGCTTCCAGGACTGC
TP53	CAGCACATGACGGAGGTTGT	TCATCCAAATACTCCACACGC
NOXA	GCTGGGGAGAAACAGTTCAG	AATGTGCTGAGTTGGCACTG

Statistical analysis

Statistical analysis was performed in GraphPad Prism 5.04 software. Statistical significance was determined from at least three independent experiments using a paired two-tailed T-test (* corresponds to p-value < 0.05; ** p-value < 0.005; *** p-value < 0.0005). Error bars indicate standard deviations. EC50 was calculated using Richard's five-parameter dose-response curve for non-linear fitting analysis.

ACKNOWLEDGMENTS

We are thankful to Rene Medema (NKI, Amsterdam), Jaroslav Truksa (IBT, Prague) and Jiri Bartek (IMG, Prague) for providing essential reagents.

CONFLICTS OF INTEREST

The authors declare no conflicts of interest.

GRANT SUPPORT

This work has been supported by the Grant Agency of the Czech Republic (P305-12-2485), Worldwide Cancer Research (14-1176) and IMG ASCR (RVO: 68378050).

REFERENCES

1. Jackson SP and Bartek J. The DNA-damage response in human biology and disease. Nature. 2009; 461: 1071-1078.
2. Halazonetis TD, Gorgoulis VG, and Bartek J. An Oncogene-Induced DNA Damage Model for Cancer Development. Science. 2008; 319:1352-1355.
3. Leontieva O, Gudkov A, and Blagosklonny M. Weak p53 permits senescence during cell cycle arrest. Cell Cycle. 2010; 9: 4323-7.
4. Kracikova M, Akiri G, George A, Sachidanandam R, and Aaronson SA. A threshold mechanism mediates p53 cell fate decision between growth arrest and apoptosis. Cell Death and Differentiation. 2013; 20:576-588.
5. Zhang X-P, Liu F, Cheng Z, and Wang W. Cell fate decision mediated by p53 pulses. Proceedings of the National Academy of Sciences of the United States of America. 2009; 106:12245-12250.
6. Pei D, Zhang Y, and Zheng J. Regulation of p53: a collaboration between Mdm2 and MdmX. Oncotarget. 2012; 3:228-235. doi: 10.18632/oncotarget.443.
7. Popowicz G, Czarna A, Rothweiler U, Szwagierczak A, Krajewski M, Weber L, and Holak T. Molecular basis for the inhibition of p53 by Mdmx. Cell Cycle. 2007; 6:2386-92.
8. Meulmeester E, Pereg Y, Shiloh Y, and Jochemsen A. ATM-mediated phosphorylations inhibit Mdmx/Mdm2 stabilization by HAUSP in favor of p53 activation. Cell Cycle. 2005; 4:1166-70.
9. Shieh SY, Ikeda M, Taya Y, and Prives C. DNA Damage-Induced Phosphorylation of p53 Alleviates Inhibition by MDM2. Cell. 1997; 91:325-334.
10. Tibbetts RS, Brumbaugh KM, Williams JM, Sarkaria JN, Cliby WA, Shieh S-Y, Taya Y, Prives C, and Abraham RT. A role for ATR in the DNA damage-induced phosphorylation of p53. Genes & Development. 1999; 13:152-157.
11. Jenkins LMM, Durell SR, Mazur SJ, and Appella E. p53 N-terminal phosphorylation: a defining layer of complex regulation. Carcinogenesis. 2012; 33:1441-1449.
12. Fiscella M, Zhang H, Fan S, Sakaguchi K, Shen S, Mercer WE, Vande Woude GF, O Connor PM, and Appella E. Wip1, a novel human protein phosphatase that is induced in response to ionizing radiation in a p53-dependent manner. Proc Natl Acad Sci USA. 1997; 94:6048-6053.
13. Lu X, Nannenga B, and Donehower L. PPM1D dephosphorylates Chk1 and p53 and abrogates cell cycle checkpoints. Genes & Development. 2005; 19:1162-74.
14. Lu X, Ma O, Nguyen T-A, Jones SN, Oren M, and Donehower LA. The Wip1 Phosphatase Acts as a Gatekeeper in the p53-Mdm2 Autoregulatory Loop. Cancer Cell. 2007; 12:342-354.
15. Lu X, Nguyen T, Zhang X, and Donehower L. The Wip1 phosphatase and Mdm2: cracking the "Wip" on p53 stability. Cell Cycle. 2008; 7:164-168.

16. Zhang X, Lin L, Guo H, Yang J, Jones SN, Jochemsen A, and Lu X. Phosphorylation and Degradation of MdmX Is Inhibited by Wip1 Phosphatase in the DNA Damage Response. Cancer Research. 2009; 69:7960-7968.

17. Lindqvist A, de Bruijn M, Macurek L, Bras A, Mensinga A, and Bruinsma W. Wip1 confers G2 checkpoint recovery competence by counteracting p53-dependent transcriptional repression. EMBO J. 2009; 28:3196-3206.

18. Shaltiel IA, Aprelia M, Saurin AT, Chowdhury D, Kops GJPL, Voest EE, and Medema RH. Distinct phosphatases antagonize the p53 response in different phases of the cell cycle. PNAS. 2014; 111:7313-7318.

19. Shreeram S, Demidov ON, Hee WK, Yamaguchi H, Onishi N, Kek C, Timofeev ON, Dudgeon C, Fornace AJ, Anderson CW, Minami Y, Appella E, and Bulavin DV. Wip1 Phosphatase Modulates ATM-Dependent Signaling Pathways. Mol. Cell. 2006; 23:757-764.

20. Macurek L, Lindqvist A, Voets O, Kool J, Vos H, and Medema R. Wip1 phosphatase is associated with chromatin and dephosphorylates gammaH2AX to promote checkpoint inhibition. Oncogene. 2010; 15;29:2281-91.

21. Le Guezennec X and Bulavin DV. WIP1 phosphatase at the crossroads of cancer and aging. Trends in Biochemical Sciences. 2010; 35:109-114.

22. Moon S, Lin L, Zhang X, Nguyen T, Darlington Y, Waldman A, Lu X, and LA. D. Wildtype p53-induced phosphatase 1 dephosphorylates histone variant gamma-H2AX and suppresses DNA double strand break repair. J Biol Chem. 2010; 23:285:12935-47.

23. Takekawa M, Adachi M, Nakahata A, Nakayama I, Itoh F, Tsukuda H, Taya Y, and Imai K. p53-inducible Wip1 phosphatase mediates a negative feedback regulation of p38 MAPK-p53 signaling in response to UV radiation. EMBO J., 2000; 19:6517-6526.

24. Fujimoto H, Onishi N, Kato N, Takekawa M, Xu X, and Kosugi A. Regulation of the antioncogenic Chk2 kinase by the oncogenic Wip1 phosphatase. Cell Death Differ. 2006; 13:1170-1180.

25. Lee JS, Lee MO, Moon BH, Shim SH, Fornace AJ, and Cha H-J. Senescent Growth Arrest in Mesenchymal Stem Cells Is Bypassed by Wip1-Mediated Downregulation of Intrinsic Stress Signaling Pathways. STEM CELLS. 2009; 27:1963-1975.

26. Sakai H, Fujigaki H, Mazur SJ, and Appella E. Wild-type p53-induced phosphatase 1 (Wip1) forestalls cellular premature senescence at physiological oxygen levels by regulating DNA damage response signaling during DNA replication. Cell Cycle. 2014; 13:1015-1029.

27. Satoh N, Maniwa Y, Bermudez VP, Nishimura K, Nishio W, Yoshimura M, Okita Y, Ohbayashi C, Hurwitz J, and Hayashi Y. Oncogenic phosphatase Wip1 is a novel prognostic marker for lung adenocarcinoma patient survival. Cancer Science. 2011; 102:1101-6.

28. Castellino R, De Bortoli M, Lu X, Moon S-H, Nguyen T-A, Shepard M, Rao P, Donehower L, and Kim J. Medulloblastomas overexpress the p53-inactivating oncogene WIP1/PPM1D. J. Neurooncol., 2008; 86:245-256.

29. Li J, Yang Y, Peng Y, Austin RJ, van Eyndhoven WG, Nguyen KCQ, Gabriele T, McCurrach ME, Marks JR, Hoey T, Lowe SW, and Powers S. Oncogenic properties of PPM1D located within a breast cancer amplification epicenter at 17q23. Nat Genet. 2002; 31:133-134.

30. Saito-Ohara F, Imoto I, Inoue J, Hosoi H, Nakagawara A, Sugimoto T, and Inazawa J. PPM1D Is a Potential Target for 17q Gain in Neuroblastoma. Cancer Res. 2003; 63:1876-1883.

31. Bulavin DV, Demidov ON, Saito Si, Kauraniemi P, Phillips C, Amundson SA, Ambrosino C, Sauter G, Nebreda AR, Anderson CW, Kallioniemi A, Fornace AJ, and Appella E. Amplification of PPM1D in human tumors abrogates p53 tumor-suppressor activity. Nat Genet. 2002; 31:210-215.

32. Tan DSP, Iravani M, McCluggage WG, Lambros MB, Milanezi F, Mackay A, Gourley C, Geyer FC, Vatcheva R, Millar J, Thomas K, Natrajan R, Savage K, et al. Genomic Analysis Reveals the Molecular Heterogeneity of Ovarian Clear Cell Carcinomas. Clinical Cancer Research. 2011; 17:1521-1534.

33. Liang C, Guo E, Lu S, Wang S, Kang C, Chang L, Liu L, Zhang G, Wu Z, Zhao Z, Ma S, Wang L, and Jiao B-h. Over-expression of Wild-type p53-induced phosphatase 1 confers poor prognosis of patients with gliomas. Brain Research. 2012; 1444:65-75.

34. Rauta J, Alarmo E-L, Kauraniemi P, Karhu R, Kuukasjärvi T, and Kallioniemi A. The serine-threonine protein phosphatase PPM1D is frequently activated through amplification in aggressive primary breast tumours. Breast Cancer Research and Treatment. 2006; 95:257-263.

35. The Cancer Genome Atlas N. Comprehensive molecular portraits of human breast tumors. Nature. 2012; 490:61-70.

36. Emelyanov A and Bulavin DV. Wip1 phosphatase in breast cancer. Oncogene. 2015; 34:4429-4438.

37. Demidov ON, Kek C, Shreeram S, Timofeev O, Fornace AJ, Appella E, and Bulavin DV. The role of the MKK6// p38 MAPK pathway in Wip1-dependent regulation of ErbB2-driven mammary gland tumorigenesis. Oncogene. 2006; 26:2502-2506.

38. Ruark E, Snape K, Humburg P, Loveday C, Bajrami I, Brough R, Rodrigues DN, Renwick A, Seal S, Ramsay E, Duarte SDV, Rivas MA, Warren-Perry M, et al. Mosaic PPM1D mutations are associated with predisposition to breast and ovarian cancer. Nature. 2013; 493:406-410.

39. Kleiblova P, Shaltiel IA, Benada J, Sevčík J, Pecháčková S, Pohlreich P, Voest EE, Dundr P, Bartek J, Kleibl Z, Medema RH, and Macurek L. Gain-of-function mutations of PPM1D/Wip1 impair the p53-dependent G1 checkpoint. The Journal of Cell Biology. 2013; 201:511-521.

40. Dudgeon C, Shreeram S, Tanoue K, Mazur SJ, Sayadi A, Robinson RC, Appella E, and Bulavin DV. Genetic variants and mutations of PPM1D control the response to DNA damage. Cell Cycle. 2013; 12:2656-2664.

41. Hoe KK, Verma CS, and Lane DP. Drugging the p53 pathway: understanding the route to clinical efficacy. Nat Rev Drug Discov. 2014; 13:217-236.

42. Brown CJ, Lain S, Verma CS, Fersht AR, and Lane DP. Awakening guardian angels: drugging the p53 pathway. Nat Rev Cancer. 2009; 9:862-873.

43. Dong P, Ihira K, Hamada J, Watari H, Yamada T, Hosaka M, Hanley SJB, Kudo M, and Sakuragi N. Reactivating p53 functions by suppressing its novel inhibitor iASPP: a potential therapeutic opportunity in p53 wild-type tumors. Oncotarget. 2015; 6:19968-75. doi: 10.18632/oncotarget.4847.

44. Qin J-J, Wang W, Voruganti S, Wang H, Zhang W-D, and Zhang R. Identification of a new class of natural product MDM2 inhibitor: In vitro and in vivo anti-breast cancer activities and target validation. Oncotarget. 2015; 6:2623-40. doi: 10.18632/oncotarget.3098.

45. Reed D, Shen Y, Shelat AA, Arnold LA, Ferreira AM, Zhu F, Mills N, Smithson DC, Regni CA, Bashford D, Cicero SA, Schulman BA, Jochemsen AG, et al. Identification and Characterization of the First Small Molecule Inhibitor of MDMX. Journal of Biological Chemistry. 2010; 285:10786-10796.

46. Vassilev LT, Vu BT, Graves B, Carvajal D, Podlaski F, Filipovic Z, Kong N, Kammlott U, Lukacs C, Klein C, Fotouhi N, and Liu EA. In Vivo Activation of the p53 Pathway by Small-Molecule Antagonists of MDM2. Science. 2004; 303:844-848.

47. Ding Q, Zhang Z, Liu J-J, Jiang N, Zhang J, Ross TM, Chu X-J, Bartkovitz D, Podlaski F, Janson C, Tovar C, Filipovic ZM, Higgins B, et al. Discovery of RG7388, a Potent and Selective p53–MDM2 Inhibitor in Clinical Development. Journal of Medicinal Chemistry. 2013; 56:5979-5983.

48. Harrison M, Li J, Degenhardt Y, Hoey T, and Powers S. Wip1-deficient mice are resistant to common cancer genes. Trends Mol Med., 2004; 10:359-361.

49. Bulavin DV, Phillips C, Nannenga B, Timofeev O, Donehower LA, Anderson CW, Appella E, and Fornace AJ. Inactivation of the Wip1 phosphatase inhibits mammary tumorigenesis through p38 MAPK-mediated activation of the p16Ink4a-p19Arf pathway. Nat Genet. 2004; 36:343-350.

50. Shreeram S, Hee WK, Demidov ON, Kek C, Yamaguchi H, Fornace AJ, Jr., Anderson CW, Appella E, and Bulavin DV. Regulation of ATM/p53-dependent suppression of myc-induced lymphomas by Wip1 phosphatase. J. Exp. Med., 2006; 203:2793-2799.

51. Demidov ON, Timofeev O, Lwin HNY, Kek C, Appella E, and Bulavin DV. Wip1 Phosphatase Regulates p53-Dependent Apoptosis of Stem Cells and Tumorigenesis in the Mouse Intestine. Cell Stem Cell. 2007; 1:180-190.

52. Demidov ON, Zhu Y, Kek C, Goloudina AR, Motoyama N, and Bulavin DV. Role of Gadd45a in Wip1-dependent regulation of intestinal tumorigenesis. Cell Death and Differentiation. 2012; 19:1761-1768.

53. Pärssinen J, Alarmo E-L, Karhu R, and Kallioniemi A. PPM1D silencing by RNA interference inhibits proliferation and induces apoptosis in breast cancer cell lines with wild-type p53. Cancer Genetics and Cytogenetics. 2008; 182:33-39.

54. Tan DSP, Lambros MBK, Rayter S, Natrajan R, Vatcheva R, Gao Q, Marchiò C, Geyer FC, Savage K, Parry S, Fenwick K, Tamber N, Mackay A, et al. PPM1D Is a Potential Therapeutic Target in Ovarian Clear Cell Carcinomas. Clinical Cancer Research. 2009; 15:2269-2280.

55. Wang P, Rao J, Yang H, Zhao H, and Yang L. PPM1D silencing by lentiviral-mediated RNA interference inhibits proliferation and invasion of human glioma cells. Journal of Huazhong University of Science and Technology. 2011; 31:94-99.

56. Yamaguchi H, Durell SR, Feng H, Bai Y, Anderson CW, and Appella E. Development of a Substrate-Based Cyclic Phosphopeptide Inhibitor of Protein Phosphatase 2Cδ, Wip1†. Biochemistry. 2006; 45:13193-13202.

57. Hayashi R, Tanoue K, Durell SR, Chatterjee DK, Miller Jenkins LM, Appella DH, and Appella E. Optimization of a Cyclic Peptide Inhibitor of Ser/Thr Phosphatase PPM1D (Wip1). Biochemistry. 2011; 50:4537-4549.

58. Rayter S, Elliott R, Travers J, Rowlands MG, Richardson TB, Boxall K, Jones K, Linardopoulos S, Workman P, Aherne W, Lord CJ, and Ashworth A. A chemical inhibitor of PPM1D that selectively kills cells overexpressing PPM1D. Oncogene. 2007; 27:1036-1044.

59. Lee JS, Park JR, Kwon OS, Kim H, Fornace AJ, and Cha HJ. Off-target response of a Wip1 chemical inhibitor in skin keratinocytes. Journal of Dermatological Science. 2014; 73:125-134.

60. Yagi H, Chuman Y, Kozakai Y, Imagawa T, Tkahashi Y, Yoshimura F, Tanino K, and Sakaguchi K. A small molecule inhibitor of p53-inducible protein phosphatase PPM1D. Bioorg Med Chem Lett. 2012; 22:729-32.

61. Kozakai Y, Kamada R, Kiyota Y, Yoshimura F, Tanino K, and Sakaguchi K. Inhibition of C-terminal truncated PPM1D enhances the effect of doxorubicin on cell viability in human colorectal carcinoma cell line. Bioorganic & Med. Chem. Lett. 2014; 24:5593-5596.

62. Ogasawara S, Kiyota Y, Chuman Y, Kowata A, Yoshimura F, Tanino K, Kamada R, and Sakaguchi K. Novel inhibitors targeting PPM1D phosphatase potently suppress cancer cell proliferation. Bioorganic & Medicinal Chemistry. 2015; 23:6246-6249.

63. Gilmartin AG, Faitg TH, Richter M, Groy A, Seefeld MA, Darcy MG, Peng X, Federowicz K, Yang J, Zhang S-Y, Minthorn E, Jaworski J-P, Schaber M, et al. Allosteric Wip1 phosphatase inhibition through flap-subdomain interaction. Nat Chem Biol. 2014; 10:181-187.

64. Richter M, Dayaram T, Gilmartin AG, Ganji G, Pemmasani SK, Van Der Key H, Shohet JM, Donehower LA, and Kumar R. WIP1 Phosphatase as a Potential Therapeutic Target in Neuroblastoma. PLoS ONE. 2015; 10:e0115635.

65. Forbes SA, Beare D, Gunasekaran P, Leung K, Bindal N, Boutselakis H, Ding M, Bamford S, Cole C, Ward S, Kok CY, Jia M, De T, et al. COSMIC: exploring the world's

knowledge of somatic mutations in human cancer. Nucleic Acids Research. 2015; 43:D805-D811.

66. Macurek L, Benada J, Müllers E, Halim VA, Krejčíková K, Burdová K, Pecháčková S, Hodný Z, Lindqvist A, Medema RH, and Bartek J. Downregulation of Wip1 phosphatase modulates the cellular threshold of DNA damage signaling in mitosis. Cell Cycle. 2013; 12:251-262.

67. Hock AK and Vousden KH. The role of ubiquitin modification in the regulation of p53. Biochimica et Biophysica Acta (BBA) - Molecular Cell Research. 2014; 1843:137-149.

68. Kruse J-P and Gu W. Modes of p53 Regulation. Cell. 2009; 137:609-622.

69. Mirza A, McGuirk M, Hockenberry T, Wu Q, Ashar H, Black S, Wen S, Wang L, Kirschmeier P, Bishop W, Nielsen L, Pickett C, and Liu S. Human survivin is negatively regulated by wild-type p53 and participates in p53-dependent apoptotic pathway. Oncogene. 2002; 21:2613-2622.

70. Hoffman WH, Biade S, Zilfou JT, Chen J, and Murphy M. Transcriptional Repression of the Anti-apoptoticsurvivin Gene by Wild Type p53. Journal of Biological Chemistry. 2002; 277:3247-3257.

71. Lam S, Lodder K, Teunisse AFAS, Rabelink MJWE, Schutte M, and Jochemsen AG. Role of Mdm4 in drug sensitivity of breast cancer cells. Oncogene. 2010; 29:2415-2426.

72. Johnson C and Jarvis W. Caspase-9 regulation: an update. Apoptosis. 2004; 9:423-7.

73. Debacq-Chainiaux F, Erusalimsky JD, Campisi J, and Toussaint O. Protocols to detect senescence-associated beta-galactosidase (SA-betagal) activity, a biomarker of senescent cells in culture and in vivo. Nat. Protocols. 2009; 4:1798-1806.

74. Choi J, Nannenga B, Demidov O, Bulavin D, Cooney A, and Brayton C. Mice deficient for the wild-type p53-induced phosphatase gene (Wip1) exhibit defects in reproductive organs, immune function, and cell cycle control. Mol Cell Biol. 2002; 22:1094-1105.

75. Spencer Sabrina L, Cappell Steven D, Tsai F-C, Overton KW, Wang Clifford L, and Meyer T. The Proliferation-Quiescence Decision Is Controlled by a Bifurcation in CDK2 Activity at Mitotic Exit. Cell. 2013; 155:369-383.

76. Overton KW, Spencer SL, Noderer WL, Meyer T, and Wang CL. Basal p21 controls population heterogeneity in cycling and quiescent cell cycle states. Proceedings of the National Academy of Sciences. 2014; 111:E4386-E4393.

77. Krenning L, Feringa Femke M, Shaltiel Indra A, van den Berg J, and Medema René H. Transient Activation of p53 in G2 Phase Is Sufficient to Induce Senescence. Molecular Cell. 2014; 55:59-72.

78. Müllers E, Cascales HS, Jaiswal H, Saurin AT, and Lindqvist A. Nuclear translocation of Cyclin B1 marks the restriction point for terminal cell cycle exit in G2 phase. Cell Cycle. 2014; 13:2733-2743.

79. Kong W, Jiang X, and Mercer W. Downregulation of Wip-1 phosphatase expression in MCF-7 breast cancer cells enhances doxorubicin-induced apoptosis through p53-mediated transcriptional activation of Bax. Cancer Biol Ther. 2009; 8:555-63.

80. Coll-Mulet L, Iglesias-Serret D, Santidrián AF, Cosialls AM, de Frias M, Castaño E, Campàs C, Barragán M, de Sevilla AF, Domingo A, Vassilev LT, Pons G, and Gil J. MDM2 antagonists activate p53 and synergize with genotoxic drugs in B-cell chronic lymphocytic leukemia cells. Blood. 2006; 107:4109-4114.

81. Bertheau P, Lehmann-Che J, Varna M, Dumay A, Poirot B, Porcher R, Turpin E, Plassa L-F, de Roquancourt A, Bourstyn E, de Cremoux P, Janin A, Giacchetti S, et al. p53 in breast cancer subtypes and new insights into response to chemotherapy. The Breast. 2013; 22, Supplement 2:S27-S29.

82. Jackson JG, Pant V, Li Q, Chang LL, Quintás-Cardama A, Garza D, Tavana O, Yang P, Manshouri T, Li Y, El-Naggar AK, and Lozano G. p53 mediated senescence impairs the apoptotic response to chemotherapy and clinical outcome in breast cancer. Cancer Cell. 2012; 21:793-806.

83. Rochette L, Guenancia C, Gudjoncik A, Hachet O, Zeller M, Cottin Y, and Vergely C. Anthracyclines/trastuzumab: new aspects of cardiotoxicity and molecular mechanisms. Trends in Pharmacological Sciences. 2015; 36:326-348.

84. Song JY, Ryu SH, Cho YM, Kim YS, Lee BM, Lee SW, and Choi J. Wip1 suppresses apoptotic cell death through direct dephosphorylation of BAX in response to γ-radiation. Cell Death & Disease. 2013; 4:e744.

85. Goloudina AR, Tanoue K, Hammann A, Fourmaux E, Le Guezennec X, Bulavin DV, Mazur SJ, Appella E, Garrido C, and Demidov ON. Wip1 promotes RUNX2-dependent apoptosis in p53-negative tumors and protects normal tissues during treatment with anticancer agents. Proceedings of the National Academy of Sciences. 2012; 109:E68–E75.

86. Goloudina AR, Mazur SJ, Appella E, Garrido C, and Demidov ON. Wip1 sensitizes p53-negative tumors to apoptosis by regulating the Bax/Bcl-xL ratio. Cell Cycle. 2012; 11:1883-1887.

87. Hu B, Gilkes DM, Farooqi B, Sebti SM, and Chen J. MDMX Overexpression Prevents p53 Activation by the MDM2 Inhibitor Nutlin. J Biol Chem. 2006; 281:33030-33035.

88. Xia M, Knezevic D, Tovar C, Huang B, Heimbrook DC, and Vassilev LT. Elevated MDM2 boosts the apoptotic activity of p53-MDM2 binding inhibitors by facilitating MDMX degradation. Cell Cycle. 2008; 7:1604-1612.

89. Quah BJC, Warren HS, and Parish CR. Monitoring lymphocyte proliferation in vitro and in vivo with the intracellular fluorescent dye carboxyfluorescein diacetate succinimidyl ester. Nat. Protocols. 2007; 2:2049-2056.

90. Gary RK and Kindell SM. Quantitative assay of senescence-associated β-galactosidase activity in mammalian cell extracts. Analytical Biochemistry. 2005; 343:329-334.

3.4 WIP1 phosphatase as pharmacological target in cancer therapy

Pecháčková S, Burdová K, Macůrek L.

Journal of Molecular Medicine (under consideration)

In this review, we discuss how could be used WIP1 inhibition in cancer therapy and which type of currently published inhibitors of WIP1 are specific in cancer cells. We focused on tumors with *PPM1D* amplification or gain-of-function mutation which carry intact of the TP53 locus.

P. S created the figures, wrote and coordinated the manuscript.

WIP1 phosphatase as pharmacological target in cancer therapy

Soňa Pecháčková, Kamila Burdová, Libor Macurek

Department of Cancer Cell Biology, Institute of Molecular Genetics of the ASCR, CZ-14220 Prague, *Czech Republic*

Correspondence to:

Libor Macurek, MD, PhD
Cancer Cell Biology
Institute of Molecular Genetics ASCR
Videnska 1083
14200 Prague
Czech Republic
tel: +420241063210
email: macurek@img.cas.cz

Keywords: cancer, phosphatase, checkpoint, DNA damage response, inhibitor, p53

Abstract

DNA damage response (DDR) pathway protects cells from genome instability and prevents cancer development. Tumor suppressor p53 is a key molecule that interconnects DDR, cell cycle checkpoints and cell fate decisions in the presence of genotoxic stress. Inactivating mutations in *TP53* and other genes implicated in DDR potentiate cancer development and also influence the sensitivity of cancer cells to treatment. Protein phosphatase 2C delta (referred to as WIP1) is a negative regulator of DDR and has been proposed as potential pharmaceutical target. Until recently, exploitation of WIP1 inhibition for suppression of cancer cell growth was compromised by the lack of selective small molecule inhibitors effective at cellular and organismal levels. Here we review recent advances in development of WIP1 inhibitors and discuss their potential use in cancer treatment.

Introduction

Genetic information is continuously endangered by erroneous DNA metabolism as well as by various environmental factors that include ionizing radiation or chemotherapy representing two major non-surgical approaches in cancer therapy. Cells respond to genotoxic stress by activation of a conserved DNA damage response pathway (DDR) that abrogates cell cycle progression and facilitates DNA repair. This safeguard mechanism represents an intrinsic barrier preventing genome instability and protecting cells against tumor development [1-4]. Depending on the mode and level of DNA damage, DDR signaling network promotes temporary cell cycle arrest (checkpoint), permanent growth arrest (senescence) or programmed cell death (apoptosis). Genes coding for proteins involved in DDR are typically tumor suppressors and are commonly mutated in cancer. The DDR pathway is regulated by a spatiotemporally controlled cascade of posttranslational modifications of key proteins including protein phosphorylation and ubiquitination [5]. Following DNA damage, upstream protein kinases ATM and ATR are activated and spread the signal through phosphorylation of downstream transducing kinases CHK2 and CHK1 to rapidly establish the checkpoint arrest. Subsequently, checkpoint is reinforced by activation of the tumor suppressor protein p53 and its transcriptional target p21 that inactivates cyclin dependent kinases.

After completion of DNA repair, activity of the DDR pathway is terminated by protein phosphatases that allow checkpoint recovery and restart cell proliferation. Serine/threonine phosphatases of PP2C family are evolutionary conserved negative regulators of cell stress response pathways and function as monomeric enzymes comprising of a conserved N-terminal phosphatase domain and non-catalytic C-terminal part [6]. Protein phosphatase 2C isoform delta is ubiquitously expressed at basal levels and its expression is strongly induced after exposure of cells to genotoxic stress in a p53-dependent manner (hence its alternative name WIP1 for wild-type p53 induced protein 1) [7]. Substrate specificity of the chromatin-bound WIP1 matches the phosphorylation sites imposed by ATM kinase and thus WIP1 can efficiently dephosphorylate p53, γH2AX and possibly also other proteins involved in DDR [8, 9]. Downregulation of WIP1 by RNA interference leads to prolongation of the G2 checkpoint whereas overexpression of WIP1 causes checkpoint override [10, 11]. WIP1 phosphatase is overexpressed in multiple human cancers and was reported to act as oncogene. Conversely, loss of WIP1 delayed the onset of tumor development in mouse models [12-14]. Similarly,

RNAi-mediated depletion of WIP1 inhibited cancer cell growth implicating WIP1 as promising pharmacological target [14]. Here we discuss recent advances in development of a selective WIP1 inhibitor with proven efficiency in animal models and its potential use in cancer therapy.

DNA damage response and role of WIP1 in checkpoint recovery

Various kinds of genotoxic stress activate kinases of PI3-kinase like family, including activation of ATM by DNA double strand breaks (DSBs) and ATR by exposed single stranded DNA (ssDNA) at stalled replication forks or resected DSBs (Figure 1). ATM and ATR phosphorylate the effector checkpoint kinases CHK2 and CHK1 that target phosphatases Cdc25A/B/C leading to inactivation of cyclin dependent kinases (CDKs) and cell cycle arrest. Under basal conditions, p53 is degraded by the E3 ubiquitin ligase MDM2 and transcriptionally inactivated at promoters by its enzymatically inactive homologue MDMX [15-18]. Following DNA damage, p53 is posttranslationally modified by ATM/CHK2, ATR/CHK1 and various acetyltransferases leading to its stabilization, oligomerization, binding to promoters and triggering transcription of various target genes involved in cell cycle arrest, DNA repair, apoptosis, senescence and metabolism [19, 20]. CDKN1/p21 is a transcriptional target of p53 and potent inhibitor of CDKs that promotes maintenance of the G1 and G2 checkpoint. In non-stressed cells, expression of CDKN1/p21 is repressed by Transcription intermediary factor 1-beta (also called KAP1) [21]. Phosphorylation of KAP1 at Ser824 by ATM and at Ser473 by CHK1/2 induced by genotoxic stress allows de-repression of CDKN1/p21 and contributes to checkpoint activation [21, 22].

Besides arresting the cell cycle progression, ATM promotes DNA repair by phosphorylating histone variant H2AX at S139 (called γH2AX) in the flanking chromatin and plethora of other DNA repair proteins. γH2AX acts as a docking platform for various mediator proteins and ubiquitin ligases that jointly regulate recruitment of either 53BP1 or BRCA1 proteins to the close proximity of the DNA lesion and thus control the DNA repair pathway choice [23]. Whereas 53BP1 in complex with RIF1 blocks DSBs resection and promotes non-homologous end joining, recruitment of BRCA1 stimulates resection and therefore facilitates homologous recombination (HR). After completion of DNA repair, cells recover from the checkpoint arrest and reenter the cell cycle. By targeting claspin, an important cofactor of ATR, PLK1 kinase terminates the activation of CHK1 and is essential for recovery from the G2 checkpoint [24]. In addition, various protein phosphatases directly reverse multiple phosphorylations imposed

by ATM/ATR and CHK1/2 and thus contribute to timely inactivation of DDR [25]. In particular, protein phosphatase PP4 targets Ser473 of KAP1 and has been implicated in recovery from the G1 checkpoint [26]. In contrast, WIP1 is needed for recovery from the G2 checkpoint [11, 26]. Whereas expression of WIP1 is potentiated by p53, it acts as a strong negative regulator of p53 pathway thus forming a negative feedback loop that allows termination of p53 response after completion of DNA repair [11]. WIP1 inhibits p53 directly by dephosphorylating Ser15 and indirectly through the stimulation of its negative regulators MDM2 and MDMX [10, 27-30]. In fact, WIP1 activity is needed throughout the G2 checkpoint to limit the level of p53/p21 pathway activation and to prevent degradation of cyclin B and a permanent cell cycle exit [31, 32]. Similarly, WIP1 was shown to suppress DNA-damage induced apoptosis in different cell types [33-35]. Besides targeting p53 pathway, WIP1 contributes to termination of DDR by dephosphorylation of ATM at Ser1981 and γH2AX at chromatin [9, 36-38]. Other reported substrates of WIP1 include active forms of CHK1, CHK2 and p38 that reside mostly in nucleoplasm [10, 39, 40]. Although WIP1 can dephosphorylate these proteins *in vitro* or when overexpressed, the physiological role of the chromatin bound WIP1 in targeting these pathways remains unclear. Similarly, WIP1 was reported to counteract phosphorylation of the p65 subunit of NF-κB at Ser536 but more data are needed to clarify to what extent WIP1 regulates NF-κB pathway in inflammation [41].

Function of WIP1 is controlled in context of the cell cycle. Expression of WIP1 protein is low in G1, peaks in S/G2 and decreases during mitosis [42]. WIP1 is phosphorylated at multiple residues within the catalytic domain during mitosis which promotes its degradation by APC/cdc20 in prometaphase [42]. Absence of WIP1 in mitosis may allow cells to recognize low levels of endogenous DNA damage present in condensed chromosomes. These sites are labeled by γH2AX during mitosis and they are repaired after mitotic exit in subsequent G1 phase. During interphase, WIP1 is constitutively phosphorylated at Ser54 and Ser85 by HIPK2 kinase that results in a rapid turnover of WIP1 [43]. Keeping basal levels of WIP1 low probably allows cells to fully activate DDR in the presence of genotoxic stress, whereas p53-dependent induction of WIP1 expression allows termination of DDR after completion of DNA repair.

WIP1 phosphatase as an oncogene

About a half of human solid tumors exhibit somatic mutations in the *TP53* gene that cause a deficient response to genotoxic stress and are commonly associated with poor prognosis [44, 45]. On the other hand, tumors carrying wild-type *TP53* frequently accumulate mutations in other genes that functionally compromise the p53 pathway and thus potentiate cell proliferation. As described above, WIP1 phosphatase is a negative regulator of DDR pathway and enhanced activity of WIP1 can contribute to tumor development.

WIP1 is encoded by *PPM1D* gene located at chromosomal locus 17q23.2 and its amplification was reported in about 10 % of breast cancers [46, 47]. Importantly, amplification of *PPM1D* occurred significantly more often in breast tumours that retained wild type *TP53* [46, 47] (Figure 2). Similarly, common amplification of *PPM1D* was found in ovarian clear cell carcinoma, where mutations in *TP53* are relatively rare, but not in a more common serous carcinoma that typically contains mutated *TP53* [48, 49]. Besides breast and ovarian cancer, *PPM1D* copy numbers gain or overexpression at mRNA level were reported also in glioma, neuroblastoma and medulloblastoma [47, 49-56]. High expression of WIP1 was also observed by immunohistological methods in a fraction of lung adenocarcinomas, gastric and colorectal cancer [53, 57, 58]. However, caution should be taken when interpreting the histopathological data, since none of the currently available antibodies was sufficiently validated in histological assays and the staining pattern does not correspond with expected nuclear localization of WIP1. Besides amplification, nonsense mutations occur in a hot spot region of the exon 6 of *PPM1D* [59, 60]. These point mutations of *PPM1D* result in expression of C-terminally truncated variants of WIP1 that exhibit higher protein stability and disable full activation of the checkpoint after genotoxic stress [60]. Besides breast and ovarian cancer, this type of mutations have been found in brainstem gliomas, lung adenocarcinoma and prostate cancer [59-65]. WIP1 truncating mutations are considerably less common than *PPM1D* amplifications (usually below 1 %) and their occurrence was reported to further increase after chemotherapy [64]. Although gain-of-function mutations in *PPM1D* efficiently suppress p53 function their pathogenic role in cancer development still needs to be experimentally tested.

Amplification of *PPM1D* was initially suggested to promote breast cancer development through inactivation of the p53 and p38 MAPK pathways [50, 66]. In the same time, however,

MMTV-driven overexpression of *PPM1D* in mice did not promote mammary tumor formation within two years suggesting that oncogenic properties of WIP1 may be relatively low [50, 67]. About one-third of breast tumors with *PPM1D* overexpression showed also amplification of *ERBB2* suggesting that these two oncogenes may cooperatively promote breast cancer development [68]. Ablation of *PPM1D* in mice impaired spermatogenesis and decreased levels of B and T-lymphocytes, both probably reflecting the decreased ability to respond adequately to endogenous DNA breaks occurring during meiosis or immunoglobulin gene rearrangements, respectively [69, 70]. Importantly, deletion of *PPM1D* strongly suppressed breast tumorigenesis in mice bearing MMTV-driven oncogenes *ERBB2* or *HRAS1* through the inactivation of p38 MAPK and p53 pathways [71]. Loss of *PPM1D* also dramatically delayed development of Eμ-myc-induced lymphomas in a p53 dependent manner [72]. In context of the colon, WIP1 was found to be highly expressed in the stem cell compartment and loss of *PPM1D* suppressed APC(Min)-driven polyp formation in mice suggesting that WIP1 might be involved also in development of colorectal cancer [73].

Exact molecular mechanism(s) by which WIP1 contributes to cell transformation still needs to be fully addressed. Data from the *PPM1D* knock-out mice and clinical specimens suggest a strong correlation between oncogenic behavior of WIP1 and the functional p53 pathway. In addition, gain-of-function mutations in *PPM1D* promote cell proliferation by overcoming p53 function and conversely, loss of *PPM1D* slows down proliferation only in p53 proficient cells further supporting the model in which active WIP1 allows cells to overcome the tumor suppressing barrier imposed by p53 pathway (Figure 3). Whereas overexpressed WIP1 may not be sufficient to fully transform the cells, it can become more important under conditions of activation of oncogenes. It is well established that oncogene activation causes replication stress and induces senescence. An attractive possibility is that WIP1 may prevent oncogene-induced senescence and thus allow accumulation of mutations caused by proliferation under condition of replication stress. In addition, WIP1 was reported to regulate epigenetic changes in heterochromatin which may increase the C-to-T substitutions and thus contribute to genome instability [74]. Finally, overexpressed WIP1 was shown to impair DNA repair through nucleotide excision and base excision pathways [75, 76]. It should be noted that all these mechanisms by which WIP1 activity promotes genome instability are not mutually exclusive, and they may jointly contribute to tumorigenesis.

Predicted structure of WIP1 phosphatase

Development of highly potent and specific small molecule inhibitors is greatly facilitated by 3D structural data of the target proteins [77]. Since WIP1 structure has still not been determined, molecular models based on its homology with PPM1A (sharing ~35% sequence identity) represent the only resource of information about WIP1 structure [78, 79]. Like the other PP2Cs, WIP1 acts as monomer consisting of the N-terminal catalytic domain (amino acids 1-375) and a presumably unstructured C-terminal tail [80]. Conserved negatively charged amino acids in the catalytic domain bind two Mg^{2+}/Mn^{2+} ions and stabilize interaction of WIP1 with the phosphorylated substrate. A unique flap sub-domain resides in the catalytic domain close to the active site and can influence binding of different substrates by allosteric modulation [78]. Part of the flap domain is a basic amino acid-rich region (called B-loop; amino acids 235-268) that was proposed to bind to negatively charged phosphate on substrates [79]. In vitro studies established that WIP1 can specifically recognize two distinct substrate motifs, namely pSQ/pTQ (present in ATM, p53, MDM2, γH2AX, Chk1, Chk2) and pTxpY (present in the active form of p38 MAPK) [8]. In comparison to other PP2Cs, catalytic domain of WIP1 contains a proline rich region (Pro-loop) that was proposed to mediate protein-protein interactions. However, the Pro-loop is not evolutionary conserved and its function in control of WIP1 activity still remains unclear. Translocation of WIP1 to the nucleus is controlled by two nuclear localization sequences (NLS). One NLS resides in the C-terminus (amino acids 535-552), while the other is located within the catalytic domain (amino acids 247-250) [60, 81]. Presence of the two NLS sequences explains why the C-terminally truncated mutants of WIP1 localize normally in the nucleus.

Small molecule inhibitors of WIP1

Based on data from *PPM1D* knockout mice and also from RNAi-mediated depletion of WIP1 in cancer cell lines, WIP1 was proposed as potential pharmacological target [71-73]. Since the structure of WIP1 is still unknown the potential inhibitors of WIP1 were found by high-throughput screening of extensive chemical libraries. During the last decade several compounds antagonizing WIP1 activity were developed, however only one of these inhibitors exhibits high specificity to WIP1 and shows promising results in preclinical analysis.

Compound M321237 was identified by screening of a chemical library based on its ability to inhibit WIP1 activity *in vitro* [82]. Cell viability assay showed that M321237 sensitized MCF7 cells to doxorubicin. *In vivo* experiments reveled that administration of M321237 decreased tumor volumes in xenograft models, however the selectivity of M321237 towards WIP1 has never been validated. Similar screening approach led to identification of CCT007093 that inhibited WIP1 in vitro with IC_{50} = 8.4 µM [83]. Cell viability in presence of CCT007093 was suppressed in human *PPM1D* amplified and p53 proficient cancer cells [83]. On the other hand, CCT007093 failed to inhibit endogenous WIP1 in skin keratinocytes, suggesting possible off-target effects of the inhibitor [84]. Recently, CCT007093 was shown to suppress cell proliferation regardless of the presence of WIP1 in U2OS cells [85]. In addition, treatment of cells with CCT007093 did not affect levels of p53-pS15 and γH2AX, both well-established substrates of WIP1 [85]. These data suggest that CCT007093 does not inhibit WIP1 in cells and highlight the urgent need for validation of specificity of small molecule inhibitors in cellular models including the CRISPR/Cas9-mediated knock-out of the expected target gene. Compared to previous compounds, SPI-001 and its analogue SL-176 were determined as noncompetitive inhibitors of recombinant WIP1 with IC_{50} = 110 and 86.9 nM, respectively [86, 87]. Moreover, SPI-001 was determined to be approximately 50-fold more specific against WIP1 than to another PP2C phosphatase, PPM1A [86]. Both, SPI-001 and SL-176 suppressed the cell proliferation in human breast cancer MCF7 cells with overexpressed wild-type *PPM1D* in a dose-dependent manner [87]. In human colorectal carcinoma HCT-116 cells expressing truncated WIP1, treatment with SPI-001 did not affect cell proliferation but combined treatment with SPI-001 and doxorubicin enhanced inhibition of cell growth through the increased phosphorylation of p53 at Ser15 [88]. In conclusion, SPI-001 and SL-176 are promising lead compounds but further analysis is needed to validate their specificity and efficiency in cellular and animal models. Another strategy for development of WIP1 inhibitors was based on modification of short peptides derived from natural WIP1 substrates [8, 89, 90]. Substitution of the pT to pS in the pT-X-pY peptide sequence corresponding to p38 prevented its dephosphorylation by WIP1. Further modification led to development of a cyclic thioether peptide c(MpSIpYVA) with micro-molar inhibitory activity towards WIP1 (Ki = 5 µM). These cyclic peptide inhibitors mimic substrates of WIP1 and block its enzymatic activity *in vitro.* Further improved cyclic peptide (F-pHse-I-pY-DDC-amide) significantly increased the inhibitory activity and selectivity for WIP1 with Ki = 2.9 µM [89]. The disadvantage of this

peptide is poor bioavailability resulting in weak absorption into cells [91]. Therefore, phosphopeptide-based inhibitors have not been tested in cell viability assays to address their anti-proliferative effect. However, the cyclic peptide could be used in future in different drug delivery system, such as nanoparticles.

The most promising compound with high selectivity to WIP1 phosphatase was identified by combination of a biochemical and biophysical screens that employed inhibition of WIP1 enzymatic activity and high-affinity binding as readouts, respectively [78]. Both screens identified compounds with overlapping structures containing an amino acid-like core region (referred to as capped amino acids, CAA) flanked by additional groups that influence pharmacokinetic properties [78]. From this series, compound GSK2830371 has been further developed and showed improved cell permeability and pharmacokinetics. According to WIP1 homology model with PPM1A structure and by photo-affinity labeling of WIP1, the binding sites of CAA were located in the Flap domain outside of the active site thus resulting in allosteric inhibition of WIP1. GSK2830371 inhibited WIP1 *in vitro* with IC_{50} = 13 nM. This compound selectively inhibited WIP1 phosphatase while other 21 phosphatases showed no inhibition of enzyme activity *in vitro*. Cell proliferation experiments revealed that GSK2830371 efficiently suppressed proliferation of tumor cells carrying *PPM1D* amplification while retaining wild-type *TP53*, including hematological cancer, neuroblastoma and breast cancer cell lines [55, 78, 85, 92, 93]. Importantly, U2OS-PPM1D-KO cells where *PPM1D* was knocked-out by CRISPR/Cas9 did not respond to GSK2830371 further confirming its specificity to WIP1 at cellular level [94]. Inhibition of WIP1 by GSK2830371 upregulated expression of p53 target genes including *CDKN1A, PUMA* and *BAX,* and caused cell cycle arrest but was not sufficient to induce cell death [78, 85, 92, 95]. In addition, GSK2830371 suppressed growth of B-cell lymphoma and neuroblastoma in xenograft mouse models demonstrating efficiency of this compound *in vivo* [78, 92]. Importantly, these studies also demonstrated that GSK2830371 is orally bioavailable. However, relatively low stability of GSK2830371 in blood could limit its clinical use. Further modification of GSK2830371 as a lead compound will hopefully allow development of a small molecule WIP1 inhibitor with more favorable pharmacokinetic properties.

Targeting of WIP1 phosphatase in cancer therapy

Restoration of p53 function was shown to cause tumor regression in a mouse model setting ground for development of various compounds capable of inducing the p53 pathway in cancer cells [96]. As described above, inhibition of WIP1 can suppress proliferation of cancer cells by activation of p53 pathway. The highest response is observed in cancer cells with the amplified *PPM1D* (such as MCF7) or truncated WIP1 (such as U2OS), suggesting that these cells might be addicted to the high level of WIP1. In contrast, healthy cells with basal expression of WIP1 are relatively resistant to WIP1 inhibition. Although inhibition of WIP1 strongly suppressed proliferation of cells with high activity of WIP1, it failed to induce massive cell death of cancer cells that would be desirable in cancer therapy [78, 85]. Several studies showed that depletion of WIP1 by RNA interference sensitized cancer cells to DNA damage-inducing chemotherapy [88, 97, 98]. Similarly, GSK2830371 potentiated cytotoxic effect of doxorubicin in breast cancer cells, neuroblastoma and lymphoma [85, 92, 93]. These results suggest that treatment with WIP1 inhibitor could allow to decrease the efficient dose of doxorubicin and thus reduce the its undesired side effects [99, 100]. Similarly, inhibition of WIP1 increased sensitivity of cells to ionizing radiation and to etoposide suggesting that a broader range of potentially beneficial treatment combinations may exist.

Reactivation of the p53 pathway by MDM2 inhibition has been suggested as a promising therapeutic strategy in cancers retaining wild-type *TP53* and several MDM2 antagonists are currently in clinical trials [101-104]. MDM2 antagonist nutlin-3 and its orally bioavailable analogues RG7388 and RG7112 disrupted interaction between p53 and MDM2 leading to stabilization of p53 [105, 106]. MDM2 antagonists efficiently induced apoptosis in p53-proficient neuroblastoma and ovarian clear cell carcinoma and blocked tumor growth in xenograft models [106-109]. Combined treatment with GSK2830371 and nutlin-3 further increased the level of p53 pathway activation and potentiated induction of senescence and apoptosis in MCF7 and HCT116 cells [85, 93, 95, 110]. These data suggest that inhibition of WIP1 that leads to increased phosphorylation of p53 may synergize with compounds that promote stabilization of p53. Besides nutlin-3, other MDM2 antagonists were reported to reactivate p53 and to strongly induce apoptosis of cancer cells, including RITA that binds to p53 at its N-terminus. Whereas, the specificity of nutlin-3 has recently been confirmed by CRISPR/Cas9-mediated deletion of p53, cytotoxic effect of RITA was completely independent

on the presence of p53, further highlighting the need for validation of the small molecule inhibitors using modern gene targeting approaches [111].

WIP1 activation in p53 negative tumors

As described above, WIP1 is a major negative regulator of p53 pathway. Besides direct or indirect inactivation of p53 pathway, WIP1 was reported to control the expression level of a pro-apoptotic protein Bax through dephosphorylation of a transcriptional factor RUNX2 [112, 113]. This pathway is particularly important in p53-negative cancer cells, where WIP1 activity promotes cisplatin-induced apoptosis. These results led to postulation of an attractive model in which activation of WIP1 can increase sensitivity of p53-negative cells to chemotherapy while protecting the healthy cells (carrying wild-type p53) from possible side effects. However, until now selective potentiation of WIP1 function remains challenging. One of the possibilities for pharmaceutical intervention, could be regulation of WIP1 stability in cells. Turnover of WIP1 in cells is relatively fast (half-life about 90 minutes) and phosphorylation of WIP1 by HIPK2 potentiates its degradation by proteasome [114]. Indeed, depletion of HIPK2 enhanced the stability of WIP1 and recently has been reported to increase the sensitivity of p53-deficient Saos2 cells to cisplatin [114, 115]. It will be interesting to address the ability of pharmacological inhibitors of HIPK2 to modulate WIP1 levels in cells. Another possibility to increase WIP1 levels in cells might be selective induction of *PPM1D* expression, possibly by RNA-guided activation of endogenous human genes [116]. Clearly, more research is needed to explore suitable approaches for selective WIP1 induction and to experimentally test its benefit for eradication of p53-negative tumors.

Conclusions and future directions

Data from cell biology and mouse genetics highlight WIP1 as an important negative regulator of p53 pathway and a terminator of the DNA damage response. When overexpressed, WIP1 impairs p53 function and contributes to tumorigenesis, usually in combination with activation of other oncogenes. Conversely, loss of WIP1 significantly delays tumor development in mice and similarly depletion of WIP1 by RNA interference allows reactivation of p53 pathway and inhibits proliferation in p53-proficient tumors. Until recently, specific inhibition of WIP1 represented a major challenge and lack of selective small molecule inhibitors limited

exploitation of WIP1 as pharmacological target in cancer therapy. Situation has changed by development of the compound GSK2830371 that has validated specificity towards WIP1 and efficiently reactivates p53 pathway in various cancer types, including breast cancer, neuroblastoma and lymphoma. In combination with DNA damage-inducing chemotherapy or with MDM2 antagonists (such as nutlin-3), WIP1 inhibition promotes cancer cell death or senescence, while it has little effect on viability of healthy cells. Importantly, GSK2830371 is orally bioavailable and its ability to suppress cancer cell growth *in vivo* was demonstrated in xenograft models. In the same time, GSK2830371 is rapidly inactivated in plasma, which may limit its further clinical use. Therefore, further development of GSK2830371 derivatives with more favorable pharmacokinetic properties is highly desirable. Also, solving the 3D structure of WIP1 could stimulate development of even more selective WIP1 inhibitors. Current results suggest that inhibition of WIP1 will be most efficient in cancers with wild type p53 and amplification or gain-of-function mutations of *PPM1D* and thus determination of the status of *TP53* and *PPM1D* in the tumors will be important for predicting the therapeutical outcome of WIP1 inhibitors. Identification of additional factors that control the ability of cells to reactivate p53 pathway is needed to allow prediction of the cancer cell sensitivity to WIP1 inhibitors. MDM2 and MDMX that are commonly overexpressed in tumors seem to be attractive candidates for testing the sensitivity to MDM2 antagonists and WIP1 inhibitors. Although loss of WIP1 is well tolerated in mice, there is emerging evidence that WIP1 plays role in differentiation of cells of the immune system (recently reviewed in [117]). In light of these newly arising physiological roles of WIP1 it will be important to address possible side effects of a temporary inhibition of WIP1 during therapeutical intervention.

Conflict of interest

Authors declare no conflict of interest.

Acknowledgements

This work was supported by Ministry of Education Youth and Sports (CZ-OPENSCREEN, LO1220).

References

1. Jackson, S.P. and J. Bartek, *The DNA-damage response in human biology and disease.* Nature, 2009. **461**(7267): p. 1071-8.
2. Halazonetis, T.D., V.G. Gorgoulis, and J. Bartek, *An oncogene-induced DNA damage model for cancer development.* Science, 2008. **319**(5868): p. 1352-5.
3. Bartek, J., J. Bartkova, and J. Lukas, *DNA damage signalling guards against activated oncogenes and tumour progression.* Oncogene, 0000. **26**(56): p. 7773-7779.
4. Bartkova, J., et al., *DNA damage response as a candidate anti-cancer barrier in early human tumorigenesis.* Nature, 2005. **434**(7035): p. 864-870.
5. Polo, S.E. and S.P. Jackson, *Dynamics of DNA damage response proteins at DNA breaks: a focus on protein modifications.* Genes Dev, 2011. **25**(5): p. 409-33.
6. Lammers, T. and S. Lavi, *Role of type 2C protein phosphatases in growth regulation and in cellular stress signaling.* Crit Rev Biochem Mol Biol, 2007. **42**(6): p. 437-61.
7. Fiscella, M., et al., *Wip1, a novel human protein phosphatase that is induced in response to ionizing radiation in a p53-dependent manner.* Proc Natl Acad Sci U S A, 1997. **94**(12): p. 6048-53.
8. Yamaguchi, H., et al., *Substrate specificity of the human protein phosphatase 2Cdelta, Wip1.* Biochemistry, 2005. **44**(14): p. 5285-94.
9. Macurek, L., et al., *Wip1 phosphatase is associated with chromatin and dephosphorylates gammaH2AX to promote checkpoint inhibition.* Oncogene, 2010. **29**(15): p. 2281-91.
10. Lu, X., B. Nannenga, and L.A. Donehower, *PPM1D dephosphorylates Chk1 and p53 and abrogates cell cycle checkpoints.* Genes Dev, 2005. **19**(10): p. 1162-74.
11. Lindqvist, A., et al., *Wip1 confers G2 checkpoint recovery competence by counteracting p53-dependent transcriptional repression.* EMBO J, 2009. **28**(20): p. 3196-206.
12. Lu, X., et al., *The type 2C phosphatase Wip1: an oncogenic regulator of tumor suppressor and DNA damage response pathways.* Cancer Metastasis Rev, 2008. **27**(2): p. 123-35.
13. Le Guezennec, X. and D.V. Bulavin, *WIP1 phosphatase at the crossroads of cancer and aging.* Trends in Biochemical Sciences, 2010. **35**(2): p. 109-114.
14. Harrison, M., et al., *Wip1-deficient mice are resistant to common cancer genes.* Trends in Molecular Medicine, 2004. **10**(8): p. 359-361.
15. Leslie, P.L. and Y. Zhang, *MDM2 oligomers: antagonizers of the guardian of the genome.* Oncogene, 2016.
16. Haupt, Y., et al., *Mdm2 promotes the rapid degradation of p53.* Nature, 1997. **387**(6630): p. 296-9.
17. Pei, D., Y. Zhang, and J. Zheng, *Regulation of p53: a collaboration between Mdm2 and Mdmx.* Oncotarget, 2012. **3**(3): p. 228-35.
18. Honda, R., H. Tanaka, and H. Yasuda, *Oncoprotein MDM2 is a ubiquitin ligase E3 for tumor suppressor p53.* FEBS Lett, 1997. **420**(1): p. 25-7.
19. Zhang, X.P., et al., *Cell fate decision mediated by p53 pulses.* Proc Natl Acad Sci U S A, 2009. **106**(30): p. 12245-50.
20. Leontieva, O.V., A.V. Gudkov, and M.V. Blagosklonny, *Weak p53 permits senescence during cell cycle arrest.* Cell Cycle, 2010. **9**(21): p. 4323-7.
21. Lee, Y.-K., et al., *Doxorubicin Down-regulates Krüppel-associated Box Domain-associated Protein 1 Sumoylation That Relieves Its Transcription Repression on p21WAF1/CIP1 in Breast Cancer MCF-7 Cells.* Journal of Biological Chemistry, 2007. **282**(3): p. 1595-1606.
22. Blasius, M., et al., *A phospho-proteomic screen identifies substrates of the checkpoint kinase Chk1.* Genome Biology, 2011. **12**(8): p. R78-R78.
23. Chapman, J.R., Martin R.G. Taylor, and Simon J. Boulton, *Playing the End Game: DNA Double-Strand Break Repair Pathway Choice.* Molecular Cell, 2012. **47**(4): p. 497-510.

24. Mamely, I., et al., *Polo-like Kinase-1 Controls Proteasome-Dependent Degradation of Claspin during Checkpoint Recovery.* Current Biology, 2006. **16**(19): p. 1950-1955.
25. Shaltiel, I.A., et al., *The same, only different – DNA damage checkpoints and their reversal throughout the cell cycle.* Journal of Cell Science, 2015. **128**(4): p. 607-620.
26. Shaltiel, I.A., et al., *Distinct phosphatases antagonize the p53 response in different phases of the cell cycle.* Proc Natl Acad Sci U S A, 2014. **111**(20): p. 7313-8.
27. Lu, X., et al., *The Wip1 phosphatase and Mdm2: cracking the "Wip" on p53 stability.* Cell Cycle, 2008. **7**(2): p. 164-8.
28. Lu, X., et al., *The Wip1 Phosphatase acts as a gatekeeper in the p53-Mdm2 autoregulatory loop.* Cancer Cell, 2007. **12**(4): p. 342-54.
29. Zhang, X., et al., *Phosphorylation and degradation of MdmX is inhibited by Wip1 phosphatase in the DNA damage response.* Cancer Res, 2009. **69**(20): p. 7960-8.
30. Meulmeester, E., et al., *ATM-mediated phosphorylations inhibit Mdmx/Mdm2 stabilization by HAUSP in favor of p53 activation.* Cell Cycle, 2005. **4**(9): p. 1166-70.
31. Krenning, L., et al., *Transient Activation of p53 in G2 Phase Is Sufficient to Induce Senescence.* Molecular Cell, 2014. **55**(1): p. 59-72.
32. Müllers, E., et al., *Nuclear translocation of Cyclin B1 marks the restriction point for terminal cell cycle exit in G2 phase.* Cell Cycle, 2014. **13**(17): p. 2733-2743.
33. Lee, J.S., et al., *Senescent growth arrest in mesenchymal stem cells is bypassed by Wip1-mediated downregulation of intrinsic stress signaling pathways.* Stem Cells, 2009. **27**(8): p. 1963-75.
34. Sakai, H., et al., *Wild-type p53-induced phosphatase 1 (Wip1) forestalls cellular premature senescence at physiological oxygen levels by regulating DNA damage response signaling during DNA replication.* Cell Cycle, 2014. **13**(6): p. 1015-29.
35. Song, J.Y., et al., *Wip1 suppresses apoptotic cell death through direct dephosphorylation of BAX in response to gamma-radiation.* Cell Death Dis, 2013. **4**: p. e744.
36. Shreeram, S., et al., *Wip1 phosphatase modulates ATM-dependent signaling pathways.* Mol Cell, 2006. **23**(5): p. 757-64.
37. Moon, S.H., et al., *Wild-type p53-induced phosphatase 1 dephosphorylates histone variant gamma-H2AX and suppresses DNA double strand break repair.* J Biol Chem, 2010. **285**(17): p. 12935-47.
38. Cha, H., et al., *Wip1 directly dephosphorylates gamma-H2AX and attenuates the DNA damage response.* Cancer Res, 2010. **70**(10): p. 4112-22.
39. Yoda, A., et al., *Intrinsic kinase activity and SQ/TQ domain of Chk2 kinase as well as N-terminal domain of Wip1 phosphatase are required for regulation of Chk2 by Wip1.* J Biol Chem, 2006. **281**(34): p. 24847-62.
40. Takekawa, M., et al., *p53-inducible wip1 phosphatase mediates a negative feedback regulation of p38 MAPK-p53 signaling in response to UV radiation.* EMBO J, 2000. **19**(23): p. 6517-26.
41. Chew, J., et al., *WIP1 phosphatase is a negative regulator of NF-[kappa]B signalling.* Nat Cell Biol, 2009. **11**(5): p. 659-666.
42. Macurek, L., et al., *Downregulation of Wip1 phosphatase modulates the cellular threshold of DNA damage signaling in mitosis.* Cell Cycle, 2013. **12**(2): p. 251-62.
43. Choi, Dong W., et al., *WIP1, a Homeostatic Regulator of the DNA Damage Response, Is Targeted by HIPK2 for Phosphorylation and Degradation*
44. Petitjean, A., et al., *TP53 mutations in human cancers: functional selection and impact on cancer prognosis and outcomes.* Oncogene, 2007. **26**(15): p. 2157-2165.
45. Wang, X. and Q. Sun, *TP53 mutations, expression and interaction networks in human cancers.* Oncotarget, 2016.
46. Natrajan, R., et al., *Tiling Path Genomic Profiling of Grade 3 Invasive Ductal Breast Cancers.* Clinical Cancer Research, 2009. **15**(8): p. 2711.

47. Li, J., et al., *Oncogenic properties of PPM1D located within a breast cancer amplification epicenter at 17q23.* Nat Genet, 2002. **31**(2): p. 133-4.
48. Shih-Chu Ho, E., et al., *p53 Mutation Is Infrequent in Clear Cell Carcinoma of the Ovary.* Gynecologic Oncology, 2001. **80**(2): p. 189-193.
49. Tan, D.S., et al., *PPM1D is a potential therapeutic target in ovarian clear cell carcinomas.* Clin Cancer Res, 2009. **15**(7): p. 2269-80.
50. Bulavin, D.V., et al., *Amplification of PPM1D in human tumors abrogates p53 tumor-suppressor activity.* Nat Genet, 2002. **31**(2): p. 210-5.
51. Liang, C., et al., *Over-expression of wild-type p53-induced phosphatase 1 confers poor prognosis of patients with gliomas.* Brain Res, 2012. **1444**: p. 65-75.
52. Rauta, J., et al., *The serine-threonine protein phosphatase PPM1D is frequently activated through amplification in aggressive primary breast tumours.* Breast Cancer Res Treat, 2006. **95**(3): p. 257-63.
53. Peng, T.S., et al., *PPM1D is a prognostic marker and therapeutic target in colorectal cancer.* Exp Ther Med, 2014. **8**(2): p. 430-434.
54. Castellino, R.C., et al., *Medulloblastomas overexpress the p53-inactivating oncogene WIP1/PPM1D.* J Neurooncol, 2008. **86**(3): p. 245-56.
55. Richter, M., et al., *WIP1 Phosphatase as a Potential Therapeutic Target in Neuroblastoma.* PLoS ONE, 2015. **10**(2): p. e0115635.
56. Saito-Ohara, F., et al., *PPM1D is a potential target for 17q gain in neuroblastoma.* Cancer Res, 2003. **63**(8): p. 1876-83.
57. Satoh, N., et al., *Oncogenic phosphatase Wip1 is a novel prognostic marker for lung adenocarcinoma patient survival.* Cancer Science, 2011. **102**(5): p. 1101-1106.
58. Fuku, T., et al., *Increased wild-type p53-induced phosphatase 1 (Wip1 or PPM1D) expression correlated with downregulation of checkpoint kinase 2 in human gastric carcinoma.* Pathology International, 2007. **57**(9): p. 566-571.
59. Ruark, E., et al., *Mosaic PPM1D mutations are associated with predisposition to breast and ovarian cancer.* Nature, 2013. **493**(7432): p. 406-10.
60. Kleiblova, P., et al., *Gain-of-function mutations of PPM1D/Wip1 impair the p53-dependent G1 checkpoint.* J Cell Biol, 2013. **201**(4): p. 511-21.
61. Dudgeon, C., et al., *Genetic variants and mutations of PPM1D control the response to DNA damage.* Cell Cycle, 2013. **12**(16): p. 2656-64.
62. Swisher, E.M., et al., *Somatic mosaic mutations in ppm1d and tp53 in the blood of women with ovarian carcinoma.* JAMA Oncology, 2016. **2**(3): p. 370-372.
63. Zhang, L., et al., *Exome sequencing identifies somatic gain-of-function PPM1D mutations in brainstem gliomas.* Nat Genet, 2014. **46**(7): p. 726-30.
64. Zajkowicz, A., et al., *Truncating mutations of PPM1D are found in blood DNA samples of lung cancer patients.* Br J Cancer, 2015. **112**(6): p. 1114-1120.
65. Cardoso, M., et al., *Truncating and missense PPM1D mutations in early-onset and/or familial/hereditary prostate cancer patients.* Genes, Chromosomes and Cancer, 2016. **55**(12): p. 954-961.
66. Yu, E., et al., *Overexpression of the wip1 gene abrogates the p38 MAPK/p53/Wip1 pathway and silences p16 expression in human breast cancers.* Breast Cancer Research and Treatment, 2007. **101**(3): p. 269-278.
67. Demidov, O.N., et al., *The role of the MKK6//p38 MAPK pathway in Wip1-dependent regulation of ErbB2-driven mammary gland tumorigenesis.* Oncogene, 2006. **26**(17): p. 2502-2506.
68. Demidov, O.N., et al., *The role of the MKK6/p38 MAPK pathway in Wip1-dependent regulation of ErbB2-driven mammary gland tumorigenesis.* Oncogene, 2007. **26**(17): p. 2502-6.

69. Choi, J., et al., *Mice deficient for the wild-type p53-induced phosphatase gene (Wip1) exhibit defects in reproductive organs, immune function, and cell cycle control.* Mol Cell Biol, 2002. **22**(4): p. 1094-105.
70. Nannenga, B., et al., *Augmented cancer resistance and DNA damage response phenotypes in PPM1D null mice.* Mol Carcinog, 2006. **45**(8): p. 594-604.
71. Bulavin, D.V., et al., *Inactivation of the Wip1 phosphatase inhibits mammary tumorigenesis through p38 MAPK-mediated activation of the p16(Ink4a)-p19(Arf) pathway.* Nat Genet, 2004. **36**(4): p. 343-50.
72. Shreeram, S., et al., *Regulation of ATM/p53-dependent suppression of myc-induced lymphomas by Wip1 phosphatase.* J Exp Med, 2006. **203**(13): p. 2793-9.
73. Demidov, O.N., et al., *Wip1 phosphatase regulates p53-dependent apoptosis of stem cells and tumorigenesis in the mouse intestine.* Cell Stem Cell, 2007. **1**(2): p. 180-90.
74. Filipponi, D., et al., *Wip1 controls global heterochromatin silencing via ATM/BRCA1-dependent DNA methylation.* Cancer Cell, 2013. **24**(4): p. 528-41.
75. Nguyen, T.A., et al., *The oncogenic phosphatase WIP1 negatively regulates nucleotide excision repair.* DNA Repair (Amst), 2010. **9**(7): p. 813-23.
76. Lu, X., et al., *The p53-Induced Oncogenic Phosphatase PPM1D Interacts with Uracil DNA Glycosylase and Suppresses Base Excision Repair.* Molecular Cell, 2004. **15**(4): p. 621-634.
77. Zhang, C. and L. Lai, *Towards structure-based protein drug design.* Biochem Soc Trans, 2011. **39**(5): p. 1382-6, suppl 1 p following 1386.
78. Gilmartin, A.G., et al., *Allosteric Wip1 phosphatase inhibition through flap-subdomain interaction.* Nat Chem Biol, 2014. **10**(3): p. 181-7.
79. Chuman, Y., et al., *Characterization of the active site and a unique uncompetitive inhibitor of the PPM1-type protein phosphatase PPM1D.* Protein Pept Lett, 2008. **15**(9): p. 938-48.
80. Nakagawa, H., et al., *Cancer whole-genome sequencing: present and future.* Oncogene, 2015. **34**(49): p. 5943-5950.
81. Chuman, Y., et al., *PPM1D430, a novel alternative splicing variant of the human PPM1D, can dephosphorylate p53 and exhibits specific tissue expression.* J Biochem, 2009. **145**(1): p. 1-12.
82. Belova, G.I., et al., *Chemical inhibition of Wip1 phosphatase contributes to suppression of tumorigenesis.* Cancer Biol Ther, 2005. **4**(10): p. 1154-8.
83. Rayter, S., et al., *A chemical inhibitor of PPM1D that selectively kills cells overexpressing PPM1D.* Oncogene, 2008. **27**(8): p. 1036-44.
84. Lee, J.S., et al., *Off-target response of a Wip1 chemical inhibitor in skin keratinocytes.* J Dermatol Sci, 2014. **73**(2): p. 125-34.
85. Pechackova, S.B., K.; Benada, J.; Kleiblova, P.; Jenikova, G., Macurek, L., *Inhibition of WIP1 phosphatase sensitizes breast cancer cells to genotoxic stress and to MDM2 antagonist nutlin-3.* 2016.
86. Yagi, H., et al., *A small molecule inhibitor of p53-inducible protein phosphatase PPM1D.* Bioorg Med Chem Lett, 2012. **22**(1): p. 729-32.
87. Ogasawara, S., et al., *Novel inhibitors targeting PPM1D phosphatase potently suppress cancer cell proliferation.* Bioorganic & Medicinal Chemistry, 2015. **23**(19): p. 6246-6249.
88. Kozakai, Y., et al., *Inhibition of C-terminal truncated PPM1D enhances the effect of doxorubicin on cell viability in human colorectal carcinoma cell line.* Bioorg Med Chem Lett, 2014. **24**(24): p. 5593-6.
89. Hayashi, R., et al., *Optimization of a cyclic peptide inhibitor of Ser/Thr phosphatase PPM1D (Wip1).* Biochemistry, 2011. **50**(21): p. 4537-49.
90. Yamaguchi, H., et al., *Development of a substrate-based cyclic phosphopeptide inhibitor of protein phosphatase 2Cdelta, Wip1.* Biochemistry, 2006. **45**(44): p. 13193-202.
91. Bang, J., et al., *A Small Molecular Scaffold for Selective Inhibition of Wip1 Phosphatase().* ChemMedChem, 2008. **3**(2): p. 10.1002/cmdc.200700281.

92. Chen, Z., et al., *Wip1 inhibitor GSK2830371 inhibits neuroblastoma growth by inducing Chk2/p53-mediated apoptosis.* Sci Rep, 2016. **6**: p. 38011.
93. Kojima, K., et al., *The pathophysiological significance of PPM1D and therapeutic targeting of PPM1D-mediated signaling by GSK2830371 in mantle cell lymphoma.* Oncotarget, 2016.
94. Pechackova, S., et al., *Inhibition of WIP1 phosphatase sensitizes breast cancer cells to genotoxic stress and to MDM2 antagonist nutlin-3.* Oncotarget, 2016. **7**(12): p. 14458-75.
95. Sriraman, A., et al., *Cooperation of Nutlin-3a and a Wip1 inhibitor to induce p53 activity.* Oncotarget, 2016. **7**(22): p. 31623-38.
96. Ventura, A., et al., *Restoration of p53 function leads to tumour regression in vivo.* Nature, 2007. **445**(7128): p. 661-5.
97. Kong, W., X. Jiang, and W.E. Mercer, *Downregulation of Wip-1 phosphatase expression in MCF-7 breast cancer cells enhances doxorubicin-induced apoptosis through p53-mediated transcriptional activation of Bax.* Cancer Biol Ther, 2009. **8**(6): p. 555-63.
98. Ali, A.Y., M.R. Abedini, and B.K. Tsang, *The oncogenic phosphatase PPM1D confers cisplatin resistance in ovarian carcinoma cells by attenuating checkpoint kinase 1 and p53 activation.* Oncogene, 2012. **31**(17): p. 2175-86.
99. Rochette, L., et al., *Anthracyclines/trastuzumab: new aspects of cardiotoxicity and molecular mechanisms.* Trends Pharmacol Sci, 2015. **36**(6): p. 326-48.
100. Derek, W.E., et al., *Role of Drug Metabolism in the Cytotoxicity and Clinical Efficacy of Anthracyclines.* Current Drug Metabolism, 2015. **16**(6): p. 412-426.
101. Qin, L., et al., *Efficient reactivation of p53 in cancer cells by a dual MdmX/Mdm2 inhibitor.* J Am Chem Soc, 2014. **136**(52): p. 18023-33.
102. Brown, C.J., et al., *Awakening guardian angels: drugging the p53 pathway.* Nat Rev Cancer, 2009. **9**(12): p. 862-73.
103. Khoo, K.H., C.S. Verma, and D.P. Lane, *Drugging the p53 pathway: understanding the route to clinical efficacy.* Nat Rev Drug Discov, 2014. **13**(3): p. 217-36.
104. Zhang, Q., S.X. Zeng, and H. Lu, *Targeting p53-MDM2-MDMX loop for cancer therapy.* Subcell Biochem, 2014. **85**: p. 281-319.
105. Vassilev, L.T., et al., *In vivo activation of the p53 pathway by small-molecule antagonists of MDM2.* Science, 2004. **303**(5659): p. 844-8.
106. Ding, Q., et al., *Discovery of RG7388, a potent and selective p53-MDM2 inhibitor in clinical development.* J Med Chem, 2013. **56**(14): p. 5979-83.
107. Chen, L., et al., *Pre-clinical evaluation of the MDM2-p53 antagonist RG7388 alone and in combination with chemotherapy in neuroblastoma.* Oncotarget, 2015. **6**(12): p. 10207-21.
108. Higgins, B., et al., *Preclinical optimization of MDM2 antagonist scheduling for cancer treatment by using a model-based approach.* Clin Cancer Res, 2014. **20**(14): p. 3742-52.
109. Makii, C., et al., *MDM2 is a potential therapeutic target and prognostic factor for ovarian clear cell carcinomas with wild type TP53.* Oncotarget; Vol 7, No 46, 2016.
110. Esfandiari, A., et al., *Chemical Inhibition of Wild-Type p53-Induced Phosphatase 1 (WIP1/PPM1D) by GSK2830371 Potentiates the Sensitivity to MDM2 Inhibitors in a p53-Dependent Manner.* Mol Cancer Ther, 2016. **15**(3): p. 379-91.
111. Wanzel, M., et al., *CRISPR-Cas9-based target validation for p53-reactivating model compounds.* Nature chemical biology, 2016. **12**(1): p. 22-28.
112. Goloudina, A.R., et al., *Wip1 sensitizes p53-negative tumors to apoptosis by regulating the Bax/Bcl-xL ratio.* Cell Cycle, 2012. **11**(10): p. 1883-7.
113. Goloudina, A.R., et al., *Wip1 promotes RUNX2-dependent apoptosis in p53-negative tumors and protects normal tissues during treatment with anticancer agents.* Proc Natl Acad Sci U S A, 2012. **109**(2): p. E68-75.
114. Choi, D.W., et al., *WIP1, a homeostatic regulator of the DNA damage response, is targeted by HIPK2 for phosphorylation and degradation.* Mol Cell, 2013. **51**(3): p. 374-85.

115. Clausse, V., et al., *Wee1 inhibition potentiates Wip1-dependent p53-negative tumor cell death during chemotherapy.* Cell Death Dis, 2016. **7**: p. e2195.
116. Perez-Pinera, P., et al., *Synergistic and tunable human gene activation by combinations of synthetic transcription factors.* Nature methods, 2013. **10**(3): p. 239-242.
117. Shen, X.-F., et al., *Phosphatase Wip1 in Immunity: An Overview and Update.* Frontiers in Immunology, 2017. **8**: p. 8.
118. Ciriello, G., et al., *Comprehensive Molecular Portraits of Invasive Lobular Breast Cancer.* Cell. **163**(2): p. 506-519.
119. Gao, J., et al., *Integrative Analysis of Complex Cancer Genomics and Clinical Profiles Using the cBioPortal.* Science Signaling, 2013. **6**(269): p. pl1-pl1.

Figure legend

Figure 1. Role of WIP1 phosphatase in termination of DNA damage response. Exposed ssDNA caused by stalled replication forks or resected DSBs activates ATR/CHK1 pathway that targets CDC25 family of phosphatases, prevents activation of CDKs and triggers cell cycle arrest. DSBs induced by ionizing radiation or chemotherapy activate ATM that orchestrates DNA repair by phosphorylating H2AX at chromatin and activates the cell cycle checkpoint. This is achieved by phosphorylation of p53 and Mdm2 that allows stabilization of p53 and triggers expression of CDKN1/p21. In addition, p53 stimulates expression of its negative regulators Mdm2 and WIP1. After accumulating sufficient protein levels, WIP1 inactivates p53 pathway and dephosphorylates other targets (indicated by dashed line) jointly contributing to termination of the DDR. Persistent genotoxic stress can continuously activate p53 leading to senescence. Very high activation of p53 pathway leads to expression of *PUMA* and *NOXA* and leads to cell death.

Figure 2. Amplification of *PPM1D* locus in breast cancer. Breast Invasive Carcinoma dataset (n=817, [118]) was analyzed for *PPM1D* amplification (11 %), *TP53* mutation (31 %) and *ERBB2* amplification, overexpression or mutation (18 %) using cBioPortal [119]. Amplification of genes was analyzed using putative copy number alterations from GISTIC. Expression analysis was based on mRNA Expression z-Scores (RNA Seq V2 RSEM) where threshold was set at 4-fold difference. Tendency to mutual exclusivity between *PPM1D* and *TP53* mutation as well

as tendency to co-occurrence between *PPM1D* and *ERBB2* activation were statistically significant.

Figure 3. Model for WIP1 involvement in tumorigenesis and in therapeutic response. Activation of oncogenes (such as *RAS* and *MYC*) causes replication stress, stimulates p53 activity and results in permanent cell cycle arrest called oncogene-induced senescence (OIS). Inactivating mutation of *TP53*, overexpression of WIP1 or amplification of *PPM1D* leads to suppression of p53 pathway, disables establishment of OIS and promotes tumor formation. Inhibition of WIP1 does not affect proliferation of cancer cells with mutant *TP53* whereas it allows partial reactivation of p53 pathway in cells with wild-type *TP53* slowing down their proliferation. Combination of WIP1 inhibition with MDM2 antagonist nutlin-3 or with DNA-damage inducing chemotherapy allows maximal activation of p53 pathway leading to induction of cell death or senescence and preventing tumor growth.

Figure 1

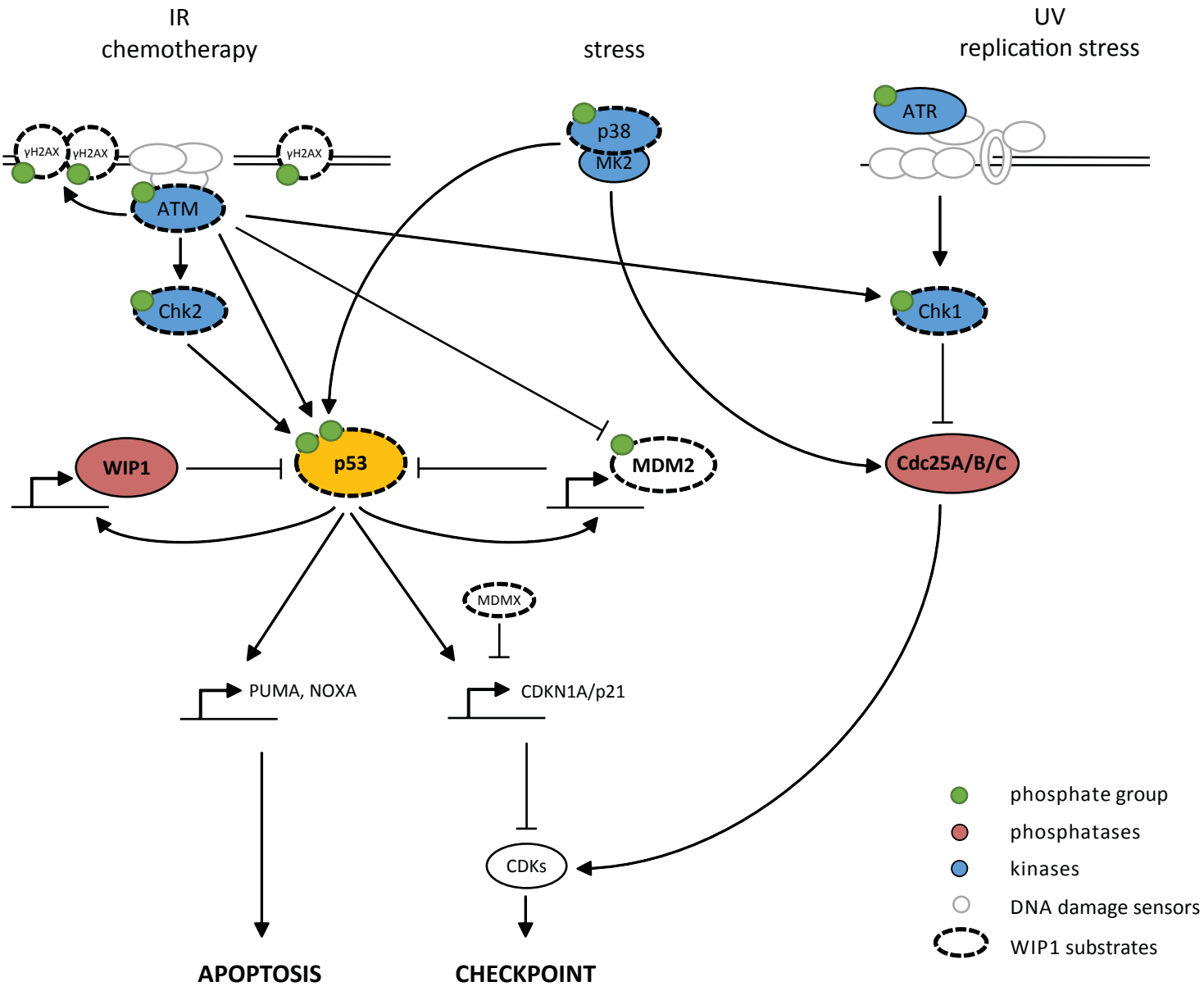
IR
chemotherapy
stress
UV
replication stress
γH2AX
γH2AX
γH2AX
ATM
p38
MK2
ATR
Chk2
Chk1
WIP1
p53
MDM2
Cdc25A/B/C
MDMX
PUMA, NOXA
CDKN1A/p21
CDKs
APOPTOSIS
CHECKPOINT
phosphate group
phosphatases
kinases
DNA damage sensors
WIP1 substrates

Figure 2.

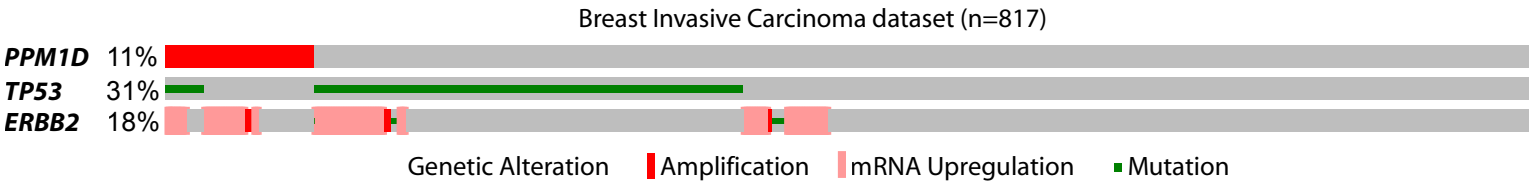
Breast Invasive Carcinoma dataset (n=817)
PPM1D 11%
TP53 31%
ERBB2 18%
Genetic Alteration
Amplification
mRNA Upregulation
Mutation

Figure 3

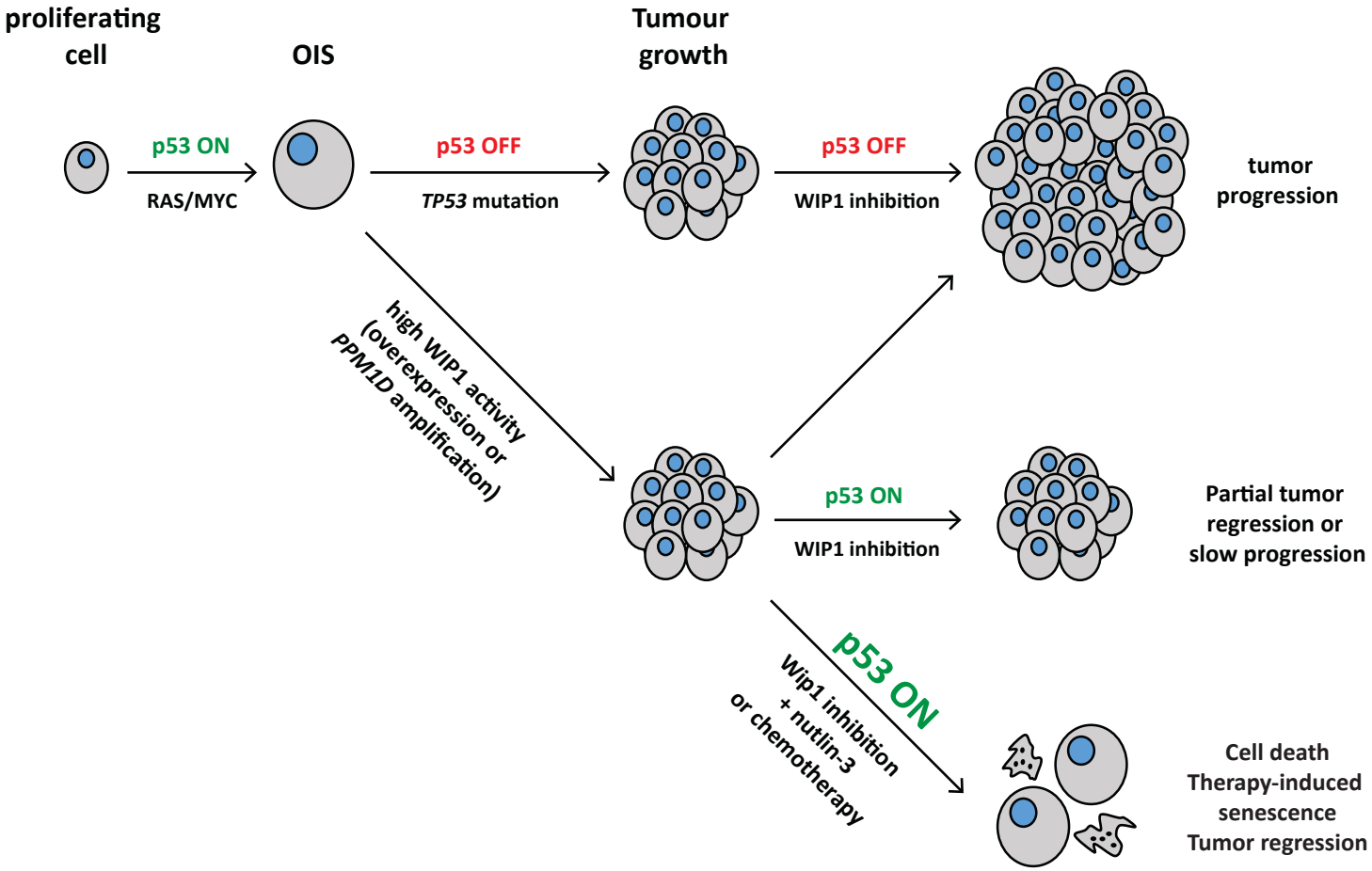
proliferating cell
OIS
Tumour growth
p53 ON
RAS/MYC
p53 OFF
TP53 mutation
p53 OFF
WIP1 inhibition
tumor progression
high WIP1 activity (overexpression or PPM1D amplification)
p53 ON
WIP1 inhibition
Partial tumor regression or slow progression
p53 ON
Wip1 inhibition + nutlin-3 or chemotherapy
Cell death
Therapy-induced senescence
Tumor regression

4 DISCUSSION

4.1 WIP1 phosphatase is downregulated during mitosis to modulates DNA damage signaling

Numerous studies reported that the WIP1 phosphatase is a major negative regulator of DNA damage response and play a crucial in termination of checkpoints in response to genotoxic insults. However, the molecular mechanism of WIP1 regulation in the cell cycle has remained unknown. In the presented study (chapter 3.1), we have examined how is the WIP1 regulated during the cell cycle progression.

To study the regulation of WIP1 during the cell cycle we have performed a biochemical synchronization of cells by thymidine followed by nocodazole treatment to allow progression of cells to and arrest in mitosis. We have observed that WIP1 was detectable during S and G2 phase and declined in mitosis. After release from nocodazole to G1 expression of WIP1 increased again to the next G2 phase. Similar expression changes of WIP1 we observed in U2OS cells, indicating that downregulation of WIP1 in mitosis was not limited to cell type. Biochemical synchronization of cells by thymidine cause a stress response and may impair protein expression. Therefore, we established biochemical approach which allowed to study the regulation of WIP1 in unsynchronized cells without perturbation and under the unstressed conditions. We made microscopic analysis of the cells with fluorescent, ubiquitination-based cell cycle indicator system (FUCCI) which facilitated to sort asynchronously growth cells according to fluorescent intensities of expressed cell cycle markers [127, 128]. Using this method we confirmed that WIP1 is highly expressed G2 cells and decreased in mitosis.

Our observations are consistent with the previous studies where it was shown that loss of WIP1 in knockout mice resulted in prolonged cell cycle and accumulation of G2 cells [99, 129]. Importantly, the mice with WIP1-knockout are viable which supports that WIP1 is not essential for cell cycle regulation [99] but may be functionally important in G2. It has been shown that WIP1 antagonized key mitotic inducers (cyclin B, Plk1) in p53-dependent manner but RNA interference of WIP1 in tissue cell lines caused only prolonged G2/M transition [48]. Thus, WIP1 is not essential for progression to mitosis but has been suggested as an enhancer of proliferation in cellular transformation. We could hypothesize that WIP1 levels during

G2/M transition may be increased in response to endogenous stress and temporarily prevent ATR/Chk1 pathway activity induced during replication.

The expression of WIP1 rapidly decline early in prometaphase phase of mitosis and we wondered by which mechanism is it caused. Since we have revealed that the levels of WIP1 mRNA remained unchanged in G2/M we investigated if WIP1 protein undergoes proteasomal degradation. Inhibitor of proteasome MG132 stabilized WIP1 levels in mitosis thus WIP1 has to be targeted by an ubiquitin ligase to proteasomal degradation. Early in mitosis, E3 ubiquitin ligase complexes SCF and APC/Cdc20 are active and therefore we performed depletion of protein components of the complexes by siRNA. We have found that only depletion of Cdc20 resulted in stabilization of WIP1 levels. These results propose that proteasomal degradation of WIP1 is controlled in mitosis in APC-Cdc20 dependent manner. In contrast with our data, recently was reported that the WIP1 is degraded in mitosis in APC/Cdh1 dependent [130] and not APC/Cdc20 dependent manner as we have demonstrated. In this study they investigated data exclusively on overexpression of Cdh1. Moreover, APC/Cdh1 complex is activate in the end of the mitosis but our results supported that WIP1 is degraded in early mitosis. Controversially, we have not observed any stabilization of WIP1 levels after downregulation of Cdh1 using siRNA (data not shown). The different observation of WIP1 regulation during mitosis could be attributed to the distinct cell lines used.

Further we have observed that the purified WIP1 protein from mitotic cells migrate slower in the gel than WIP1 protein treated with lambda phosphatase, suggesting that WIP1 is post-translationally modified during mitosis by phosphorylation. We have found that WIP1 is extensively phosphorylated at multiple sites in the catalytic domain and C-terminal part. Moreover, we have described that serine 40 is the major target of CDK1. The mutation analysis of serine 40 did not show any obvious phenotype but the phosphomimicking WIP-7D mutant lost the enzymatic activity compared to nonphosphorylatable WIP1–7A mutant protein. We assume that cells can reduce the activity of WIP1 during mitosis by inhibitory phosphorylation in combination with proteasomal degradation. However, in this study we did not resolve whether the phosphorylation of WIP1 is required for subsequent stimulation of APC/Cdc20 dependent degradation.

To analyse the phenotype of mitotic cells we established tetracycline-inducible system to allow expression of high levels of WIP1. Despite of that induction of WIP1 expression

increased its activity in mitotic cells, we did not observe any defect in the timing of mitosis, in spindle assembly nor any differences in cytokinesis.

After induction of ectopic expression of WIP1, we observed an approximately two-fold reduction in the number of H2AX foci in mitotic cells. Previously, Macurek et al. demonstrated that WIP1 is associated with the chromatin and directly dephosphorylates γH2AX after induction of double-stranded breaks [59]. During the mitosis DNA damage activates only upstream part of DDR pathway, ATM kinase which subsequently phosphorylates H2AX to recruit DNA repair mediator of MDC1 to the damage sites [131, 132]. The activity of DDR checkpoint kinases is suppressed by the Plk1 during mitosis [133]. In cells with the forced expression of WIP1, we also observed reduction of 53BP1 nuclear bodies in the following G1. Recently, our laboratory published that 53BP1 is phosphorylated by Plk1 and CDK1 during mitosis. These phosphorylations prevent of 53BP1 localize to sites of DNA damage and utilize DNA repair [134]. Cells efficiently suppress DNA repair mechanisms during mitosis but the DNA lesions are marked by γH2AX to allow repair in the following cell cycle phases. Thus, we hypothesized that WIP1 needs to be downregulated in mitosis to utilize formation of γH2AX marks on damaged DNA through the mitosis to the next G1, where they efficiently mediate the DNA repair.

In conclusion, we propose that combination of proteasome degradation and phosphorylation-mediated inhibition of WIP1 permits sensing of DNA damage that appears during unperturbed mitosis and ensures the preservation of chromatin marks on DNA lesions which can utilise repair of DNA in the subsequent G1 phase.

4.2 Gain-of-function mutations of *PPM1D* abrogates the G1 checkpoint in p53-dependent manner

As was discuss in chapter 1.5, amplification of *PPM1D* occurs particularly in tumors carrying the wild-type p53. It is known that MCF7 breast cancer cell line highly express full-length of Wip1 protein due to extensive amplification of the *PPM1D* locus [135]. We have analysed a panel of cancer cell lines which retained wild-type p53. We found out that the HCT116 and U2OS cells lines derived from colorectal adenocarcinoma and osteosarcoma expressed besides of full-length Wip1 protein also ~10–20-fold higher level of a smaller variant of the Wip1 protein recognised by specific Wip1 antibodies. In the present study

(chapter 3.2), we determined that these shorter Wip1 proteins occur by non-sense mutation in the exon 6 of *PPM1D* gene which introduces premature stop codon. These mutations create a C-terminally truncated Wip1 protein that contains the intact catalytic domain. Similarly, we found truncating mutations of PPM1D gene also in the peripheral blood of colon and breast cancer patients indicating that they are not caused in consequence of genome instability in tumors. Importantly, we show that the truncated Wip1 protein caused a gain-of-function effect in the cancer cells. Biochemical analysis of truncated Wip1 mutants revealed that they are enzymatically active and efficiently downregulate p53 activity comparable to full-length Wip1 suggesting that gain-of-function mutation is not attributed by hyperactivity of Wip1 in the cells. However, we demonstrated that C-terminally truncated Wip1 has increased protein stability in the cells, with half-life more than 6 hours in contrast to 1-2h of full-length Wip1. Thus the gain-of-function mutations in exon 6 of the *PPM1D* gene lead to increased protein levels of truncated Wip1 and in total raised up the enzymatic activity of Wip1 in cells.

Since that U2OS and HCT116 cells contain wild-type p53 we assumed that the high levels of truncated Wip1 can compromised cell cycle arrest in response to genotoxic stress. Indeed, we observed that U2OS and HCT116 cell lines have not been able to efficiently arrest in G1 checkpoint because they cannot activate p53-induced arrest, and progress to S phase. By isoform-specific RNAi, we have shown that the depletion of truncated Wip1 restores G1 checkpoint in U2OS and HCT116 cell lines in p53-dependent manner.

Structure prediction of Wip1 proposes that C-terminus is disordered and its function is for a while unclear. On the other hand, C-terminus is unique for Wip1 compere to other PP2C phosphatases but is less conserved across the species than catalytic core domain of Wip1 [47]. We hypothesise that the C-terminally truncated Wip1 are stabilised due to lack of part on the C-terminus which can mediate degradation of full-length Wip1 either by interaction with ubiquitin ligase and/or by poly-ubiquitination of the lysines within the C-terminus.

According to a low number of patients, we cannot to statistically show whether the identified gain-of-function mutations predispose tumor development. In parallel with us, was published extensive study where they also as first described truncated mutations of Wip1. Moreover, they performed a case-controlled study of 13 642 human samples which confirmed that the mutations in *PPM1D* significantly increased the relative risk of breast cancer development [136].

After the first identification of Wip1 truncating mutations were reported the similar mutations of *PPM1D* gene in ovarian cancer, brain stem gliomas and lung cancer [137-139]. Interestingly, all described mutations were located in a hotspot region of exon 6. In comparison to amplifications of PPM1D locus (10-25% (http://www.cbioportal.org/; [140-142] the Wip1 mutations occurs with lower frequency about 2% [136-139]. Notably, the *PPM1D* mutations are mutually exclusive with a mutation in *TP53* [137, 143].

The current hypothetical model of cancer development, propose that the cells firstly gain extra function mutation in important pro-proliferative oncogenes, such a Myc or Ras. This leads to uncontrolled cell proliferation. Increased cell cycle progression also elevates replication stress, breaking of DNA and subsequently activation of DDR and checkpoint signalling. Based on DNA damage level cells trigger either an apoptosis or senescence in a p53-dependent manner. This mechanism represents protecting barriers against cell transformation and following tumor development. Therefore, the cells lost the tumor-suppressive protection either by loss-of-function mutation of the key positive regulator p53 or by gain-of-function mutation of negative regulators of DDR, such as Wip1. Subsequently, the mutated cells cannot establish checkpoint and escape to apoptosis and senescence, and the precancerous lesions progress to develop cancer [2, 144, 145].

Based on our data in the cancer cells lines, high level of full-length Wip1 or truncated Wip1, seems to contribute to defects in G1 and G2 checkpoint. Truncated Wip1 could promote the tumorigenesis by impairing the proper activation of DDR through the dephosphorylation of γH2AX and ATM. The increased deactivation of ATM signalling would affect the ability of the cells to efficiently repair harmed DNA [146]. Moreover, the high levels of Wip1 could promote genomic instability by the accumulation of mutations through the negative regulation of nucleotide excision repair [54].

In almost all reported cases, mosaics mutations of *PPM1D* were observed that could explain limited hereditary transition [136, 138]. We speculate that PPM1D mutations could arise early in embryogenesis or alternatively mosaic mutations could be a result of chemotherapy by DNA-damaging agents [139]. We have also identified *PPM1D* heterozygous mutations in one tumor sample but in these cases is excluded that the mutations were caused by chemotherapy (unpublished data).

Probably, Wip1 mutations would not cause driver mutation of primary tumor but could contribute the chemoresistance of cancer cells and eventually drive of treatment-induced

secondary tumors. As we will discuss in the next chapters 4.3 and 4.4, patients with amplification of *PPM1D* and the subset of patients with Wip1 truncating mutations might represent candidates to pharmacological inhibition of Wip1. The pharmacological effects of Wip1 inhibitors *in vitro* we recently described (see chapter 4.3).

4.3 Inhibition of WIP1 phosphatase sensitizes breast cancer cells to the chemotherapy

During last decade evidence has been accumulating that WIP1 can function as an oncoprotein. As we discuss in the review (chapter 3.4) amplification and gain-of-function mutation of *PPM1D* have been identified in multiple human tumors. In particular, amplification or overexpression of *PPM1D* occurs approximately 10% of primary breast tumors which retain wild-type *TP53* [91, 94, 147]. Therefore, WIP1 was suggested as potential pharmacological target, namely in tumors that exhibit high levels of WIP1 and p53-proficiency which is in consistence with WIP1 function reflected by negative regulation of p53. Several WIP1 inhibitors were already developed but their specificity has to be more validated or their bioavailability is needs to be improved (see chapter 1.6).

In the presented study (chapter 3.3), we validated the specificity of two commercially available WIP1 inhibitors GSK2830371 [85] and CCT007093 [107]. Since that U2OS osteosarcoma cells express stabilized WIP1 protein and since that after depletion of WIP1 expression in this cell lines we have shown checkpoint restart, we generated U2OS cells with the CRISPR-Cas9-mediated knockout of the *PPM1D* as a cellular model to test specific phenotype after WIP1 inhibition by small molecule compounds. Using this tool, we demonstrated that CCT007093 suppressed cell proliferation of parental-U2OS and U2OS-*PPM1D*-KO cells in the same way thus this effect was independent of WIP1. Moreover, we have not observed any increase in phosphorylation of well-established WIP1 substrates such p53-pS15 and γH2AX upon DNA damage. In the original publication authors described that CCT007093 can stimulate the p38 pathway via WIP1 inhibition [107]. Later it was suggested that the pharmacological effects of CCT007093 could be attributed through the attenuation of JNK signaling, independently on WIP1 activity [108]. Our data proved that CCT007093 does not specifically inhibit the activity of WIP1 in cells. So, we stress here that

it is critically important to validate the specificity of small molecule inhibitors in proper cellular models including the CRISPR-mediated knock-out of the target gene.

Validation of allosteric modulator GSK2830371 showed that this compound inhibited cell proliferation in WIP1-dependent manner. Furthermore, upon GSK2830371 treatment, levels of γH2AX and p53-pS15 were increased thus our findings confirm that GSK2830371 specifically inhibits cellular activity of WIP1 phosphatase.

We have found that WIP1 inhibition by GSK2830371 reduceed cell proliferation only in transformed cell lines that express high levels of WIP1 namely in MCF7 breast cancer cells with amplified *PPM1D*. Importantly, we did not observe any effect of GSK2830371 on the proliferation of non-transformed cells with low levels of WIP1. Thus the administration of GSK2830371 could be well tolerated in normal cells without excessive adverse effect. *In vivo* study supported low toxicity of GSK2830371 with no obvious health problems or weight loss of treated groups of xenograft mouse models compared to the control group [85, 114].

MCF7 cells treated with GSK2830371 were accumulated in the G2 phase and this influence on the cell cycle was strictly dependent on the p53/21 pathway. Inhibition of WIP1 did not affect cell cycle progression of the breast cancer cell lines with amplified *PPM1D* and mutated p53 or with the CRISPR-mediated knock-out of p53 and p21. This observation supports that p53 is the functionally the most relevant target of WIP1. Reactivation of G2 arrest after WIP1 inhibition is in good agreement with previous study showing the accumulation of the G2 cells in the population of PPM1D-/- MEFs compared to the wild-type MEFs [99, 148].

Since we observed stabilization of p53-pS15 and p21 in the cancer cells treated with GSK2830371 we assumed that the cells could undergo cell death upon treatment. WIP1 inhibition by GSK2830371 did not influence cell viability and could not induce the apoptosis of breast cancer cells with amplified *PPM1D* and wild-type *TP53.* Thus WIP1 inhibition alone may not be sufficient to induce tumor regression.

There is evidence that reactivation of p53 results in suppression of tumor cells growth and induction of cell death. In the past, it was shown that inhibition of WIP1 by RNA interference sensitised cell viability of cancer cells to DNA damage-inducing chemotherapy and caused DNA damage-induced apoptosis [115-117].

Well established negative regulator of p53 is E3 ubiquitin ligase MDM2 which has been reported as oncogene identified in tumors. Nutlin-3 was developed as a potent antagonist which disrupted the interaction between p53 and MDM2, resulting in strong stabilisation of p53 and high expression of its transcriptional targets [123]. The analogues of nutlin-3 are currently tested in clinical trials. There are also reports that nutlin-3 and doxorubicin synergistically increased anti-proliferative effect in neuroblastomas, B-cell leukaemia and in breast cancer cells [125, 149, 150]. Administration of nutlin-3 analogues has been reported to cause a hematotoxic effect (reviewed in [151]). The combination of nutlin-3 analogues with a lower dose of cytotoxic drugs could allow decreasing side-effects of chemotherapy.

In the present study, we found that both WIP1 inhibitor GSK2830371 and nutlin-3 potentiated the effect of doxorubicin to induce senescence and DNA damage-induced cell death. Our data and other publications suggest that co-treatment of the WIP1 inhibitor with a low dose (50 nM) of doxorubicin can be beneficial for patients to reduce cytotoxic effects of doxorubicin [152, 153]. In addition, we have observed strong stabilisation of p53 activity even using of the combination of the WIP1 inhibitor with nutlin-3 which caused senescence and apoptosis in MCF7 cells. Cooperative effect of WIP1 inhibitor and MDM2 antagonists were supported by other studies on cancer cells with overexpressed or mutated *PPM1D* [154-157]. The response of cancer cells to nutlin-3 can be impaired by overexpression of MDMX which can alone inhibit transactivation of p53 and this can lead to the tumor resistance upon MDM2 antagonist treatment [158, 159]. Since GSK2830371 enhance the cytotoxicity of nutlin-3, we assume that the response of MDMX overexpressing cancers might be sensitised by WIP1 inhibition. Recent studies also propose that the *PPM1D* overexpression could have a beneficial role also in the treatment of cancers with a dysfunctional p53 pathway. Cancer cells with mutated *TP53* and overexpressed *PPM1D* have increased sensitivity to anticancer drugs acting by activation of pro-apoptotic Bax in a p53-independent manner [160, 161]. Further studies are now needed to analyze targeting of *PPM1D* in p53-negative tumors. However, inhibition of cell growth and induction of apoptosis by WIP1 downregulation or inhibition completely depends on the p53 pathway.

Taken together our data and other publications suggest that WIP1 inhibition by GSK2830371 could enhance senescence or cell death of the subset of tumors with amplified or mutated *PPM1D* and *TP53* wild-type cancer cells treated with nutlin-3 and/or doxorubicin [114, 155-157]. WIP1 inhibition alone slows down the proliferation of cancer cells

but is not sufficient to cause their apoptosis. On the other hand, WIP1 inhibitor sensitised the cancer cells to chemotherapy, such as doxorubicin, or MDM2 antagonist treatment. Combination treatment targeting p53/MDM2/WIP1 pathway could elevate the response to chemotherapy and partially reduce effective dose of genotoxic drugs. However, further research and *in vivo* studies are needed to prove the pharmacological usefulness of allosteric WIP1 inhibitor.

4.4 WIP1 phosphatase is potential pharmacological target in cancer therapy

Our research focusing on the role of WIP1 phosphatase in tumorigenesis lead us to summarize current knowledge in the presented review (chapter 3.4). Here, we discuss recent advance in the development of WIP1 inhibitors and their potential use in cancer treatment.

Multiple studies highlight that overexpressed WIP1 impairs p53 function and contributes to tumorigenesis, usually in combination with activation of other oncogenes. Importantly, loss of WIP1 significantly delays tumor development in mice and similarly, depletion of WIP1 by RNA interference allows reactivation of p53 pathway and inhibits proliferation in p53-proficient tumors. As we described above (chapter 4.3) specific inhibition of WIP1 by allosteric modulator GSK2830371 represents a major challenge in the targeted cancer therapy. Moreover, in combination with DNA damage-inducing chemotherapy or with MDM2 antagonists, WIP1 inhibition promotes cancer cell death or senescence, while it has little effect on the viability of non-transformed cells. GSK2830371 is orally bioavailable and its ability to suppress cancer cell growth *in vivo* was demonstrated in xenograft models [85, 114]. Since that GSK2830371 is rapidly inactivated in plasma, which may limit its further clinical use, further development of its derivatives to improving pharmacokinetic properties is desirable. Furthermore, solving the 3D structure of WIP1 could help to develop even more selective WIP1 inhibitors. Current results suggest that inhibition of WIP1 will be most efficient in cancers with wild-type p53 and amplification or gain-of-function mutations of *PPM1D*. The sufficient reactivation of p53 pathway by WIP1 inhibition and additional compounds is needed to be more tested in cancers with wild-type p53. As attractive candidates are direct negative regulators of p53, such as MDM2 which is also commonly overexpressed in tumors.

While loss of WIP1 is well tolerated in mice, there is evidence that WIP1 plays role in differentiation of cells of the immune system (recently reviewed in [162]). Further research is needed to address possible side effects of a temporary inhibition of WIP1 during therapeutical administration.

5 SUPPLEMENT – UNPUBLISHED DATA

5.1 Determination of structure of WIP1 phosphatase by X-ray crystallography

When I started this work, one of the goals was determination of the 3D structure of WIP1 phosphatase that could help to study its molecular functions. The knowledge of WIP1 structure can be useful to characterize which kind of post-translational modifications may regulate WIP1 in cells. Since the WIP1 has been suggested as a potential pharmacological target, the crystal structure could be used in the structure-based design of small molecules and allow identification of a specific inhibitor of WIP1. Until now we had not achieved to crystallize WIP1, but our efforts are summarized here as unpublished results.

5.1.1 Design of WIP1 phosphatase variants

Crystallization of protein requires preparing great yield of the protein sample with concentration 10-20 mg/ml and high purity (at 90%). The concentrated protein sample should be stable in a buffer condition for a long time without precipitating or aggregation. As expression system for production of the target protein can be used various organism from prokaryotic microorganisms to mammalian cells.

For the production of WIP1 phosphatase, we chose bacterial organism Escherichia coli. The disadvantage of bacterial production of mammalian proteins may be improper folding and/or stabilization of protein by post-translational modifications. On the other hand, expression of a recombinant enzyme in a bacterial system can increase the yield in comparison with the production of a protein in insect or mammalian cells. In collaboration with Laboratory of structural biology (Institute of molecular genetics, Prague) we designed different constructs of WIP1 protein. According to secondary structure prediction analysis, only catalytic domain of WIP1 is structured whereas the C-terminal part of WIP1 is disordered (Figure 8). We already knew that WIP1(WT) containing 605 amino acids undergoes degradation during expression or purification in the bacteria. Therefore, we truncated WIP1 protein from the C-terminal part and constructed recombinant proteins which are listed in the following table (Table 2).

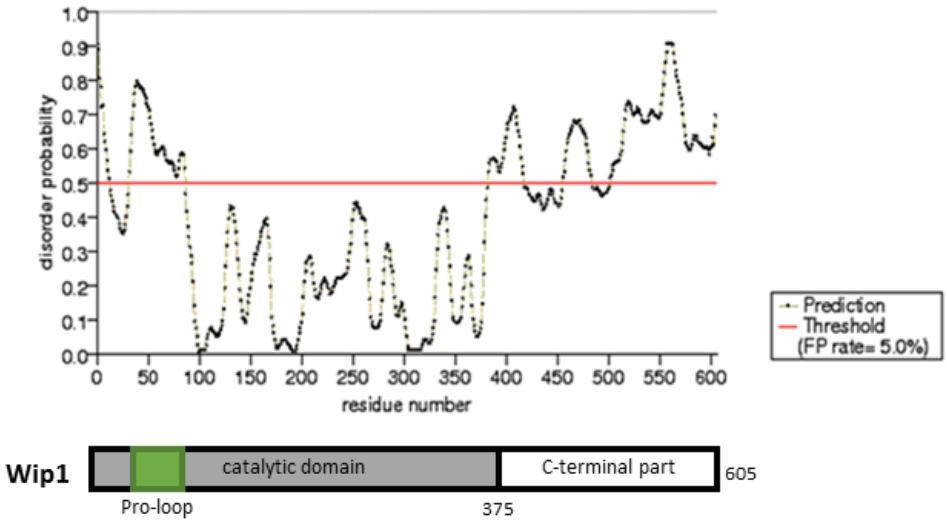

Figure 8. Secondary structure prediction of WIP1 phosphatase. Created by online tool *PrDOS* – *http://prdos.hgc.jp*. According to disorder probability, N-terminal catalytic domain has structured secondary motifs. The C-terminal part, from amino acid 375 is partially disordered thus exhibit no secondary motifs (alpha helix or beta strand).

Table 2. WIP1 phosphatase recombinant variant.

Protein variant	Location of 6xHis tag
WIP1(WT)	N-terminus
WIP1(1-380)	N-terminus
WIP(1-382)	C-terminus
WIP(1-410)	C-terminus
WIP(1-420)	N-terminus
WIP1(1-449) [a]	C-terminus
WIP1(1-457) [a]	C-terminus

[a] truncated variant founded in breast cancer patients

All constructs of recombinant WIP1 proteins were tagged by 6xHis on the N- or C-terminus of the proteins. Proteins were isolated by small-scale batch purification using affinity chromatography, namely immobilized-metal affinity chromatography (IMAC) (Figure 9). From these WIP1 variants, we further focused on WIP1(1-410)-6xHis because of its high purity and good yield.

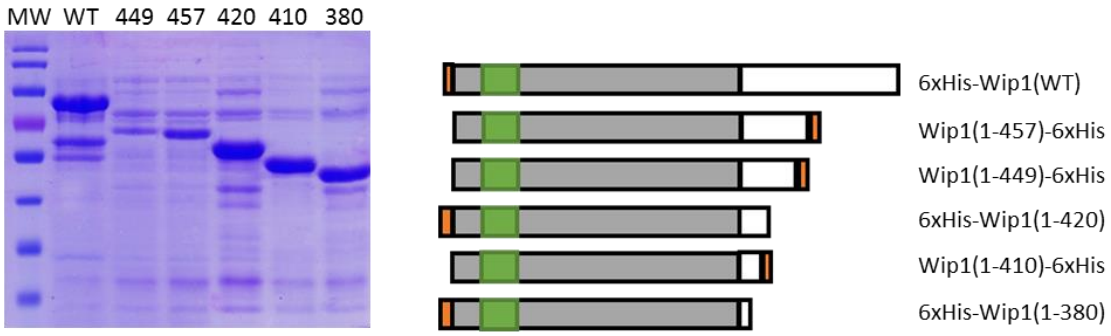

Figure 9. Small-scale purification of WIP1 recombinant proteins. Isolation was done from 100 ml of culture by affinity purification using Ni-beds in batch. The numbers indicate the type of recombinant protein listed in table 2.

5.1.2 Optimization of protein solubility

To identify optimal protein formulation for crystallization we performed thermofluor-based method as a high-throughput approach for determination of suitable buffer conditions [163]. Thermal stability of the protein was detected using a hydrophobic fluoroprobe (SyproOrange) that binds to the unfolded protein with increasing temperature. WIP1(1-410)-6xHis was analyzed in different buffers including pH range from 4-10 and low and high sodium salt concentration (Figure 10). We found out that the WIP1(1-410)-6xHis protein is the most stable in buffers at pH = 7-7,5 with higher concentration of magnesium salts (50-200 mM). On the other hand, so high concentration of magnesium salts may increase the risk of growth of inorganic salt crystals during crystalization. The selected buffer was 50 mM Hepes at pH 7.5 with 200 mM NaCl, 10 mM MgCl2 and 5 % (v/v) glycerol and we used it further for purification of all WIP1 protein recombinant proteins.

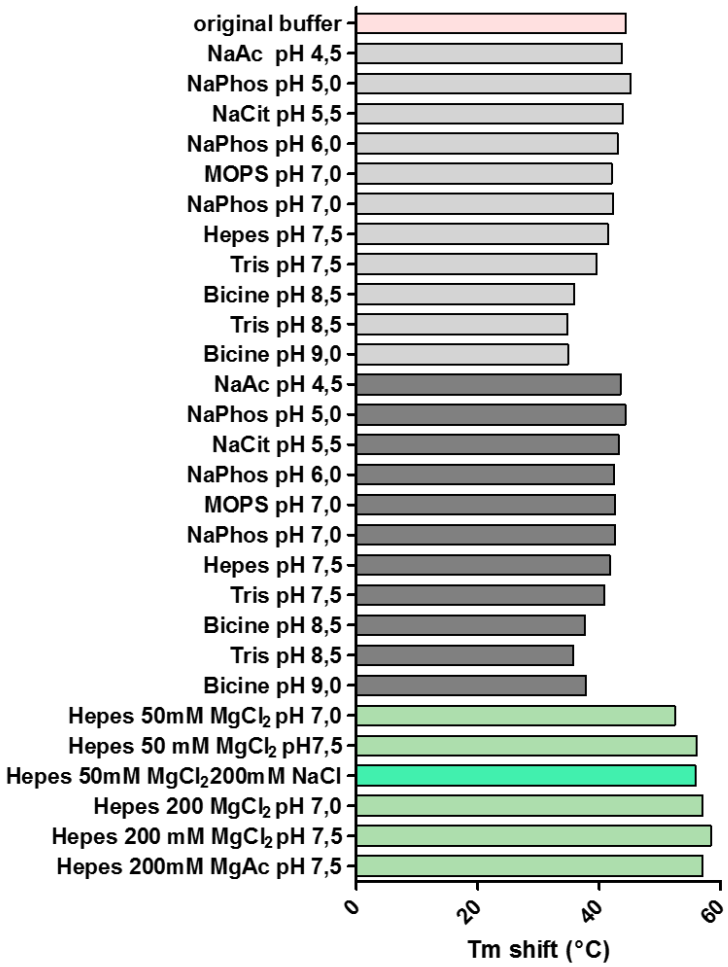

Figure 10. Thermal stability screen of WIP1(1-410)-6xHis. Thermal shift (Tm) assay of the protein in buffer conditions was performed by real-time PCR instrument. Original buffer was 50 mM NaPhos, 1 mM $MgCl_2$, 5% glycerol. Light gray columns – buffers with 1 mM $MgCl_2$ and without NaCl. Dark gray columns – buffers with 200 mM NaCl and 1 mM $MgCl_2$. Columns colored green indicates buffers with the highest thermal shift.

5.1.3 Mutagenesis of WIP1 Pro-loop increase protein purity and stability

Large-scale purification of WIP1(1-410)-6xHis was performed by immobilized-metal affinity chromatography column compatible with HPLC system. The peak fractions of WIP1(1-410)-6xHis contained approximately 20 mg of protein that indicates good purification efficiency (Figure 11a). Coomassie blue staining of the acrylamide gel showed lower migrating fragments (Figure 11b) which were co-purified with the target protein. Fractions with the peak amount of WIP1(1-410)-6xHis was concentrated to the maximal concentration 4 mg/ml because the protein was lost by aggregation on the surface of contractor membrane (data

not shown). Silver staining of the concentrated sample showed very low purity of WIP1(1-410)-6xHis (Figure 11c) and suggesting that another purification step was necessary. Firstly, we investigated whereas the contaminating fragments may come from WIP1 and if the fragment contains 6xHis tag on the C-terminus. Using specific antibody anti-His and anti-WIP1 we revealed that the nearest contaminant and others were fragments of WIP1(1-410)-6xHis (Figure 11d).

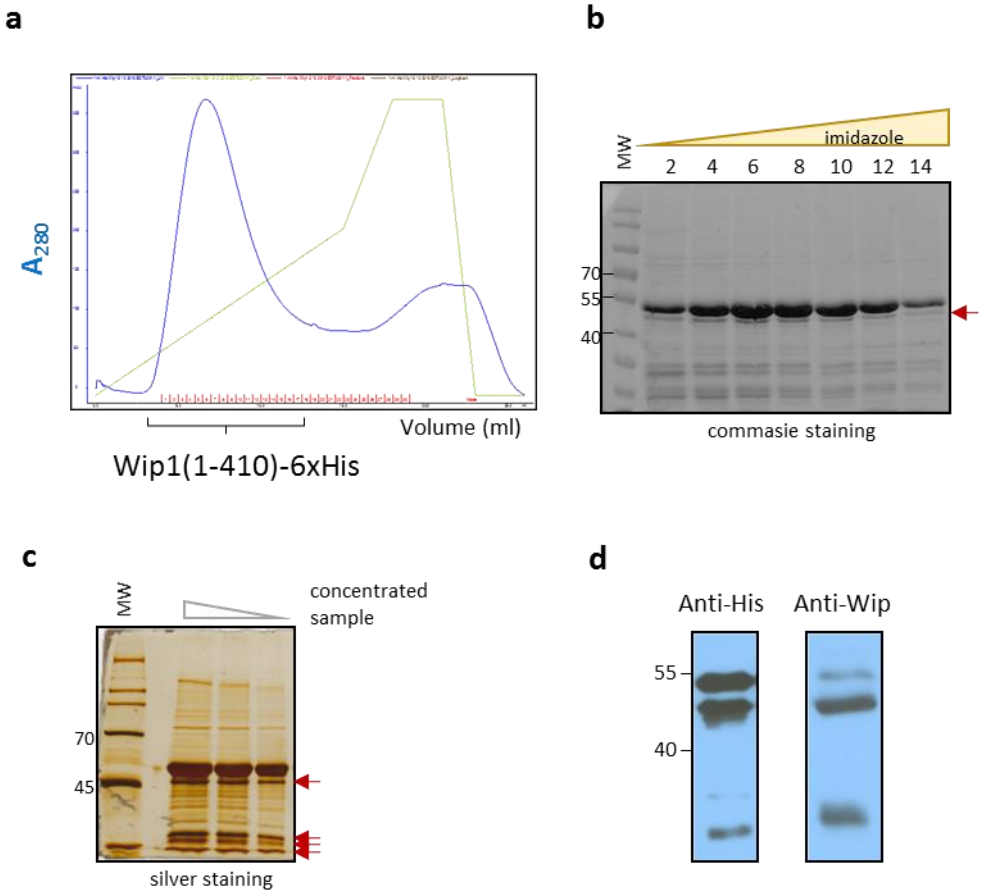

Figure 11. Large-scale purification of WIP1(1-410)-6xHis. a) Chromatogram of imidazole gradient elution of WIP1(1-410)-6xHis from His-tag purification column. **b)** Coomassie gel staining of peak fractions from IMAC chromatography. **c)** The silver-stained gel of concentrated WIP1(1-410)-6xHis sample (decreased dilution in the gel lines). **d)** Western blot of purified sample of WIP1(1-410)-6xHis stained by anti-His and anti-WIP antibodies.

We were not able to separate the nearest contaminating fragment by ion exchange chromatography or gel filtration because probably it has the similar behavior in the buffer

as WIP1(1-410)-6xHis (data not shown). This fragment contains His-tag on the C-terminus (Figure 11d) and we supposed that it might be the product of N-terminal cleavage of WIP1(1-410)-6xHis. According to the molecular weight of problematic fragment, we assumed that it may be cleaved in Pro-loop which is not conserved across PP2Cδ orthologues in the different species and it supposed to be unstructured (Figure 12a). Probably, Pro-loop is located outside of the catalytic domain of WIP1 and therefore it could be attacked by bacterial proteases during purification or it may be sensitive to cleavage during improper protein folding. To address this question, we analyzed fragments of WIP1(1-410)-6xHis by N-terminal sequencing followed by mass spectrometry (this experiment was done by Research-Service Groups of Mass Spectrometry at IOCB in Prague). As we expected, N-terminal sequencing revealed that the nearest fragment of WIP1(1-410)-6xHis was cleaved in the Pro-loop in (45)LSQPL sequence (Figure 12b).

a

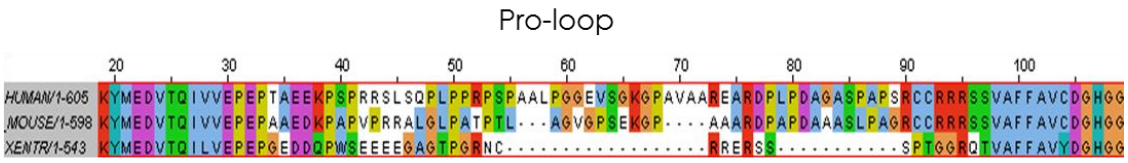

b

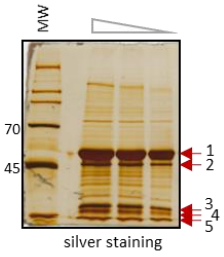

N-terminal sequencing

Fragments	determined sequences	consensus
1	AGLYSLG	**AGLYSLG**
2	GPQPL LVEYY ASPNA	**45-LSQPL**
3	AGLYS GLY	**AGLYS**
4	AGLYS GLVEK MPYAV	**AGLYS**
5	AGLYS GEVAK	**AGLYS**

Figure 12. N-terminal sequencing of WIP1(1-410)-6xHis fragments. a) Alignment of WIP1 Pro-loop between human, mouse and Xenopus orthologues. **b)** N-terminal sequencing of 1-5 isolated fragments and their mass spectrometry analysis revealed consensus sequences. Fragment 2 started at lysine 45, others lower migrating fragments are probably cleaved from C-terminus because were sequenced from the first amino acid of WIP1.

These results led us to exchange the part of Pro-loop to a short glycine-serine repeat which is well established in protein engineering and crystallography fields as a flexible and stable liker [164, 165]. In addition, we replaced Pro-loop to correspond to the sequence from *Xenopus laevis* WIP1 orthologue which does not contain the cleavage site. We created other three variants WIP1(1-410)-GGGS-6xHis, WIP1(1-382)-GGGS-6xHis and WIP1(1-410)-Xenopus-6xHis (Figure 13a) and purified by established protocol for large-scale isolation by HPLC (Figure 13b). As we expected, mutation of Pro-loop of WIP1 successfully removed of the nearest fragment. Between the WIP1(1-410)-GGGS-6xHis and WIP1(1-410)-Xenopus-6xHis we did not see any differences in purity. Therefore, we used variant WIP1(1-410)-GGGS-6xHis for other work. However, the stability of WIP1(1-410)-GGGS-6xHis was still very low. The protein sample repeatedly aggregates after freezing/thawing and even at 4°C in defined buffer after 1 day.

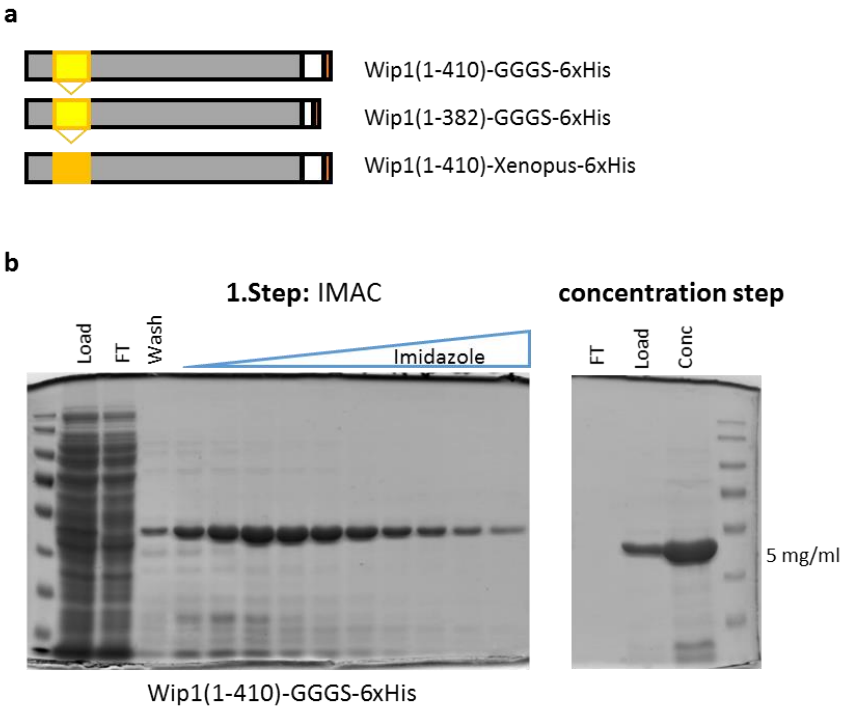

Figure 13. Pro-loop mutated WIP1 recombinant proteins. a) WIP1(1-410)-GGGS-6xHis and WIP1(1-382)-GGGS-6xHis variants contains instead of Pro-loop 7xGGGS linkers (yellow box). WIP1(1-410)-Xenopus-6xHis variant contains corresponding sequence 34-GEDELPWSEEEEGTPAKNCRSENRQT-92 from *Xenopus laevis*. **b)** Coomassie blue staining of gels with samples from gradient elution by IMAC/HPLC (left) and with the concentrated sample to 5 mg/ml (right).

5.1.4 T4 lysozyme fusion protein enhance expression and stability of WIP1

A well-folded and soluble protein T4 lysozyme (T4L) was crystallized under many different conditions [166, 167]. Recently, a number of published crystal structures has been gained by fusing T4L to the amino terminus of target proteins. This approach could also facilitate crystallization of proteins [168]. Hence, we created T4L fusion construct with WIP1(1-410). In our case, we replaced the Pro-loop to T4L to prevent degradation and to exclude the disordered part of WIP1 (Figure 14a).

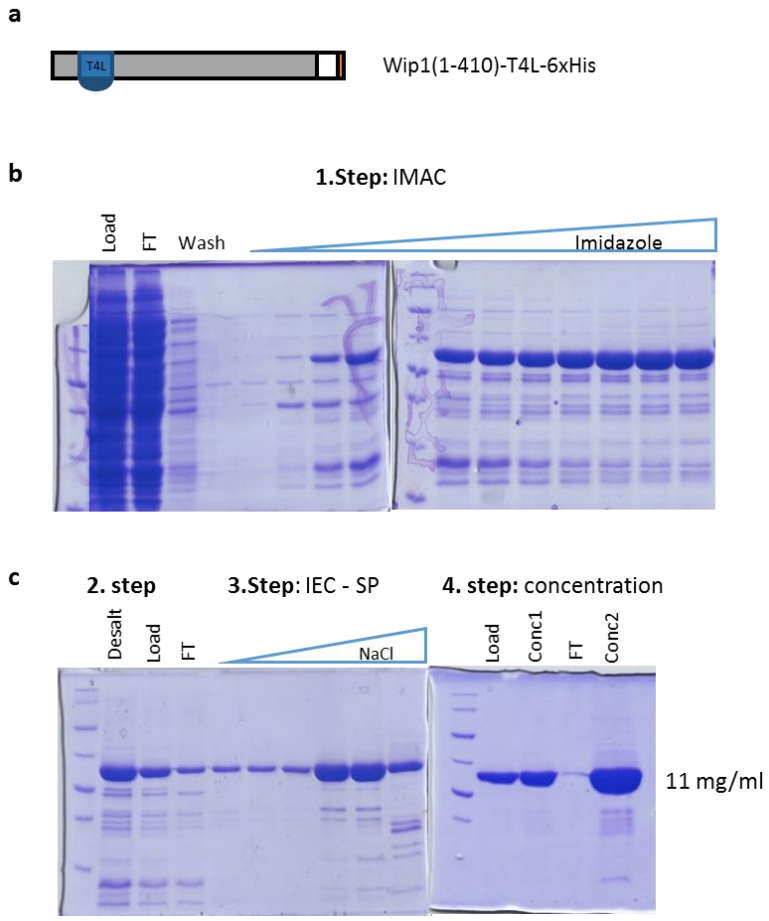

Figure 14. Large-scale purification of T4 lysozyme fusion WIP1 protein. a) Scheme of T4 lysozyme (blue part) fusion WIP1 protein - WIP1(1-410)-T4L-6xHis. **b)** First step purification - coomassie blue staining of gels with samples of WIP1(1-410)-T4L-6xHis from gradient elution by IMAC/HPLC. **c)** Coomassie blue-stained gels. 2.step – desalting of WIP1(1-410)-T4L-6xHis to low salt buffer by Hitrap 2x5ml desalting column. 3.step – gradient elution from cation (SP) exchange column chromatography (IEC). 4.step – Concentration of peak fractions from IEC to 11 mg/ml.

The fusion variant WIP1(1-410)-T4L-6xHis was expressed and purified by the standard protocol in the HEPES buffer at pH 7,5 (Figure 14b). The T4L fusion WIP1 protein improved expression yield, solubility and protein sample did not undergo aggregation in time or after freezing at higher concentration (> 5 mg/ml). WIP1(1-410)-T4L-6xHis variant was further used to increase its purity suitable for crystallization.

To determine whether recombinant proteins of WIP1 are enzymatically active we performed in vitro assay with purified proteins and nuclear extract from etoposide-treated RPE cells where *PPM1D* was knocked out by CRISPR/Cas9 and that were (Figure 15). Western blot analysis revealed that recombinant variants of WIP1(1-410)-T4L-6xHis decreased levels of endogenous substrates of WIP1 KAP1-pS824 and p53-pS15.

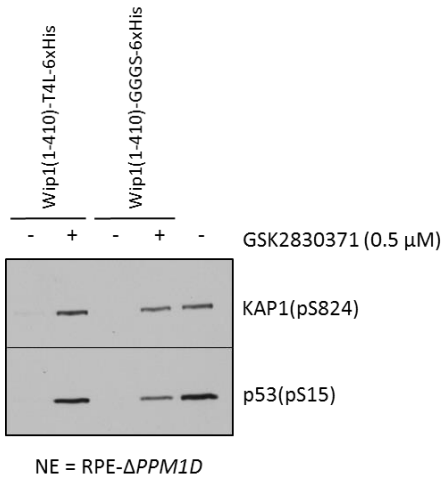

Figure 15. Phosphatase reaction of recombinant WIP1 with nuclear extract. Western blot analysis. RPE cells with CRISPR/Cas9-mediated knock-out of *PPM1D* was treated by etoposide for 2h were harvested and the nuclear fraction was extracted. Recombinant WIP1(1-410)-GGGS-6xHis and WIP1(1-410)-T4L-6xHis (4 nM) were incubated with 10 µl of nuclear extract, and with or without 0,5 µM of GSK2830371 for 30 minutes at 37°C. Dephosphorylated endogenous substrates were detected by antibodies anti-KAP1-pS824 and anti-p53-pS15.

5.1.5 Ion exchange chromatography increase purity of WIP1

To increase the purity of WIP1 recombinant proteins we included second purification step. The ion exchange chromatography (IEC) separates proteins according to their charge at certain pH of the buffer. To predict which IEC we based on the theoretical isoelectric points of WIP1 variants (Table 3).

Table 3. Theoretical pI of WIP1 recombinant variants.

Protein variant	Theoretical pI [a]
WIP-(1-410)-GGGS-6xHis	7.03
WIP-(1-382)-GGGS-6xHis	8.67
WIP-(1-410)-T4-6xHis	8.85

[a] theoretical pI were calculated by http://web.expasy.org/compute_pi/

For WIP1(1-410)-T4L-6xHis and WIP1(1-382)-GGGS-6xHis at buffer pH 7,5, and WIP1(1-410)-GGGS-6xHis at buffer pH 6 we chose strong cation exchanger SP (sulfopropyl matrix), respectively. Successfully, WIP1(1-410)-T4L-6xHis bound to cation exchanger and was eluted by sodium salt gradient (Figure 14c). The cation IEC increased the purity of WIP1 by removing higher and a lower migrating fragments. The most improved purity was observed in case of WIP1(1-410)-T4L-6xHis and therefore we further concentrated the samples from IEC for crystallization screen (Figure 14c).

In the case of WIP1(1-382)-GGGS-6xHis we found that protein had low solubility during the expression in bacteria comparable to the non-mutated version WIP1(1-382)-6xHis (data not shown). On the other hand, the second purification step improved the purity of WIP1(1-382)-GGGS-6xHis, but its yield was not sufficient for growth of crystals. Therefore, we excluded the shortest WIP1 variants from crystallization trials. Possible protein purification in denaturation conditions has to be followed by protein renaturation which can cause improper folding and loss of native behavior of the protein. Results from purification step of selected WIP1 recombinant variant are summarized in table 4.

Table 4. Purification characteristics of selected WIP1 recombinant proteins.

Protein variant	Soluble fraction[a]/stability[b]	Yield from first purification step[c]	Second purification step	Concentration[d] (mg/ml)
WIP(1-410)-6xHis	yes/precipitation	3 mg	-	3,5
WIP(1-382)-6xHis	no	1mg	-	-
WIP(1-410)-GGGS-6xHis	yes/precipitation	2,5 mg	IEC (SP)	5
WIP(1-382)-GGGS-6xHis	no	1mg	IEC (SP)	2
WIP(1-410)-T4-6xHis	yes/good stability	6 mg	IEC (SP)	5-11

[a] majority of the target protein was in soluble fraction (lysate extracted form bacterial pelete)
[b] stability or precipitation of the protein at > 5 mg/ml
[c] approximate yield isolated from 1 litre of culture
[d] final concentration of the protein sample after concentration

5.1.6 HTP screening of buffer condition for crystallization

Concentrated recombinant proteins WIP1(1-410)-6xHis and WIP1(1-410)-T4L-6xHis (Table 5) were used for screening of crystallization conditions. We performed 96-well commercial crystalyzation screens (JB Phosphatases screen, JBScreen JCSG++, Morpheus screen). Protein drops were seeded automatically by vapor diffusion, sitting drop method in the 1:1 ratio with the precipitant. The wells were scanned by light and UV microscopy automatically for two months. We did not observe any crystals growth of WIP1(1-410)-6xHis in commercial designed buffer screen (Jena bioscience) for phosphatases. We suppose that sample of WIP1(1-410)-6xHis had too low purity, homogeneity, or very low stability. All crystallization trials which were set with the most promising construct WIP1(1-410)-T4L-6xHis are summarized in table 5.

5.1.7 Application of *in situ* proteolysis for crystallization

In situ proteolysis or limited proteolysis by non-specific proteases has been used as a classical approach to determine the stable and structured domains of target proteins[169]. The addition of trace amounts of protease to the crystallization drops can rescue of protein targets that had failed in previous crystallization screens [170].

Table 5. Crystallization trials of WIP1(1-410)-T4L-6xHis

Number of screen [a]	Type of screen	Concentration (mg/ml)	Setting and special additives [b]
MCSP01	Morpheus screen	5.33	Drop1 – 1:1
MCSP02	JBScreen JCSG++	5.33	Drop1 – 1:1
MCSP03	Morpheus screen	5.33	Drop1 – 1:1 Drop2 – 2:1
MCSP04	JBScreen JCSG++	5.33	incubation at 4°C Drop1 – 1:1 Drop2 – 2:1
MCSP05	JBScreen JCSG++	5.33	Drop1 – 1:1 protein + Trypsin Drop2 – 1:1 protein + Chymotrypsin
S0SP06	JBScreen JCSG++	5.33	Drop – 1:1 protein + 10 µM GSK2830371 + Chymotrypsin
MCSP07	JBScreen JCSG++	11	Drop1 – 1:1 protein + 10 µM GSK2830371 Drop2 – 1:1 protein + Chymotrypsin
MCSP08	Morpheus screen	11	Drop1 – 1:1 protein + 10 µM GSK2830371 Drop2 – 1:1 protein + Chymotrypsin

[a] number of screens are based on the type of 96-well plate for crystallization
[b] plates were incubated at 18°C, if it not specified differently

In situ proteolysis has been commercialized for protein crystallization to improve growth of protein crystals, and enhance crystal with low diffraction resolution. Since WIP1(1-410)-T4L-6xHis was unable to crystallize in previous screens, we investigated whether the addition of non-specific proteases to the crystallization trials could help to promote crystal growth. Firstly, we pre-screened the WIP1(1-410)-T4L-6xHis to identified promising proteases (Figure 16). For crystallization screens, we selected chymotrypsin and trypsin in ratio 1:5000 and 1:10,000 with concentrated WIP1(1-410)-T4L-6xHis,respectively. We did not observe the growth of crystals but only atypical changes in several conditions after 13 days which could lead to crystal formation (Figure 17). However, after 1 month we did not see any other changes neither protein crystals. Surprisingly, when we repeated *in situ* proteolysis technique with new purified and higher concentrated protein WIP1(1-410)-T4L-6xHis (screen MCSP07) we did not observe same changes as before even after 27 days and later (Figure 17).

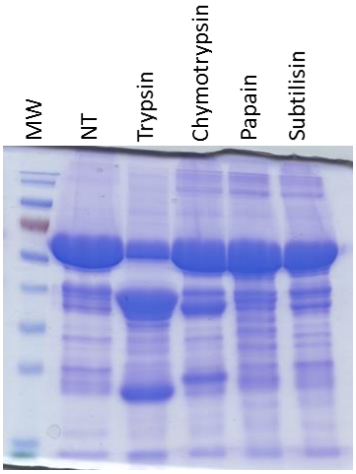

Figure 16. Pre-screening of WIP1(1-410)-T4L-6xHis to identify a promising protease. Coomassie stained gel. 100 µg of WIP1(1-410)-T4L-6xHis was incubated with 0,01 µg of proteases at room temperature for 30 minutes. MW - protein marker, NT – non-treated protein sample.

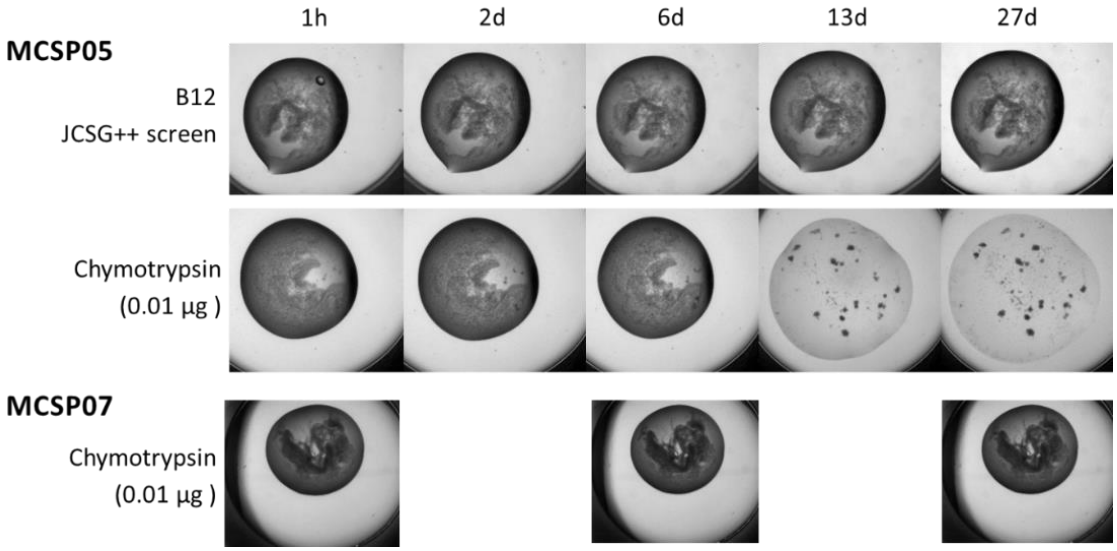

Figure 17. Crystallization trials of WIP1(1-410)-T4L-6xHis. MCSP05 – B12/drop2, JCSG++ screen, 5,33 mg/ml of the protein. (first line) protein, protein + 0,01 µg of chymotrypsin (second line). MCSP07 – B12/drop2, JCSG++ screen, 11 mg/ml of the protein + 0,01µg of chymotrypsin (last line)

5.1.8 Specific inhibitor of WIP1 phosphatase increased stability of protein

Protein crystallization can be facilitated by the specific ligands or inhibitors, which bind to the protein and increase its stability and homogeneity. The novel allosteric inhibitor GSK2830371 was published as a compound capable to inhibit WIP1 phosphatase in cells. In this study, they also determined that binding of inhibitor increased the thermal stability of WIP1 in vitro [85]. Firstly, we analysed the thermal stability of WIP1(1-410)-T4L-6xHis and WIP1(1-410)-6xHis by the thermofluor-based method. Similarly, we observed that inhibitor GSK2830371 enhanced the stability of recombinant WIP1 proteins in the consistent with the original publication (Figure 18).

Further, we performed crystallization screens with WIP1(1-410)-6xT4L-His and added 10 μM of GSK2830371 to crystallization screen conditions. We observed formation of a crystal in condition E7/JBS JCSG++ screen, but further analysis by UV and X-ray diffraction did not confirm the presence of protein crystal (Figure 19). WIP1(1-410)-6xT4L-His was not able to crystallize even in the presence of the allosteric inhibitory compound.

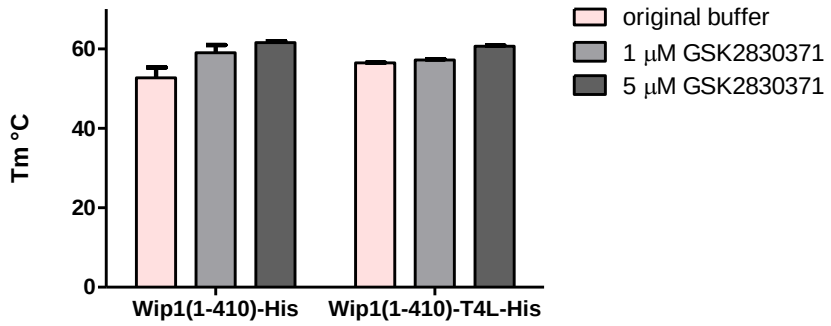

Figure 18. Thermal stability of WIP1 in the presence of its allosteric inhibitor (GSK2830371). Thermal shift (Tm) of the protein in buffer conditions were performed by real-time PCR instrument. Original buffer was 50 mM Hepes, 200 mM NaCl, 10 mM MgCl2, 5% glycerol. Protein was incubated with indicated concentration of GSK2830371 for 30 minutes before thermofluor analysis.

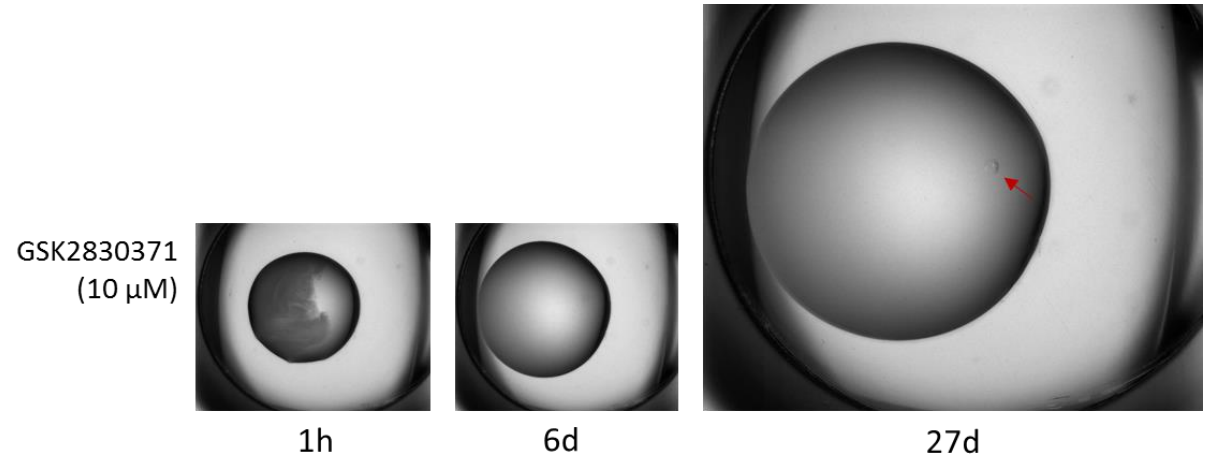

Figure 19. Crystallization trials of WIP1 in the presence of allosteric inhibitor (GSK2830371). Screen MCSP07 - Drop1 – condition E7 (0,2 M zinc acetate, 0,1 M sodium cacodylate, 10 % isopropanol).

5.2 Materials and methods

Materials and chemicals

GSK2830371 (MedChem Express), Hepes (Sigma), IPTG (Applichem), EDTA (Sigma), SYPRO®Orange Protein Gel Stain (5,000X Concentrate in DMSO) (Thermo Fisher Scientific), Sodium chloride (Sigma), Magnesium chloride (Sigma), glycerol (Labnet), Coomassie Brilliant Blue R-250 Dye (Sigma), Silver staining solution (homemade)

Cell lines

RPE cells with CRISPR/Cas9-mediated *PPM1D* knocked out. Cells were grown at 37°C and 5% CO2 in DMEM supplemented with 6% FBS (Gibco), penicillin (100 U/ml), and streptomycin (0.1 mg/ml). All cell lines were regularly checked for absence of mycoplasma infection using MycoAlert Plus reagent (Lonza).

Antibodies

The following antibodies were used: WIP1 (sc-130655), p53-pS15 (#9284), KAP1-pS824 (ab70369), Anti-6X His tag (ab18184).

Plasmid construction, expression and purification of WIP1

All WIP1 protein variants were produced as a C-terminal or N-termianl 6xHis-tag fusion protein using pET21b vector in *Escherichia coli* BL21 gold cells. Proteins expression was induced by 0,5 mM IPTG at OD = 0,6 for 16 hours at 21°C. Initially, for lysis of bacterial pellet we used phosphatase buffer (50 mM NaH_2PO_4, 0,5 M NaCl, 10 mM imidazole, 5 % (v/v) glycerol, 1 mM $MgCl_2$, pH = 8.0). Using thermal stability assay we selected more suitable lysis buffer which contains 50 mM HEPES, 200 mM NaCl, 5 % (v/v) glycerol, 10 mM $MgCl_2$, pH = 7,5. This buffer was used for large-scale purification of selected WIP1 proteins to crystallization. To the lysis buffer we freshly added 0,5 mM TCEP, protease inhibitors, 25 U/µl benzonase, 1 mg/ml lysozyme, 10 mM imidazole and 1 mM EDTA. Proteins were purified using Immobilized-metal affinity chromatography (IMAC) (HisTrap HP, GE Healthcare or cOmplete His-Tag Purification Columns, Roche). The peak fractions from imidazole gradient elution (from 10-500 mM of imidazole) were desalted (Hitrap Desalting column, GE Healthcare) into the buffer without imidazole (50 mM HEPES, 200 mM NaCl, 5 % (v/v) glycerol, 10 mM MgCl2, pH = 7,5) to minimize proteins precipitation. Desalted fractions were loaded into the ion exchange chromatography. SP column (strong catex; 1 ml SP Hitrap column, GE Healthcare) was in tandem with Q column (strong annex; 1 ml Q Hitrap column, GE Healthcare). Protein was eluted by NaCl (from 0,2-1 M) gradient only from SP chromatography column, Q column was removed after loading of sample. Isolated proteins were concentrated by Vivaspin 2, 30 kD MWCO (GE Healthcare) to 1ml, subsequently by Microcon 10 kD MWCO (Merck Millipore) to 5 and 11 mg/ml and stored at -80° until needed. The purity of final protein samples were validated by coomassie blue or silver staining.

Thermofluor assay

Solutions of 7,5 µl of 300x Sypro Orange (Molecular Probes), 12.5 µl of test compounds (buffer or additive, see in Figure 10), and 2 µl of 0,5 mg/ml protein were added to the wells of a 96-well thin-wall PCR plate (BioRad). Water was added instead of test compound in the control samples. The plates were sealed with Optical-Quality Sealing Tape (Bio-Rad) and heated in LightCycler 480SW1.5 Real Time PCR Detection System (Bio-Rad) from 20 to 90 °C in increments of 0.2 °C. Fluorescence changes in the wells of the plate were monitored simultaneously with a charge-coupled device (CCD) camera. The wavelengths for excitation and emission were 490 and 575 nm, respectively.(procedure details see in [163])

In situ proteolysis for crystallization

Using JBS Floppy-Choppy (JenaBioscience) we pre-screened 100 µg of WIP1(1-410)-T4L-6xHis. Protein was incubated with 0,01 µg of proteases (chymotrypsin, trypsin, subtilisin, papain) at room temperature for 30 minutes. Samples were analysed by SDS-PAGE and the gel was stained by Coomassie Brilliant Blue R-250 Dye. In situ proteolysis was done with 5 and 11 mg/ml of WIP1(1-410)-T4L-6xHis in ration 1:5000 and 1:10,000 with proteases chymotrypsin and trypsin (1mg/ml in the stocks), respectively. Proteases were added exactly before crystallization experiments.

HTP crystallization screening

All Crystallization screens were performed 96-well format. We used commercial crystalyzation buffer screens (JB Phosphatases screen, JBScreen JCSG++, Morpheus screen). Reservoir volume was 50 µl, automatically loaded by ArtRobins instrument. Protein drops were seeded as sitting drop with vapor diffusion. The protein solutions were mixed in a 1:1 (0,2 µl:0,2 µl) ratio with the reservoir solution by Dougles Instrument Oryx8. The crystallization trials were scanned by light and UV microscopy automatically for two months (Rigaku Xtal Detect R^{TM} UV).

6 SUMMARY AND CONCLUSION

In conclusion, the results achieved during the work on this thesis contribute to our knowledge of how Wip1 is regulated during the cell cycle, how can Wip1 be implicated in the regulation of cancer cells and if the inhibition of Wip1 could enhance cancer therapy response. In general, the negative regulation of DNA damage response pathway plays a role in both cancer development and cancer treatment. Since the Wip1 terminates DDR signalling, we believe that better understanding of its molecular mechanism in DDR will lead to the development of more targeted cancer treatment. Moreover, the knowledge of Wip1 structure can help to determine the molecular function of Wip1 and could be used for design specific small molecule inhibitors.

The novel findings obtained during the work on this thesis can be summarised as follows:

- We characterised the regulation of Wip1 during the cell cycle. Wip1 protein levels decline during mitosis by APC-Cdc20 dependent proteasomal degradation. Wip1 protein abundance increase during G1 and peaks at the end of G2. During mitosis, Wip1 is phosphorylated at multiple residues which inhibit its enzymatic activity. We propose that combination of proteasome degradation and phosphorylation-mediated inhibition of Wip1 permits sensing of DNA damage that appears during unperturbed mitosis and provides the preservation of chromatin marks on DNA lesions which facilitate repair of DNA in the subsequent G1 phase.

- We newly identified gain-of-function mutations of *PPM1D* which result in expression of C-terminally truncated Wip1. These truncated Wip1 variants are enzymatically active and exhibit increased protein stability. We identified these mutations in cancer cell lines and also in the peripheral blood of breast cancer patients. Stabilised form of Wip1 impairs the p53-dependent G1 checkpoint We suggest that these gain-of-mutations of *PPM1D* could predispose to cancer development.

- We validated of commercially available inhibitors of Wip1. Using the cell CRISPR-Cas9 knock-out model we confirmed the specificity of allosteric Wip1 inhibitor GSK2830371 and off-target function of the second compound CCT007093.

- We characterised the effects of Wip1 inhibition in cancer cell lines. Inhibition of Wip1 significantly reduced the cell proliferation in cancer cell lines which carry amplification of *PPM1D*. Wip1 inhibition did not affect the proliferation of non-transformed cells with low levels of Wip1. We showed that inhibition of Wip1 by GSK2830371 sensitises breast cancer cells with amplified *PPM1D* and wild-type p53 to DNA damage-induced chemotherapy and to MDM2 antagonist (Nutlin-3) treatment.

- As the unpublished result, we optimized conditions of purification of active Wip1 variants from bacteria and performed crystallization trials. The most promising construct was T4 lysozyme fusion protein Wip1(1-410)-T4L-6xHis with the highest purity, stability and solubility behaviour in the buffer. Unfortunately, we have not succeeded to crystallize and determine the crystal structure of Wip1 phosphatase.

7 REFERENCES

1. Jackson, S.P. and J. Bartek, *The DNA-damage response in human biology and disease.* Nature, 2009. **461**(7267): p. 1071-8.
2. Halazonetis, T.D., V.G. Gorgoulis, and J. Bartek, *An oncogene-induced DNA damage model for cancer development.* Science, 2008. **319**(5868): p. 1352-5.
3. Polo, S.E. and S.P. Jackson, *Dynamics of DNA damage response proteins at DNA breaks: a focus on protein modifications.* Genes Dev, 2011. **25**(5): p. 409-33.
4. Motoyama, N. and K. Naka, *DNA damage tumor suppressor genes and genomic instability.* Curr Opin Genet Dev, 2004. **14**(1): p. 11-6.
5. Yang, J., et al., *ATM, ATR and DNA-PK: initiators of the cellular genotoxic stress responses.* Carcinogenesis, 2003. **24**(10): p. 1571-80.
6. Bartek, J. and J. Lukas, *DNA damage checkpoints: from initiation to recovery or adaptation.* Curr Opin Cell Biol, 2007. **19**(2): p. 238-45.
7. Zhang, X.P., et al., *Cell fate decision mediated by p53 pulses.* Proc Natl Acad Sci U S A, 2009. **106**(30): p. 12245-50.
8. Leontieva, O.V., A.V. Gudkov, and M.V. Blagosklonny, *Weak p53 permits senescence during cell cycle arrest.* Cell Cycle, 2010. **9**(21): p. 4323-7.
9. Bartek, J. and J. Lukas, *Chk1 and Chk2 kinases in checkpoint control and cancer.* Cancer Cell, 2003. **3**(5): p. 421-9.
10. Canman, C.E., et al., *Activation of the ATM kinase by ionizing radiation and phosphorylation of p53.* Science, 1998. **281**(5383): p. 1677-9.
11. Burma, S., et al., *ATM phosphorylates histone H2AX in response to DNA double-strand breaks.* J Biol Chem, 2001. **276**(45): p. 42462-7.
12. Doil, C., et al., *RNF168 binds and amplifies ubiquitin conjugates on damaged chromosomes to allow accumulation of repair proteins.* Cell, 2009. **136**(3): p. 435-46.
13. Morgan, D.O., *Principles of CDK regulation.* Nature, 1995. **374**(6518): p. 131-4.
14. Parker, L.L., et al., *Phosphorylation and inactivation of the mitotic inhibitor Wee1 by the nim1/cdr1 kinase.* Nature, 1993. **363**(6431): p. 736-8.
15. Chow, J.P., et al., *Differential contribution of inhibitory phosphorylation of CDC2 and CDK2 for unperturbed cell cycle control and DNA integrity checkpoints.* J Biol Chem, 2003. **278**(42): p. 40815-28.
16. Kasahara, K., et al., *14-3-3gamma mediates Cdc25A proteolysis to block premature mitotic entry after DNA damage.* EMBO J, 2010. **29**(16): p. 2802-12.
17. Forrest, A. and B. Gabrielli, *Cdc25B activity is regulated by 14-3-3.* Oncogene, 2001. **20**(32): p. 4393-401.
18. Peng, C.Y., et al., *Mitotic and G2 checkpoint control: regulation of 14-3-3 protein binding by phosphorylation of Cdc25C on serine-216.* Science, 1997. **277**(5331): p. 1501-5.
19. Sanchez, Y., et al., *Conservation of the Chk1 checkpoint pathway in mammals: linkage of DNA damage to Cdk regulation through Cdc25.* Science, 1997. **277**(5331): p. 1497-501.
20. O'Connell, M.J., et al., *Chk1 is a wee1 kinase in the G2 DNA damage checkpoint inhibiting cdc2 by Y15 phosphorylation.* EMBO J, 1997. **16**(3): p. 545-54.
21. el-Deiry, W.S., et al., *WAF1, a potential mediator of p53 tumor suppression.* Cell, 1993. **75**(4): p. 817-25.
22. McKenzie, L., et al., *p53-dependent repression of polo-like kinase-1 (PLK1).* Cell Cycle, 2010. **9**(20): p. 4200-12.
23. Bulavin, D.V., et al., *Initiation of a G2/M checkpoint after ultraviolet radiation requires p38 kinase.* Nature, 2001. **411**(6833): p. 102-7.
24. Medema, R.H. and L. Macurek, *Checkpoint control and cancer.* Oncogene, 2012. **31**(21): p. 2601-13.

25. Shaltiel, I.A., et al., *The same, only different – DNA damage checkpoints and their reversal throughout the cell cycle.* Journal of Cell Science, 2015. **128**(4): p. 607-620.
26. Macurek, L., et al., *Polo-like kinase-1 is activated by aurora A to promote checkpoint recovery.* Nature, 2008. **455**(7209): p. 119-23.
27. Watanabe, N., et al., *M-phase kinases induce phospho-dependent ubiquitination of somatic Wee1 by SCFbeta-TrCP.* Proc Natl Acad Sci U S A, 2004. **101**(13): p. 4419-24.
28. Toyoshima-Morimoto, F., E. Taniguchi, and E. Nishida, *Plk1 promotes nuclear translocation of human Cdc25C during prophase.* EMBO Rep, 2002. **3**(4): p. 341-8.
29. Liu, X.S., et al., *Polo-like kinase 1 phosphorylation of G2 and S-phase-expressed 1 protein is essential for p53 inactivation during G2 checkpoint recovery.* EMBO Rep, 2010. **11**(8): p. 626-32.
30. Shi, Y., *Serine/threonine phosphatases: mechanism through structure.* Cell, 2009. **139**(3): p. 468-84.
31. Shaltiel, I.A., et al., *Distinct phosphatases antagonize the p53 response in different phases of the cell cycle.* Proc Natl Acad Sci U S A, 2014. **111**(20): p. 7313-8.
32. Leung-Pineda, V., C.E. Ryan, and H. Piwnica-Worms, *Phosphorylation of Chk1 by ATR is antagonized by a Chk1-regulated protein phosphatase 2A circuit.* Mol Cell Biol, 2006. **26**(20): p. 7529-38.
33. Dozier, C., et al., *Regulation of Chk2 phosphorylation by interaction with protein phosphatase 2A via its B' regulatory subunit.* Biol Cell, 2004. **96**(7): p. 509-17.
34. Liang, X., E. Reed, and J.J. Yu, *Protein phosphatase 2A interacts with Chk2 and regulates phosphorylation at Thr-68 after cisplatin treatment of human ovarian cancer cells.* Int J Mol Med, 2006. **17**(5): p. 703-8.
35. Peng, A. and J.L. Maller, *Serine/threonine phosphatases in the DNA damage response and cancer.* Oncogene, 2010. **29**(45): p. 5977-88.
36. Chowdhury, D., et al., *A PP4-phosphatase complex dephosphorylates gamma-H2AX generated during DNA replication.* Mol Cell, 2008. **31**(1): p. 33-46.
37. Keogh, M.C., et al., *A phosphatase complex that dephosphorylates gammaH2AX regulates DNA damage checkpoint recovery.* Nature, 2006. **439**(7075): p. 497-501.
38. Nazarov, I.B., et al., *Dephosphorylation of histone gamma-H2AX during repair of DNA double-strand breaks in mammalian cells and its inhibition by calyculin A.* Radiat Res, 2003. **160**(3): p. 309-17.
39. Goodarzi, A.A., et al., *Autophosphorylation of ataxia-telangiectasia mutated is regulated by protein phosphatase 2A.* EMBO J, 2004. **23**(22): p. 4451-61.
40. Haneda, M., et al., *Protein phosphatase 1, but not protein phosphatase 2A, dephosphorylates DNA-damaging stress-induced phospho-serine 15 of p53.* FEBS Lett, 2004. **567**(2-3): p. 171-4.
41. Shouse, G.P., X. Cai, and X. Liu, *Serine 15 phosphorylation of p53 directs its interaction with B56gamma and the tumor suppressor activity of B56gamma-specific protein phosphatase 2A.* Mol Cell Biol, 2008. **28**(1): p. 448-56.
42. Janssens, V. and J. Goris, *Protein phosphatase 2A: a highly regulated family of serine/threonine phosphatases implicated in cell growth and signalling.* Biochem J, 2001. **353**(Pt 3): p. 417-39.
43. Hong, C.S., et al., *LB100, a small molecule inhibitor of PP2A with potent chemo- and radio-sensitizing potential.* Cancer Biology & Therapy, 2015. **16**(6): p. 821-833.
44. Lu, J., et al., *Inhibition of serine/threonine phosphatase PP2A enhances cancer chemotherapy by blocking DNA damage induced defense mechanisms.* Proceedings of the National Academy of Sciences, 2009. **106**(28): p. 11697-11702.
45. Wang, B., et al., *Protein phosphatase PP4 is overexpressed in human breast and lung tumors.* Cell Res, 2008. **18**(9): p. 974-7.
46. Lammers, T. and S. Lavi, *Role of type 2C protein phosphatases in growth regulation and in cellular stress signaling.* Crit Rev Biochem Mol Biol, 2007. **42**(6): p. 437-61.

47. Lu, X., et al., *The type 2C phosphatase Wip1: an oncogenic regulator of tumor suppressor and DNA damage response pathways.* Cancer Metastasis Rev, 2008. **27**(2): p. 123-35.
48. Lindqvist, A., et al., *Wip1 confers G2 checkpoint recovery competence by counteracting p53-dependent transcriptional repression.* EMBO J, 2009. **28**(20): p. 3196-206.
49. Shreeram, S., et al., *Wip1 phosphatase modulates ATM-dependent signaling pathways.* Mol Cell, 2006. **23**(5): p. 757-64.
50. Lu, X., B. Nannenga, and L.A. Donehower, *PPM1D dephosphorylates Chk1 and p53 and abrogates cell cycle checkpoints.* Genes Dev, 2005. **19**(10): p. 1162-74.
51. Yoda, A., et al., *Intrinsic kinase activity and SQ/TQ domain of Chk2 kinase as well as N-terminal domain of Wip1 phosphatase are required for regulation of Chk2 by Wip1.* J Biol Chem, 2006. **281**(34): p. 24847-62.
52. Fujimoto, H., et al., *Regulation of the antioncogenic Chk2 kinase by the oncogenic Wip1 phosphatase.* Cell Death Differ, 2006. **13**(7): p. 1170-80.
53. Brazina, J., et al., *DNA damage-induced regulatory interplay between DAXX, p53, ATM kinase and Wip1 phosphatase.* Cell Cycle, 2015. **14**(3): p. 375-87.
54. Nguyen, T.A., et al., *The oncogenic phosphatase WIP1 negatively regulates nucleotide excision repair.* DNA Repair (Amst), 2010. **9**(7): p. 813-23.
55. Peng, B., et al., *Modulation of LSD1 phosphorylation by CK2/WIP1 regulates RNF168-dependent 53BP1 recruitment in response to DNA damage.* Nucleic Acids Res, 2015. **43**(12): p. 5936-47.
56. Zhang, M., et al., *PPM1D phosphatase, a target of p53 and RBM38 RNA-binding protein, inhibits p53 mRNA translation via dephosphorylation of RBM38.* Oncogene, 2015. **34**(48): p. 5900-11.
57. Lowe, J.M., et al., *Nuclear factor-kappaB (NF-kappaB) is a novel positive transcriptional regulator of the oncogenic Wip1 phosphatase.* J Biol Chem, 2010. **285**(8): p. 5249-57.
58. Chew, J., et al., *WIP1 phosphatase is a negative regulator of NF-kappaB signalling.* Nat Cell Biol, 2009. **11**(5): p. 659-66.
59. Macurek, L., et al., *Wip1 phosphatase is associated with chromatin and dephosphorylates gammaH2AX to promote checkpoint inhibition.* Oncogene, 2010. **29**(15): p. 2281-91.
60. Moon, S.H., et al., *Wild-type p53-induced phosphatase 1 dephosphorylates histone variant gamma-H2AX and suppresses DNA double strand break repair.* J Biol Chem, 2010. **285**(17): p. 12935-47.
61. Cha, H., et al., *Wip1 directly dephosphorylates gamma-H2AX and attenuates the DNA damage response.* Cancer Res, 2010. **70**(10): p. 4112-22.
62. Lu, X., et al., *The Wip1 Phosphatase acts as a gatekeeper in the p53-Mdm2 autoregulatory loop.* Cancer Cell, 2007. **12**(4): p. 342-54.
63. Zhang, X., et al., *Phosphorylation and degradation of MdmX is inhibited by Wip1 phosphatase in the DNA damage response.* Cancer Res, 2009. **69**(20): p. 7960-8.
64. Takekawa, M., et al., *p53-inducible wip1 phosphatase mediates a negative feedback regulation of p38 MAPK-p53 signaling in response to UV radiation.* EMBO J, 2000. **19**(23): p. 6517-26.
65. Lu, X., et al., *The p53-induced oncogenic phosphatase PPM1D interacts with uracil DNA glycosylase and suppresses base excision repair.* Mol Cell, 2004. **15**(4): p. 621-34.
66. Fiscella, M., et al., *Wip1, a novel human protein phosphatase that is induced in response to ionizing radiation in a p53-dependent manner.* Proc Natl Acad Sci U S A, 1997. **94**(12): p. 6048-53.
67. Maltzman, W. and L. Czyzyk, *UV irradiation stimulates levels of p53 cellular tumor antigen in nontransformed mouse cells.* Mol Cell Biol, 1984. **4**(9): p. 1689-94.
68. Momand, J., et al., *The mdm-2 oncogene product forms a complex with the p53 protein and inhibits p53-mediated transactivation.* Cell, 1992. **69**(7): p. 1237-45.

69. Honda, R., H. Tanaka, and H. Yasuda, *Oncoprotein MDM2 is a ubiquitin ligase E3 for tumor suppressor p53.* FEBS Lett, 1997. **420**(1): p. 25-7.
70. Leslie, P.L. and Y. Zhang, *MDM2 oligomers: antagonizers of the guardian of the genome.* Oncogene, 2016.
71. Haupt, Y., et al., *Mdm2 promotes the rapid degradation of p53.* Nature, 1997. **387**(6630): p. 296-9.
72. Pei, D., Y. Zhang, and J. Zheng, *Regulation of p53: a collaboration between Mdm2 and Mdmx.* Oncotarget, 2012. **3**(3): p. 228-35.
73. Wang, X., J. Wang, and X. Jiang, *MdmX protein is essential for Mdm2 protein-mediated p53 polyubiquitination.* J Biol Chem, 2011. **286**(27): p. 23725-34.
74. Barak, Y., et al., *mdm2 expression is induced by wild type p53 activity.* EMBO J, 1993. **12**(2): p. 461-8.
75. Meulmeester, E., et al., *ATM-mediated phosphorylations inhibit Mdmx/Mdm2 stabilization by HAUSP in favor of p53 activation.* Cell Cycle, 2005. **4**(9): p. 1166-70.
76. Lu, X., et al., *The Wip1 phosphatase and Mdm2: cracking the "Wip" on p53 stability.* Cell Cycle, 2008. **7**(2): p. 164-8.
77. Lee, J.S., et al., *Senescent growth arrest in mesenchymal stem cells is bypassed by Wip1-mediated downregulation of intrinsic stress signaling pathways.* Stem Cells, 2009. **27**(8): p. 1963-75.
78. Sakai, H., et al., *Wild-type p53-induced phosphatase 1 (Wip1) forestalls cellular premature senescence at physiological oxygen levels by regulating DNA damage response signaling during DNA replication.* Cell Cycle, 2014. **13**(6): p. 1015-29.
79. Song, J.Y., et al., *Wip1 suppresses apoptotic cell death through direct dephosphorylation of BAX in response to gamma-radiation.* Cell Death Dis, 2013. **4**: p. e744.
80. Choi, Dong W., et al., *WIP1, a Homeostatic Regulator of the DNA Damage Response, Is Targeted by HIPK2 for Phosphorylation and Degradation*
81. Yamaguchi, H., et al., *Substrate specificity of the human protein phosphatase 2Cdelta, Wip1.* Biochemistry, 2005. **44**(14): p. 5285-94.
82. Chuman, Y., et al., *PPM1D430, a novel alternative splicing variant of the human PPM1D, can dephosphorylate p53 and exhibits specific tissue expression.* J Biochem, 2009. **145**(1): p. 1-12.
83. Chuman, Y., et al., *Characterization of the active site and a unique uncompetitive inhibitor of the PPM1-type protein phosphatase PPM1D.* Protein Pept Lett, 2008. **15**(9): p. 938-48.
84. Kleiblova, P., et al., *Gain-of-function mutations of PPM1D/Wip1 impair the p53-dependent G1 checkpoint.* J Cell Biol, 2013. **201**(4): p. 511-21.
85. Gilmartin, A.G., et al., *Allosteric Wip1 phosphatase inhibition through flap-subdomain interaction.* Nat Chem Biol, 2014. **10**(3): p. 181-7.
86. Petitjean, A., et al., *TP53 mutations in human cancers: functional selection and impact on cancer prognosis and outcomes.* Oncogene, 2007. **26**(15): p. 2157-2165.
87. Wang, X. and Q. Sun, *TP53 mutations, expression and interaction networks in human cancers.* Oncotarget, 2016.
88. Li, J., et al., *Oncogenic properties of PPM1D located within a breast cancer amplification epicenter at 17q23.* Nat Genet, 2002. **31**(2): p. 133-4.
89. Natrajan, R., et al., *Tiling Path Genomic Profiling of Grade 3 Invasive Ductal Breast Cancers.* Clinical Cancer Research, 2009. **15**(8): p. 2711.
90. Satoh, N., et al., *Oncogenic phosphatase Wip1 is a novel prognostic marker for lung adenocarcinoma patient survival.* Cancer Science, 2011. **102**(5): p. 1101-1106.
91. Bulavin, D.V., et al., *Amplification of PPM1D in human tumors abrogates p53 tumor-suppressor activity.* Nat Genet, 2002. **31**(2): p. 210-5.
92. Tan, D.S., et al., *Genomic analysis reveals the molecular heterogeneity of ovarian clear cell carcinomas.* Clin Cancer Res, 2011. **17**(6): p. 1521-34.

93. Liang, C., et al., *Over-expression of wild-type p53-induced phosphatase 1 confers poor prognosis of patients with gliomas.* Brain Res, 2012. **1444**: p. 65-75.
94. Rauta, J., et al., *The serine-threonine protein phosphatase PPM1D is frequently activated through amplification in aggressive primary breast tumours.* Breast Cancer Res Treat, 2006. **95**(3): p. 257-63.
95. Castellino, R.C., et al., *Medulloblastomas overexpress the p53-inactivating oncogene WIP1/PPM1D.* J Neurooncol, 2008. **86**(3): p. 245-56.
96. Peng, T.S., et al., *PPM1D is a prognostic marker and therapeutic target in colorectal cancer.* Exp Ther Med, 2014. **8**(2): p. 430-434.
97. Fuku, T., et al., *Increased wild-type p53-induced phosphatase 1 (Wip1 or PPM1D) expression correlated with downregulation of checkpoint kinase 2 in human gastric carcinoma.* Pathology International, 2007. **57**(9): p. 566-571.
98. Demidov, O.N., et al., *The role of the MKK6/p38 MAPK pathway in Wip1-dependent regulation of ErbB2-driven mammary gland tumorigenesis.* Oncogene, 2007. **26**(17): p. 2502-6.
99. Choi, J., et al., *Mice deficient for the wild-type p53-induced phosphatase gene (Wip1) exhibit defects in reproductive organs, immune function, and cell cycle control.* Mol Cell Biol, 2002. **22**(4): p. 1094-105.
100. Nannenga, B., et al., *Augmented cancer resistance and DNA damage response phenotypes in PPM1D null mice.* Mol Carcinog, 2006. **45**(8): p. 594-604.
101. Bulavin, D.V., et al., *Inactivation of the Wip1 phosphatase inhibits mammary tumorigenesis through p38 MAPK-mediated activation of the p16(Ink4a)-p19(Arf) pathway.* Nat Genet, 2004. **36**(4): p. 343-50.
102. Shreeram, S., et al., *Regulation of ATM/p53-dependent suppression of myc-induced lymphomas by Wip1 phosphatase.* J Exp Med, 2006. **203**(13): p. 2793-9.
103. Demidov, O.N., et al., *Wip1 phosphatase regulates p53-dependent apoptosis of stem cells and tumorigenesis in the mouse intestine.* Cell Stem Cell, 2007. **1**(2): p. 180-90.
104. Filipponi, D., et al., *Wip1 controls global heterochromatin silencing via ATM/BRCA1-dependent DNA methylation.* Cancer Cell, 2013. **24**(4): p. 528-41.
105. Zhang, C. and L. Lai, *Towards structure-based protein drug design.* Biochem Soc Trans, 2011. **39**(5): p. 1382-6, suppl 1 p following 1386.
106. Belova, G.I., et al., *Chemical inhibition of Wip1 phosphatase contributes to suppression of tumorigenesis.* Cancer Biol Ther, 2005. **4**(10): p. 1154-8.
107. Rayter, S., et al., *A chemical inhibitor of PPM1D that selectively kills cells overexpressing PPM1D.* Oncogene, 2008. **27**(8): p. 1036-44.
108. Lee, J.S., et al., *Off-target response of a Wip1 chemical inhibitor in skin keratinocytes.* J Dermatol Sci, 2014. **73**(2): p. 125-34.
109. Yagi, H., et al., *A small molecule inhibitor of p53-inducible protein phosphatase PPM1D.* Bioorg Med Chem Lett, 2012. **22**(1): p. 729-32.
110. Ogasawara, S., et al., *Novel inhibitors targeting PPM1D phosphatase potently suppress cancer cell proliferation.* Bioorganic & Medicinal Chemistry, 2015. **23**(19): p. 6246-6249.
111. Hayashi, R., et al., *Optimization of a cyclic peptide inhibitor of Ser/Thr phosphatase PPM1D (Wip1).* Biochemistry, 2011. **50**(21): p. 4537-49.
112. Yamaguchi, H., et al., *Development of a substrate-based cyclic phosphopeptide inhibitor of protein phosphatase 2Cdelta, Wip1.* Biochemistry, 2006. **45**(44): p. 13193-202.
113. Bang, J., et al., *A Small Molecular Scaffold for Selective Inhibition of Wip1 Phosphatase().* ChemMedChem, 2008. **3**(2): p. 10.1002/cmdc.200700281.
114. Chen, Z., et al., *Wip1 inhibitor GSK2830371 inhibits neuroblastoma growth by inducing Chk2/p53-mediated apoptosis.* Sci Rep, 2016. **6**: p. 38011.
115. Kong, W., X. Jiang, and W.E. Mercer, *Downregulation of Wip-1 phosphatase expression in MCF-7 breast cancer cells enhances doxorubicin-induced apoptosis through p53-mediated transcriptional activation of Bax.* Cancer Biol Ther, 2009. **8**(6): p. 555-63.

116. Ali, A.Y., M.R. Abedini, and B.K. Tsang, *The oncogenic phosphatase PPM1D confers cisplatin resistance in ovarian carcinoma cells by attenuating checkpoint kinase 1 and p53 activation.* Oncogene, 2012. **31**(17): p. 2175-86.
117. Kozakai, Y., et al., *Inhibition of C-terminal truncated PPM1D enhances the effect of doxorubicin on cell viability in human colorectal carcinoma cell line.* Bioorg Med Chem Lett, 2014. **24**(24): p. 5593-6.
118. Ventura, A., et al., *Restoration of p53 function leads to tumour regression in vivo.* Nature, 2007. **445**(7128): p. 661-5.
119. Qin, L., et al., *Efficient reactivation of p53 in cancer cells by a dual MdmX/Mdm2 inhibitor.* J Am Chem Soc, 2014. **136**(52): p. 18023-33.
120. Brown, C.J., et al., *Awakening guardian angels: drugging the p53 pathway.* Nat Rev Cancer, 2009. **9**(12): p. 862-73.
121. Khoo, K.H., C.S. Verma, and D.P. Lane, *Drugging the p53 pathway: understanding the route to clinical efficacy.* Nat Rev Drug Discov, 2014. **13**(3): p. 217-36.
122. Zhang, Q., S.X. Zeng, and H. Lu, *Targeting p53-MDM2-MDMX loop for cancer therapy.* Subcell Biochem, 2014. **85**: p. 281-319.
123. Vassilev, L.T., et al., *In vivo activation of the p53 pathway by small-molecule antagonists of MDM2.* Science, 2004. **303**(5659): p. 844-8.
124. Ding, Q., et al., *Discovery of RG7388, a potent and selective p53-MDM2 inhibitor in clinical development.* J Med Chem, 2013. **56**(14): p. 5979-83.
125. Chen, L., et al., *Pre-clinical evaluation of the MDM2-p53 antagonist RG7388 alone and in combination with chemotherapy in neuroblastoma.* Oncotarget, 2015. **6**(12): p. 10207-21.
126. Higgins, B., et al., *Preclinical optimization of MDM2 antagonist scheduling for cancer treatment by using a model-based approach.* Clin Cancer Res, 2014. **20**(14): p. 3742-52.
127. Sakaue-Sawano, A., et al., *Visualizing spatiotemporal dynamics of multicellular cell-cycle progression.* Cell, 2008. **132**(3): p. 487-98.
128. Sakaue-Sawano, A., et al., *Tracing the silhouette of individual cells in S/G2/M phases with fluorescence.* Chem Biol, 2008. **15**(12): p. 1243-8.
129. Zhu, Y.H., et al., *Wip1 regulates the generation of new neural cells in the adult olfactory bulb through p53-dependent cell cycle control.* Stem Cells, 2009. **27**(6): p. 1433-42.
130. Jeong, H.C., et al., *Timely Degradation of Wip1 Phosphatase by APC/C Activator Protein Cdh1 is Necessary for Normal Mitotic Progression.* J Cell Biochem, 2015. **116**(8): p. 1602-12.
131. Nelson, G., M. Buhmann, and T. von Zglinicki, *DNA damage foci in mitosis are devoid of 53BP1.* Cell Cycle, 2009. **8**(20): p. 3379-83.
132. Giunta, S., R. Belotserkovskaya, and S.P. Jackson, *DNA damage signaling in response to double-strand breaks during mitosis.* J Cell Biol, 2010. **190**(2): p. 197-207.
133. van Vugt, M.A., A. Bras, and R.H. Medema, *Polo-like kinase-1 controls recovery from a G2 DNA damage-induced arrest in mammalian cells.* Mol Cell, 2004. **15**(5): p. 799-811.
134. Benada, J., et al., *Polo-like kinase 1 inhibits DNA damage response during mitosis.* Cell Cycle, 2015. **14**(2): p. 219-31.
135. Parssinen, J., et al., *PPM1D silencing by RNA interference inhibits proliferation and induces apoptosis in breast cancer cell lines with wild-type p53.* Cancer Genet Cytogenet, 2008. **182**(1): p. 33-9.
136. Ruark, E., et al., *Mosaic PPM1D mutations are associated with predisposition to breast and ovarian cancer.* Nature, 2013. **493**(7432): p. 406-10.
137. Zhang, L., et al., *Exome sequencing identifies somatic gain-of-function PPM1D mutations in brainstem gliomas.* Nat Genet, 2014. **46**(7): p. 726-30.
138. Akbari, M.R., et al., *PPM1D mutations in circulating white blood cells and the risk for ovarian cancer.* J Natl Cancer Inst, 2014. **106**(1): p. djt323.
139. Zajkowicz, A., et al., *Truncating mutations of PPM1D are found in blood DNA samples of lung cancer patients.* Br J Cancer, 2015. **112**(6): p. 1114-20.

140. Eirew, P., et al., *Dynamics of genomic clones in breast cancer patient xenografts at single-cell resolution.* Nature, 2015. **518**(7539): p. 422-6.
141. Ciriello, G., et al., *Comprehensive Molecular Portraits of Invasive Lobular Breast Cancer.* Cell. **163**(2): p. 506-519.
142. Martelotto, L.G., et al., *Genomic landscape of adenoid cystic carcinoma of the breast.* J Pathol, 2015. **237**(2): p. 179-89.
143. Swisher, E.M., et al., *Somatic mosaic mutations in ppm1d and tp53 in the blood of women with ovarian carcinoma.* JAMA Oncology, 2016. **2**(3): p. 370-372.
144. Bartkova, J., et al., *DNA damage response as a candidate anti-cancer barrier in early human tumorigenesis.* Nature, 2005. **434**(7035): p. 864-70.
145. Bartkova, J., et al., *Oncogene-induced senescence is part of the tumorigenesis barrier imposed by DNA damage checkpoints.* Nature, 2006. **444**(7119): p. 633-7.
146. Shiloh, Y., *ATM and related protein kinases: safeguarding genome integrity.* Nat Rev Cancer, 2003. **3**(3): p. 155-68.
147. Emelyanov, A. and D.V. Bulavin, *Wip1 phosphatase in breast cancer.* Oncogene, 2015. **34**(34): p. 4429-38.
148. Macurek, L., et al., *Downregulation of Wip1 phosphatase modulates the cellular threshold of DNA damage signaling in mitosis.* Cell Cycle, 2013. **12**(2): p. 251-62.
149. Coll-Mulet, L., et al., *MDM2 antagonists activate p53 and synergize with genotoxic drugs in B-cell chronic lymphocytic leukemia cells.* Blood, 2006. **107**(10): p. 4109-14.
150. Lam, S., et al., *Role of Mdm4 in drug sensitivity of breast cancer cells.* Oncogene, 2010. **29**(16): p. 2415-26.
151. Burgess, A., et al., *Clinical Overview of MDM2/X-Targeted Therapies.* Front Oncol, 2016. **6**: p. 7.
152. Rochette, L., et al., *Anthracyclines/trastuzumab: new aspects of cardiotoxicity and molecular mechanisms.* Trends Pharmacol Sci, 2015. **36**(6): p. 326-48.
153. Derek, W.E., et al., *Role of Drug Metabolism in the Cytotoxicity and Clinical Efficacy of Anthracyclines.* Current Drug Metabolism, 2015. **16**(6): p. 412-426.
154. Sriraman, A., et al., *Cooperation of Nutlin-3a and a Wip1 inhibitor to induce p53 activity.* Oncotarget, 2016. **7**(22): p. 31623-38.
155. Pechackova, S.B., K.; Benada, J.; Kleiblova, P.; Jenikova, G., Macurek, L., *Inhibition of WIP1 phosphatase sensitizes breast cancer cells to genotoxic stress and to MDM2 antagonist nutlin-3.* 2016.
156. Kojima, K., et al., *The pathophysiological significance of PPM1D and therapeutic targeting of PPM1D-mediated signaling by GSK2830371 in mantle cell lymphoma.* Oncotarget, 2016.
157. Esfandiari, A., et al., *Chemical Inhibition of Wild-Type p53-Induced Phosphatase 1 (WIP1/PPM1D) by GSK2830371 Potentiates the Sensitivity to MDM2 Inhibitors in a p53-Dependent Manner.* Mol Cancer Ther, 2016. **15**(3): p. 379-91.
158. Hu, B., et al., *MDMX overexpression prevents p53 activation by the MDM2 inhibitor Nutlin.* J Biol Chem, 2006. **281**(44): p. 33030-5.
159. Xia, M., et al., *Elevated MDM2 boosts the apoptotic activity of p53-MDM2 binding inhibitors by facilitating MDMX degradation.* Cell Cycle, 2008. **7**(11): p. 1604-12.
160. Goloudina, A.R., et al., *Wip1 sensitizes p53-negative tumors to apoptosis by regulating the Bax/Bcl-xL ratio.* Cell Cycle, 2012. **11**(10): p. 1883-7.
161. Goloudina, A.R., et al., *Wip1 promotes RUNX2-dependent apoptosis in p53-negative tumors and protects normal tissues during treatment with anticancer agents.* Proc Natl Acad Sci U S A, 2012. **109**(2): p. E68-75.
162. Shen, X.-F., et al., *Phosphatase Wip1 in Immunity: An Overview and Update.* Frontiers in Immunology, 2017. **8**: p. 8.
163. Ericsson, U.B., et al., *Thermofluor-based high-throughput stability optimization of proteins for structural studies.* Anal Biochem, 2006. **357**(2): p. 289-98.

164. Chen, X., *Fusion Protein Linkers: Property, Design and Functionality.* 2013. **65**(10): p. 1357-69.
165. Trinh, R., et al., *Optimization of codon pair use within the (GGGGS)3 linker sequence results in enhanced protein expression.* Molecular Immunology, 2004. **40**(10): p. 717-722.
166. Baase, W.A., et al., *Lessons from the lysozyme of phage T4.* Protein Sci, 2010. **19**(4): p. 631-41.
167. Rasmussen, S.G., et al., *Crystal structure of the human beta2 adrenergic G-protein-coupled receptor.* Nature, 2007. **450**(7168): p. 383-7.
168. Zou, Y., W.I. Weis, and B.K. Kobilka, *N-terminal T4 lysozyme fusion facilitates crystallization of a G protein coupled receptor.* PLoS One, 2012. **7**(10): p. e46039.
169. Longhi, S., F. Ferron, and M.P. Egloff, *Protein engineering.* Methods Mol Biol, 2007. **363**: p. 59-89.
170. Dong, A., X. Xu, and A.M. Edwards, *In situ proteolysis for protein crystallization and structure determination.* Nat Meth, 2007. **4**(12): p. 1019-1021.